This document was produced by scanning the original publication.

Ce document est le produit d'une numérisation par balayage de la publication originale.

GEOLOGICAL SURVEY OF CANADA
BULLETIN 383

PETROLOGY, TECTONIC SETTING, AND ECONOMIC POTENTIAL OF DEVONIAN PERALUMINOUS GRANITOID PLUTONS IN THE CANSO AND FOREST HILL AREAS, EASTERN MEGUMA TERRANE, NOVA SCOTIA

J.D. Hill

1991

Energy, Mines and Resources Canada
Énergie, Mines et Ressources Canada

Canada

THE ENERGY OF OUR RESOURCES

THE POWER OF OUR IDEAS

GEOLOGICAL SURVEY OF CANADA
BULLETIN 383

PETROLOGY, TECTONIC SETTING, AND ECONOMIC POTENTIAL OF DEVONIAN PERALUMINOUS GRANITOID PLUTONS IN THE CANSO AND FOREST HILL AREAS, EASTERN MEGUMA TERRANE, NOVA SCOTIA

J.D. Hill

1991

©Minister of Supply and Services Canada 1991

Available in Canada through
authorized bookstore agents and other bookstores
or by mail from

Canadian Government Publishing Centre
Supply and Services Canada
Ottawa, Canada K1A 0S9

and from

Geological Survey of Canada offices:

601 Booth Street
Ottawa, Canada K1A 0E8

3303-33rd Street N.W.,
Calgary, Alberta T2L 2A7

A deposit copy of this publication is also available for
reference in public libraries across Canada

Cat. No. M42-383E
ISBN 0-660-13837-9

Price subject to change without notice

Critical reader

K. Currie

Author's address

Dept. of Mining and Engineering,
Technical University of Nova Scotia
P.O. Box 1000
Halifax, N.S.
B3J 2X4

Original manuscript submitted: 1987 - 11
Final version approved for publication: 1989 - 05

Preface

The Geological Survey of Canada carries out petrological studies of igneous rocks to gain a better understanding of the geological evolution and economic potential of particular regions. The Meguma Terrane in mainland Nova Scotia consists primarily of peraluminous granitoid plutons which intrude Cambro-Ordovician metasedimentary rocks of the Meguma Group. Interest in granitoid plutons in the Meguma Terrane has been stimulated in recent years by the discovery of granite-hosted mineralization such as the East Kemptville tin deposit. In addition, the Meguma Group has considerable potential for gold, as evidenced by the opening of a new mine at Forest Hill in 1987.

Two segments of the eastern Meguma Terrane, the Canso and Forest Hill areas, were selected for an integrated program involving mapping, structural analysis, petrography, geochemistry and isotopic investigation. The granitoid rocks in these areas have received very little attention in the past. The Canso area in particular is well suited for study because of the superb exposure in nearly continuous, clean outcrops along the coast. Although mapping did not reveal any important new economic mineral showings, comparison with granitic rocks associated with tin mineralization in western Nova Scotia suggests that three muscovite leucogranite intrusions are favourable targets for exploration.

Elkanah A. Babcock
Assistant Deputy Minister
Geological Survey of Canada

Préface

La Commission géologique du Canada effectue des analyses pétrologiques de roches ignées afin d'acquérir une meilleure connaissance de l'évolution géologique et de la valeur économique possible de certaines régions. Le terrane de Meguma, dans la masse continentale de la Nouvelle-Écosse, est composé principalement de plutons granitoïdes hyperalumineux pénétrant les roches métasédimentaires cambro-ordoviciennes du groupe de Meguma. La découverte de dépôts minéralisés dans le granite, comme le gisement d'étain d'East Kemptville, a incité les scientifiques à s'intéresser davantage à ces plutons granitoïdes au cours des dernières années. De fait, ainsi qu'en témoigne la nouvelle mine de Forest Hill mise en exploitation en 1987, le groupe de Meguma pourrait contenir une quantité considérable d'or.

On a choisi de mettre en oeuvre un programme de recherche intégré, touchant à la cartographie, à l'analyse structurale, à la pétrographie, à la géochimie et à l'analyse isotopique du sol, dans deux segments du terrane de Meguma de l'est, soit dans les régions de Canso et de Forest Hill. Jusqu'à maintenant, les roches granitoïdes de ces régions ont suscité bien peu d'intérêt. La région de Canso se prête particulièrement bien à ce genre d'étude étant donné ses affleurements quasi continus très visibles le long de la côte. Bien que la cartographie du sol n'y ait pas révélé de nouveaux gisements importants de minéraux de grande valeur économique, la présence de roches granitiques associées à la minéralisation de l'étain dans l'ouest de la Nouvelle-Écosse laisse croire que l'exploration de trois intrusions de leucogranite à muscovite pourrait donner de bons résultats.

Elkanah A. Babcock
Sous-ministre adjoint
Commission géologique du Canada

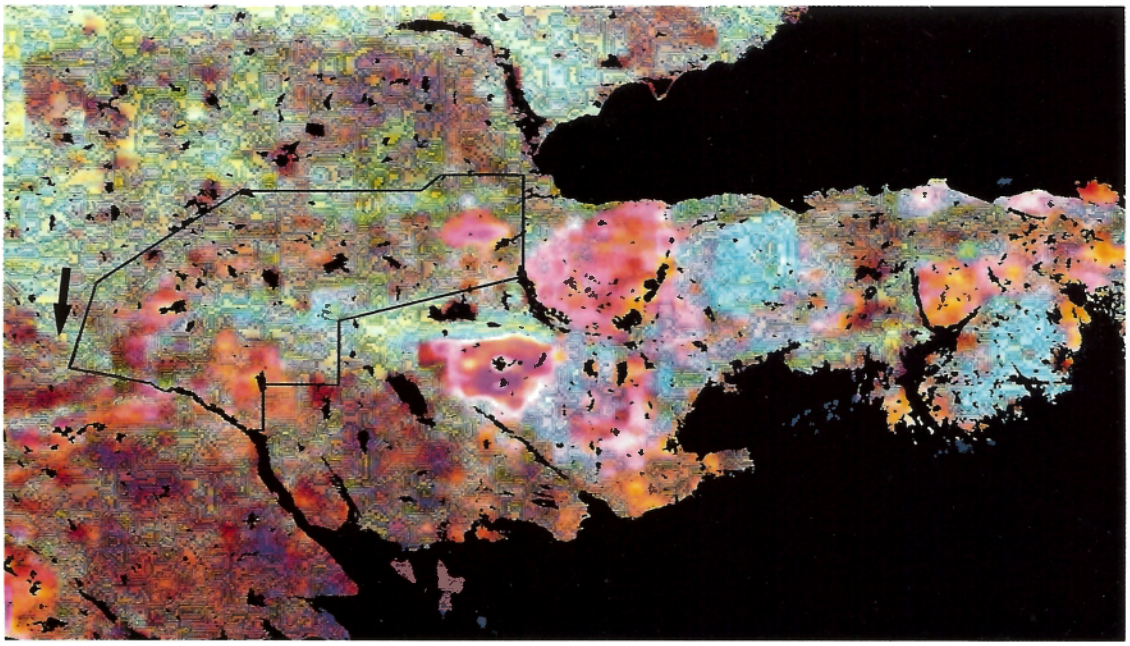

Airborne gamma ray spectrometer image of the eastern Meguma Terrane, generated by computer-enhancement of integrated U-Th-K measurements. Granitic plutons stand out in purple and yellow-green, indicating low and high U/Th respectively. Black arrow points to trace of Country Harbour fault in the Gunns Brook formation. The Forest Hill area is outlined in black.

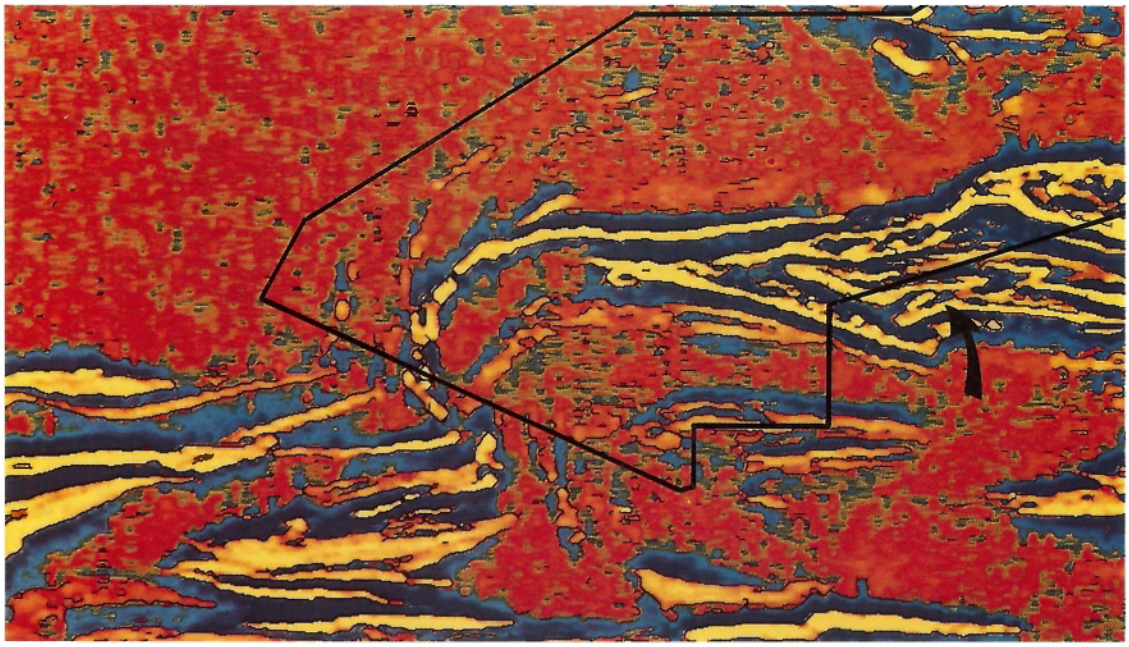

Computer-enhanced aeromagnetic vertical gradient image of the Forest Hill area (outlined in black). The Halifax Formation, shown by closely spaced blue and yellow bands, occupies the core of the D_1 Loon Lake synclinorium in the eastern half of the area. Black arrow points to possible Z-shaped F_2 folds.

CONTENTS

1 Abstract/Résumé

2 Summary/Sommaire
7 Introduction
7 General statement
8 Previous work
8 Acknowledgments

9 Geological setting
9 General statement
9 Meguma Group
9 Granitoid plutons
10 Fundy Basin
10 Summary of tectonic history
11 General geology of the Canso and Forest Hill areas

13 Geology of the country rocks
13 Meguma Group
13 General statement
13 Goldenville Formation (unit CO_G)
16 Goldenville-Halifax transition zone
16 Halifax Formation (unit CO_H)
18 Chemistry of the Meguma Group
19 Quartz veins in the Meguma Group
20 Devono-Carboniferous rocks
20 General statement
20 Minister Brook formation (unit DC_M)
20 Mylonitic inliers in the Minister Brook formation
21 Sunnyville formation (unit DC_S)
21 Tower formation (unit DC_T)
21 Gunns Brook formation (unit C_G)

22 Macroscopic features of the granitoid plutons
22 General statement
23 Rock textures
23 Tonalite plutons (unit D_T)
25 Granitic plutons (unit D_G)
26 Big Branch, Sheep Island, Rocky Lake plutons (unit D_{Ga})
26 Andrew Island, Dover Head, Madeline Point, Prince Island plutons (unit D_{Gb})
26 False Cove pluton (unit D_{Gc})
26 Bantry Road and related plutons (unit D_{Gd})
26 Charles Lake, Ketch Harbour, Portage Cove, Port Howe plutons (unit D_{Ge})
27 Buchanans Mountain, Gammon Islands, Snyders Lake plutons (unit D_{Gf})
27 Contact and age relationships
27 Country rock contacts and xenoliths
27 Interplutonic contacts
27 Age relationships
28 Internal igneous structures and pluton shapes
28 Magmatic structures
29 Late magmatic structures
29 Pluton shapes and sizes
30 Miscellaneous plutonic rocks
31 Pegmatite and aplite
32 Quartz veins

32 Petrography and chemistry of the granitoid plutons
32 General statement

32 Pluton modal compositions
32 Mineral relationships and compositions
32 Analytical methods and accuracy
34 Plagioclase
34 Microcline
36 Biotite and muscovite
36 Hornblende
37 Accessory minerals
38 Pluton chemistry
38 Analytical methods and accuracy
38 Effect of deformation on rock chemistry
39 Major and trace element variation
41 Rare-earth elements
41 Isotopic data and geochronology
41 U-Pb data
43 Rb-Sr data

43 Structure and metamorphism
43 General statement
43 D_1
44 D_2 – dextral shearing event
44 General statement
45 D_{2a}
48 Static metamorphism (M_S)
50 Contact metamorphism (M_K) caused by granitic plutonism
50 D_{2b}
54 D_{2c}
55 D_{2d}
57 D_{2e}
58 D_3 – Late faulting

58 Summary and discussion of tectonic history and granitoid petrogenesis
58 Tectonic history
58 Overview
58 D_1 – Regional deformation
58 D_2 – Dextral transcurrent shearing
60 D_3 – Carboniferous faulting
60 Metamorphism and P-T conditions
63 Compositions of the granitoid plutons
64 Comparison with other Meguma Terrane granitoid plutons
65 Sequence and style of granitoid intrusion
67 Causes of lithological variation of the granitoid rocks
69 Nature of source area

72 Economic geology
72 General statement
72 Meguma Group
72 Gold
73 Base metals
73 Aluminum
73 Granitoid rocks
74 Devono-Carboniferous rocks

75 References

Appendices

80 I. Pluton descriptions
85 II. Representative mineral analyses
87 III. Average pluton compositions and norms
89 IV. Rock chemical analyses

Tables

11 1. Simplified sequence of lithological and tectonic events in the eastern Meguma Terrane and adjacent part of the Fundy basin
12 2. Lithological units
33 3. Approximate average pluton modes
34 4. List of accessory minerals
45 5. Outcrop features where isotopic samples were collected
46 6. Rb-Sr isotopic data
46 7. Summary of the structural, metamorphic and intrusive history of the Canso and Forest Hill areas
59 8. Summary of lithological, tectonic and isotopic age relationships
62 9. Biotite-garnet equilibration temperatures
64 10. Characteristics of granitic plutons in the Canso and Forest Hill areas compared with S-type granites
65 11. Average analyses of selected granitoid lithologies in the Canso and Forest Hill areas, Musquodoboit batholith, South Mountain batholith, and southern plutons
71 12. Results of least-squares mass balance calculations
74 13. Average trace element contents of selected rocks and plutons in the Canso and Forest Hill areas compared to various lithologies in the South Mountain batholith

Figures

7 1. Simplified geological map of mainland Nova Scotia
in pocket 2. Geology of the Canso area (scale 1:50 000)
in pocket 3. Geology of the Forest Hill area (scale 1:50 000)
13 4. Inferred stratigraphy and macroscopic structure of the western part of the Canso area
14 5. Photomicrographs showing country rock textures
15 6. Outcrop features of the Meguma Group
18 7. Relationship between MnO content and inferred stratigraphic position of Meguma samples in the Canso area
19 8. Ternary plot showing the relationship between pelite chemistry and the presence of andalusite and cordierite porphyroblasts
22 9. Sketch maps showing the locations and two-letter codes of granitoid plutons in the Canso and Forest Hill areas
23 10. Sketch map of the eastern Meguma Terrane showing the variation in intensity of post-granite D2 strain
24 11. Photomicrographs of granitoid rock textures
25 12. Structures associated with tonalite plutons in the Canso area
28 13. Structures in granitic plutons in the Canso area
29 14. Inferred intrusive sequence of the granitoid plutons
30 15. Comparison of magmatic and late magmatic structures in granitic plutons in the Canso area
31 16. Structural relationships between pegmatite dykes and the Andrew Island pluton
33 17. Average modal compositions of the granitoid plutons
35 18. Photomicrographs showing mineral relationships in granitic rocks
36 19. Plagioclase compositions
37 20. Ternary plot showing biotite compositions
37 21. Comparison of biotite composition with respect to crystal habit and degree of deformation in the host rock
38 22. Variation in Al^{iv} in biotite with Al/Na+K+2Ca in the host rock
38 23. Comparison of primary-looking, secondary, and metamorphic muscovite compositions

39 24. Variation in rock chemistry with distance from the centre of the Harbour Island shear zone
39 25. Compositional variation within four plutons compared to the total range of granitic rocks in the Canso area
40 26. Variation diagram for the granitoid rocks
41 27. Modified ACF diagram for the granitoid rocks
42 28. Selected parameters plotted against MgO
43 29. Rare-earth element plot
44 30. Variation in ΣREE, La/Yb, and Eu/Eu* with MgO
45 31. U-Pb concordia plot
45 32. Rb-Sr isochron diagram
47 33. Structural relationships in the Prices Island domain
47 34. Structural relationships in the Spears Cove domain
49 35. Photomicrographs showing deformation and metamorphic textures in the Meguma Group
51 36. Photomicrographs showing deformation and metamorphic textures in the Meguma Group and granitoid plutons
53 37. D_2 structures in the Canso area
54 38. Structural relationships in the Poule Point domain
55 39. Differences in granitic rock texture resulting from variations in post-granite D_2 strain
56 40. Structural relationships in the Harbour Island shear zone
56 41. Structural relationships in the George Island domain
57 42. Equal area projections of poles to brittle structures in the Canso area
60 43. Riedel shear package of faults and brittle-ductile shear zones developed along the north shore of the Canso area
61 44. Inferred relationships between time, deformation, and metamorphic grade in the Canso and Forest Hill areas
62 45. Probable pressure-temperature conditions during the peak of D_2 metamorphism
65 46. REE plot of various granitoid lithologies from the Meguma Terrane
66 47. Variation in modal muscovite and biotite contents in granitic plutons from the Canso and Forest Hill areas
66 48. Bivariate plot illustrating the main chemical differences between granitic rocks in the Canso-Forest Hill area, Musquodoboit batholith, South Mountain batholith, and southern plutons
66 49. Gravity profile of the upper crust in the eastern Meguma Terrane
67 50. K/Rb versus Rb/Sr in granitic plutons from the Canso and Forest Hill areas
68 51. Variation in initial $^{87}Sr/^{86}Sr$ with normative corundum
68 52. Na_2O-FeO and Zr-FeO plots for the granitic plutons in the Canso area compared to metasedimentary rocks from the Meguma Group
69 53. Proportions of normative quartz, albite, orthoclase, and anorthite in the qz-ab-or-H_2O and or-ab-an-H_2O systems
70 54. Variation of selected elements with FeO in granitic plutons from the Canso area
70 55. Variation in La, Zr, and Rb in granitic rocks from the Canso area
72 56. Boudinaged quartz vein at Forest Hill
75 57. Rb-K_2O variation in granitic rocks from the Canso and Forest Hill areas
75 58. Ternary plots of specialized granitic rocks from the Canso and Forest Hill areas

PETROLOGY, TECTONIC SETTING, AND ECONOMIC POTENTIAL OF DEVONIAN PERALUMINOUS GRANITOID PLUTONS IN THE CANSO AND FOREST HILL AREAS, EASTERN MEGUMA TERRANE, NOVA SCOTIA

Abstract

The Devonian peraluminous granitoid plutons in the eastern Meguma Terrane can be divided into two independent suites, based on differences in age, composition, and areal extent. The older suite consists of a few small, widely separated bodies of biotite tonalite, some of which contain significant amounts of hornblende or muscovite. Concordant U-Pb dates suggest that at least two of the tonalite intrusions crystallized at about 378 Ma. The younger suite is composed of numerous biotite-muscovite granite and minor granodiorite plutons, each of which is relatively homogeneous within a total range of granitic rock types that is already compositionally restricted. Contact relationships require at least six episodes of intrusion, although U-Pb monazite isotopic data indicate that emplacement of most or all the plutons occurred between 371 and 373 Ma.

The tonalite plutons have relatively high K and Rb contents and initial $^{87}Sr/^{86}Sr$, suggesting an origin involving significant crustal material. However, participation of a small mantle component cannot be ruled out. The granitic plutons show no systematic relationship between composition and age of intrusion, which implies that lithological variation resulted either from uprise of various independent magmas or from the tapping at different times of parts of one or more zoned magma chambers below the current level of exposure. Poor inter-element correlation, initial $^{87}Sr/^{86}Sr$ ratios that range from 0.703 to 0.709, and the fact that most plutons have close to minimum melt compositions favour the former model. Thus, it is postulated that plutons ranging from biotite-rich granodiorite to muscovite-rich granite formed by the intrusion of several unrelated magmas generated in a somewhat heterogeneous source volume in lower crust composed of intermediate to felsic rocks that contained a significant proportion of aluminous material.

The tonalite and granitic plutons were emplaced respectively at the beginning and during the early stages of a ductile shearing event associated with dextral transcurrent movements in the Cobequid-Chedabucto fault system. Tectonism was probably caused by readjustments among the outboard blocks of the northern Appalachian Orogen following initial collision between the Meguma and Avalon terranes during the early Devonian. High thermal gradients preceding granitic intrusion suggest that crustal anatexis was facilitated by the addition of heat from mafic magmas generated in the mantle or subducted oceanic crust.

No significant economic mineral occurrences were found, and gold in the Goldenville Formation remains the primary exploration target. However, three muscovite leucogranite intrusions that are highly enriched in F, Li, and Sn appear to have some economic potential.

Résumé

On peut diviser les plutons granitoïdes peralumineux dévoniens qui se trouvent dans l'est du terrain de Meguma en deux suites indépendantes fondées sur des différences d'âge, de composition et d'extension. La suite la plus ancienne est composée de quelques petits massifs de tonalite à biotite distancés, dont quelques'uns ont des teneurs importantes en hornblende ou muscovite. Des datations U-Pb concordantes indiquent qu'au moins deux des intrusions de tonalite se seraient cristallisées vers 378 Ma. La suite la plus récente est composée de plusieurs plutons de granite à biotite-muscovite et de granodiorite mineur, qui sont tous relativement homogènes dans une gamme complète de roches de type granitique dont la composition est déjà limitée. Les relations de contact observées nécessitent au moins six épisodes d'intrusion bien que des données isotopiques U-Pb monazite indiquent que l'intrusion de la plupart des plutons, sinon tous, s'est produite entre 371 et 373 Ma.

Les plutons de tonalite ont des teneurs en K et Rb et un rapport initial $^{87}Sr/^{86}Sr$ relativement élevés, indiquant qu'à l'origine, ils comportaient une quantité importante de matériau crustal. Cependant, il n'est pas possible d'établir si une petite composante du manteau a été incluse. Les plutons granitiques ne permettent pas d'établir de lien systématique entre la composition et l'âge de l'intrusion. La lithologie aurait donc varié par suite d'une montée de divers magmas indépendants ou

du soutirage à différentes périodes d'une ou plusieurs chambres magmatiques zonées, au-dessous du niveau actuel d'exposition. Une faible corrélation inter-éléments, des rapports $^{87}Sr/^{86}Sr$ initiaux variant de 0,703 à 0,709 et le fait que la plupart des plutons soient composés de roches en fusion en quantités presque minimales favorisent l'utilisation du premier modèle. Par conséquent, il est postulé que des plutons variant de granodiorite à forte teneur en biotite à granite à forte teneur en muscovite, se sont formés par l'intrusion de plusieurs magmas non associés issus d'une roche crustale quelque peu hétérogène composée de roches intermédiaires à felsiques qui contenaient une fraction importante de matériaux alumineux.

Les plutons de tonalite et de granite se sont introduits respectivement au début et pendant les premières étapes d'un cisaillement ductile associé à des déplacements transversaux dextres dans le système de failles de Cobequid-Chedabucto. Ce tectonisme a probablement été causé par des réajustements au sein des blocs extérieurs de la partie septentrionale de l'orogène des Appalaches survenus après la collision initiale entre les terrains de Meguma et d'Avalon au début du Dévonien. Des gradients thermiques élevés avant l'intrusion granitique indique que l'anatexie crustale a été facilitée par l'ajout de chaleur fournie par des magmas mafiques formés dans le manteau ou dans la croûte océanique subductée.

Aucun gisement d'importance économique n'a été découvert et l'or demeure la principale cible d'exploration dans la formation de Goldenville. Toutefois, trois intrusions de leucogranite à muscovite à forte teneur en P, Li et Sn semblent présenter des possibilités économiques.

SUMMARY

The Meguma Terrane of Nova Scotia is composed mainly of the Meguma Group, a thick sequence of Cambro-Ordovician clastic metasedimentary rocks, intruded by numerous Devonian peraluminous granitoid plutons. These rocks form a unique lithological assemblage within the Appalachian Orogen. For this reason, the Meguma Terrane is thought to be allochthonous, possibly representing a segment of northwestern Africa or western Europe accreted to North America during the middle to late Devonian Acadian Orogeny. Recent discoveries of tin and uranium mineralization as well as renewed interest in gold exploration have indicated the need for more detailed information on the geology of the Meguma Terrane. This need is emphasized by the fact that parts of the terrane have not been mapped since Faribault's work in the late 1800s. Furthermore, most mapping projects have concentrated on the Meguma Group at the expense of the granitoid plutons. This report partly fills this gap in knowledge by presenting the results of a two year field-based research project on the petrology, tectonic history and economic potential of granitoid plutons and their country rocks in two areas of the eastern Meguma Terrane.

In general, two separate suites of granitoid plutons can be distinguished: an older tonalite group and a younger granitic group. Both suites intruded the Meguma Group more or less concurrently with late Devonian deformation and metamorphism.

Tonalite plutons. Tonalite forms less than 10% of the two mapped areas in the eastern Meguma Terrane, forming numerous small bodies lying within and adja-

SOMMAIRE

Le terrane de Meguma de la Nouvelle-Écosse est constitué surtout du groupe de Meguma, séquence épaisse de roches métasédimentaires détritiques du Cambrian et de l'Ordovicien, pénétré par de nombreux plutons granitoïdes hyperalumineux du Dévonien. Ces roches forment un ensemble lithologique unique à l'intérieur de l'orogène appalachien. C'est pour cette raison qu'on pense que le terrane de Meguma est allochtone, représentant probablement un segment du nord-ouest de l'Afrique ou de l'Europe occidentale qui serait venu s'ajouter à l'Amérique du Nord au cours de l'orogenèse acadienne du Dévonien supérieur. Des découvertes récentes de minéralisation en étain et en uranium ainsi que l'intérêt renouvelé dans l'exploration de l'or, ont souligné la nécessité de recueillir de meilleurs renseignements sur la géologie du terrane de Meguma. Le fait que certaines parties du terrane n'ont pas été cartographiées depuis les travaux de Faribault menés à la fin du XIXe siècle accentue le besoin. De plus, la plupart des levés cartographiques ont été concentrés sur le groupe de Meguma plutôt que sur les plutons granitoïdes. Le présent rapport corrige partiellement cette lacune des connaissances en présentant les résultats de travaux de recherche effectués sur le terrain pendant deux ans, consacrés à la pétrologie, la tectonique et les possibilités économiques de plutons granitoïdes, ainsi que de celles de leurs roches encaissantes, dans deux secteurs de la partie est du terrane de Meguma.

En général, on peut distinguer deux différentes séries de plutons granitoïdes, soit un groupe ancien de plutons constitués de tonalite et un groupe plus récent constitué de granite. Ces deux séries ont pénétré le groupe de Meguma à peu près à l'époque ou se sont produits la déformation et le métamorphisme au Dévonien supérieur.

Plutons de tonalite. La tonalite constitue moins de 10 % des deux zones cartographiées dans la partie est du terrane de Meguma, créant de nombreux petits amas à l'intérieur

cent to larger masses of younger granitic rocks. Hornblende-biotite, biotite and migmatitic biotite-muscovite variants have been recognized. The tonalite has been variably deformed and metamorphosed depending on its location, and as a result ranges from decussate to gneissose in fabric. Plagioclase, which is typically oriented parallel to the tectonic foliation and may be at least partly metamorphic in origin, varies from An_{51} in the hornblende-rich variant to An_{26} in rocks lacking hornblende. The high muscovite content of the migmatitic variant may be the result of metamorphic decomposition of magmatic alkali feldspar or metasomatic contamination during granitic injection. Clear, unzoned zircon crystals from two hornblende-biotite and biotite tonalite plutons have given concordant U-Pb ages of about 378 ± 2 Ma. This isotopic age is consistent with the fact that the tonalite plutons contain xenoliths of Meguma metasedimentary rocks and are crosscut by dykes of adjacent granitic plutons.

Granitic plutons. Thirty granitic plutons, ranging up to 40 km² in area, have been distinguished in the two mapped areas, although the precise number depends on correlation of rock types that vary only slightly in lithology. Pluton margins are commonly agmatitic and the few planar contacts observed suggest that individual intrusions are steep-walled. An east-west profile using regional-scale gravity data indicates that plutons in the more eastern map area extend to a maximum depth of about 3 km. Each pluton is relatively homogeneous in composition and texture compared to the total range of granitic rock types. In addition, interplutonic contacts are invariably intrusive wherever seen in outcrop. Thus, the term 'pluton' used herein refers to a body of granitic rock which is lithologically distinct from its neighbours and appears to represent a single pulse of magma (melt plus crystals) at the current level of exposure. The thirty plutons have been assigned to six map units based on age relationships and lithology. These six units are inferred to represent sequential emplacement of six or more batches of granitic magma into the upper crust, each of which gave rise to more than one individual intrusion. However, concordant to nearly concordant $^{207}Pb/^{235}U$ monazite ages for three plutons suggest that most and perhaps all of the granitic rocks crystallized between 371 and 373 Ma. This short time span implies that magmas assigned to different units probably coexisted during emplacement.

The granitic rocks are composed of only five essential minerals: quartz, plagioclase, microcline, biotite and muscovite. Common accessory phases include zircon, monazite, garnet, ilmenite, apatite, tourmaline and possible cordierite pseudomorphed by smectite. Magmatic-appearing spinel was found in one thin section and subsolidus sillimanite is common in several

et autour de grands massifs de roches granitiques plus jeunes. On signale la présence de variétés à hornblende et biotite, à biotite et à biotite et muscovite migmatitique. La tonalite a été plus ou moins déformée et métamorphisée selon son emplacement, épisodes qui lui ont conféré une fabrique variant de décussée à gneissique. Les plagioclases dont l'orientation caractéristique est parallèle à la foliation tectonique et auxquels on peut attribuer une origine partiellement métamorphique, ont une composition qui varie de An_{51} dans la variété riche en hornblende à An_{26} dans les roches où la hornblende est absente. La teneur élevée en muscovite de la variété migmatitique peut être le résultat d'une décomposition par métamorphisme d'un feldspath alcalin de nature magmatique ou d'un métasomatisme au cours de l'intrusion granitique. Des cristaux clairs, non zonés, de zircon provenant de deux plutons de tonalite à hornblende et biotite et à biotite, sont d'âge radiométrique (couple U-Pb) concordant d'environ 378 ± 2 Ma. Cet âge est conforme au fait que les plutons de tonalite renferment des xénolites de roches métasédimentaires de Meguma et qu'ils sont recoupés par des dykes de plutons granitiques adjacents.

Plutons granitiques. On trouve dans les deux secteurs cartographiés 30 plutons granitiques, atteignant parfois 40 km², bien que le nombre précis de ces plutons dépende de la corrélation des types de roche dont la lithologie varie à peine. Les bords des plutons sont généralement agmatitiques et les quelques contacts planaires observés semblent indiquer que les différentes intrusions sont à parois abruptes. Un profil est-ouest obtenu à partir de données gravimétriques à l'échelle régionale indique que les plutons qui se trouvent dans la partie située le plus à l'est de la région de la carte atteignent une profondeur maximale d'environ 3 km. La composition et la texture de chaque pluton est relativement homogène par rapport à la gamme totale des types de roches granitiques. De plus, les contacts entre les plutons sont invariablement intrusifs chaque fois qu'ils se manifestent en affleurement. Ainsi, le terme «pluton» utilisé dans le présent bulletin, se rapporte à un massif de roches granitiques dont la lithologie diffère de celle des roches avoisinantes et semble représenter une seule montée de magma (liquide plus cristaux) au niveau actuel d'affleurement. Les 30 plutons ont été regroupés en six unités cartographiques selon leur âge et leur lithologie. On pense que ces six unités représentent une mise en place séquentielle d'au moins six lots de magma granitique dans la croûte supérieure, dont chacun a donné naissance à plus d'une intrusion. Toutefois, la présence de monazites d'âges radiométriques (couple $^{207}Pb/^{235}U$) concordants à presque concordants pour trois plutons porte à croire que la plupart et peut-être toutes les roches granitiques se sont cristallisées il y a entre 371 et 373 Ma. Cette courte période de temps suppose que des magmas attribués à différentes unités coexistaient probablement lors de la mise en place.

Les roches granitiques sont constituées uniquement de cinq minéraux importants, à savoir du quartz, des plagioclases, de la microcline, de la biotite et de la muscovite. Des phases secondaires communes comprennent du zircon, de la monazite, du grenat, de l'ilménite, de l'apatite, de la tourmaline et probablement de la cordiérite pseudomorphosée par de la smectite. Du spinelle d'apparence

plutons. The granitic rocks range from biotite-muscovite granodiorite to muscovite-biotite granite. Overall, they appear to be more enriched in muscovite and depleted in biotite than similar rocks farther west in the Meguma Terrane (e.g. the South Mountain Batholith). Plagioclase varies from An_{29} to An_0 with the more calcic compositions occurring in rocks with higher biotite contents.

The granitic rocks have been variably deformed within about 9 km of the northern margin of the eastern Meguma Terrane. As a result, all gradations between virtually undeformed granite and true mylonite with well-developed S-C fabric are present. Although the undeformed varieties have typical granitoid textures in hand specimen, textural evidence in thin section indicates extensive subsolidus recrystallization has occurred that is more extensive than is common for similar rocks farther west in the South Mountain Batholith. In areas transitional between undeformed and deformed granitic rocks, the time relationship between these subsolidus minerals and regional metamorphic fabrics implies that this subsolidus recrystallization probably closely followed magmatic crystallization at near-magmatic temperatures.

Chemistry. The tonalite plutons are enriched in Ca, Fe and Mg relative to granitic plutons in the same area. Compositions of individual samples are variable, reflecting the large range in modal contents of hornblende, biotite and muscovite. All of the tonalite plutons are peraluminous, containing 1.3 to 2.9% normative corundum. Bivariate elemental plots reveal that the tonalite plutons do not lie on the same trend lines defined by granitic plutons for some elements, although the amount of scatter in the data makes this interpretation questionable. Initial $^{87}Sr/^{86}Sr$ ratios, calculated using the U-Pb monazite age of 378 Ma, range from 0.706 to 0.707.

The granitic plutons have a restricted compositional range, containing 70.6 to 75.5% SiO_2 and 0.1 to 0.8% MgO. The chemical homogeneity of each pluton implies that average pluton compositions approximate magma compositions (i.e. melt plus crystals) emplaced at the current level of exposure. All of the granitic intrusions are peraluminous with normative corundum varying between 1.5 and 4.8%. Inter-element correlation is good for some pairs (e.g. FeO and MgO) and poor for others (e.g. Al_2O_3 and MgO). Furthermore, no simple correlation exists between the degree of differentiation of each pluton and its relative age of intrusion. Rare-earth element patterns are characterized by strong negative europium anomalies and moderate to strong enrichment in light rare-earth elements. Total rare-earth element contents tend to increase with increasing degree of felsicity. The

magmatique a été trouvé dans une lame mince et de la sillimanite à l'état de subsolidus est commune dans plusieurs plutons. La composition des roches granitiques varie de la granodiorite à biotite et muscovite à du granite à muscovite et biotite. Dans leur ensemble, ces roches semblent être plus riches en muscovite et moins riches en biotite que des roches similaires se trouvant plus à l'ouest dans le terrane de Meguma (par exemple le batholite de South Mountain). Les plagioclases varient de An_{29} à An_0, les plus calciques se trouvant dans des roches à teneur plus élevée en biotite.

Les roches granitiques ont été plus ou moins déformées dans un rayon d'environ 9 km de la bordure septentrionale de la partie est du terrane de Meguma. On trouve, par conséquent, toutes les variétés entre un granite presque non déformé et une vraie mylonite qui se caractérise par une fabrique S-C bien représentée. Bien que les variétés non déformées présentent des textures granitoïdes caractéristiques dans un échantillon, la texture observée dans une lame mince indique qu'il y a eu une importante recristallisation à l'état subsolidus, recristallisation plus importante que ce qui est habituel pour des roches similaires situées plus à l'ouest dans le batholite de South Mountain. Dans les secteurs de transition situés entre des roches granitiques non déformées et des roches granitiques déformées, la relation temporelle entre ces minéraux à l'état subsolidus et les fabriques métamorphiques régionales suppose que cette recristallisation à l'état subsolidus a probablement suivi de très près la cristallisation magmatique et qu'elle s'est effectuée à des températures proches de celle du magma.

Chimie. Les plutons de tonalite sont riches en Ca, en Fe et en Mg par rapport aux plutons granitiques du même secteur. Les compositions des différents échantillons sont variables, reflétant ainsi la grande variété en teneurs modales de la hornblende, de la biotite et de la muscovite. Tous les plutons de tonalite sont hyperalumineux, renfermant de 1,3 à 2,9 % de corindon normatif. Des courbes des éléments à deux variables révèlent que les plutons de tonalite ne se trouvent pas sur les mêmes lignes de tendance définies par des plutons granitiques pour certains éléments, bien que la dispersion des données rende cette interprétation douteuse. Des rapports initiaux $^{87}Sr/^{86}Sr$, calculés à partir de l'âge radiométrique (couple U-Pb) de 378 Ma de la monazite, varient de 0,706 à 0,707.

Les plutons granitiques ont une composition qui varie trés peu et renferment de 70,6 à 75,5 % de SiO_2 et de 0,1 à 0,8 % de MgO. L'homogénéité chimique de chaque pluton suppose que les compositions moyennes des plutons sont proches de celles des magmas (c'est-à-dire liquide plus cristaux) mis en place au niveau actuel de l'affleurement. Toutes les intrusions granitiques sont hyperalumineuses, où le corindon normatif varie de 1,5 à 4,8 %. La corrélation entre les éléments est bonne pour certaines paires (p. ex. FeO et MgO) et mauvaise pour d'autres (p. ex. Al_2O_3 et MgO). De plus, il n'existe aucune corrélation simple entre le degré de différenciation de chaque pluton et son âge relatif d'intrusion. Les structures des terres rares sont caractérisées par de fortes anomalies négatives de l'europium et par un enrichissement modéré à fort en terres rares légères. Les teneurs totales en terres rares ont tendance à augmenter avec le degré felsitique observé. Les plutons possèdent un grand

plutons have many but not all of the characteristics of S-type granites. For example, they have high normative corundum, restricted compositional range and contain Al-rich minerals such as muscovite, garnet and cordierite(?). On the other hand, compared to S-type granites in the Lachlan fold belt in southeastern Australia, granitic plutons in the eastern Meguma Terrane have relatively high Na_2O contents (2.9 to 5.2%) and low initial $^{87}Sr/^{86}Sr$ ratios of 0.703 to 0.709 (calculated using the U-Pb monazite age of 372 Ma).

Tectonic history. Deformation and metamorphism are assigned to three main events (D_1, D_2 and D_3) which together represent continuous or nearly continuous tectonism from early Devonian (D_1–ca. 410 Ma) to early Carboniferous (D_3–350-360 Ma). D_1 structures are difficult to recognize because of the overprinting effects of younger deformation. Limited field evidence suggests that regional stratigraphic repetition is the result of subhorizontal, east-trending D_1 synclines and anticlines which are correlative with similar structures farther west in less deformed parts of the Meguma Terrane. D_2 involved a complex series of progressive phases of deformation associated with dextral transcurrent movements along the Cobequid-Chedabucto Fault System. D_2 strain was heterogeneous in space and time. As a result, strongly mylonitic rocks are concentrated in narrow east-trending bands bounded north and south by less deformed rocks. Deformation became increasingly more brittle and localized as D_2 progressed, culminating in the development of a Riedel shear package of transcurrent faults and brittle-ductile shear zones along the northern boundary of the terrane. The brittle end-stages of D_2 passed into D_3 with the formation of discrete normal and left-lateral faults which affected both the Meguma Terrane and the early Carboniferous rocks.

Although evidence is scanty, regional metamorphism seems to have attained upper greenschist to lower amphibolite facies conditions during D_1. As D_1 progressed into D_2, deformation became more localized adjacent to the Cobequid-Chedabucto Fault System and temperature increased. The tonalite plutons (ca. 378 Ma) appear to have been emplaced during the initial stages of D_2. Regional metamorphism culminated during widespread emplacement of granitic intrusions at about 372 Ma with the development of middle amphibolite facies assemblages. Mineral equilibria indicate that the granitic plutons were intruded at depths of about 10 to 13 km. From that time to the early Carboniferous, temperature gradually decreased as the area was uplifted and eroded to near-surface conditions.

nombre de caractéristiques des granites du type S, mais pas toutes. Ces derniers présentent par exemple une teneur élevée en corindon normatif et une composition très peu variée, et renferment des minéraux riches en aluminium comme la muscovite, le grenat et la cordiérite (?). Par contre, en les comparant aux granites de type S de la zone de plissements de Lachlan située dans la partie sud-est de l'Australie, les plutons granitiques de la partie est du terrane de Meguma ont des teneurs relativement élevées en Na_2O (de 2,9 à 5,2 %) et des faibles rapports initiaux $^{87}Sr/^{86}Sr$ de 0,703 à 0,709 (calculés à partir de l'âge radiométrique U-Pb de 372 Ma de la monazite).

Tectonique. On attribue les déformations et le métamorphisme à trois principaux évènements (D_1, D_2 et D_3) qui représentent des événements tectoniques continus ou presque continus, allant du Dévonien inférieur (D_1 – ca 410 Ma) au Carbonifère inférieur (D_3 – 350 à 360 Ma). Les structures de l'évènement D_1 sont difficiles à reconnaître à cause des effets de superposition de déformations plus récentes. Des observations limitées sur le terrain semblent indiquer que la répétition de la stratigraphie régionale est le résultat de synclinaux et d'anticlinaux subhorizontaux, de direction est de l'évènement D_1, qu'on peut corréler avec des structures similaires situées plus loin à l'ouest dans des zones moins déformées du terrane de Meguma. L'évènement D_2 comprenait une série complexe de phases progressives de déformation associées à des mouvements dextres transversaux le long du système de failles de Cobequid-Chedabucto. Les déformations survenues au cours de l'évènement D_2 sont hétérogènes dans l'espace et dans le temps. Cela a eu pour résultat la concentration de roches fortement mylonitiques dans des bandes étroites de direction est, bordées au nord et au sud par des roches moins déformées. Les déformations deviennaient de plus en plus fragiles et localisées à mesure que l'évènement D_2 progressait, se terminant par la formation de l'ensemble du cisaillement de Riedel constitué de failles transversales et de zones de cisaillement fragiles et ductiles le long de la limite nord du terrane de Meguma. Les étapes finales fragiles de l'évènement D_2 ont été suivies dans l'évènement D_3 par la formation de failles distinctes, normales, sénestres et latérales qui ont modifié le terrane de Meguma et les roches du Carbonifère inférieur.

En dépit du peu de données établissant le fait, il semble que le métamorphisme régional ait atteint le niveau de faciés supérieur des schistes verts au faciés inférieur des amphibolites pendant l'évènement D_1. À mesure que l'évènement D_1 se transformait en évènement D_2, les déformations se localisaient devenant adjacentes au système de failles de Cobequid-Chedabucto, et la température augmentait. Les plutons de tonalite (ca 378 Ma) semblent avoir été mis en place pendant les étapes initiales de l'évènement D_2. Le métamorphisme régional a atteint son paroxysme pendant la mise en place générale des intrusions granitiques, il y a environ 372 Ma, avec la formation d'assemblages de faciés intermédiaires des amphibolites. Les équilibres des minéraux indiquent que l'intrusion des plutons granitiques a commencé à des profondeurs d'environ 10 à 13 km. Depuis ce moment et jusqu'au Carbonifère inférieur, la température a diminué progressivement à mesure que la région se soulevait et s'érodait jusqu'aux conditions actuelles près de la surface.

Petrogenesis. The high K, Rb and normative corundum contents and high initial $^{87}Sr/^{86}Sr$ ratios of the tonalite plutons imply involvement of continental crust in their generation. Thus, the tonalite plutons could have formed by crustal contamination of basaltic magma generated in the upper mantle or by partial melting of intermediate to mafic rocks in the lower continental crust. The tonalite and granitic plutons represent two separate magmatic events because of their significant differences in composition, age, aerial abundance and zircon morphology.

The granitic plutons formed by sequential intrusion of separate pulses of magma. The compositions of some dykes and smaller plutons can be attributed to local fractional crystallization based on least-squares mass balance calculations. However, the lack of simple correlation between pluton chemistry and relative age and the large range in initial $^{87}Sr/^{86}Sr$ ratios imply that most of these magmas were not the result of simple in situ fractionation. Instead, a supply of magma that varied irregularly in time must have been available below the current level of exposure. The most plausible mechanism would involve more or less simultaneous generation of two or more independent batches of magma in a heterogenous source. Although other process such as restite unmixing, volatile transfer and assimilation may have played some part in this process, the data suggest that they were relatively unimportant. The highly felsic, peraluminous compositions favour a source composed of quartzofeldspathic rocks containing some proportion of peraluminous material. The low initial $^{87}Sr/^{86}Sr$ ratios compared to most S-type granites suggest that the source was low in Rb and/or had a short residence time in the crust.

The tonalite and granitic plutons were emplaced syntectonically during the early stages of ductile shearing associated with dextral transcurrent movements along the Cobequid-Chedabucto Fault System. The presence of tonalite, which has liquidus temperatures on the order of 1000-1100°C, indicates that mafic magma was involved in some way, either by supplying heat or by giving rise to the tonalite plutons more directly. Thus, crustal thickening during Devonian continental collision, augmented by underplating or uprise of mafic magma, is thought to be the most likely source of heat for generation of the granitic magmas. The peak in regional metamorphism appears to have been caused by widespread intrusion of the granitic magmas into crust that was already preheated. This event of thickening and thermal expansion led to immediate uplift and erosion with the consequent removal of about 10-13 km of crustal material by the early Carboniferous.

Pétrogenèse. Les teneurs élevées en K, en Rb et en corindon normatif, ainsi que les rapports élevés initiaux $^{87}Sr/^{86}Sr$ des plutons de tonalite supposent l'intervention de la croûte continentale dans la formation de ces derniers. Ainsi, les plutons de tonalite peuvent avoir été formés par la contamination par la croûte d'un magma basaltique généré dans le manteau supérieur ou par la fusion partielle de roches neutres à mafiques au sein de la croûte continentale inférieure. Les plutons de tonalite et les plutons de granite représentent deux évènements magmatiques distincts à cause des grandes différences dans leur composition, leur âge, leur abondance en surface et la morphologie de leurs zircons.

Les plutons granitiques ont été formés par une intrusion séquentielle de montées distinctes de magma. Les compositions de certains dykes et de plutons plus petits peuvent être attribuées à une cristallisation fractionnée locale fondée sur des calculs du bilan massique par la méthode des moindres carrés. Le manque de corrélation simple entre la chimie et l'âge relatif des plutons, ainsi que la grande variété des rapports initiaux $^{87}Sr/^{86}Sr$ supposent, toutefois, que la plupart de ces magmas n'étaient pas le résultat d'un fractionnement simple in situ. Au lieu de cela, un apport de magma variant irrégulièrement avec le temps, devait exister au-dessous du niveau actuel d'affleurement. Le mécanisme le plus plausible devrait comporter la formation plus ou moins simultanée d'au moins deux lots indépendants de magma dans une source hérétogène. Bien que d'autres processus comme l'exsolution de restites, l'assimilation et le transfert de matières volatiles aient pu jouer un rôle dans ce processus, les données semblent indiquer que ces processus étaient relativement peu importants. L'abondance en roches felsiques et hyperalumineuses soutient la théorie d'une source constituée de roches quartzo-feldspathiques renfermant une certaine proportion de matériaux hyperalumineux. Les faibles rapports initiaux $^{87}Sr/^{86}Sr$, par rapport à la plupart des granites de type S, laissent supposer que la source contenait peu de Rb et a eu un temps de séjour court dans la croûte.

Les plutons de tonalite et les plutons de granite ont été mis en place syntectoniquement pendant les premières phases du cisaillement ductile, associé à des mouvements transversaux dextres le long du système de failles de Cobequid-Chedabucto. La présence de la tonalite, à température à l'état liquidus de l'ordre de 1000 à 1100°C, indique qu'un magma mafique était présent d'une façon ou d'une autre, soit en fournissant de la chaleur, soit en donnant naissance aux plutons de tonalite d'une façon plus directe. On pense donc que l'épaississement de la croûte pendant la collision continentale du Dévonien, accru par le sous-charriage d'une plaque sous-jacente ou une montée du magma mafique, est la source la plus probable de chaleur à l'origine de la formation de magmas granitiques. Le maximum du métamorphisme régional semble avoir été produit par l'intrusion générale de magmas granitiques dans la croûte qui était déjà préchauffée. Cet épisode d'épaississement et de dilation thermique a été à l'origine du soulèvement et de l'érosion immédiats, suivis de l'enlèvement d'environ 10 à 13 km de matériau crustal dès le début du Carbonifère.

Economic potential. Gold in the Meguma Group continues to provide the highest economic potential in the eastern Meguma Terrane. Only very minor showings of beryl and sulphide minerals were found in a few of the granitic plutons. However, three muscovite-rich, albite-bearing granitic plutons are enriched in Sn and F and are similar in composition to the granite which hosts the East Kemptville tin mine in the southwestern part of the terrane. These plutons may offer the best targets for future mineral exploration.

Possibilités économiques. L'or du groupe de Meguma continue de présenter les meilleures possibilités économiques de la partie est du terrane de Meguma. On n'a trouvé que de très petites manifestations de béryl et de minéraux sulfurés dans quelques-uns des plutons granitiques. Trois plutons granitiques riches en muscovite et en albite sont toutefois riches en Sn et F et présentent une composition similaire à celle du granite où se trouve la mine d'étain d'East Kemptville, située dans la partie sud-ouest du même terrane de Meguma. Ces plutons peuvent offrir les meilleures cibles pour une prospection ultérieure.

INTRODUCTION

General statement

This project was undertaken to gain a better understanding of the petrology, tectonic history, and economic potential of Devonian granitoid plutons and their country rocks in the eastern Meguma Terrane of Nova Scotia. Mid-Paleozoic peraluminous granitoid rocks form a minor but widespread component of the Appalachian orogen (see summary by Pitcher, 1982). However, the Meguma Terrane is unique in that all of its plutonic rocks are peraluminous. Largely ignored prior to 1974, these intrusions have been the subject of numerous recent studies concerning their petrogenesis and age relationships. This work, as well as the current project, has been stimulated both by worldwide interest in peraluminous granitic rocks (e.g., Chappell and White, 1974) and by recent discoveries of tin and uranium mineralization in the South Mountain batholith in Nova Scotia (e.g., Chatterjee and Muecke, 1982).

Two segments of the eastern Meguma Terrane were selected for study – the Canso and Forest Hill areas (Fig. 1). Until now, granitoid plutons in both map areas had not been examined in detail. Intrusions situated between the Canso and Forest Hill areas are the subjects of recent M.Sc. theses (Ham, 1988; O'Reilly, 1988). The Canso area (about 210 km^2; Fig. 2, in pocket) encompasses all of the Cape Canso peninsula east of longitude 61°13′W. Access to parts of the interior is provided by three paved highways leading to the town of Canso and the villages of Dover and Whitehead. About 200 islands and most of the coastline can be reached only by boat. Fog, rolling swells from the open ocean, and lack of good landing sites make it difficult and sometimes dangerous

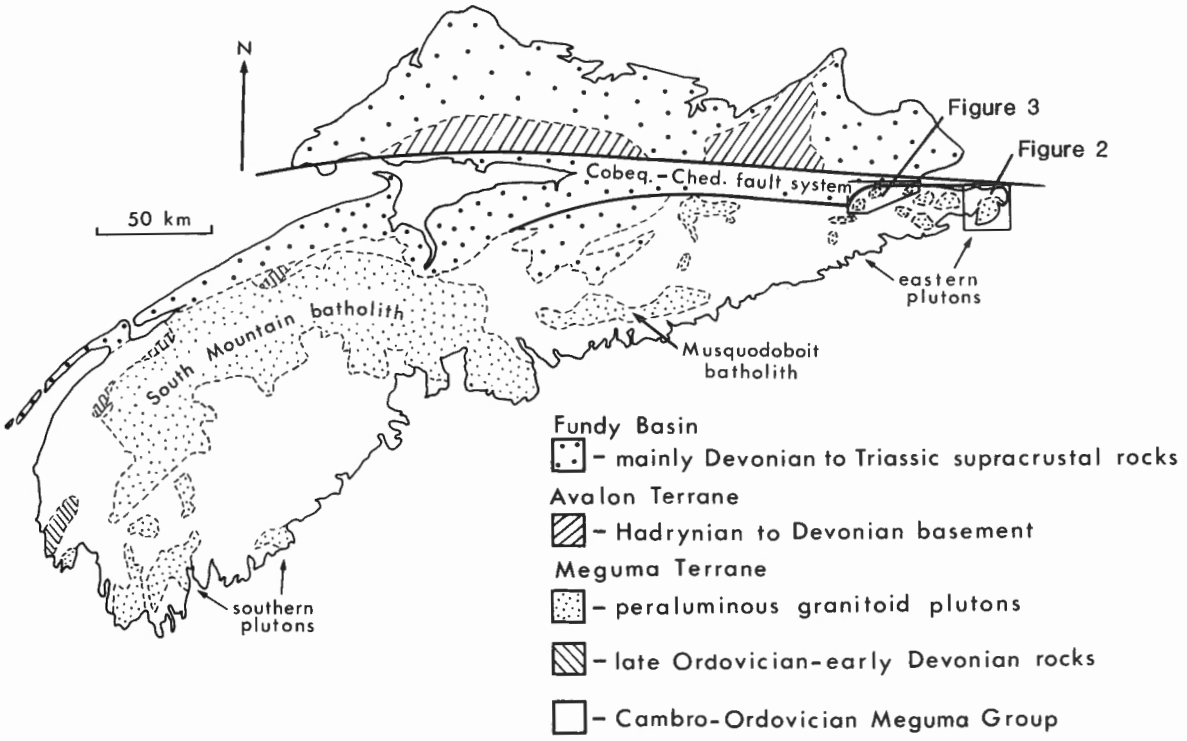

Figure 1. Simplified geological map of mainland Nova Scotia. The Canso (Fig. 2, in pocket) and Forest Hill (Fig. 3, in pocket) areas are outlined.

to reach exposed coastal sections, especially on the outer islands, many of which are bare rock. Mapping these places was done between 15 July and 15 August when the ocean was relatively calm. The Forest Hill area (about 300 km^2; Fig. 3, in pocket) is irregularly shaped and includes all granitoid plutons between Country Harbour and the town of Guysborough. Access is provided by several paved and gravel highways as well as numerous logging roads and trails. No communities lie within the map area. However, an underground gold mine is currently being developed at Forest Hill (production suspended in 1989) by Westminer Canada Limited.

The eastern Meguma Terrane is characterized by a rolling peneplain that slopes gently southeast toward the Atlantic Ocean. With maximum elevations of 110 m in the Canso area and 200 m in the Forest Hill area, relief is minimal except along the partly eroded, east-trending escarpment of the Guysborough County fault in the northern part of the latter area. Bedrock exposure is highly variable. Magnificent outcrops, which are clean and almost continuous along the Canso area shoreline, diminish in both quality and quantity inland. Granitoid plutons are relatively well exposed, especially in barrens in the southern part of the Canso area, whereas metasedimentary rocks are poorly exposed. The Forest Hill area is covered by a thick mantle of glacial drift and is heavily forested. As a result, outcrops are exceedingly sparse, except along some streams and in exploration trenches at Forest Hill mine site.

All fieldwork was carried out using colour aerial photographs at a scale of 1:10 000 supplied by Maritime Resource Management Service of Amherst, Nova Scotia. The Canso area was mapped from 20 May to 15 September in 1985 and 17 July to 8 August in 1986. Most time was spent along the coast, more than 90% of which was examined in person, because of superb bedrock exposure, much of which had not been previously studied. Inland traverses, which were geologically much less rewarding, were confined to roads, trails, power lines, streams, lake shores, and well-exposed barrens. The Forest Hill area was mapped from 2 June to 16 July and 9 August to 2 September in 1986. Virtually all of the roads, trails, and power lines and most of the streams were followed in a sometimes futile search for outcrops. Cross-country traverses were used only where necessary to fill in gaps in the geological data base.

The geology of the Canso and Forest Hill areas (Fig. 2, 3, in pocket) is shown at 1:50 000 scale. Individual outcrops are plotted and traverse lines lacking outcrops are indicated. Outcrop data recorded by earlier workers are marked with a different symbol and used wherever they are available and important. All occurrences of significant metamorphic minerals are plotted as well.

Previous work

The first significant geological work in the eastern Meguma Terrane involved regional mapping by Faribault (1893a,b,c) at a scale of 1 inch to 1 mile between 1882 and 1886. Faribault, like most subsequent workers, concentrated on the Meguma Group because of the common occurrence of gold mineralization. More recently, the Canso area was remapped by Weeks (1960) and Stevenson (1964) at the same scale. Schiller (1961, 1963) remapped the Forest Hill area as part of a Ph.D. study.

The Meguma Group has received considerable attention since the late 1800s by companies exploring for gold and base metals. Several small gold mines have operated at various places and times near Forest Hill and Country Harbour Mines in the Forest Hill area. Some exploration for copper and tungsten, including diamond drilling, has been carried out along the north shore of the Canso area since 1950. In addition, andalusite schist from Doughboy Point and Black Point was tested as a possible source of aluminum. Information on these and other mineral showings in the eastern Meguma Terrane is available in the assessment files of the Nova Scotia Department of Mines and Energy in Halifax.

More detailed work on specific geological problems has been done by various people in the last 30 years. Schiller (1959) studied the petrography of the andalusite schist belt north of Whitehead. Nichols (1976) and Poole (1984) completed B.Sc. theses on the structure and metamorphism of the Halifax Formation in the same area. The structural evolution of rocks at the east end of Durells Island has been described by Keppie (1985). During the current project, a B.Sc. thesis on the structure of two small areas north and east of Whitehead was done by Eddy (1987). More detailed structural studies have been completed by Mawer and Williams (1986) in the Canso area and by Haynes et al. (1986) in the Forest Hill area. The relationships between geology and lineaments defined on Landsat and aeromagnetic images of the Forest Hill area have been examined by Harmeson (1986). Shaw (1983) studied the Lazy Head tungsten showing on the north shore of the Canso area. The granitoid plutons have been largely ignored. However, McKenzie and MacGillivary (1974) briefly described and sampled several plutons in the eastern Meguma Terrane. An $^{40}Ar/^{39}Ar$ age was determined on pegmatite collected south of Whitehead by Reynolds et al. (1981). Ford and Ballantyne (1983) have studied the lithogeochemistry and U-Th distribution patterns in granitoid rocks throughout the eastern Meguma Terrane.

Preliminary reports on the current project have been given by Hill (1986, 1987a,b), Hill and Raeside (1988), and Raeside et al. (1988).

Acknowledgments

This project is part of the Canada – Nova Scotia Mineral Development Agreement of 1984-89. Able assistance in the field was provided by J.M. Hill (1985) and B.G. Eddy (1986). Additional information on the geology of the area around the Forest Hill mine site was kindly provided by K.D. Adams of Westminer Canada Limited.

Several people have contributed to various aspects of the research. T.E. Krogh of the Royal Ontario Museum

in Toronto completed all the U-Pb isotope work. V.R. Slaney and P.H. McGrath of Geological Survey of Canada provided computer-enhanced images of airborne radiometric and gradiometer data respectively. J.H. Maley of Geological Survey of Canada supplied the computer program which was used to plot equal-area stereographic projections of structural data. Computer modelling of regional gravity data was done by M.D. Thomas, and Rb-Sr isotopic analyses were done by R.G. Theriault, both of Geological Survey of Canada. R.P. Raeside of Acadia University undertook a preliminary study of metamorphic mineral compositions and paleotemperatures in the Canso area.

Discussions with C.R. van Staal, G.M. Yeo, and F.W. Chandler have resulted in numerous improvements to the manuscript. The final version has been critically reviewed by K.L. Currie.

GEOLOGICAL SETTING

General statement

All the Canso area and most of the Forest Hill area lie within the Meguma Terrane (Williams and Hatcher, 1982), a 33 000 km^2 belt of rocks forming the southern half of mainland Nova Scotia (see Fig. 1). The Meguma Terrane is composed mainly of the Meguma Group, a thick sequence of folded and metamorphosed clastic sedimentary rocks, intruded by numerous granitoid plutons. Its northern boundary is marked by the east-trending transcurrent Cobequid-Chedabucto fault system, believed to represent a major break between the allochthonous Meguma Terrane to the south and the Avalon Terrane to the north (Schenk, 1975, 1978). The northwestern margin of the Forest Hill area is underlain by variably deformed supracrustal cover rocks of probable Devono-Carboniferous age, part of the larger Fundy Basin (as defined by Webb, 1969). Fundy Basin strata cover much of the Avalon Terrane and overstep parts of the Meguma Terrane and the Cobequid-Chedabucto fault system.

Meguma Group

The Meguma Group, which is deformed and metamorphosed from lower greenschist to middle amphibolite grade, is traditionally divided into an older psammitic Goldenville Formation and a younger pelitic Halifax Formation. The Meguma Group appears to be Cambro-Ordovician in age (e.g., Cumming, 1985) and has a minimum thickness of about 10-14 km (e.g., Schenk, 1970). It is generally believed to have formed by turbidite deposition in a relatively deep, continental rise, marine environment (Schenk, 1970; Waldron, 1987) derived from a source in western Europe or northwestern Africa (Schenk, 1978). Seismic data suggest that it was deposited on continental rather than oceanic crust (Dainty et al., 1966).

The Goldenville Formation consists of quartz, feldspathic and lithic wacke interbedded with minor shale and has a sandstone to shale ratio of about 20-40:1 (Schenk, 1970). Less common lithologies include secondary concretions of ferruginous and manganiferous carbonate and very rare, thin beds of polymictic and intraclastic conglomerate (e.g., Smith, 1981). Sandstone beds are typically massive and 1-20 m thick. Subdivision of the Goldenville Formation has proved difficult because of lithological homogeneity and the lack of fossils. However, Waldron (1987) has stated that the uppermost 1 km or so is more thinly bedded and contains more shale than the bulk of the Goldenville Formation. The base of the formation has not been observed.

The Halifax Formation is mainly pelitic with a shale to sandstone ratio of about 1-5:1. The dominant lithology is black shale interbedded with pyritic sandstone and cross-laminated siltstone. Black shale may either overlie (McBride, 1978) or underlie (O'Brien, 1986) grey shale. Beds are usually less than 1 m thick. Although regional stratigraphic subdivision of the Halifax Formation has not been attempted, local subdivision based on colour, the presence or absence of porphyroblasts, and other criteria is possible.

Although the contact between the Goldenville and Halifax formations is abrupt at map scale in most places, the two may be partly coeval (Schenk, 1970, 1975). The transition zone is commonly marked by a rapid upward decrease in sandstone to shale ratio over a stratigraphic height of a few metres (Smith, 1981; Waldron, 1987). The boundary may be more complex in the Mahone Bay area where O'Brien (1986) has recognized a 1-2 km thick transition zone of thinly bedded sandstone and shale, which he informally named the Green Bay formation. Waldron (1987) has argued for the retention of the traditional bipartite division into the Goldenville and Halifax formations. The upper 150-300 m of the Green Bay formation (Moshers Island member) appear to be geochemically anomalous, being enriched in Mn, Ba, Cu, Pb, and Zn compared to other parts of the Meguma Group (Zentilli et al., 1986).

The Halifax Formation is overlain by the White Rock, Kentville, New Canaan, and Torbrook formations along the northwestern margin of the Meguma Terrane (see Fig. 1). They form a folded sequence of shallow marine sedimentary and volcanic rocks ranging from late Ordovician or early Silurian to early Devonian in age. These rocks form an apparently conformable succession, at least in part, although the Halifax-Kentville contact may be marked locally by an angular unconformity (see Keppie, 1977).

Granitoid plutons

The Meguma Terrane is intruded by numerous granitoid plutons, which are remarkably homogeneous in composition considering their large areal extent. Except for minor tonalite, they are composed of only five essential minerals: quartz, plagioclase, alkali feldspar, biotite, and muscovite. The occurrence of accessory phases such as cordierite, andalusite, garnet, and tourmaline and the

ubiquitous presence of normative corundum attest to peraluminous compositions. Although most of the plutons are relatively pristine, some of those in the southwestern Meguma Terrane and those near the Cobequid-Chedabucto fault system in the eastern Meguma Terrane are deformed and possess well developed tectonic fabrics.

The intrusions can be divided into four local groups, each of which has distinguishing characteristics; namely the South Mountain batholith, Musquodoboit batholith, southern plutons, and eastern plutons (see Fig. 1). The South Mountain batholith is composed of numerous separate intrusions, the dominant lithologies of which are biotite granodiorite and biotite-muscovite granite (Clarke et al., 1985; MacDonald and Horne, 1986). It is generally massive, discordant to the country rocks, and has a well developed contact aureole that overprints regional Acadian metamorphic mineral assemblages. The Musquodoboit batholith is a poorly exposed body of 80-90% porphyritic muscovite-cordierite-biotite granite intruded by small masses and dykes of biotite-muscovite granite (MacDonald and Clarke, 1985). It appears to have been emplaced by passive stoping and clearly truncates regional Acadian folds. The southern plutons consist of several discrete intrusions separated by screens and larger areas of Meguma Group (Albuquerque, 1977; Rogers, 1986). They are composed mainly of biotite-muscovite granite and lesser amounts of granodiorite, tonalite, and more mafic rocks, many having a tectonic foliation. The eastern plutons, consisting of numerous separate intrusions some of which are composite, are made up almost entirely of biotite-muscovite granite, except for a few small bodies of granodiorite and tonalite.

Rb-Sr whole-rock isochron and $^{40}Ar/^{39}Ar$ mineral plateau dates suggest that most of the granitoid rocks in the Meguma Terrane crystallized at about 370 ± 10 Ma (Reynolds et al., 1981; Clarke and Halliday, 1980). However, Ordovician and Carboniferous ages have been determined for three of the southern plutons. These ages include a preliminary Rb-Sr isochron date of 466 ± 17 Ma for the Shelburne granite (Rogers, 1986), a U-Pb zircon age of 451 ± 11 Ma for the Brenton pluton (Krogh, cited in Rogers, 1986), and a U-Pb zircon date of 313 ± 3 Ma for the Wedgeport pluton (Keppie et al., 1983).

Fundy Basin

The Fundy Basin is mainly filled with a thick sequence of shallow marine and continental sedimentary and volcanic rocks ranging in age from middle Devonian to Triassic (Webb, 1969). Deposition was apparently confined to a series of fault-controlled intermontane basins extending from the Bay of Fundy to western Newfoundland. Episodic block faulting and subsidence probably accompanied deposition throughout the late Paleozoic and early Mesozoic (Howie and Barss, 1974; Keppie, 1977). The rocks vary from almost undeformed to strongly folded and deformation is most intense along faults and close to the margins of the Fundy Basin. They unconformably overlie most of the Avalon Terrane and part of the northern Meguma Terrane in Nova Scotia (see Fig. 1).

The base of the Fundy basin succession is made up of middle to late Devonian molasse redbeds and intercalated subaerial volcanic rocks that are restricted to areas within and north of the Cobequid-Chedabucto fault system. They are overlain by piedmont and fluviolacustrine strata of the late Devonian to early Carboniferous Horton Group. Vertical fault movements during deposition appear to have confined part of the Horton Group to the St. Marys River graben along the northern margin of the Meguma Terrane. The Horton Group oversteps parts of the Cobequid-Chedabucto fault system and locally contains lithic fragments of Goldenville metawacke, Halifax schist, and Meguma Terrane granite (e.g., Benson, 1967). In this regard, the Horton Group provides a younger age limit for at least the initial stages of uplift and erosion of the northern part of the Meguma Terrane.

Summary of tectonic history

The Meguma Terrane appears to be a unique lithologic and tectonic entity in the Appalachian Orogen. It is believed to be allochthonous, accreted to the Avalon Terrane during the Devonian Acadian Orogeny (Schenk, 1970; Keppie, 1985). The boundary between the two terranes is marked by the dextral transcurrent Cobequid-Chedabucto fault system (see Fig. 1). The deformation and metamorphic history of the Meguma Terrane and adjacent Fundy Basin can be divided into three main events (Table 1). These events are inferred, at least in part, to be related to collision of the Meguma Terrane with North America (Keppie, 1983, 1985).

The oldest event recognized (D_1 herein), which is dominant throughout most of the Meguma Terrane, resulted in the formation of kilometre-scale, open to tight, gently plunging anticlines and synclines in the Meguma Group (O'Brien, 1983; Keppie, 1985). A regionally developed slaty to spaced cleavage defined by greenschist grade minerals is associated with the folds. The folds bend from northeast-trending in the southwest Meguma Terrane to east-trending in the northeast, a feature that may be related to subsequent shearing along the Cobequid-Chedabucto fault system (e.g., Mawer and Williams, 1986). This phase of deformation was preceded locally by the formation of monoclinal folds and was followed by the local development of a subhorizontal crenulation cleavage (Keppie, 1983). Subhorizontal crenulation cleavages, which both predate and postdate the slaty cleavage, are developed sporadically in pelitic layers in the Sherbrooke area (e.g., O'Brien, 1983).

A period of low-pressure static metamorphism following D_1 is marked by the growth of decussate porphyroblasts of biotite, cordierite, andalusite, and staurolite that generally overprint the regional tectonic foliation (Keppie, 1985). This event was widespread; it reached amphibolite grade in the easternmost Meguma Terrane (including the Canso and Forest Hill areas) and

Table 1. Simplified sequence of lithological and tectonic events in the eastern Meguma Terrane and adjacent part of the Fundy Basin

Age (Ma)	Period		Lithological record	Tectonism
	Triassic		Supracrustal rocks formed in Fundy Basin	D_3: Faulting and open folding in the Fundy Basin and faulting in the Meguma Terrane
245				
	Permian			
286				
	Carboniferous			
360				
	Devonian	Late	Intrusion of most Meguma Terrane granitoid plutons	D_2: Ductile and brittle deformation caused by movements along the Cobequid-Chedabucto fault zone
		Middle		
		Early		D_1: Regional folding and metamorphism
408	Silurian		Deposition of Meguma Group and Torbrook, New Canaan, Kentville, and White Rock formations	
438	Ordovician			
505	Cambrian			

around the southern granitoid plutons in southwestern Nova Scotia. It began at about the same time or slightly before emplacement of most of the granitoid plutons. Isograds defined by the porphyroblasts are truncated by the Sherbrooke pluton (Smith, 1981), which has been dated at 369 ± 2 Ma (Keppie, 1983).

The structural and metamorphic history of the eastern Meguma Terrane is more complex adjacent to the Cobequid-Chedabucto fault system. There, a broad zone of ductile shear is developed in which older structures are transposed and locally obliterated. This event (D_2 herein) involved a series of overlapping phases of deformation, which was accompanied by static metamorphism and granitoid intrusion (Keppie, 1985; Mawer and Williams, 1986; Hill and Raeside, 1988). Although strain is highly variable, in general it intensifies northward, and for this reason, it has been attributed to movements along the Cobequid-Chedabucto fault system (Keppie, 1985). Kinematic indicators are consistent with dextral subhorizontal shear (Keppie, 1985; Mawer and Williams, 1986). D_2 culminated with localized brittle deformation along discrete segments of the Cobequid-Chedabucto fault system (Mawer and White, 1987).

The last orogenic event is loosely defined to include all Carboniferous and younger tectonism. Referred to as D_3 in this report, it has also been called the Maritime Disturbance by Poole (1976) and the Hercynian Orogeny by Keppie (1985). It appears to have involved low grade metamorphism, folding, and cataclasis in restricted parts of the Fundy Basin and Meguma Terrane. Vertical movements along segments of the Cobequid-Chedabucto fault system appear to have been responsible for localizing deposition of the Horton Group in the St. Mary's graben. In addition, shearing and a thermal disturbance are postulated at 300-320 Ma for parts of southwestern Nova Scotia, based on $^{40}Ar/^{39}Ar$ geochronology (Elias et al., 1987).

General geology of the Canso and Forest Hill areas

Rocks in the Canso and Forest Hill areas can be divided into three lithological age groups: Cambro-Ordovician Meguma Group, Devonian granitoid plutons, and Devono-Carboniferous supracrustal rocks (Table 2). The latter includes probable inliers of mylonite of unknown age. Schiller (1963) reported the existence of a small outcrop of friable, red, calcareous sandstone in the Salmon River bed, 2 km west of the river's mouth, which he correlated with Triassic rocks farther east. This outcrop was not observed during mapping but may have been overlooked because of high water level.

Following Schenk (1970) and Waldron (1987), the Meguma Group is divided into the older Goldenville Formation (unit CO_G) and younger Halifax Formation (unit CO_H), with the boundary mapped at a 1:1 sandstone to shale ratio. The Goldenville Formation is subdivided into two members (units CO_{Ga} and CO_{Gb}) that may be partly time-equivalent; they are not separated by a geological boundary on the maps. The Halifax Formation is subdivided into five lithostratigraphic members (units CO_{Ha} to CO_{He}), the upper three of which are found only in the Canso area. Differences between members have been accentuated by metamorphism.

The granitoid plutons include numerous granitic intrusions (unit D_G) and a few small bodies of tonalite (unit D_T). Plutons in the northern parts of the Canso and Forest Hill areas are deformed and metamorphosed to varying degrees, with textures ranging from a weakly

Table 2. Lithological units in the Canso and Forest Hill areas

AGE	UNIT	DESCRIPTION
Early Carboniferous	Horton Group	
	C_G Gunns Brook fm.	green-grey to red-brown, lithic feldspathic, and minor quartz wacke; conglomerate; rare carbonaceous shale
Middle Devonian to Early Carboniferous	DC_T Tower fm.	maroon to red hematitic quartz arenite; minor siltstone, sedimentary and volcanic-pebble conglomerate
	DC_S Sunnyville fm.	hydrothermally altered, amygdaloidal, plagioclase-phyric basalt
	DC_M Minister Brooks fm.	light to very dark grey, locally graphitic argillite and laminated phyllite; minor metabasalt(?); includes possible outliers of arenite, mudstone and conglomerate.
Pre-Carboniferous	Inliers in unit DC_M	mylonite containing porphyroclasts of plagioclase-biotite-quartz-garnet granofels
Late Devonian	Granitic plutons (D_G)	
	D_{Gf}	medium grained equigranular muscovite leucogranite
	D_{Ge}	coarse grained seriate muscovite-biotite granite
	D_{Gd}	medium grained, equigranular to slightly porphyritic biotite-muscovite granite; D_{Gdl} indicates plutons with <4% biotite
	D_{Gc}	fine grained porphyritic biotite-muscovite granite
	D_{Gb}	very coarse grained seriate muscovite-biotite granite and minor granodiorite
	D_{Ga}	fine- to medium-grained biotite-muscovite leucogranite
Middle Devonian	Tonalite plutons (D_T)	medium grained, locally plagioclase-phyric biotite tonalite (D_{Tb}), hornblende-biotite tonalite (D_{Th}), and migmatitic muscovite-biotite tonalite (D_{Tm})
Cambro-Ordovician	Meguma Group	
	Halifax Fm. (CO_H)	
	CO_{He}	laminated phyllite, minor metawacke
	CO_{Hd}	andalusite schist with coticules
	CO_{Hc}	metawacke, minor phyllite, and coticules
	CO_{Hb}	laminated schist with coticules
	CO_{Ha}	graphite schist interbedded with grey schist and metawacke
	Goldenville Fm. (CO_G)	metawacke; minor metapelite and calc-silicate layers; varies from thickly bedded with <5% metapelite (CO_{Ga}) to thinly bedded with 5-20% metapelite (CO_{Gb}); agmatitic (aCO_G) where intruded by numerous dykes and irregular lenses of granite

defined mica foliation to a mylonitic S-C fabric. For simplicity however, only igneous terminology (Streckeisen, 1976) is used. Unit D_T consists of small tonalite bodies that occur in both map areas, some of which are represented by single outcrops. The unit is subdivided into biotite tonalite (unit D_{Tb}), hornblende-biotite tonalite (unit D_{Th}), and migmatitic muscovite-biotite tonalite (unit D_{Tm}), the relative ages of which are unknown. Granitic plutons (unit D_G) are fairly homogeneous in composition and texture and are composed of biotite-muscovite granite and minor granodiorite. The unit is divided into six (units D_{Ga} to D_{Gf}), based on age relationships, composition, and texture (see Table 2). However, the sequence of emplacement is only partly known. Numerous dykes, sills, and irregular masses of aplitic to pegmatitic leucogranite intrude the Meguma Group in areas adjacent to the plutons.

Mapping was extended 1-2 km north and west of the Meguma Terrane in the Forest Hill area to help determine the movement history along the Guysborough County fault, part of the Cobequid-Chedabucto fault system. This area is underlain by supracrustal rocks belonging to the Fundy Basin. They are divided into the Minister Brook formation (unit DC_M), Sunnyville formation (unit DC_S), Tower formation (unit DC_T), and Gunns Brook formation (unit C_G) using informal names taken from Schiller (1963) and Mooney (1987).

GEOLOGY OF THE COUNTRY ROCKS

Meguma Group

General statement

D_2 deformation and metamorphism have affected the northern parts of both map areas, resulting in diminution of grain size, boudinage of competent layers, formation of well developed tectonic fabrics, and obliteration of primary structures. The least deformed Meguma Group rocks (i.e., those affected mainly by D_1 only) are preserved around the East Branch pluton in the Forest Hill area and on Sheep Island near Whitehead in the Canso area. Most stratigraphic and lithological data described in the following sections are taken from the Canso area where the Meguma Group is locally well exposed.

Goldenville Formation (unit CO_G)

The Goldenville Formation consists of psammite with minor pelite, calc-silicate beds, and rare coticules. It is locally intruded by numerous dykes and lenses of aplitic to pegmatitic leucogranite (correlated with unit D_G), especially near granitoid plutons. Where granite dykes and lenses are particularly abundant, the rocks are mapped as agmatite (unit aCO_G). Inferred structure of the western part of the Canso area is shown in Figure 4. It implies a thickness of about 1800 m for the Goldenville Formation in the core of the Dobsons Lake anticline. This value is very approximate because exposure is inadequate to delineate all folds and faults in that area. Individual rock types are described first as they occur in both members, after which differences between the two members are noted.

The dominant lithology is light to dark grey metawacke, commonly marked by blocky fracturing and a micaceous sheen on cleavage surfaces. It is made up of 40-80% quartz with lesser amounts of plagioclase, muscovite, biotite, and chlorite. Accessory minerals include microcline (up to 5%), garnet, zircon, sphene, fluorite, opaques, tourmaline, rutile, dolomite, and apatite. Grain size is generally 0.01-0.1 mm except in less deformed rocks near the East Branch pluton where angular, unstrained quartz grains up to 1.5 mm in diameter are present (Fig. 5a). Platy to schistose metapelite with 50-80% mica and chlorite is a common but minor lithology in many outcrops. It is locally spotted with 0.3-2 cm long porphyroblasts of staurolite, andalusite, cordierite, and biotite. Meta-arenite containing up to 90% quartz and feldspar occurs in a few places as discontinuous beds up to 10 cm thick.

Fine grained, granoblastic to very weakly schistose calc-silicate layers form up to 10% of some outcrops (Fig. 6a). They contain variable amounts of plagioclase, quartz, amphibole, and biotite and one or more of sphene, garnet, epidote, clinozoisite, apatite, opaques, and clinopyroxene; mineralogical zonation is common. They occur as lensoid beds, 1-25 cm thick, that can only rarely be traced for more than a few metres along strike. However, individual layers of constant thickness can be followed for at least 100 m in exploration trenches at the Forest Hill mine site. Several 1-5 cm thick beds of buff-weathering calc-silicate granofels at Forest Hill were incorrectly described as coticules in an earlier report (Hill, 1987a). A few dark grey to light brown-weathering coticules are present as 1-10 cm thick beds at two localities in the Canso area, 1500 m west of Lazy Head and 1 km west of Fogerty Head. They contain 30-80% fine grained granoblastic garnet, 20-60% quartz, and minor mica and chlorite. They are confined to Goldenville rocks within a few metres of the Goldenville-Halifax boundary.

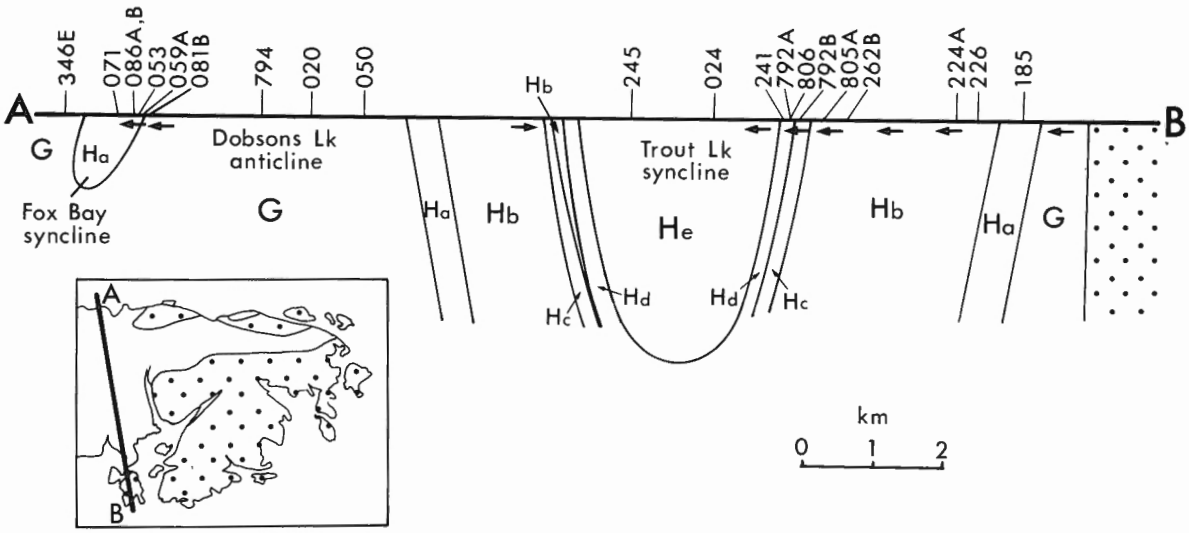

Figure 4. Inferred stratigraphy and macroscopic structure of the Goldenville (CO_G) and Halifax (CO_{Ha}-CO_{He}) formations in the western part of the Canso area. Bold arrows indicate observed younging directions. Numbers are geochemistry samples (Appendix IV) projected onto the cross-section in their approximate stratigraphic positions. Stippled areas are late Devonian granite.

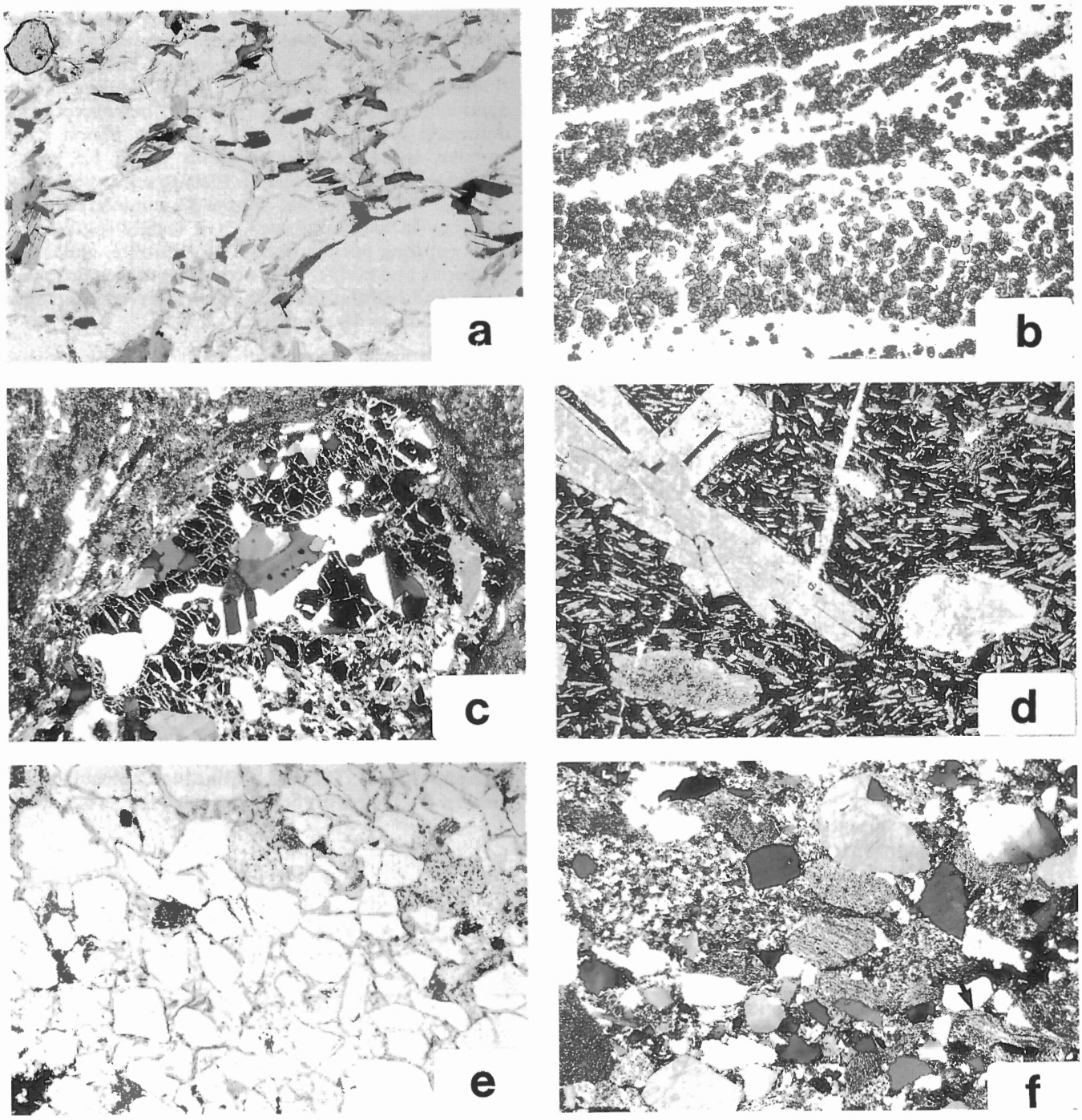

Figure 5. Country rock textures. Field widths (e.g., 3 mm) and light polarization (plane polarized light or crossed nicols) are given in brackets. (a) Relatively undeformed Goldenville metawacke collected just south of the East Branch pluton in the Forest Hill area. Note the large rounded quartz grains, which are only mildly strained and which are absent in mylonitic rocks in areas affected by D_2 farther north (3 mm; ppl). (b) Laminated coticule composed almost entirely of quartz and spessartine garnet. Unit CO_{Hb} at Spears Head, Canso area (4 mm; ppl). (c) Porphyroclast in mylonitic inlier in unit DC_M, composed of unstrained quartz, biotite, and garnet (4 mm; X-nicols). (d) Plagioclase-phyric amygdaloidal basalt from the Sunnyville formation. Note flow fabric defined by plagioclase microphenocrysts (6 mm; ppl). (e) Hematitic quartz arenite from the Tower formation (2 mm; ppl). (f) Lithic wacke from the Gunns Brook formation. Black arrow points to crenulated schist clast believed to have been derived from Meguma rocks deformed by D_2 (6 mm; X-nicols).

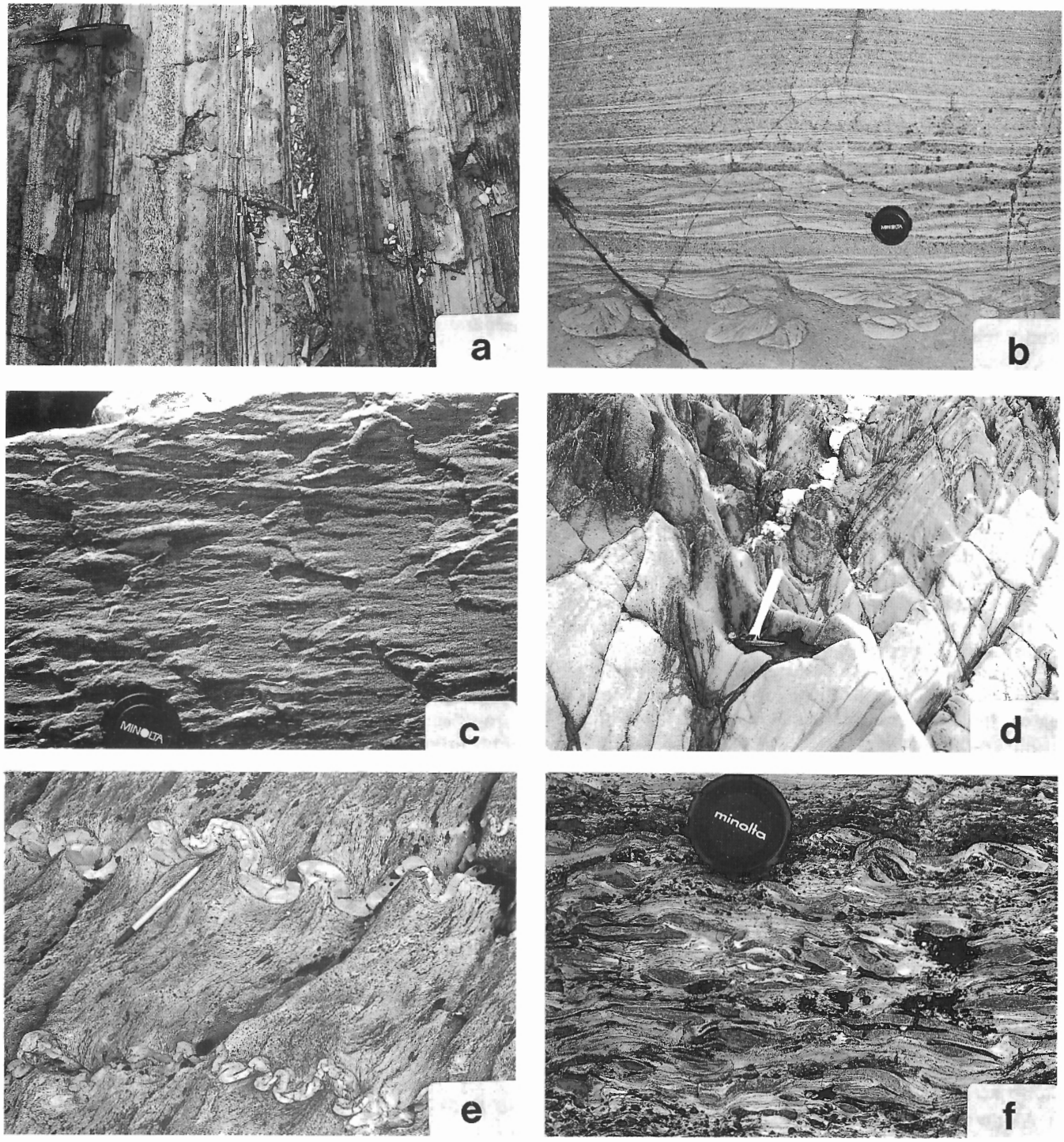

Figure 6. Outcrop features in the Meguma Group. (a) Thinly bedded metawacke, phyllite, and calc-silicate layers (light speckled band to right of hammer head) in unit CO_{Gb} at Forest Hill. GSC 204508-P (b) Cross-laminated psammite with load casts in underlying pelite, unit CO_{Gb}, Sheep Island near Whitehead. GSC 204508-D (c) Flute casts on the basal surface of a psammite bed, unit CO_{Gb}, Sheep Island near Whitehead. GSC 204508-N (d) Interbedded graphite schist (dark) and metawacke in small F_{2b} fold, unit CO_{Ha}, Fox Bay. GSC 204508-M (e) Muscovite-quartz schist with two folded coticule beds in unit CO_{Hb} at Poule Point in the Canso area. GSC 204508-E (f) Nodular coticule bed in unit CO_{Hb} at Poule Point. GSC 204508-A

The Goldenville Formation is subdivided into two members (units CO_{Ga} and CO_{Gb}) on the basis of sedimentary structures and proportion of metapelite. Unit CO_{Ga} is composed of thickly bedded, relatively massive to weakly schistose metawacke containing less than 5% interbedded metapelite and calc-silicate layers. It is best exposed along the north shore of the Canso area. Metawacke beds are typically 1-5 m thick, although beds up to 14 m thick were found in a few places. Bedding is generally weakly developed, being marked by slight differences in composition causing variations in colour, degree of weathering, and intensity of the tectonic fabric. More obvious but much less common bedding features are caused by millimetre-scale laminations and intercalated 1 mm to 1 m thick layers of metapelite.

Unit CO_{Gb} is composed of thinly bedded metawacke with 5-20% metapelite, minor calc-silicate layers, and rare coticules (see Fig. 6a). The best exposures are found on Sheep Island near Whitehead in the Canso area and in exploration trenches at the Forest Hill mine site. Individual beds are commonly 1 cm to 1 m thick, with occasional beds up to 3 m thick. They are characterized by the presence of numerous sedimentary structures that are particularly well displayed on Sheep Island and on islands farther west. These structures include parallel and cross-lamination, load casts (Fig. 6b), grading, slump structures such as intraformational breccia and contorted laminae, flute casts (Fig. 6c), and rip-up clasts of pelite in psammite. Unit CO_{Gb} is restricted to the uppermost 700 m of the Goldenville Formation, a sedimentological feature that has been observed elsewhere in the Meguma Group (Waldron, 1987). In this respect, it is at least partly younger than the more massive metawacke of unit CO_{Ga}. However, 1.6 km west of Fogerty Head on the north shore of the Canso area, massive metawacke lies in direct and apparently conformable contact with grey phyllite of the lowermost Halifax Formation (unit CO_{Ha}), which suggests that units CO_{Ga} and CO_{Gb} are time equivalent in some places.

Goldenville-Halifax transition zone

Although an abrupt contact between relatively massive Goldenville metawacke and Halifax metapelite occurs 1.6 km west of Fogerty Head, a 20-200 m thick transition zone was observed at four other localities in the Canso area as follows:

a) Along the shore 1700 m west of Lazy Head, thinly bedded metawacke intercalated with 10% graphite schist, 5% grey schist, and 1% coticule lies immediately south of the Halifax Formation (unit CO_{Ha}).
b) 700 m west of Lazy Head, metawacke is thinly interbedded with 20% grey phyllite. These rocks are in apparently conformable contact with underlying massive metawacke (unit CO_{Ga}) and overlying grey phyllite (unit CO_{Ha}).
c) A sill-like projection of the Fogherty Lake pluton runs into the sea 1 km west of Fogerty Head. On the south side of the granite, thinly bedded metawacke, phyllite, and one thin layer of dark-weathering coticule overlie massive metawacke. The Goldenville-Halifax contact is projected to lie in the water just north of the granite.
d) Thinly bedded metawacke with 10-20% phyllite is exposed in a 200 m thick section on the west side of Sheep Island near Whitehead. These rocks are separated from an outcrop of Halifax schist (unit CO_{Ha}) to the north by a few metres of beach gravel.

The transition zone is generally marked by a gradual upward thinning of beds and an increase in the proportion of metapelite. In addition, it contains the only coticules found within the Goldenville Formation. The transition zone is included here within unit CO_{Gb}. However, more detailed mapping in the future may permit its separation into a new unit.

Halifax Formation (unit CO_H)

The lower part of the Halifax Formation (unit CO_{Ha} and the Goldenville-Halifax contact) is well exposed along the north shore of the Canso area. The middle and upper parts are best exposed north of Whitehead. About 80% of the Halifax Formation is metapelite; beds are generally 1-50 cm thick except in a few places where they are up to 2 m thick. Centimetre-scale porphyroblasts of staurolite, andalusite, cordierite, and biotite locally form up to 35% of outcrops. Matrix grain size varies along and across strike between 0.02 mm and about 0.2 mm. This feature is particularly obvious in the Canso area where rocks grade eastward from platy phyllite at Port Felix to fine grained schist at Doughboy Point. Cross-stratification and grading in quartz-rich laminae were the only primary structures found. Pelitic rocks within 300 m of granite are thermally metamorphosed to hornfels in the southern part of the Canso area wherever post-granite deformation is weak or absent. Relative ages are only well defined on the south limb of the Trout Lake syncline in the southwest Canso area where younging directions point consistently north (see Fig. 4). There, the Halifax Formation is 5300 m thick, although that number is believed to be inflated by the presence of numerous D_2 folds. The 3900 m width of the formation on the north limb of the syncline may be a more realistic stratigraphic thickness. Unlike many other parts of the Meguma Terrane, the Halifax Formation in the Canso area is dominated by nongraphitic pelite.

Unit CO_{Ha}

The oldest member of the Halifax Formation consists of 30-60% fine grained graphite schist and phyllite, interbedded with 0-30% grey schist and phyllite, 5-40% rusty metawacke and rare coticules (Fig. 6d). It is about 300 m thick along the north shore of the Canso area. Thicknesses of up to 800 m may exist near Whitehead where outcrops are scarce. The continuous occurrence of unit CO_{Ha} at the base of the Halifax Formation is only well established along the north shore of the Canso area and in the Forest Hill area. Elsewhere, the member is poorly exposed and may pinch out along strike, bringing unit CO_{Hb} into contact with the underlying Goldenville Formation.

The pelitic rocks are composed of muscovite and quartz, with or without graphite, and smaller amounts of biotite or chlorite, or both. Pyrite and pyrrhotite constitute 5-50% of individual beds, occurring as disseminated grains, lensoid clusters, and irregular veinlets. The high proportion of pyrrhotite is probably responsible for the + 100-300 nT aeromagnetic anomaly that marks the unit in most places (see Geological Survey of Canada aeromagnetic Maps 237G and 241G). Porphyroblasts of cordierite, andalusite, biotite, and rare staurolite form up to 30% of some beds. Cordierite grains, up to 1 cm long, are more common in grey schist, whereas pink andalusite is confined to graphitic layers. Although andalusite porphyroblasts are usually less than 5 cm long, crystals up to 12 cm long occur 250 m south of Black Point in the Canso area. In addition, elliptical knots (up to 15 cm long) composed of radiating and intergrown andalusite crystals are a sporadic feature between Lewis Brook and Buchanans Mountain in the Forest Hill area. Medium grey to grey-green schist and phyllite, which could be equivalent to the Moshers Island member of O'Brien (1986), form the basal 20-50 m of the unit in a few places (e.g., 750 m west of Lazy Head and 2 km east of Buchanans Mountain). The section 750 m west of Lazy Head includes a 1-1.5 m thick and several thinner beds of coticule. Shaw (1983) placed these rocks within the upper part of the Goldenville Formation, even though phyllite forms more than 90% of the sequence. Along the shore 2200 m west of Lazy Head, graphite schist lies within 1 m of the Goldenville Formation, although gravel covers the actual contact.

Unit CO_{Hb}

Light brown to medium grey phyllite and fine grained schist with minor but ubiquitous thin coticule beds characterize unit CO_{Hb}. The unit is only well exposed along the north shore of Whitehead Harbour. The member is about 2500 m thick in the tectonically thickened south limb of the Trout Lake syncline and about 1500 m thick on the north limb (see Fig. 4).

The phyllite and schist consist of 20-40% quartz, 30-40% muscovite, 5-20% biotite and chlorite, and 5-20% garnet. Accessories include plagioclase, apatite, zircon, tourmaline, and opaques. Rocks are generally marked by the presence of discontinuous, millimetre-scale, quartz-rich laminations. Up to 30% porphyroblasts, mainly andalusite and cordierite from 0.1 to 3 cm long, are present in the Forest Hill area and in the eastern part of the unit in the Canso area. Light brown- to pink-weathering coticule beds, 1 mm to 5 cm thick, make up <1 to 10% of individual outcrops (Fig. 6e). They are fine- to very fine-grained, granoblastic and consist of subequal proportions of garnet and quartz (see Fig. 5b), with small amounts of mica, chlorite, and opaques. The coticules are commonly laminated, with pelitic, quartz, and garnet-rich layers and are typically spaced at intervals of 10 cm to several metres. Of special note are 10-30 cm thick stratabound layers composed of coticule nodules (0.1-4 cm long) embedded in a pelitic matrix (Fig. 6f). Individual nodules are commonly zoned having garnet-rich rims and quartz-rich cores. At least some of the nodules appear to be disrupted F_2 fold closures.

A few outcrops of unit CO_{Hb} in the Canso area include 1-30 cm thick beds of metawacke. Some metawacke beds are laminated and show grading and cross-stratification. They form up to 40% of single outcrops but, overall, constitute less than 1% of the member. Thin beds of graphite phyllite make up to 50% of a few outcrops on the shore at Port Felix East, the southwest corner of Spears Cove, and the north end of the Northwest Branch in the Canso area. Locally they contain small porphyroblasts of garnet and andalusite. Where graphite phyllite occurs, coticules are absent. Five 1-5 m thick sills of porphyritic felsite, tentatively correlated with unit D_G, intrude unit CO_{Hb} between Monroe and Doughboy points in the Canso area.

Unit CO_{Hc}

This member consists mainly of light- to medium-grey metawacke with very minor metapelite, calc-silicate lenses, and coticules. It is well exposed on the south limb of the Trout Lake syncline where it is 100-150 m thick (see Fig. 4). Its only exposure on the north limb is on the east side of the Northwest Branch of Whitehead Harbour. There it is separated from unit CO_{Hd} by about 200 m of metapelite (correlated with unit CO_{Hb}). Outcrop control is insufficient to determine whether the metawacke continues or pinches out to the west. Although unit CO_{Hc} is virtually identical to the Goldenville Formation, its inclusion in the Halifax Formation is indicated by consistent north-trending younging directions within and both above and below the member at Port Felix Harbour.

Unit CO_{Hc} generally consists of about 70% metawacke and up to 30% phyllite. Metawacke beds are 10 cm to 3 m thick and vary from massive to laminated and crosslaminated. Phyllite beds are locally spotted with small cordierite and biotite porphyroblasts. Calc-silicate lenses with garnet-rich cores were found in a few places. Several 1-8 cm thick coticules occur at the north end of Port Felix Harbour. Generally, the rocks are similar to unit CO_{Gb} in the Goldenville Formation. However, 700 m west of Spears Lake the member consists of relatively massive metawacke similar to that in unit CO_{Ga}.

Unit CO_{Hd}

A 150-250 m thick belt of medium grey andalusite schist is repeated on both limbs of the Trout Lake syncline in the southwest part of the Canso area (see Fig. 4). It forms a resistant ridge that is easily visible on aerial photographs. It is also distinguished by a + 100-400 nT aeromagnetic anomaly (see Geological Survey of Canada aeromagnetic Maps 237G and 241G), which appears to be caused by the presence of accessory magnetite. Schiller (1959) has indicated that the unit can be traced westward for at least 20 km on the south limb of the syncline. Both Faribault (1893a) and Schiller (1959) noted the occurrence of a third layer at Whitehead. Although andalusite porphyroblasts do occur locally in a few pelitic outcrops,

they are mainly pink and prismatic rather than the grey, equant crystals characteristic of unit CO_{Hd}.

The schist consists of 30-40% muscovite, 10-30% quartz, 5-20% biotite and/or chlorite, and 1-20% garnet. It has 5-25% grey, equant andalusite porphyroblasts (0.5-2 cm across) that stand out in positive relief on weathered surfaces. The eastern part of the member also contains up to 20% ovoid cordierite porphyroblasts (<1 cm long), which commonly weather out giving outcrops a pockmarked appearance. It contains up to 10% millimetre-scale, discontinuous laminations and centimetre-thick beds rich in quartz. Repeated 1-10 cm thick beds of coticule locally form up to 20% of individual outcrops.

Unit CO_{He}

This member, which is very poorly exposed in the core of the Trout Lake syncline, is 1300-1400 m thick (see Fig. 4). It is virtually identical to unit CO_{Hb} except that garnet is a very minor component and coticule beds appear to be absent. Mostly it consists of medium to very dark grey quartz-mica phyllite characterized by the presence of discontinuous millimetre-scale laminations enriched in quartz. The laminations show local grading and cross-stratification. Porphyroblasts of pink andalusite, biotite, garnet, and staurolite up to 2 cm long were found within 500 m of the Northwest Branch and along the Northeast Branch of Whitehead Harbour. Beds of metawacke up to 2 m thick occur in some places. Metawacke, andalusite schist, and minor graphite schist are exposed along the north side of the Northeast Branch, where the stratigraphy is poorly known and correlation with unit CO_{He} is tentative. Centimetre-thick calc-silicate layers containing plagioclase, amphibole, garnet, clinozoisite, and quartz were observed in laminated phyllite 2 km west of Port Felix Harbour.

Chemistry of the Meguma Group

Twenty-one samples were collected from the Meguma Group in the Canso area to examine their chemistry and to determine compositional control on porphyroblast type. Of the 16 Halifax Formation samples, 2 are coticules (059A, 226) and the others are metapelites. One metawacke (346E), one coticule (081B), and three metapelites were collected from the Goldenville Formation. The data are tabulated in Appendix IV.

Manganese enrichment

The lowermost 150-300 m of the Halifax Formation in the Mahone Bay area (Moshers Island member) is characterized by green-grey slate containing calcareous nodules and locally abundant spessartine (Waldron, 1987). These rocks, part of the Goldenville-Halifax transition zone, are unusually enriched in Mn, Ba, Cu, Pb, and Zn compared to other parts of the Meguma Group (Zentilli et al., 1986).

The samples collected for geochemistry in the Canso area cover a much larger part of the Meguma stratigraphic column than those studied by Zentilli et al. (1986). In addition, the green-grey phyllite locally present at the base of unit CO_{Ha} (which may be equivalent to the Moshers Island member) was not sampled. Therefore the two data sets are not directly comparable. In the Canso area, units CO_{Hb}, CO_{Hc}, and CO_{Hd} are unusually enriched in Mn (Fig. 7). The Mn mainly resides in fine grained garnet, ranging from $al_{76}sp_{18}py_6$ to $al_{35}sp_{53}py_{12}$ (data from Eddy, 1987 and Raeside et al., 1988), which forms up to 30% of pelitic beds and 80% of coticules. Accessory ilmenite in unit CO_{Hb} in the Poule Point area is also manganiferous (Raeside et al., 1988). Graphite schist and grey schist in unit CO_{Ha}, which have 0-10% garnet, have a very low Mn content. However, rare coticules at the base of unit CO_{Ha} and in the uppermost part of the Goldenville Formation are Mn-rich. The bulk of the Goldenville Formation and unit CO_{He}, both of which lack abundant garnet, appear to have uniformly low Mn contents (see Fig. 7). These data suggest that

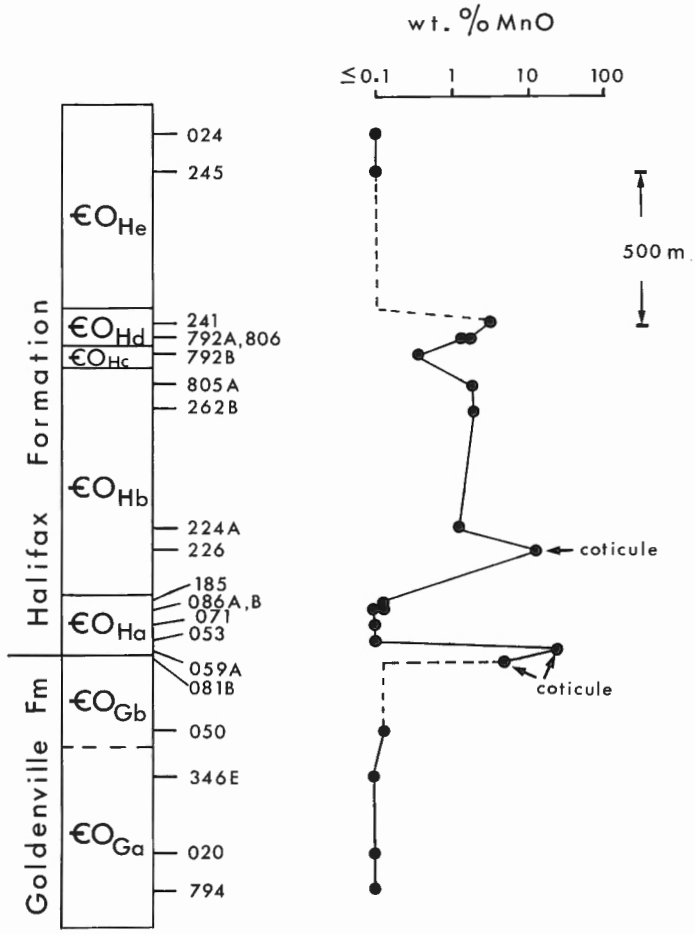

Figure 7. Relationship between MnO content and inferred stratigraphic position of Meguma samples in the Canso area. The Goldenville-Halifax transition zone and units CO_{Hb}, CO_{Hc} and CO_{Hd} are enriched in MnO compared to other parts of the sequence. Coticules and sample numbers are indicated.

Mn-enrichment is not restricted to the transition zone between the Goldenville and Halifax formations. In the Canso area at least, Mn is abnormally enriched in non-graphitic pelites up to about 1800 m above the Goldenville-Halifax contact.

Chemical control of porphyroblast type

Cordierite and andalusite, the two most common porphyroblast minerals in the Halifax Formation in the Canso area, are locally stratabound. For example, light brown-grey schist containing 25-35% cordierite (samples 262B, 805A) is interbedded with dark grey schist with 15-20% andalusite and 20-25% cordierite (samples 241, 806) between Spears Head and Loon Point (unit CO_{Hb}). Along the north shore at Yellow Rocks in unit CO_{Ha}, graphite schist with 15-20% andalusite (sample 086A) is interbedded with grey phyllite containing 20-25% cordierite (sample 086B). Along the paved highway 1.5 km west of Port Felix Harbour, unit CO_{Hd} has about 15-20% andalusite porphyroblasts (sample 792A) whereas grey phyllite in unit CO_{Hc} 50 m to the south (sample 792B) lacks porphyroblasts.

Although chemical differences are slight, comparison of the four pairs of samples suggests that andalusite is favoured over cordierite by higher Al and lower Si (Fig. 8). Fe, Mn, and Mg values seem not to be crucial in controlling the occurrence of cordierite and andalusite, as shown by the variation in slopes of the tie lines in Figure 8. The lack of porphyroblasts in sample 792B, which is only 50 m south of andalusite schist, is probably related to metamorphic grade as well as composition.

Quartz veins in the Meguma Group

Quartz veins are more abundant in fold closures and fault and shear zones and are more common in the Goldenville than the Halifax Formation. Although they comprise <1% of the whole Meguma Group, they constitute up to 5% of single outcrops. Most of the veins are 1-30 cm thick but veins up to 2 m thick occur in a few places. Quartz is by far the dominant mineral, with one or more of muscovite, feldspar, andalusite, tourmaline, garnet, chlorite, graphite, arsenopyrite, and pyrite occurring as accessory phases. Trace element contents of selected quartz veins are given in Appendix IV.

Notable quartz vein occurrences include the following:

a) Gold and arsenopyrite are important accessories in quartz veins at the Forest Hill mine site.
b) Quartz veinlets with either garnet or andalusite (crystals up to 3 cm long) occur at Forest Hill and between Poule and Doughboy points.
c) Coarse grained pink andalusite with minor quartz forms discontinuous vein-like streaks in unit CO_{Ha} at Yellow Rocks on the north shore of the Canso area. The veins trend approximately 010°/90°, crosscut bedding and S_{2a} (terminology defined in Chapter 6), and are deformed by S_{2b}.
d) Quartz-tourmaline veins with tourmaline crystals up to 8 cm long occur north of Poule Point and on Durells Island and other islands farther east in the Canso area.
e) Thick quartz veins between Forest Hill and Fraser Brook are locally rimmed by discontinuous selvages (≤30 cm thick) enriched in coarse grained biotite and one or more of garnet, andalusite, staurolite, sillimanite, quartz, and muscovite.

The quartz veins have various structural styles and ages of formation (cf. Mawer and Williams, 1986). Most are parallel to bedding and are deformed by S_{2b}. Between Doughboy and Poule points in the Canso area, apparently undeformed quartz veins carrying andalusite and garnet are concentrated in F_{2b} fold closures and along S_{2b} cleavage planes. Quartz-tourmaline veinlets in the same area are sheared by S_{2b}. In unit D_{Tm} north of Canso, most quartz veins are deformed by S_{2b}. A few have intruded along F_{2c} axial surfaces and others partly

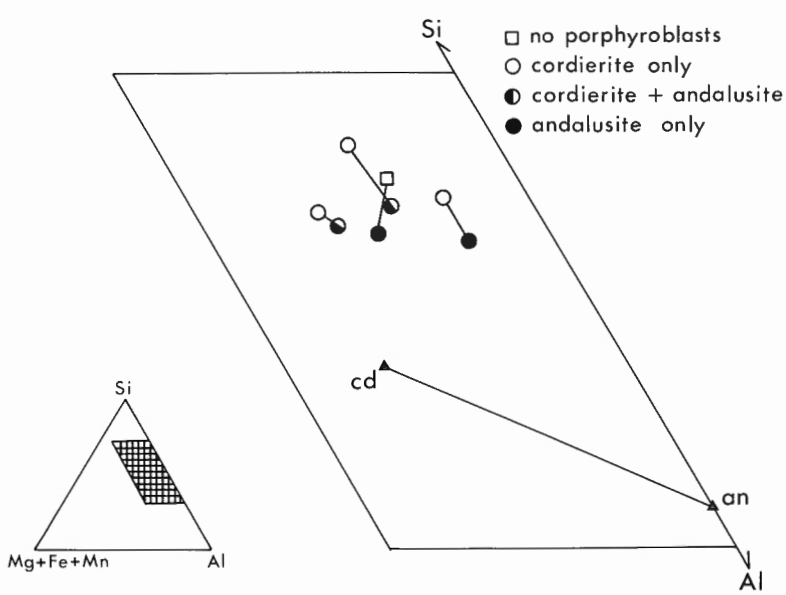

Figure 8. Ternary plot in cation proportions showing the relationship between pelite chemistry and the presence of andalusite and cordierite porphyroblasts in the Meguma Group in the Canso area. Sample pairs joined by tie-lines were collected in the same outcrops. Stoichiometric andalusite (an) and cordierite (cd) compositions are indicated.

crosscut and are partly deformed by F_{2c} folds. Therefore, these veins appear to be syn-D_{2c}. Along the north shore of the Canso area, rare quartz veins have been emplaced along, and are deformed by, late brittle-ductile shear zones that postdate D_{2c}. Taken together, these observations suggest that quartz vein emplacement extended over a more protracted interval than that envisaged by Mawer and Williams (1986).

Devono-Carboniferous rocks

General statement

The Devono-Carboniferous rocks are divided into the Minister Brook formation (unit DC_M), Sunnyville formation (unit DC_S), Tower formation (unit DC_T), and Gunns Brook formation (unit C_G). Probable inliers of mylonite of unknown age occur within the Minister Brook formation. Clastic sedimentary and mafic volcanic rocks are the dominant lithologies. Quartz and specular hematite veins up to 10 cm thick and running in several directions crosscut the Minister Brook, Tower, and Sunnyville formations. They are locally accompanied by open fractures and cavities lined with small quartz euhedra. Chlorite and dolomite veins also crosscut the Minister Brook formation. Epidote, calcite, and zeolite veinlets are restricted to the Sunnyville formation volcanic rocks. The contact and age relationships of these four units are poorly known because of little exposure and limited mapping. They are inferred to be middle Devonian to early Carboniferous in age, from fossil evidence given by Schiller (1963) and correlation with similar rocks farther north and west.

Minister Brook formation (unit DC_M)

The Minister Brook formation forms an east-trending belt of metapelitic rocks that appears to be bounded by faults on three sides. The southern boundary is the well defined Guysborough County fault. A fault breccia of Goldenville metawacke and Minister Brook metapelite is exposed on a northward meander of Salmon River, 600 m east of Roachvale. The western boundary fault is inferred not only from the coincidence of a linear valley with the projected contact but also from the fact that the Minister Brook and Gunns Brook formations strike into each other. No substantial evidence was found for the northern fault contact (i.e., Chedabucto fault). It was taken from earlier work by Schiller (1961) who mapped a much larger area.

The main rock type is a light to dark grey, very fine grained pelite that varies from blocky argillite to fissile phyllite. It is locally marked by the presence of discontinuous quartz-rich laminae up to 1 cm thick. Muscovite, chlorite, biotite, and highly strained quartz are the main constituents, with minor plagioclase, pyrite, epidote, and tourmaline. Darker varieties appear to be slightly graphitic. Deformed and altered, fine grained, green-black rock was found at two localities – where Horton Brook intersects the main highway and 1400 m to the northwest. It contains prismatic, decussate pseudomorphs up to 3 mm long that are outlined by iron oxide. The pseudomorphs might represent pyroxene or plagioclase phenocrysts in a highly altered metabasalt. The relationships of these two outcrops with the surrounding phyllite are unknown, although both lithologies have suffered about the same degree of deformation and metamorphism.

Schiller (1963) described these rocks as phyllonites and considered them to be a sheared equivalent of the Strathlorne Formation of the Horton Group. Fossil evidence collected by Schiller (1963) is ambiguous, giving possible ages ranging from Silurian to early Carboniferous. The age of the Minister Brook formation relative to the other three Devono-Carboniferous units is unknown. If its deformation and metamorphism are correlative with D_{2c} as inferred in Chapter 6, then the Minister Brook formation is late Devonian or older. The deformation and metamorphism may simply be related to its location within the Cobequid-Chedabucto fault zone during repeated fault movements. This latter possibility is supported by the fact that the rocks appear to become less deformed and metamorphosed farther north and west, based on descriptions given by Schiller (1963).

Three outcrops of relatively undeformed and unmetamorphosed sedimentary rock that could be outliers of other Devono-Carboniferous units occur within unit DC_M. A small exposure of light-coloured, blocky arenite containing 1% disseminated pyrite lies in McAllister Brook, 600 m north of the highway. Conglomerate with unmetamorphosed clastic sedimentary pebbles was found in the same brook, 500 m farther north. The conglomerate sits on an irregular surface above argillite. About 150 m upstream from the mouth of Horton Brook is a 4 m thick horizon of light brown, dolomitic, pebbly, argillaceous mudstone. The pebbles, up to 2 cm long, consist of phyllite, polycrystalline quartz, and metawacke.

Mylonite inliers in the Minister Brook formation

Three isolated outcrops of porphyroclastic mylonite lie within the Minister Brook formation. They are believed to be fault-bounded inliers, although contact relationships with surrounding rocks were not observed. Two of the outcrops occur 1000 and 1500 m north of the highway on McAllister Brook. The third is exposed at the edge of a dirt road 900 m to the east. In hand specimen, the rock is dark grey and rather nondescript, being easily mistaken for altered tuff with feldspar phenocrysts. Porphyroclasts vary between 0.1 and 2 cm long and are composed of one or more of garnet, biotite, quartz, plagioclase, and minor orthoclase and sillimanite (see Fig. 5c). Schiller (1963) has reported the presence of hornblende-bearing porphyroclasts as well. Mineral grains in some of the porphyroclasts are granoblastic, unstrained, and compositionally unzoned. Microprobe analyses of minerals in three of the porphyroclasts indicate plagioclase, garnet, and biotite are $An_{18\text{-}21}$, $al_{77}py_{18}sp_4$, and $X_{2.0}(Fe_{2.4}Mg_{2.3}Ti_{0.5}Al_{0.3})(Si_{5.3}Al_{2.7})O_{20}(OH)_4$ respectively. The porphyroclasts are enveloped by a fine- to very fine-grained mylonitic matrix of biotite,

chlorite, plagioclase, opaques, quartz, dolomite, and sericite. The age of the inliers is unknown, although their degree of deformation and metamorphism suggests that they are pre-Carboniferous.

Sunnyville formation (unit DC_S)

The Sunnyville formation is known from only two outcrops and scattered float of porphyritic, amygdaloidal basalt (called andesite in Hill, 1987a). Plagioclase is by far the most common phenocryst phase. It typically occurs in two size ranges, 1-5 mm and 0.03-0.3 mm, and defines an irregular flow fabric (see Fig. 5d). Altered clinopyroxene and olivine phenocrysts were observed in one thin section. The rocks are invariably hydrothermally altered, showing the formation of abundant secondary chlorite, tremolite, epidote, sericite, hematite, and zeolite in both original mineral grains and crosscutting veinlets. Vesicles are commonly flattened and many are filled with calcite, quartz, chlorophaeite, and zeolite. The groundmass consists of very fine grained, indeterminate, dark grey to red-brown material. A single outcrop of the same rock was found within the Tower formation, just north of Poder Lake.

Irregular vein-like fracture-fillings of red-brown mudstone to fine grained sandstone occur in all of the basalt outcrops examined. On the south side of the Sunnyville crossroads 3 km west of Guysborough (north of the map area), altered amygdaloidal basalt is structurally overlain by unbedded red to maroon sandstone to mudstone. The contact is abrupt and dips steeply to the north. More outcrops of basalt lie just north of the crossroads. Red-brown mudstone fills irregular cavities and fractures in the underlying basalt. The contact relationships are not clear, although Schiller (1963) has interpreted the exposure as an unconformity. About 200 m south of the crossroads, conglomerate is interbedded with maroon to dark grey, immature sandstone and shale. The conglomerate contains numerous pebbles of Sunnyville basalt. According to Schiller (1963) and Mooney (1987), welded tuffs, agglomerate, and minor red clastic sedimentary rocks are interbedded with amygdaloidal basalt farther north.

Schiller (1963) included these rocks in the Black Settlement Formation. They may be correlative with the middle to late Devonian McAras Brook Formation that outcrops on St. Georges Bay farther north (Dostal et al., 1983). Benson (1974) has noted the occurrence of red sandstone dykes in altered plagioclase-phyric basalt in the McAras Brook Formation at Cape George.

Tower formation (unit DC_T)

The Tower formation is represented by only six outcrops and some glacial float of unmetamorphosed sandstone, siltstone, and conglomerate. Bedding has a very low dip in the only outcrop in which it was found. The main rock type is maroon to pink quartz arenite (see Fig. 5e). It is well sorted, consisting of up to 90% subangular to subrounded sand-sized grains in a matrix of hematite and sericite. The clastic component is dominated by quartz, with minor amounts of feldspar, opaques, tourmaline, chert, mylonitic quartzite, crenulated schist, and zircon. Many of the quartz grains have rounded cores and subangular silica overgrowths. Arenite is locally interbedded with minor siltstone and conglomerate. Conglomerate, found in three small outcrops north of Priest Lake, is unbedded and contains pebbles of unmetamorphosed sedimentary and felsic to intermediate aphyric volcanic rocks. In addition, maroon and red conglomerate, which may be correlative with the Tower formation and which contains numerous pebbles of Sunnyville basalt, occurs 400 m southwest of the Sunnyville crossroads and in float west of Godfry Brook.

Schiller (1963) has correlated these rocks with the Craignish Formation of the early Carboniferous Horton Brook. Five features point to a close relationship between the Sunnyville and Tower formations as follows:

a) the common occurrence of fracture-fillings of red-brown mudstone to quartzose sandstone in the Sunnyville basalt;
b) the presence of hematitic mudstone to sandstone structurally overlying Sunnyville basalt at the Sunnyville crossroads;
c) the isolated outcrop of Sunnyville basalt within the Tower formation;
d) the local occurrence of maroon to red conglomerate containing pebbles of Sunnyville basalt; and
e) intercalation of red clastic rocks with Sunnyville basalt north of the map area (Schiller, 1963).

These features suggest that the Sunnyville and Tower formations are coeval, although an unconformable relationship cannot be discounted. This interpretation is indirectly supported by the fact that the McAras Brook Formation (a possible Sunnyville correlative) consists of red conglomerate and sandstone interbedded with basalt (Dostal et al., 1983).

Gunns Brook formation (unit C_G)

The Gunns Brook formation lies on the west side of the Forest Hill map area and is separated from the Meguma Terrane by the Guysborough County fault. The rocks, consisting mainly of sandstone, conglomerate, and very minor shale are unmetamorphosed and undeformed, except for broad, open folds. Dips are generally $<35°$ except along the fault where beds as steep as 80° occur.

The dominant lithology is sandstone that varies from lithic and feldspathic to minor quartz wacke (see Fig. 5f), characterized by poor sorting and pebbly horizons. The sandstone is normally green grey on fresh surfaces but is oxidized to red brown along flaggy partings. Subangular grains up to 2 mm long of quartz, rock fragments, plagioclase, microcline, muscovite and minor opaques, biotite, and tourmaline are the main clastic components, with feldspar and rock fragments each forming up to 25% of individual beds. Detrital muscovite flakes are concentrated along bedding planes. The matrix consists of dolomite, silt, clay, and limonite. Conglomerate, including subrounded boulders up to 1 m in diameter, appears

to be more abundant and coarser grained closer to the Guysborough County fault. Carbonaceous shale is a very minor component, forming a few beds up to 2 cm thick east of Salmon River Lake.

Most lithic fragments in the sandstone and conglomerate are derived from the Meguma Terrane. Goldenville metawacke and both grey and black Halifax schist are the main components. Keppie (1985) has reported the presence of andalusite porphyroblasts in clasts of crenulated Halifax schist at the crossroads east of Salmon River Lake. In spite of diligent search, no granite clasts were found, although Benson (1967) has described boulders of granite in Horton conglomerate unconformably overlying the Meguma Terrane about 30 km west of the Forest Hill area. Pebbles of vein quartz, which are also likely derived from the Meguma Terrane, and unmetamorphosed sandstone and shale, which are probably derived from Fundy basin strata, occur in conglomerate along Gunns Brook.

The sandstone is flaggy and friable. It forms beds from 1 cm to 3 m thick, which are often difficult to see, except where pebbly and shaly horizons occur. Discontinuous conglomerate beds that appear to have shoestring shapes are 1-3 m wide and were traced along strike for up to 10 m. Metre-scale, trough-shaped crossbeds and centimetre-scale, asymmetric ripples are common in sandstone. Numerous root casts are exposed on a dip slope along the road 400 m southwest of Salmon River Lake. Fractures are commonly stained with manganese oxide and lined with quartz euhedra.

These rocks appear to be part of the Horton Group, and Schiller (1963) considered them to be equivalent to either the Ainslie or Strathlorne formations. The westward extension of the Gunns Brook formation was interpreted by Benson (1967) to be correlative with the Craignish Formation. Fossils in the Gunns Brook formation collected just outside the Forest Hill area substantiate an early Carboniferous age (Schiller, 1963).

MACROSCOPIC FEATURES OF THE GRANITOID PLUTONS

General statement

Granitoid rocks are divided into 33 plutons, based on composition, texture, and contact relationships with neighbouring intrusions. Each pluton is assigned a geographic name and a two-letter code (e.g., Snyders Lake pluton–SL). Plutons are located in Figure 9 and are described individually in Appendix I. Most are lithologically homogeneous at map scale. However, the term "pluton" is used in a somewhat liberal sense. Geographically paired plutons, which are virtually identical in composition but separated by water, may actually comprise single intrusions (e.g., Port Howe and Ketch Harbour plutons, Fig. 9). Others are composed of more than one

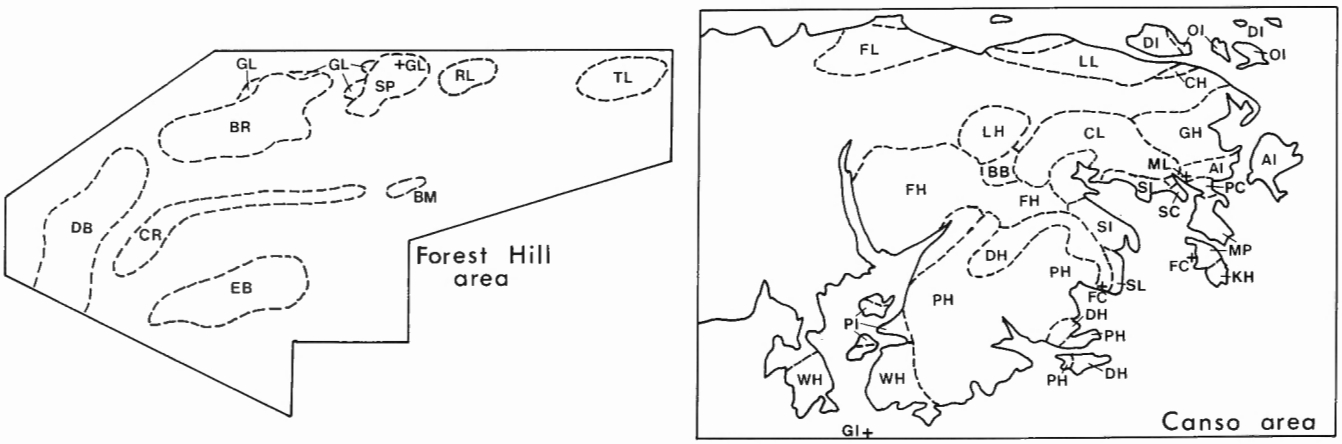

Forest Hill area

BM- Buchanans Mountain
BR- Bantry Road
CR- Costley River
DB- Doctors Brook
EB- East Branch
GL- Garry Lakes
RL- Rocky Lake
SP- Sloans Pond
TL- Tom Lake

Canso area

AI- Andrew Island
BB- Big Branch
CH- Canso Harbour
CL- Charles Lake
DH- Dover Head
DI- Durells Island
FC- False Cove
FH- Flagstaff Hill
FL- Fogherty Lake
GH- Glasgow Harbour
GI- Gammon Islands
KH- Ketch Harbour
LH- Lookout Hill
LL- Lumsdens Lake
ML- Mahons Lake
MP- Madeline Point
OI- Oliver Island
PC- Portage Cove
PH- Port Howe
PI- Prices Island
SC- Shag Cove
SI- Sheep Island
SL- Snyders Lake
WH- Whitehead

Figure 9. Sketch maps showing the locations and two-letter codes of granitoid plutons in the Canso and Forest Hill areas. Plutons too small to plot separately are indicated by crosses.

discrete body (e.g., Garry Lakes pluton, Fig. 9). Igneous rocks that are not assigned to specific plutons include the following:

a) dykes and xenoliths of miscellaneous granitic rocks that cannot be correlated with the pluton in which they occur;
b) pegmatite and aplite dykes and lenses that intrude both plutons and country rocks; and
c) numerous dykes, sills, and irregular masses of fine- to coarse-grained granite that intrude the country rocks adjacent to plutons. They are mapped as intrusive agmatite where, together with pegmatite and aplite, they form 25-50% of the country rocks (e.g., unit aCO_G around Dover Basin).

Rock textures

Post-granite D_2 deformation has affected most of the plutons within 10-15 km of the Cobequid-Chedabucto fault system (Fig. 10). As a result, all variations between highly deformed and almost pristine granitoid rocks are represented. The least deformed rocks occur in the southern parts of the two map areas. South of the Harbour Island shear zone (Fig. 10), they are comparable to "undeformed" parts of the South Mountain batholith, the only indications of strain being minor subgrain formation in quartz and rare kink bands in mica. Undeformed granitoid rocks are typically massive with granular to weakly decussate fabrics (Fig. 11a,b). Grain size varies from fine to very coarse, with medium being predominant. Coarser phases contain 1-30% microcline phenocrysts ranging from 1 to 15 cm long that are blocky to tabular and appear subhedral in hand specimen. Locally they define an impersistent igneous lamination and rare lineation (described below). Specific textures characteristic of each plutonic unit are described in the following sections.

Strain effects in deformed plutons vary considerably from outcrop to outcrop. Slightly deformed rocks retain most of their igneous texture but have a weakly developed tectonic foliation defined by recrystallized quartz and mica (e.g., Fig. 11c). As zones of greater strain are approached, the foliation intensifies and grain size decreases. The most deformed rocks occur in east-trending shear zones, particularly the Harbour Island, Tittle, and Black Lakes shear zones (see Fig. 10). They are marked by platy fracturing and mylonitic S-C fabric defined by feldspar augen, which are enveloped by ribbon quartz and shredded mica (Fig. 11d). Locally, ductile tectonic textures are obliterated by brittle features such as breccia and cataclasite. Deformation textures and structures are described in more detail below.

Tonalite plutons (unit D_T)

Tonalite comprises <1% of the Canso and Forest Hill areas, forming several small bodies lying within and adjacent to granitic intrusions. They are grouped into three plutons and are subdivided into biotite (unit D_{Tb}), hornblende-biotite (unit D_{Th}), and migmatitic muscovite-biotite (unit D_{Tm}) varieties. The three tonalite plutons are the Garry Lakes pluton in the Forest Hill area and the Shag Cove and Oliver Island plutons in the Canso area.

The Shag Cove pluton is made up of numerous variously sized fragments enclosed in several granitic intrusions (units D_{Gb} and D_{Ge}) between Andrew and Gun Cove islands. The fragments range from angular xenoliths <1 m long (Fig. 12a) to mappable bodies up to 0.3 km^2 in area. They are intruded by numerous granitic dykes of the host plutons as well as pegmatite and aplite. Individual samples are variable in composition, containing 13 to 37% biotite, and may represent fragmentation of more than one original intrusion. The tonalite contains 1-10% disc-shaped enclaves of biotite microtonalite (Fig. 12b). These are oriented parallel to the foliation, are ≤1 m long, and are similar in composition to the host rock. Although they are deformed along with their host, the enclaves locally preserve igneous textures (i.e., decussate plagioclase phenocrysts with oscillatory zoning) and

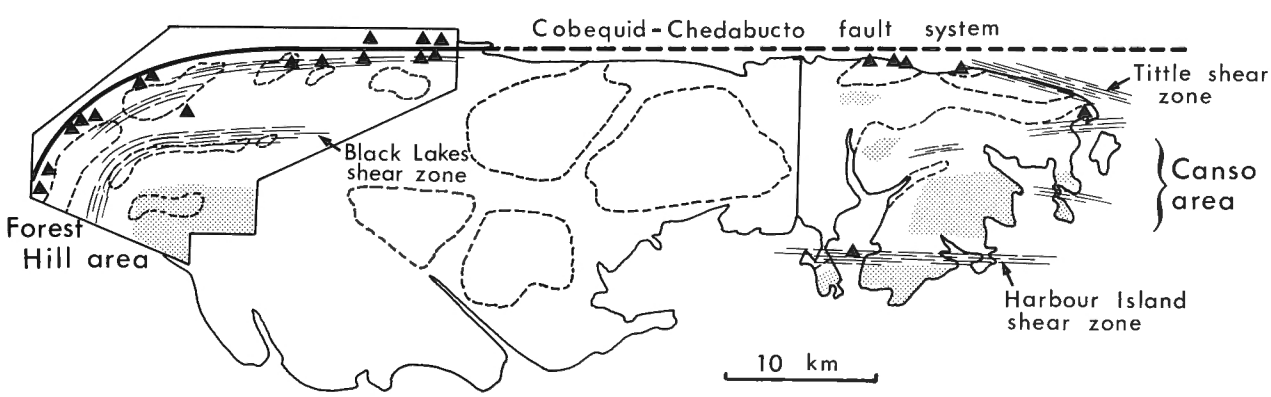

Figure 10. Sketch map of the eastern Meguma Terrane showing the variation in intensity of post-granite D_2 strain in the Canso and Forest Hill areas. Strongly deformed areas are indicated by dashes, moderately deformed areas are unpatterned, and relatively undeformed areas are stippled. Triangles mark occurrences of fault breccia and cataclasite. Three D_2 ductile shear zones are named. The pronounced bend in the orientation of D_2 structures in the western part of the Forest Hill area appears to be caused by sinistral drag along the northwest-trending Country Harbour fault, which marks the southwest corner of the map area.

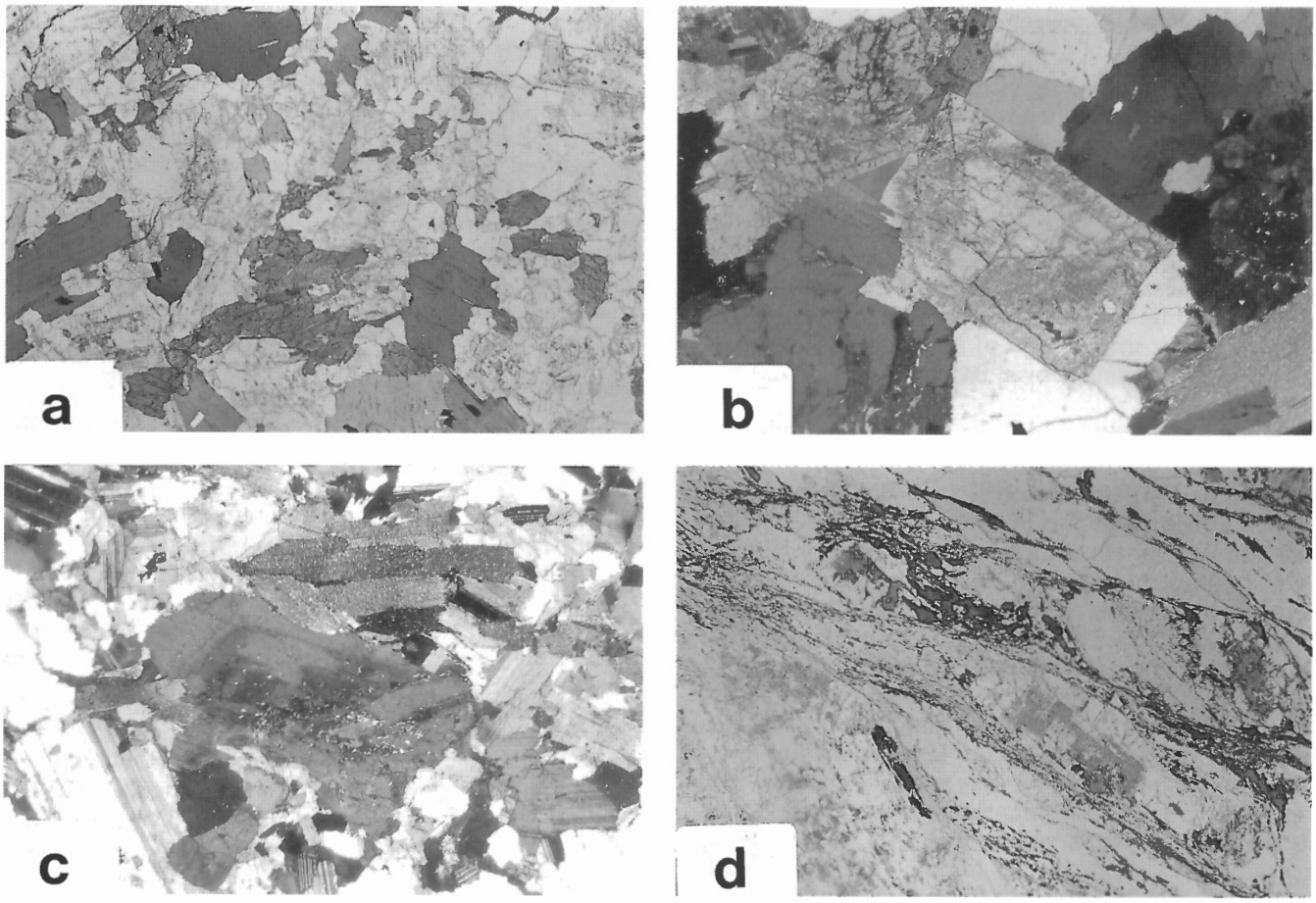

Figure 11. Granitoid rock textures. Field widths (e.g., 3 mm) and light polarization (plane polarized light or crossed nicols) are given in brackets. (a) Relatively undeformed hornblende-biotite tonalite from the Garry Lakes pluton (6 mm; ppl). (b) Undeformed biotite-muscovite granite from the Whitehead pluton, collected 2 km south of the Harbour Island shear zone (6 mm; X-nicols). (c) Weakly deformed biotite tonalite from the Shag Cove pluton. Biotite (left and upper centre) defines S_{2b} (6 mm; X-nicols). (d) Well developed S-C fabric in mylonitic granite from the Whitehead pluton, collected from the centre of the Harbour Island shear zone. S-C fabric relationship is reversed in the photograph (6 mm; ppl).

may be quenched globules of more mafic magma or rounded pieces of chilled margin tonalite, as suggested by Vernon (1983). Dykes of biotite tonalite crosscut Goldenville metawacke at the southeast end of Shag Cove.

The Garry Lakes pluton includes five separate bodies, four of which are represented by single outcrops. They lie along and within the margins of the Sloans Pond and Bantry Road granitic plutons in the Forest Hill area. The largest body just north of Garry Lakes contains scattered biotite schlieren and disc-shaped inclusions of Goldenville metawacke oriented parallel to a weak tectonic foliation. Two of the bodies have biotite as the sole mafic mineral whereas the three between Garry Lakes and Whites Lake also have hornblende.

The Oliver Island pluton is unique in that it is migmatitic. The migmatite consists of the following four phases:

a) The dominant lithology is muscovite-biotite tonalite that is foliate and locally gneissic. It contains numerous streaks and clots (0.1-3 cm thick) enriched in mica (Fig. 12c). Tonalite generally comprises 30-70% of individual outcrops. It is this tonalite that is meant by the term "Oliver Island pluton".
b) Abundant xenoliths of Goldenville metawacke and minor biotite schist occur within the tonalite. They are locally marked by micaceous laminations and centimetre-sized microcline and muscovite porphyroblasts (Fig. 12c).
c) Dykes and irregular lenses of medium grained, white-weathering biotite-muscovite leucogranite intrude the tonalite and metasedimentary rocks. The leucogranite contains scattered millimetre-thick micaceous schlieren and microcline augen up to 2 cm long.
d) Leucogranite pegmatite dykes, forming up to 10% of single outcrops, crosscut all of the other rock types. In addition, pegmatitic microcline, quartz, and muscovite form ovoid knots 5-20 cm long in the tonalite and metawacke.

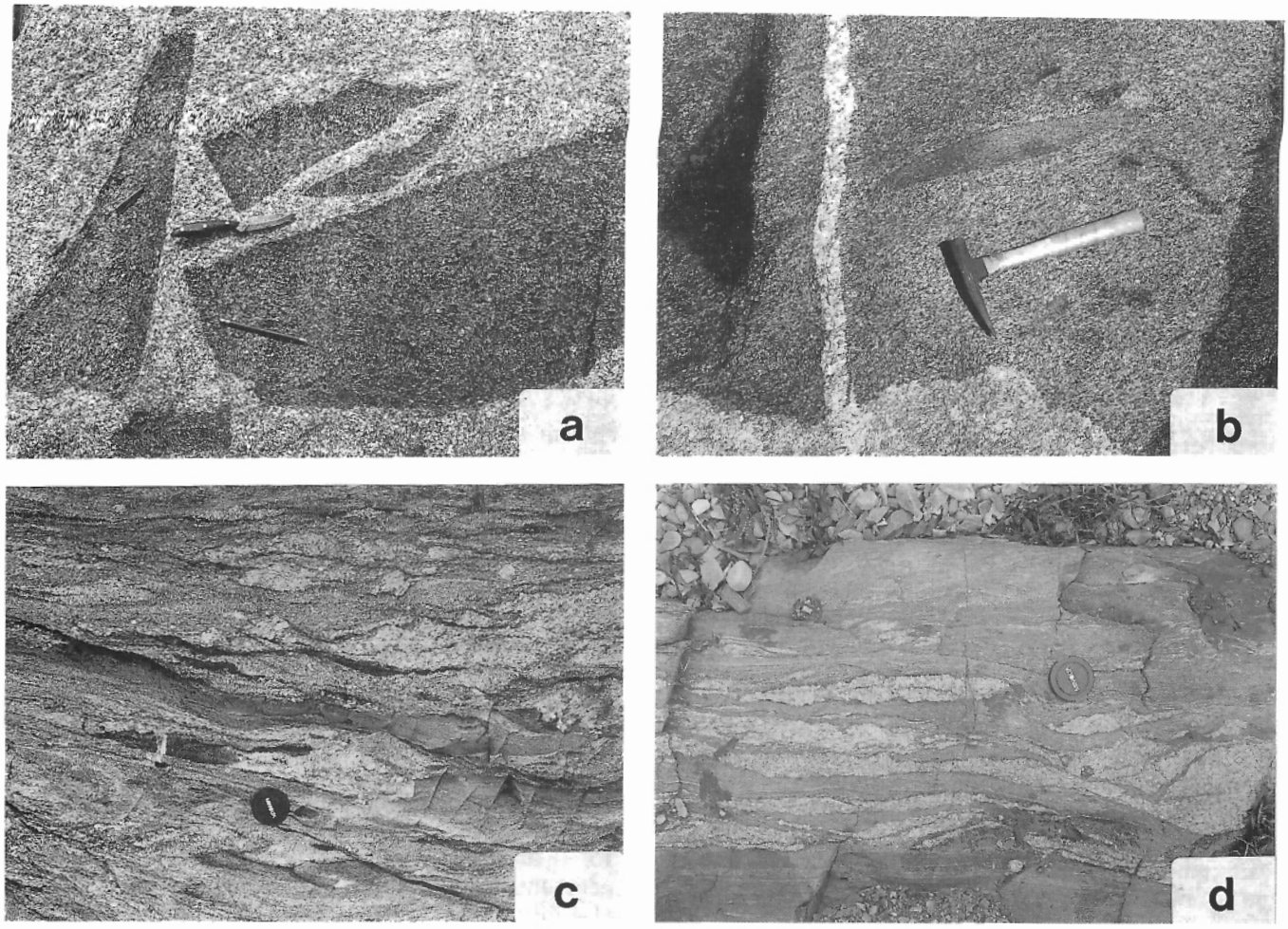

Figure 12. Structures associated with tonalite plutons in the Canso area. (a) Angular xenoliths of Shag Cove tonalite in Portage Cove granite at Haulover Ledge. The pencil and pen cap are oriented parallel to a mylonitic foliation, correlated with S_{2a}, in two xenoliths. The knife is parallel to weakly developed S_{2b} in the granite. GSC 204508-J. (b) Flattened microtonalite xenolith (autolith?) in Shag Cove biotite tonalite at Shag Cove. Hammer is parallel to S_{2b}. White-weathering leucogranite pegmatite crosscuts the tonalite. GSC 204508-K. (c) Migmatite on Piscatiqui Island formed by pre-D_{2b} injection of Oliver Island tonalite (medium grey) containing Goldenville xenoliths (dark grey) by leucogranite and pegmatite (light grey). GSC 204508-C. (d) Goldenville metawacke with numerous transposed pegmatite dykes at the south end of Piscatiqui Island. GSC 204508-AA.

Strong post-tonalite D_2 deformation has transposed the rocks into migmatite composed of discontinuous layers of tonalite, Goldenville metasedimentary rocks, granite, and pegmatite ranging from <1 to 40 m thick. The layers are deformed into repeated Z-shaped folds in a few places. Interlayer angles are small and intrusive relationships are only visible locally. The white-weathering leucogranite may be correlative with the Durells Island pluton (unit D_{Gd}) that borders the Oliver Island pluton to the north. The migmatite passes southward into Goldenville metawacke (unit aCO_{Ga}) injected by numerous pegmatite dykes (Fig. 12d) by the abrupt disappearance of tonalite (e.g., south end of Crow Island).

These rocks have been mapped as granitized and injected Goldenville strata by Weeks (1960) and Stevenson (1964). Shaw (1983) called them migmatitic paragneiss. However, the host rock is tonalite with 40-60% plagioclase, quite unlike any metasedimentary rocks in the Meguma Group. For this reason, the tonalite is tentatively correlated with unit D_T and the Oliver Island pluton is interpreted as deformed intrusive agmatite. Discontinuous, 0.1-1 cm thick, biotite-rich selvages locally separating granite and metawacke layers, appear to represent restite associated with small-scale partial melting along the margins of transposed granite dykes.

Granitic plutons (unit D_G)

Granitic rocks make up 59% of the Canso area and 28% of the Forest Hill area. The 30 plutons are grouped into six units (units D_{Ga} to D_{Gf}) using three criteria as follows:

a) age relationships–based on intrusive structures, primarily observed in the superb coastal exposures in the southern part of the Canso area;

b) lithology–based mainly on the proportions of muscovite and biotite; and
c) texture–based on grain size, which is only reliable in the southern parts of the two map areas where post-granite deformation is weak or absent.

The division into six granitic units has certain limitations. Pluton age relationships are only partly known in the Canso area and are unknown in the Forest Hill area. The three listed criteria sometimes conflict with each other when assigning outcrops to plutons and plutons to units; if so, relative age is given priority. Finally, the subtle differences in composition and texture between some plutons make recognition difficult, especially inland where the quality and quantity of outcrops are limited. Division into units with meaningful relative ages would have been impossible without the excellent coastal exposures in the southern part of the Canso area. Thus some plutons may be grouped with the wrong unit, within a complete sequence of magmatic events that is only partly known. The intrusive history of the Canso and Forest Hill areas is probably more complicated than that implied by division into one tonalite and six granitic units.

Big Branch, Sheep Island, Rocky Lake plutons (unit D_{Ga})

Unit D_{Ga} rocks consist of fine- to medium-grained biotite-muscovite leucogranite and are recognized in the field by aplitic texture and the presence of 2-3% biotite and 9-12% muscovite. They are equigranular except for scattered biotite and muscovite flakes up to 1 cm across and a few microcline phenocrysts ≤ 3 cm long in one outcrop in the Sheep Island pluton. In general, xenoliths and dykes are lacking and the plutons are quite homogeneous in texture and composition. However, grain size in the Sheep Island pluton varies from 0.5-1 mm in the eastern third to 1-3 mm in the western part, with the contact between the two phases being sharply gradational over 1-5 cm and irregular in orientation. The contact is exposed along the shore 600 m ENE of Meades Point.

Andrew Island, Dover Head, Madeline Point, Prices Island plutons (unit D_{Gb})

These plutons are composed of very coarse grained, porphyritic to seriate muscovite-biotite granite and minor granodiorite. They are characterized by the presence of 10-30% microcline phenocrysts that generally range from 1 to 8 cm long, although individual grains up to 15 cm long occur in a few places. Groundmass grain size is 0.2-1 cm. Biotite is generally more abundant than muscovite; muscovite is commonly difficult to recognize in hand specimen. The Andrew Island pluton is distinguished by the presence of accessory garnet, which is visible in outcrop except in the western part around Mahons Lake. The Dover Head and Madeline Point plutons, which are separated by Dover Bay, are lithologically similar and may comprise a single intrusion. The Prices Island pluton and the western part of the Andrew Island pluton are somewhat finer grained than normal, generally lacking phenocrysts longer than about 2 cm. The Andrew Island, Dover Head and Madeline Point plutons are further distinguished by the development of extensive plutonic agmatite (unit aD_{Gb}–see below).

False Cove pluton (unit D_{Gc})

The False Cove pluton, composed of fine grained biotite-muscovite granite is recognized in the field by medium grey colour on both fresh and weathered surfaces, aplitic texture, and the presence of 1-10% small phenocrysts of one or more of biotite, muscovite, quartz, plagioclase, and microcline. Groundmass grain size is about 0.3-0.5 mm. The False Cove pluton includes several dykes and small bodies that intrude and are spatially associated with unit D_{Gb} between Louse Harbour and Andrew Island in the Canso area. Mappable bodies occur only at the north end of Louse Harbour and at False Cove on Little Dover Island.

Bantry Road, Canso Harbour, Costley River, Doctors Brook, Durells Island, East Branch, Flagstaff Hill, Fogherty Lake, Glasgow Harbour, Lookout Hill, Lumsdens Lake, Mahons Lake, Sloans Pond, Tom Lake, Whitehead plutons (unit D_{Gd})

The age relationships of most unit D_{Gd} plutons are unknown and it is possible that unit D_{Gd} includes intrusions of more than one generation, which may account for their large range of compositions and textures. In general, they are distinguished by medium grained (1-4 mm) equigranular textures and moderate amounts of mica with muscovite in excess of biotite. Phenocrysts of microcline (0.5-2 cm long) and muscovite (≤ 1 cm long) form up to 5% of the rock in a few outcrops. Unusual variants are the Durells Island and Canso Harbour plutons, which have abundant feldspar augen up to 2 cm long and the Sloans Pond pluton, which has more biotite than muscovite. Most of the plutons are relatively homogeneous, lacking xenoliths and dykes except along their margins. However, the Durells Island pluton contains numerous pegmatite dykes as well as plate-shaped inclusions of Goldenville metawacke and minor biotite schist up to 40 m long. Plutons with less than 4% biotite are termed "leucocratic" (unit D_{Gdl}).

Charles Lake, Ketch Harbour, Portage Cove, Port Howe plutons (unit D_{Ge})

These plutons are recognized by coarse grained seriate textures and compositions with biotite more abundant than muscovite. They are similar in lithology to unit D_{Gb} but are finer grained, having 1-20% microcline phenocrysts 0.5-3 cm long set in a 2-5 mm groundmass. Very rare microcline phenocrysts up to 8 cm long occur in a few outcrops. The Charles Lake pluton and dykes of the Portage Cove pluton north of Portage Cove are anomalous because they lack phenocrysts longer than about 1 cm and are commonly medium grained and equigranular. The Portage Cove, Ketch Harbour, and

Port Howe plutons are agmatitic (unit aD_{Ge}), containing numerous blocks of unit D_{Gb}, unit D_T, and Meguma Group up to 100 m across as well as dykes of pegmatite and aplite (discussed below).

Buchanans Mountain, Gammon Islands, Snyders Lake plutons (unit D_{gf})

Unit D_{Gf} consists of leucogranite, which is recognized by the presence of about 10% muscovite and almost no biotite. Rocks are medium grained, equigranular, and lack phenocrysts. No dykes or xenoliths were found.

Contact and age relationships

Country rock contacts and xenoliths

Contacts between granitoid plutons and country rocks vary from simple and abrupt to agmatite developed over large areas (≤ 6 km^2). Simple contacts dip moderately to steeply inward and outward where observed. They truncate both bedding and a single tectonic foliation in the country rocks where post-granite deformation is weak or absent. In those areas, pelitic rocks are thermally metamorphosed to hornfels. Where post-granite deformation is relatively strong, dykes, xenoliths, and contacts are partly transposed parallel to the tectonic foliation and pelitic rocks are schistose. A few granitic dykes usually intrude the country rocks and a few xenoliths occur in the plutons close to contacts. All the nonplutonic xenoliths appear to be derived from the Meguma Group. They generally constitute much less than 1% of individual plutons and, as has been observed in the South Mountain batholith (McKenzie and Clarke, 1975), are more abundant in more mafic plutons. However, metasedimentary xenoliths are unusually common in the Durells Island, Port Howe, and Dover Head plutons and along many intrusion margins. Locally the Durells Island pluton contains up to 30% tabular rafts of Goldenville metawacke up to 40 m long. They have been transposed parallel to the tectonic foliation during D_2. Variably oriented angular blocks of Halifax hornfels up to 0.1 km^2 in size are scattered in the relatively undeformed Port Howe and Dover Head plutons between Snyders Lake and Kyak Brook. Leucogranite pegmatite lenses and dykes are unusually abundant within and adjacent to xenoliths, and coarse grained muscovite is commonly developed in xenoliths along their rims.

Agmatite (unit aCO_G) composed of highly variable mixtures of Goldenville Formation (50-75% of the unit) and granitic rocks is found along the margins of some plutons (small-scale example is shown in Fig. 13a). It is particularly widespread around Dover Basin and Chapel Gulley in the Canso area and between the Tom Lake and Doctors Brook plutons in the Forest Hill area. Metawacke and minor schist are intimately injected by medium grained, aplitic and pegmatitic granite (unit D_G) at all scales from small dykelets and lenses to undefined masses up to 150 m across. The pegmatitic, medium grained, and aplitic granite phases are commonly gradational with each other. The medium grained phase is biotite-muscovite granite that cannot always be correlated with adjacent plutons. Agmatite passes into plutons by gradual decrease in the size and proportion of both pegmatite bodies and enclaves. Where post-granite deformation is strong, the rocks are transposed forming a discontinuous lensoid layering in which intrusive relationships are difficult to discern.

Interplutonic contacts

All interplutonic contacts observed in the Canso area are abrupt and intrusive, except possibly between the Whitehead and Port Howe plutons. Relative ages, particularly along the south coast where exposure is almost continuous, can usually be determined by dyke-xenolith-host relationships (Fig. 13b,c,d). Plutonic xenoliths tend to be equidimensional or lensoid with rounded to subangular corners. Many interplutonic contacts and virtually all pluton-dyke contacts appear to follow fracture-controlled planes. Brittle movement along some of these planes is demonstrated by comminution of the wallrocks and small offsets of intersected structures (Fig. 16). The Whitehead-Port Howe interplutonic contact, which is not exposed, is confined within 20 m at the east end of Raspberry Cove West. However, Port Howe rocks gradually become more like the Whitehead pluton (i.e., increase in muscovite content, decrease in biotite, and decrease in phenocryst grain size and abundance) over a distance of 1.5 km as the contact is approached from the east. Thus, the possibility of a gradational boundary cannot be discounted. No interplutonic contacts were observed in the Forest Hill area.

In the southeastern part of the Canso area, intrusions of units D_{Gb} and D_{Ge} are characterized by the development of widespread plutonic agmatite (units aD_{Gb} and aD_{Ge}), making it difficult to define pluton boundaries at map scale. Plutonic agmatite is shown on the maps wherever the host lithology comprises 50-90% of the intrusion. Unit D_{Gb} plutons are intimately injected by masses of unit D_{Ge} granite ranging from variously oriented planar dykes <1 m thick to mappable intrusions. Unit D_{Ge} plutons contain numerous blocky xenoliths of unit D_{Gb} that vary from <1 to 100 m in diameter. In addition to these lithologies, lesser amounts of up to four other rock types may be present within single outcrops. These include xenoliths of tonalite (unit D_T) and Meguma Group (units CO_G and CO_H), leucogranite pegmatite and aplite dykes, and xenoliths and dykes of other plutons and miscellaneous granitic rock types. Plutonic agmatite is especially well displayed in coastal exposures between Andrew Island and Port Howe.

Age relationships

The relative ages of the granitoid units are based on xenolith-dyke-host relationships found in outcrops (see Fig. 13). The contact relationships observed for each pluton are listed and described in Appendix I. The seven granitoid units are believed to correspond to at least seven episodes of magma emplacement.

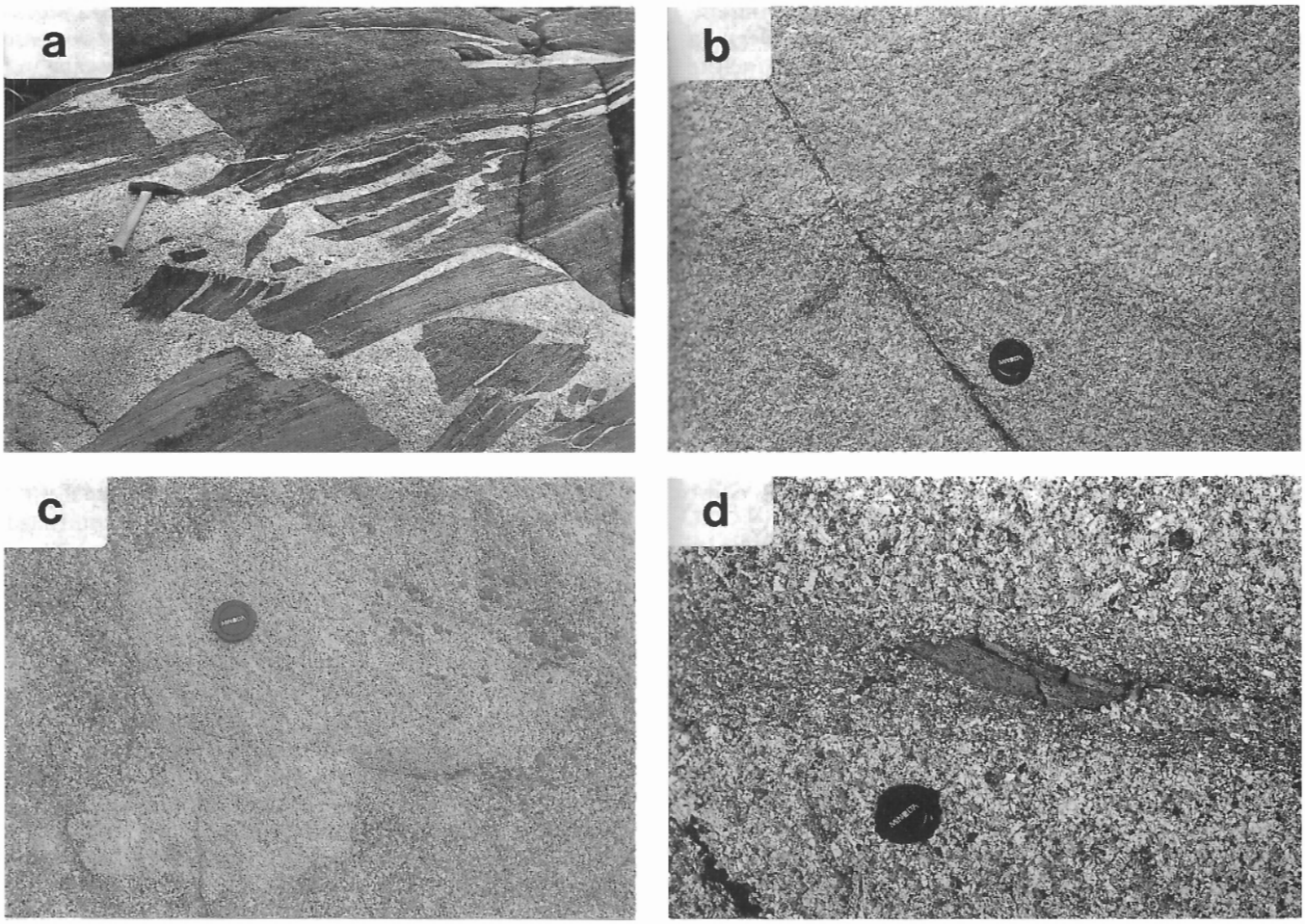

Figure 13. Structures in granitic plutons in the Canso area. (a) Agmatitic contact between undeformed muscovite-biotite granite of the Prices Island pluton (light) and Halifax hornfels, west side of Prices Island. GSC 204509. (b) A 2 m x 3 m xenolith of medium grained biotite-muscovite granite (a miscellaneous granitic lithology) is partly shown in the top half of the photograph. It is crosscut by a dyke of unit D_{Gb} granite (centre) and both phases are enclosed in the Ketch Harbour pluton (unit D_{Ge}-bottom half). Outcrop is at Ketch Harbour Head. GSC 204508. (c) Rounded xenolith of Glasgow Harbour granite (unit D_{Gd}) enclosed in large dyke of unit D_{Ge} at Whistler Point. GSC 204508-CC. (d) Dyke of Ketch Harbour granite (unit D_{Ge}) containing a small xenolith of Goldenville metawacke crosscuts the Madeline Point pluton (unit D_{Gb}) on Little Dover Island. GSC 204508-H.

The inferred sequence of intrusive events is shown in Figure 14. Fifteen plutons have partly or wholly defined age relationships. The remaining 18 plutons have unknown ages and are assigned to specific units based on similarities in composition and texture. The Sheep Island, Gammon Islands, and Buchanans Mountain plutons are assigned to unit D_{Gf} of unknown relative age because they have distinctive lithology and chemistry, unlike any of the other plutons.

Internal igneous structures and pluton shapes

Magmatic structures

Plutonic structures inferred to be magmatic in origin include compositional layering, igneous lamination and lineation, and autoliths. Layering is only visible in some of the clean, relatively undeformed outcrops along the south coast of the Canso area. The best examples occur on Louse Harbour and Whale and White Head islands. Layers are distinguished by the presence of 2-30% additional biotite and 0-5% additional muscovite relative to the host granite (Fig. 15a). In addition, they are locally marked by slightly finer grain size and may lack phenocrysts where they occur in porphyritic granite. Individual layers are 1 cm to 1 m thick and vary from planar to curved and somewhat irregular. They can rarely be traced for more than 20 m along strike and usually occur in groups with 0.1-2 m spacings. Boundaries with the host granite are sharply gradational. Their relative age of formation is demonstrated on the west side of White Head Island where massive granite truncates curved layers and pegmatite dykes crosscut both the massive and layered granite (Fig. 15a). These layers are similar in structure and composition to some of those observed in the South Mountain batholith near Halifax (Smith, 1975).

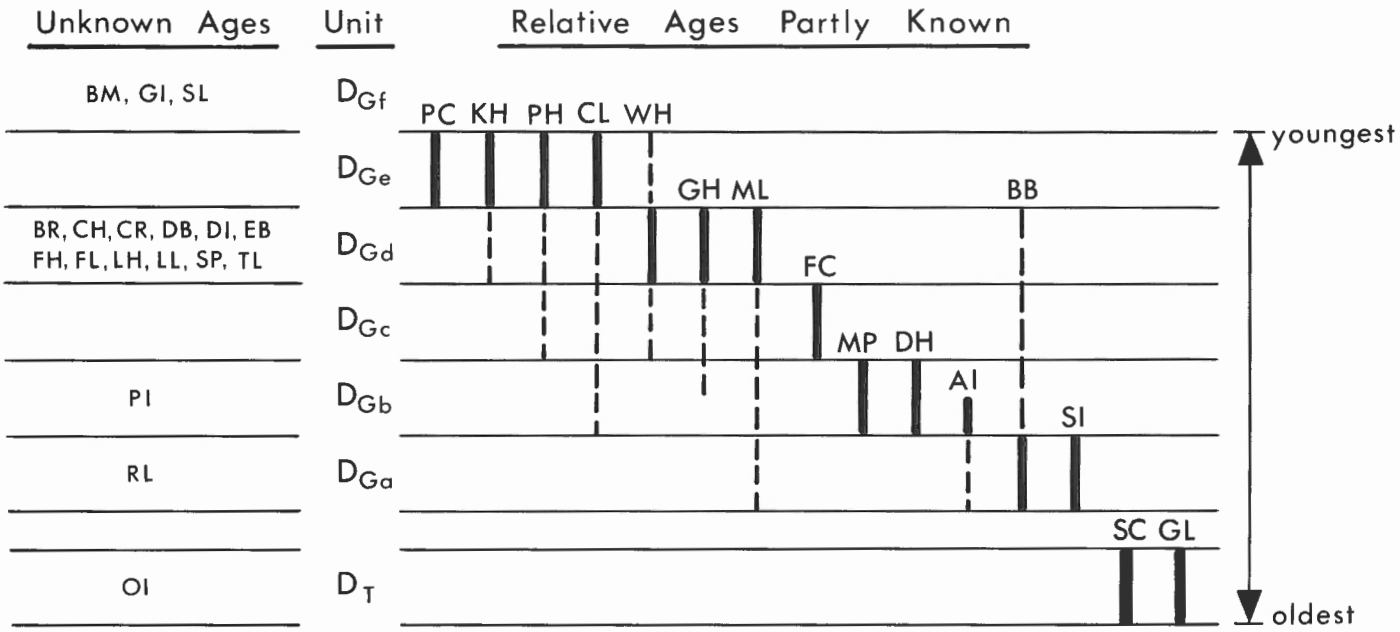

Figure 14. Inferred intrusive sequence based on xenolith-host-dyke relationships in the eastern and southern parts of the Canso area. Interpreted and possible age ranges are indicated by solid and broken lines respectively. Plutons with unknown ages are correlated with the inferred sequence on the basis of composition and texture. The relative ages of unit D_{Gf} plutons are unknown. (See Fig. 9 for two-letter pluton codes.)

Microcline phenocrysts in units D_{Gb} and D_{Ge} locally define a weak and impersistent igneous lamination in the southern part of the Canso area. Strike and dip are variable, even within the same outcrop, although dips less than 35° are prevalent. Layering, lamination, and elongate xenoliths are approximately parallel where they occur together. Microcline phenocrysts also define a weak lineation in a few places, which lies in the plane of the lamination. Plunges are generally less than 15°.

Probable autoliths were found at Louse Head in the Snyders Lake pluton and at Flying Point in the Whitehead pluton. They are rounded, up to 5 m long, and virtually identical in composition and texture to the host granite.

Late magmatic structures

Late magmatic and deuteric structures, recognized mainly in the Canso area, include schlieren, orbicules, monomineralic clots, and miarolitic cavities. Schlieren are common and well displayed on the west side of White Head Island. They are composed of 10-100% quartz, biotite, and/or muscovite (Fig. 15b). Boundaries with the host granite range from abrupt to sharply gradational. They are 0.1-10 cm thick, discontinuous, and can rarely be traced for more than 10 m. The formation of magmatic layers (already described) and schlieren appear to have been part of a continuously evolving process because all gradations between the two structures exist. Two main types of schlieren occur. One type is irregular to strongly curved streaks that bifurcate, merge, and pinch out (see Fig. 15b). They abut against interplutonic and pluton-dyke contacts and appear to be an integral part of the plutons in which they occur. Micaceous schlieren crosscut mica-enriched magmatic layers on the west side of White Head Island. The other type is regular, planar fracture fillings (<1 cm thick) that locally crosscut individual igneous crystals. On White Head Island, a fracture filling passes along strike into normal granite at one end and into a magmatic layer at the other end.

Spherical orbicules, 2-4 cm in diameter, form up to 30% of the Snyders Lake pluton at Louse Head. They are unlayered (proto-orbicules of Leveson, 1966), finer grained, and contain only about one-tenth as much muscovite compared to the surrounding granite. The orbicules were not studied in detail and their origin is uncertain. The lack of sharp contacts and similarity in composition to their host suggest that they formed at either a late magmatic or deuteric stage of crystallization.

Monomineralic clots of coarse grained quartz, biotite, or muscovite occur in a few places in the Dover Head, Madeline Point, Port Howe, Portage Cove, and Whitehead plutons. They are ovoid and range from 1 to 30 cm in diameter. Contacts with the host granite are abrupt to sharply gradational. Miarolitic cavities up to 30 cm in diameter were found at Dogfish Point in the Whitehead pluton, on Shag Ledge in the Gammon Islands pluton, and at Louse Head in the Snyders Lake pluton. They are lined with coarse euhedral crystals of quartz, muscovite, feldspar and tourmaline.

Pluton shapes and sizes

The granitoid plutons vary from <1 to 40 km² in plan view. They are about equidimensional in areas where

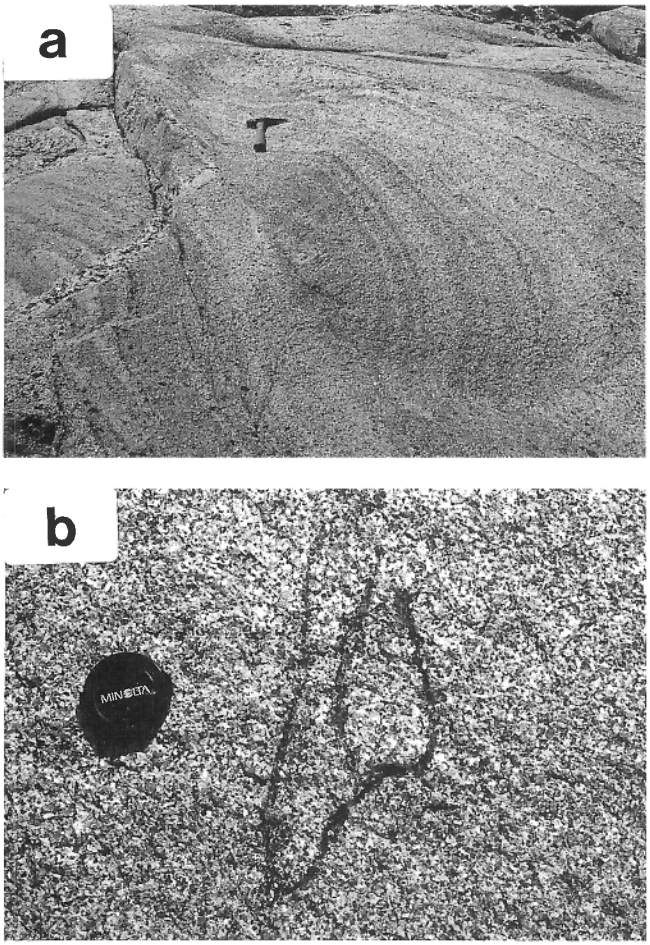

Figure 15. Comparison of magmatic and late magmatic structures in granitic plutons in the Canso area. (a) Wavy magmatic layers in the Whitehead pluton on the west side of White Head Island. The layers are truncated by massive granite at lower right and crosscut by a pegmatite dyke on left. GSC 204508-U. (b) Irregular streak containing nearly 100% biotite in the Gammon Islands pluton. GSC 204508-I.

post-granite deformation is weak or absent. Where post-granite strain is intense, plutons are commonly elongate. The most obvious example is the Costley River pluton, which is highly elongate (flattened?) parallel to the Black Lakes shear zone in the Forest Hill area (see Fig. 10). Contacts with the country rocks observed at the surface dip moderately to steeply both inward and outward. In addition, diamond drilling by Sulpetro Minerals in 1981 (NSDME[1]) has shown that the southeast corner of the Lumsdens Lake pluton dips about 60° to the south to a depth of 40 m.

Miscellaneous plutonic rocks

Small dykes, xenoliths, and undefined masses of various types and ages of granite that cannot be assigned directly to units D_{Ga} to D_{Gf} are associated with some of the granitic plutons. These are described to illustrate the complexity of the intrusive history of the area. Abbreviations are used for biotite (bi) and muscovite (ms) with subscripts to indicate visually estimated modal percentages.

a) Quartz-bearing syenite occurs in the Fogherty Lake and Lumsdens Lake plutons on the east side and 2 km west of Indian Cove. It forms poorly defined zones up to several tens of metres across that are gradational with the host granite over 1 cm. The syenite is nearly identical to the granite except for slightly finer grain size and the presence of only about 5% quartz. The two syenite zones would lie in close proximity if inferred displacement along the dextral transcurrent fault in that area was removed. (The syenite bodies associated with the Fogherty Lake and Lumsdens Lake plutons are designated as FLs and LLs in Appendices III and IV.)
b) Fine grained, buff-coloured bi_1-ms_{3-6} leucogranite intrudes the Durells Island pluton as small masses and dykes between Hog and Welsh islands. It is locally gradational with pegmatite, which forms numerous dykes in the Durells Island pluton. (The leucogranite is designated as DIa in Appendices III and IV.)
c) Medium grained, granular bi_{3-5}-ms_{5-8} granite (sample 414, Appendix IV) occurs as a few xenoliths in the Madeline Point and Ketch Harbour plutons at Ketch Harbour Head and in the Portage Cove pluton on Pea Island (Fig. 13b). It is similar in lithology to the Glasgow Harbour pluton but differs in relative age.
d) One xenolith of fine- to medium-grained ms_{3-4}-bi_{5-8} granite containing 5-10% microcline phenocrysts ($\leq$1 cm long) occurs in the Prices Island pluton at the northwest corner of Harbour Island.
e) Several small dykes of medium grained, bi_{3-4}-ms_{3-5} leucogranite crosscut the Andrew Island pluton at Black Duck Cove. They may be correlative with the Glasgow Harbour pluton (unit D_{Gdl}).
f) Several dykes of medium grained ms_{3-4}-bi_{6-9} granite (sample 458B, Appendix IV) with a few microcline phenocrysts up to 1.5 cm long intrude medium grained bi_2-ms_{3-5} leucogranite (sample 458A, Appendix IV) on Black Island. The bi-ms leucogranite is tentatively correlated with unit D_{Gdl}.
g) A few xenoliths of medium grained bi_{10} granite were found in the Dover Head pluton about 0.5 km north of Fluid Point. The xenoliths are rounded and up to 5 m in diameter and are the most mafic granitic rocks found in the Canso and Forest Hill map areas.
h) Medium- to coarse-grained, equigranular bi_{1-3}-ms_{2-3} leucogranite (sample 553, Appendix IV) occurs in three places. Dykes up to 4 m thick crosscut the Dover Head pluton on the south side of Dover Island. A small xenolith of the leucogranite was found in the Port Howe pluton on the southwest side of Whale Island. A tabular body that may be a dyke (sample 411C, Appendix IV) is in abrupt contact with the Andrew Island granodiorite at Castle Rock.
i) Isolated outcrops of fine grained, bi_{1-2}-ms_{3-10} leucogranite occur in the Bantry Road and Doctors

[1] Reference denotes assessment files available at the Nova Scotia Department of Mines and Energy, Halifax, Nova Scotia.

Brook plutons in the Forest Hill area. Contact relationships with their hosts are unknown. They are shown as aplite dykes on the map.

j) Medium grained, white-weathering bi_{1-2}-ms_{2-6} leucogranite (Fig. 12c; samples 346A and 384A, Appendix IV) intrudes the migmatitic Oliver Island tonalite pluton. It may be correlative with the Durells Island pluton, although the textures and compositions are a little different.

k) Six sills of felsite from 1 to 5 m thick (samples 236, 253, and 802, Appendix IV) containing small phenocrysts of quartz, feldspar, biotite, muscovite, and garnet intrude the Halifax Formation between Monroe and Doughboy points and farther east in the Canso area. Although they are deformed and their chemical compositions are quite variable, at least three of them are peraluminous and thus are tentatively correlated with unit D_G.

l) A xenolith of medium- to coarse-grained ms_2-bi_5 granite (sample 441A, Appendix IV) occurs in the Portage Cove pluton along the north side of Portage Cove. It is similar in texture to the Andrew Island pluton but is a little unusual in composition.

Pegmatite and aplite

Dykes and irregular lenses of leucogranite pegmatite and minor aplite, ranging from a few centimetres to 5 m thick, intrude the granitoid plutons and adjacent country rocks. They consist of quartz, microcline, plagioclase, 1-30% muscovite, and 0-5% each of garnet, apatite, tourmaline, and biotite. Accessory graphite occurs in pegmatite and aplite at the east end of the Buchanans Mountain pluton in the Forest Hill area. Beryl has been reported in pegmatite intruding the Goldenville Formation north and west of Reynolds Brook in the Canso area (Shaw, 1983; K. Ford, personal communication, 1987) and southwest of Camerons Lake in the Forest Hill area (Schiller, 1963). Andalusite was found in pegmatite south of Costley Lake in the Forest Hill area (Schiller, 1963). Nichols (1976) noted the occurrence of lazulite in a small pegmatite dyke at Spears Head. Some of the dykes are compositionally zoned with quartz-rich centres. Pegmatite is gradational with both aplite and host granite in many plutons. Although several ages of pegmatite and aplite intrusion can be recognized in outcrop based on crosscutting relationships, it was not possible to relate a specific type to any granitic unit.

Generally, pegmatite and aplite constitute less than 1% of the plutonic rocks. They are unusually abundant in three areas:

a) along the boundaries between granitic plutons and metasedimentary country rocks and xenoliths, especially in agmatitic zones in the Goldenville Formation (unit aCO_G) developed around Dover Basin, Chapel Gulley, and close to the Guysborough County fault;

b) in the Durells Island and Rocky Lake plutons where pegmatite dykes locally form up to 75% of individual outcrops; and

c) in the Whitehead, Port Howe, Ketch Harbour, and Madeline Point plutons where northwest-trending pegmatite and aplite dykes are common and in the Portage Cove and Andrew Island plutons where variously oriented dykes locally form up to 20% of individual outcrops.

In areas where post-granite deformation is strong, dykes are commonly transposed and boudinaged into discontinuous, tabular to lensoid bodies oriented parallel or at small angles to the dominant tectonic foliation. Where post-granite deformation is weak or absent, dykes generally follow variously oriented planes that appear to be fracture-controlled. Movement during or after intrusion is demonstrated by offset of one dyke along another (Fig. 16a) and by displacement of opposite dyke walls (Fig. 16b). Granite bordering open fractures associated with, and parallel to, dyke sets is locally comminuted.

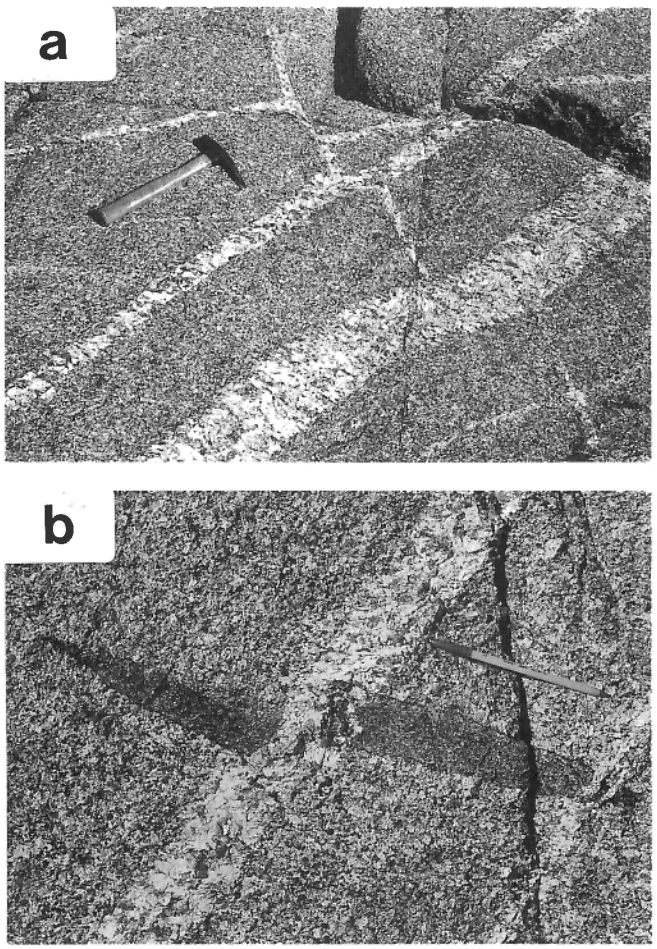

Figure 16. Structural relationships between pegmatite dykes and the Andrew Island granodiorite pluton on the northeast side of Andrew Island. (a) At least three ages of dyke intrusion are suggested by dextral and sinistral displacements along dyke walls. The regular planar orientations of the dykes suggest that emplacement was controlled by pre-existing fractures in the host granodiorite. GSC 204508-G. (b) A Goldenville metawacke xenolith, oriented parallel to S_{2b}, is sinistrally offset along a pegmatite dyke. S_{2b} crosscuts both the dykes and the host granodiorite. GSC 204508-Z.

Quartz veins

Quartz veins containing one or more of accessory muscovite, tourmaline, and microcline occur in many granitic plutons but are common only in strongly deformed plutons, such as along the Harbour Island shear zone where they are up to 2 m thick. They are relatively rare and less than 1 m thick in undeformed granitic rocks and generally crosscut the latest igneous phase in any particular outcrop. However, more than one age of emplacement has occurred, as shown on the east side of Louse Harbour Island where quartz veins that intrude the Dover Head pluton are, in turn, crosscut by dykes of the False Cove pluton. Elsewhere, quartz veins intrude plutons younger than the False Cove pluton. The genetic association of quartz veins and pegmatite-aplite dykes is demonstrated by gradational boundaries between the two and by the fact that both follow the same northwest-trending fracture set in the southern part of the Canso area.

PETROGRAPHY AND CHEMISTRY OF THE GRANITOID PLUTONS

General statement

This section describes the petrography, mineral compositions, and rock chemistry of the granitoid rocks. In all cases, the freshest and least deformed samples were selected from each pluton for modal and chemical analysis. However, data for many of the plutons still partly reflect deuteric alteration and metamorphic recrystallization. Despite the many modal and chemical data obtained, the results are inadequate for detailed description of internal compositional variation within individual plutons. Rather, this overview gives average modal and chemical compositions for the 33 plutons. This approach, although neglecting details, is considered valid as most of the intrusions are lithologically homogeneous at map scale. (Lithologic inhomogeneities in plutons are described in Appendix I.)

Pluton modal compositions

Average modes for the 33 plutons are given in Table 3. They were determined by point-counting stained thin sections rather than rock slabs because of complex textural relationships and the presence of small grains in many samples. Although deuteric alteration products form 1-10% of most samples, they were counted as their igneous parent minerals wherever possible. Counts were accumulated using one to six separate samples for each pluton to alleviate some of the problems associated with coarse grain size. However, the results should only be considered as approximate, particularly for plutons in units D_{Gb} and D_{Ge}, which contain large microcline phenocrysts.

Plagioclase, quartz, and biotite are essential minerals in the three tonalite plutons (unit D_T). In addition, muscovite and hornblende are important in the Oliver Island and Garry Lakes plutons respectively. These rocks are similar to tonalite associated with the southern plutons (see Fig. 1). Both suites are variably deformed, contain biotite and hornblende-bearing varieties, and are locally migmatitic (Rogers, 1986). However, unlike the eastern Meguma Terrane, the southern plutons include rocks as mafic as plagioclase-rich peridotite and norite (Albuquerque, 1979). Furthermore, the Oliver Island tonalite, which plots on the tonalite-granodiorite boundary in Figure 17, is distinguished by an unusually high muscovite content. However, the Oliver Island pluton is migmatitic and highly deformed and the high muscovite content may reflect contamination or metamorphism rather than an original igneous composition.

Quartz, microcline, plagioclase, biotite, and muscovite are essential minerals in the 30 granitic plutons (unit D_G). Amphibole has not been found. They plot in a diffuse cluster centred in the monzogranite field (Fig. 17). The Andrew Island pluton in unit D_{Gb} and all three plutons in unit D_{Gf} plot within or along the boundary of the granodiorite field[1]. In terms of quartz and feldspar only, unit D_G plutons are similar to the Musquodoboit batholith but are much more restricted in composition than the southern plutons and South Mountain batholith (Fig. 17). Neither muscovite-cordierite-biotite granite, which is the dominant lithology in the Musquodoboit batholith (MacDonald, 1981), nor porphyritic biotite mesogranodiorite, which is abundant in the South Mountain batholith (McKenzie and Clarke, 1975), have been recognized in the Canso and Forest Hill areas.

Accessory minerals recognized in the granitoid plutons are listed in Table 4. Apatite occurs as relatively large subhedral to euhedral grains and is by far the most common accessory phase, forming 0.1-0.5% of most rocks. Zircon and monazite, although relatively low in abundance, occur in all the plutons. Garnet is rare, except in the Andrew Island and Mahons Lake plutons where it is readily visible in most hand specimens. Sillimanite, ilmenite, and cordierite(?) generally occur together in small amounts in relatively undeformed rocks in the southern part of the Canso area. Andalusite, which is a common accessory in the South Mountain and Musquodoboit batholiths (Clarke et al., 1976; MacDonald, 1981), was not identified. However, Schiller (1963) found andalusite in pegmatite near Costley Lake and McKenzie and MacGillivary (1974) noted its occurrence in the Tom Lake pluton. The remaining accessory minerals were recognized only in a few thin sections.

Mineral relationships and compositions

Analytical methods and accuracy

Mineral compositions were determined with an energy-dispersive MAC electron microprobe interfaced with

[1] The three plutons in unit D_{Gf} are muscovite-rich, have albitic plagioclase, and are chemically akin to granite. For these reasons, they are referred to as leucogranite.

Table 3. Approximate average pluton modes for the Canso and Forest Hill areas. Alteration products are counted as the host mineral wherever possible (e.g., chlorite after biotite).

Canso area

	Pluton name and mode[d]										
	Al[e]	BB[e]	CH[e]	CL[e]	DH	Dl[e]	FC	FH	FL[e]	GH[e]	Gl
qz	28.1	30.7	22.9	40.2	26.9	31.1	27.6	35.2	32.8	28.1	36.0
mi	19.8	24.4	38.9	27.7	34.5	25.2	27.3	23.5	23.9	26.7	16.1
pl	42.7	32.4	32.3	21.4	24.5	32.2	33.1	30.3	33.2	31.3	34.3
hb											
bi	8.2	3.3	1.5	6.1	7.0	4.8	5.6	2.7	2.8	3.7	1.4
ms	0.9	8.7	4.4	4.4	5.0	6.5	6.3	7.9	6.9	10.1	12.2
ac[a]	0.4	0.4	0.0	0.2	1.1	0.2	0.2	0.4	0.3	0.1	0.1
cts[b]	1114	1080	1024	1259	1490	1048	1265	1529	1006	1343	1059
area[c]	16.6	12.4	8.0	16.6	20.7	12.4	12.4	20.7	12.4	16.6	8.3

	KH	LH[e]	LL[e]	ML[e]	MP	Ol*	PC	PH	Pl	SC[e]	Sl[e]
qz	31.7	31.9	31.1	30.5	21.9	36.3	37.4	32.5	30.7	27.2	33.6
mi	31.6	15.9	23.9	31.1	36.6	4.6	27.6	32.7	32.1	2.5	23.5
pl	24.9	29.2	31.8	29.8	30.3	37.5	24.0	25.1	25.5	47.1	30.9
hb											
bi	6.7	8.7	2.5	1.0	5.7	13.2	6.2	5.7	5.2	22.2	2.7
ms	4.7	13.6	10.4	7.6	5.1	8.0	4.3	3.5	6.5	0.3	9.3
ac	0.5	0.8	0.2	0.1	0.5	0.3	0.6	0.6	0.1	0.8	0.2
cts	1118	1017	1095	1000	1369	1368	1254	1948	1165	1050	1167
area	16.6	8.3	12.4	6.0	24.8	12.4	16.6	24.8	16.6	16.6	16.6

Forest Hill area

	SL	WH	BM[e]	BR[e]	CR[e]	DB[e]	EB	GL[e]	RL[e]	SP[e]	TL[e]
qz	34.1	35.4	27.3	30.3	28.4	28.1	33.2	22.2	29.3	31.9	37.5
mi	17.8	22.3	22.1	24.5	24.1	24.1	22.1	1.6	22.3	25.9	23.7
pl	37.3	33.8	40.7	32.5	32.8	31.5	32.8	48.8	34.5	35.5	26.6
hb								3.9			
bi	0.7	2.4	0.0	5.6	5.2	6.9	2.9	23.3	1.8	4.3	1.8
ms	10.0	6.0	9.2	6.9	9.3	8.7	8.4	0.0	11.5	2.2	9.8
ac	0.2	0.1	0.7	0.3	0.3	0.7	0.6	0.4	0.7	0.2	0.7
cts	1378	1314	1026	1585	1148	1059	1222	2048	1020	1312	1537
area	8.3	20.7	6.0	24.8	16.6	12.4	12.4	11.0	6.0	16.6	12.4

a) ac = accessory minerals
b) cts = number of points counted
c) area = total sample surface area counted (in cm^2)
d) Pluton names and locations are given in Figure 9
e) Mode which includes partly or wholly metamorphosed rock

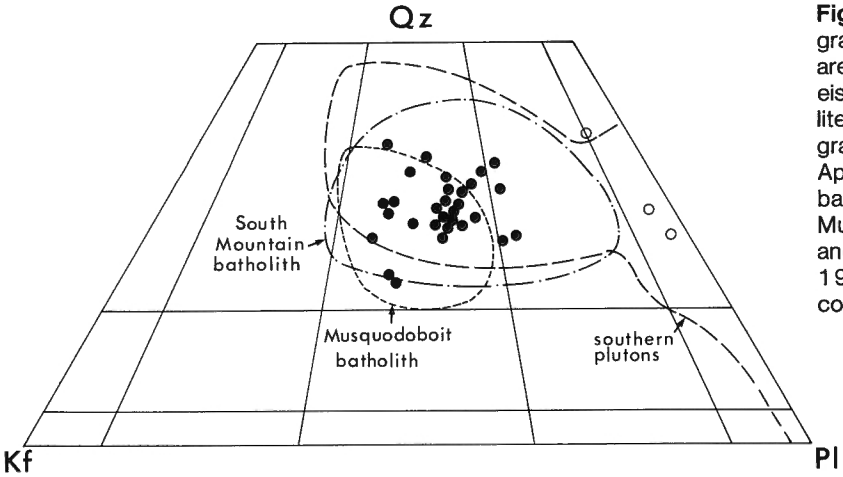

Figure 17. Average modal compositions of 33 granitoid plutons in the Canso and Forest Hill areas, using the classification triangle of Streckeisen (1976). Plagioclase includes albite. Tonalite plutons are shown with open circles and granitic plutons are shown with closed circles. Approximate fields for the South Mountain batholith (McKenzie and Clarke, 1975), Musquodoboit batholith (MacDonald, 1981), and southern plutons (Albuquerque, 1977, 1979; Rogers, 1986) are shown for comparison.

Table 4. List of accessory minerals recognized in each plutonic unit in the Canso and Forest Hill areas

Unit	Accessory minerals[a]
D_{Gf}	Apatite, monazite, zircon, allanite, ilmenite (GI)[b], pyrite (BM)
D_{Ge}	Apatite, monazite, zircon, ilmenite, sillimanite, cordierite(?), garnet, tourmaline, sphene, fluorite (KH)
D_{Gd}	Apatite, monazite, zircon, garnet, ilmenite, sillimanite, rutile (DI), tourmaline (FL), cordierite(?) (FH), sphene (WH), spinel (WH)
D_{Gc}	Apatite, monazite, zircon, ilmenite
D_{Gb}	Apatite, monazite, zircon, ilmenite, garnet, sillimanite, cordierite(?), allanite, sphene (MP), anatase (MP)
D_{Ga}	Apatite, monazite, zircon, allanite, garnet (BB), tourmaline (RL), sphene (RL), ilmenite (RL)
D_T	Apatite, ilmenite, zircon, monazite, sphene, augite (GL), epidote (SC), garnet (SC)

a) Accessories are given in approximate order of decreasing abundance
b) The pluton name is given in brackets for minerals found only in one pluton

automated data correction and reduction. More than 350 analyses of plagioclase, microcline, biotite, muscovite, ilmenite, garnet, spinel, hornblende, and cordierite(?) were determined in 27 samples. Each analysis is an average of one to six spot measurements of single grains. (Representative analyses are given in Appendix II.) The least deformed rocks and least altered grains from each pluton were used wherever possible. Accuracy was checked by periodic analysis of known standards. Mean relative deviation from accepted values is approximately $\pm 1\%$ at the 10% concentration level and $\pm 5\%$ at the 1% level. Except where specifically indicated, all textures described below apply to relatively undeformed granitoid rocks.

Plagioclase

Plagioclase typically occurs as subhedral decussate laths, although in detail some grain boundaries are highly irregular. It is the only essential mineral that has a recognizable igneous habit. Albite and Carlsbad twinning and diffuse oscillatory zoning with both normal and reversed zones are common in the most pristine rocks. Most plagioclase grains are cloudy because of the presence of small decussate laths of secondary muscovite and dispersed microgranules of iron oxide. Where plagioclase lies in contact with microcline, locally it contains myrmekitic blebs of quartz. Small inclusions of biotite and accessory minerals are common but minor features. Generally, plagioclase does not show the effects of remobilization, which are characteristic of other rock-forming minerals. Instead, plagioclase is commonly cross-cut and replaced by microcline, mica, and quartz (e.g., Fig. 18a). An exception was found in one thin section from the Dover Head pluton where a microveinlet of plagioclase transects microcline.

Plagioclase in the tonalite plutons is generally oriented parallel to the tectonic foliation and may be metamorphic in origin. It varies from An_{24} to An_{52} (Fig. 19), which is almost identical to the compositional range of $An_{26\text{-}51}$ in tonalite associated with the southern granitoid plutons in southwest Nova Scotia (Albuquerque, 1977, 1979). Individual grains are typically zoned with core to rim differences of up to An_{14}.

Granitic plutons contain plagioclase from An_0 to An_{29} (Fig. 19). These compositions are slightly more sodic than the maximum values of $An_{30\text{-}35}$ found in granite and granodiorite in the South Mountain batholith (McKenzie and Clarke, 1975). Each pluton has a specific range of plagioclase composition, with the most calcic occurring in plutons of units D_{Gb} and D_{Ge}. Unit D_{Gf} plutons contain unusually sodic plagioclase ($An_{0\text{-}1}$). Individual grains are unzoned to strongly zoned with variations of as much as An_{20} from grain cores to rims. Plagioclase compositions in relatively undeformed and moderately to strongly deformed rocks in the Whitehead and Port Howe plutons are compared in Figure 19. No detectable difference was found. Small, clear, equant grains of almost pure albite occur in some rocks containing more calcic plagioclase. They are spatially associated with perthitic microcline grains and appear to be the result of subsolidus exsolution.

Microcline

All the potassium feldspar appears to be microcline, based on the ubiquitous occurrence of well developed cross-hatch twinning, which contrasts with the optical homogeneity of potassium feldspar in the South Mountain batholith. The microcline is perthitic with 1-20% patch and string lamellae. It has two habits, forming equant anhedra similar in size to the other essential minerals as well as 1-15 cm long tabular to blocky phenocrysts that appear subhedral in hand

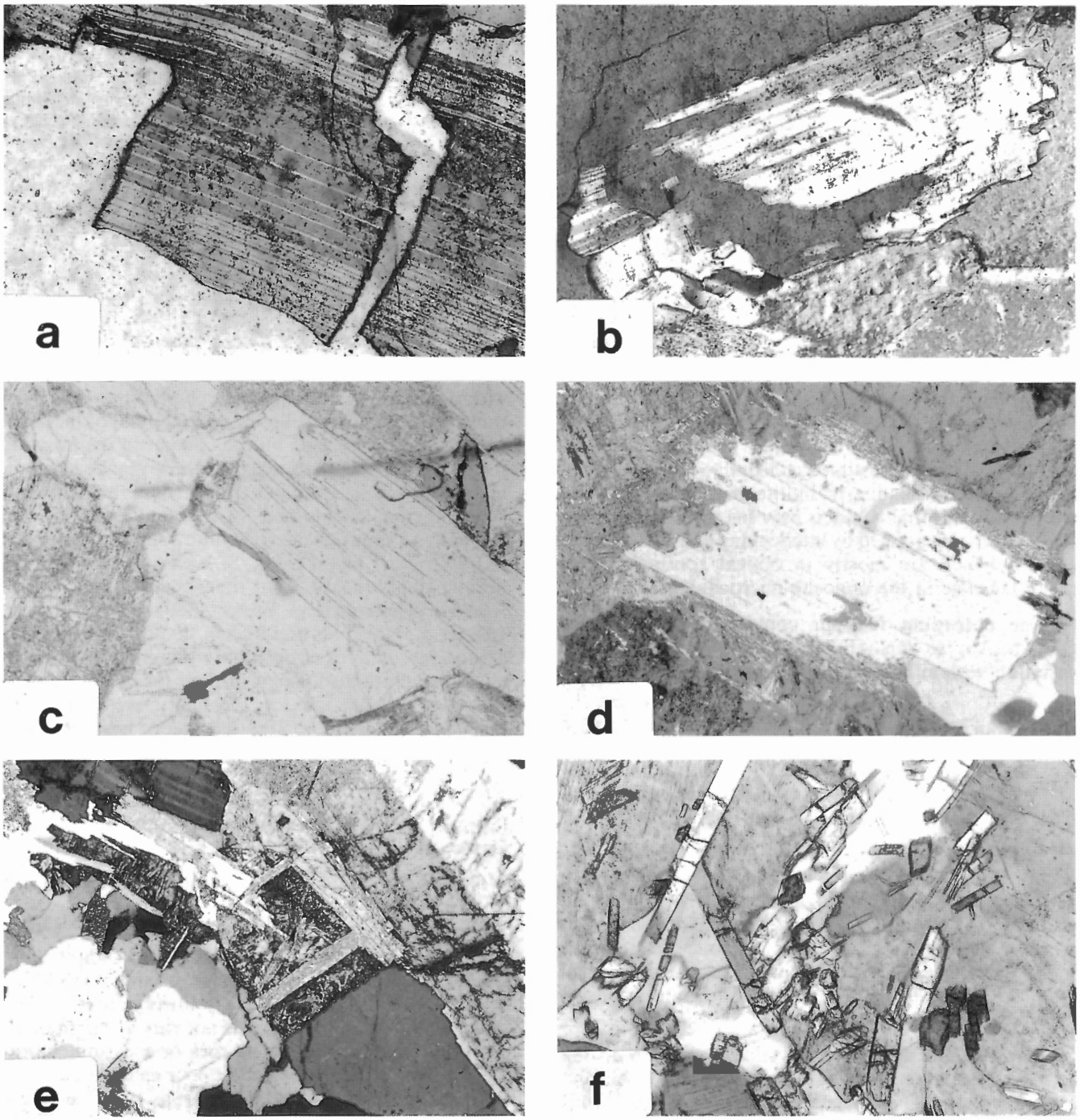

Figure 18. Mineral relationships in weakly deformed to undeformed granitic rocks. Field widths (e.g., 3 mm) and light polarization (plane polarized, oblique or crossed nicols) are given in brackets. (a) Quartz veinlet, in optical continuity with an adjacent quartz grain, crosscuts and replaces a plagioclase lath along a kink plane boundary, Sloans Pond pluton (6 mm; X-nicols). (b) Microcline (dark grey) protrudes into and replaces a plagioclase lath in the Doctors Brook granite (6 mm; X-nicols). (c) Primary-looking muscovite lath (right centre) in biotite-muscovite granite from the Flagstaff Hill pluton (4 mm; ppl). (d) Secondary muscovite lath (centre) with spongy terminations and very fine grained marginal laths replaces adjacent feldspar, Whitehead pluton (2 mm; oblique nicols). (e) Smectite pseudomorph (dark grey, centre) after cordierite(?) in muscovite-biotite granite from the Port Howe pluton (3 mm; X-nicols). (f) Acicular sillimanite crystals crosscut quartz and feldspar in muscovite-biotite granite from the Portage Cove pluton (1.2 mm; ppl).

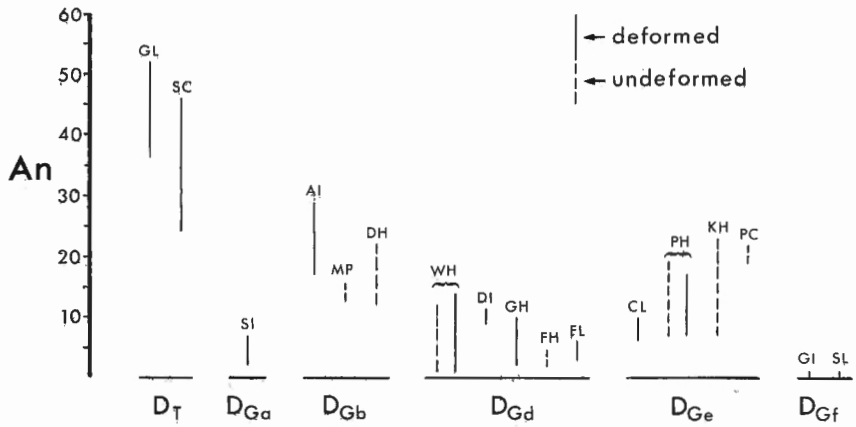

Figure 19. Compositional ranges of plagioclase determined by microprobe analysis of 26 samples from 17 plutons. Ranges reflect both compositional zoning in individual grains as well as inter-sample variation within plutons. Only primary-looking, relatively unaltered grains were analyzed, although samples varied from essentially undeformed to strongly deformed.

specimen. In thin section, both grain boundaries of phenocryst and groundmass microcline are highly irregular, penetrating and locally replacing adjacent plagioclase (Fig. 18b). Larger grains, especially phenocrysts, enclose scattered euhedral to anhedral inclusions of plagioclase, quartz, biotite, muscovite, ilmenite, and apatite. Mutual contacts between microcline grains are commonly separated by interlocking granules of albite (An_{0-3}), which are mostly in optical continuity with albite lamellae in the opposite microcline grain.

The potassium feldspar component ranges from $Or_{80}Ab_{18}An_2$ to $Or_{95}Ab_5An_0$, showing no systematic variation with either sample or pluton composition.

Biotite and muscovite

Although a continuum of mica habits occurs in the granitoid rocks, three main types can be defined using textural criteria outlined by Speer (1984) as follows:

Primary-looking. These large (0.1-1.0 cm) subhedral laths occur singly or in clusters (Fig. 18c) and locally contain subhedral inclusions of plagioclase, microcline, and accessory minerals. The term primary-looking is used to indicate habit only and carries no genetic connotation. In actual fact, as discussed in " . . . Tectonic history . . . " all mica grains have undergone extensive subsolidus recrystallization.

Secondary. Small decussate laths and clusters of radiating acicular crystals (generally <1 mm long) occur within and replace feldspar. This category includes spongy to fibrous terminations of primary-looking laths that project into feldspar grains (Fig. 18d) and very fine grained mica filling microfractures that crosscut quartz and feldspar. Although both biotite and muscovite exhibit these textural variations, they are much more common with muscovite. They occur in both undeformed and deformed rocks.

Metamorphic. Large augen (≤1 cm long) and small laths (generally 0.01-0.1 mm long) are commonly kinked and define a tectonic foliation in deformed granitoid rocks. The augen may be remnants of original primary grains.

Biotite varies from pale yellow brown to dark red brown and is locally altered to chlorite. Total chloritization is restricted to fault zones. Most of the biotites fall within the field of normal biotite compositions in granitic rocks (Fig. 20). They follow a general trend of increasing Fe/Mg with decreasing biotite content in the host rock (i.e., from tonalite to muscovite-biotite granite to biotite-muscovite granite to muscovite leucogranite). Biotite in the Gammon Islands and Snyders Lake plutons (unit D_{Gf}) has an unusual siderophyllite composition characterized by very high Fe/Mg, Si, and Al. It is atypical of normal granitic rocks, being more comparable to biotites found in pegmatite (e.g., Foster, 1960) and hydrothermal veins (e.g., Nockolds and Richey, 1939). Although there are too few data for rigorous interpretation, biotite composition cannot be distinguished on the basis of textural type (i.e., primary-looking, secondary, metamorphic) in individual samples (Fig. 21a) or degree of host rock deformation (Fig. 21b). Several workers have shown that, in specific cases, Al^{iv} in biotite varies systematically with Al/Na + K + 2Ca (Clarke, 1981) or associated mineralogy (Speer, 1981). Similar variation was not detected in the Canso area (Fig. 22).

Muscovite in unit D_G has an average composition of

$$X_{1.94}(Y^{2+}{}_{0.32}Y^{3+}{}_{3.66})(Si_{6.34}Al_{1.66})O_{20}(OH)_4$$

It shows little variation from sample to sample and is similar to the average muscovite in granitic rocks (Miller et al., 1981), except for slightly lower content of Y^{2+} ions. Fe/Mg in muscovite does not vary sympathetically with either Fe/Mg in the host rock or coexisting biotite, although this finding may reflect poor analytical accuracy at low concentration levels. Miller et al. (1981) and Speer (1984) noted that primary-looking muscovite in granitic rocks is commonly enriched in titanium. Titanium content in muscovite in unit D_G is quite variable and shows no systematic enrichment in primary-looking relative to secondary and metamorphic grains (Fig. 23).

Hornblende

Hornblende is restricted to parts of the Garry Lakes pluton (unit D_T) in the Forest Hill area. It forms subhedral, equant to prismatic grains partly altered to secondary amphibole. Pleochroism is pale brown to dark olive green. (A representative analysis is given in Appendix II.)

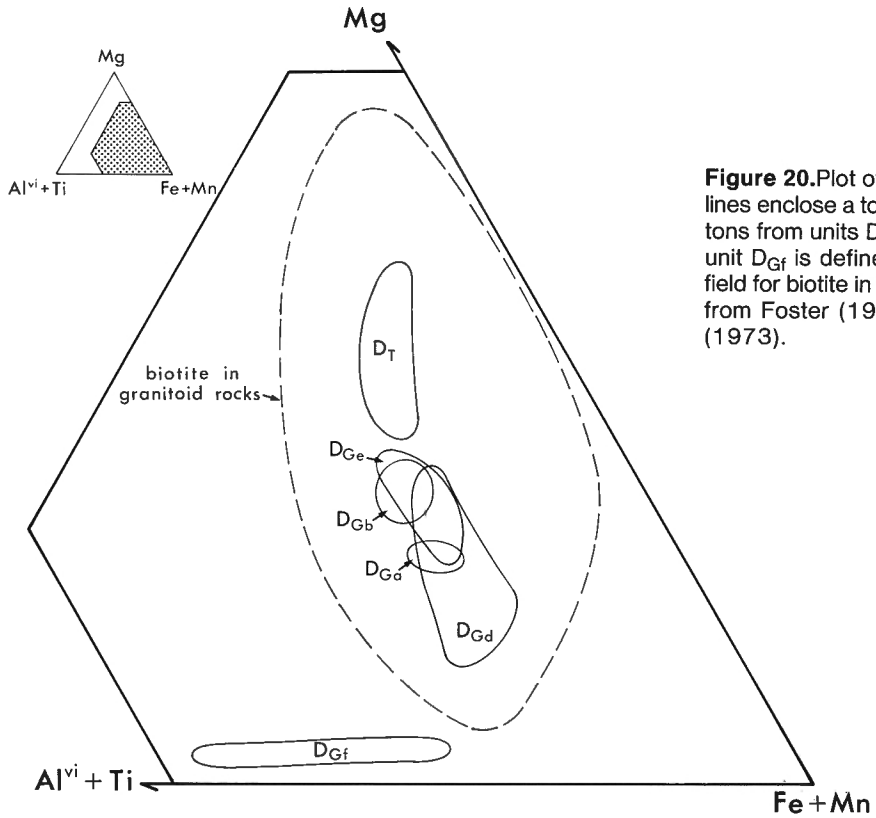

Figure 20. Plot of Y-site cations in biotite. Solid lines enclose a total of 81 analyses from 17 plutons from units D_T and D_{Ga} to D_{Gf}. The field for unit D_{Gf} is defined only by two analyses. The field for biotite in normal granitoid rocks is taken from Foster (1960) and Neilson and Haynes (1973).

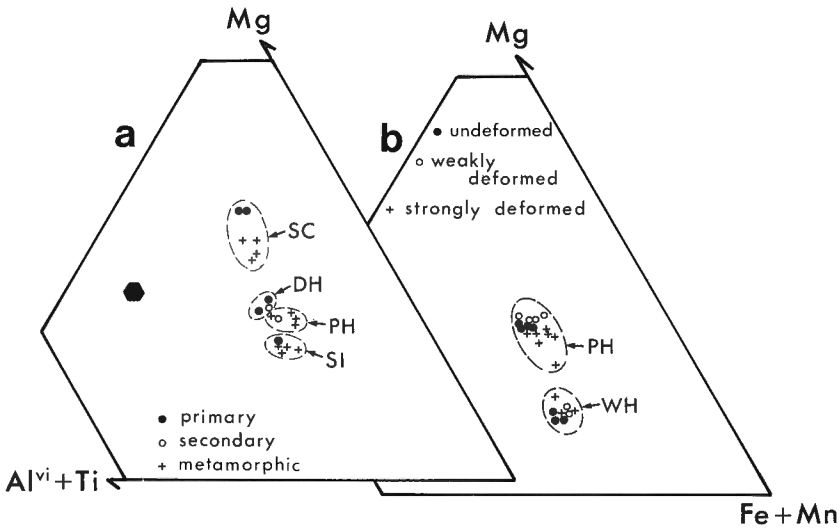

Figure 21. Plots of Y-site cations in biotite. (a) Comparison of primary-looking, secondary, and metamorphic biotite in the Shag Cove, Dover Head, Port Howe, and Sheep Island plutons. Solid hexagon shows compositional variation due to analytical error. (b) Comparison of biotite in undeformed, weakly deformed, and strongly deformed rocks in the Port Howe and Whitehead plutons.

Accessory minerals

Accessory minerals usually occur in clusters associated with biotite and as inclusions in essential minerals. Grains are generally subhedral to euhedral and 0.01-0.5 mm in diameter. Garnet is an exception, occurring as cracked, rounded, inclusion-free grains up to 3 mm across. One grain from the Andrew Island pluton was analyzed. It is $al_{67}sp_{23}py_{10}$ zoned to slightly higher Mn/Fe in its rim. Garnet in the South Mountain batholith, inferred to be of magmatic origin, has a much lower spessartine content (Allan and Clarke, 1981). One grain of green spinel was found in the Whitehead pluton. It is a hercynite-gahnite solid solution, similar to spinels found by Farley (cited in Clarke et al., 1985) in altered aplite and pegmatite in the South Mountain batholith. Ilmenite is the only opaque oxide that has been identified. It has variable but relatively high amounts of MnO, ranging from 2.6 to 8.6%. A pale brown nonpleochroic material that forms scattered equant anhedra (0.1-0.5 mm in diameter) in the Port Howe, Dover Head, Flagstaff Hill (rare), Ketch Harbour, Madeline Point, and Portage Cove plutons was identified as smectite by X-ray diffraction (Fig. 18e). (An

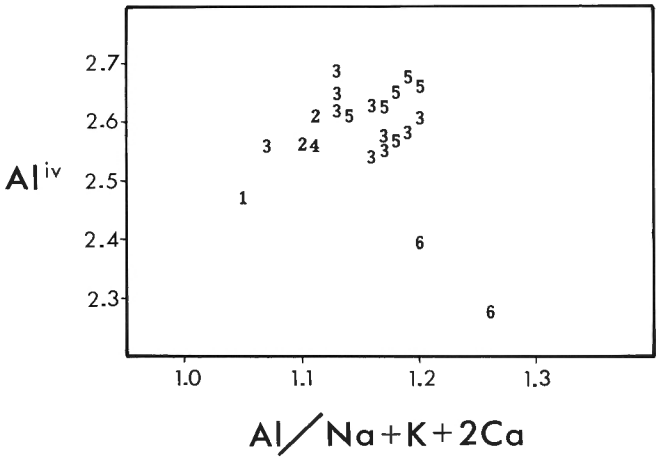

Figure 22. Variation in Al^{iv} in biotite with Al/Na+K+2Ca in the host rock. Numbers correspond to granitoid rocks with biotite + hornblende (1), biotite only (2), biotite + muscovite (3), biotite + muscovite + garnet (4), biotite + muscovite + cordierite(?) (5), and essentially muscovite only (6).

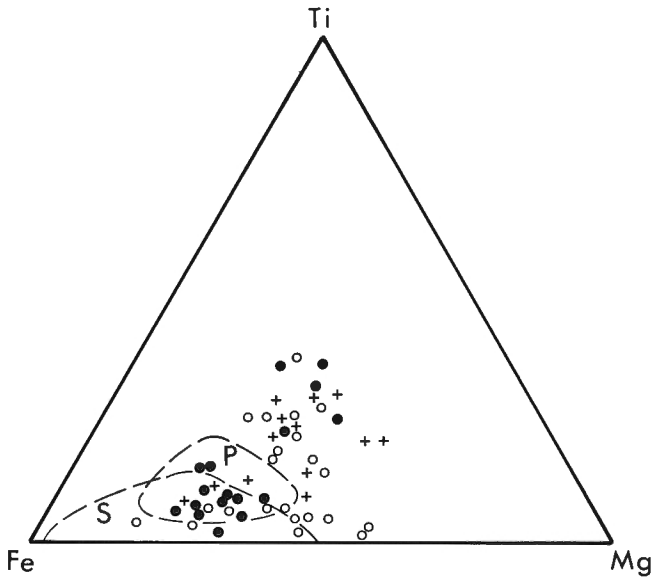

Figure 23. Ternary plot of primary-looking (solid circles), secondary (open circles), and metamorphic (crosses) muscovite compositions in granitic rocks from the Canso area. Dashed lines enclose fields of primary (P) and secondary (S) muscovite defined by Miller et al. (1981) and Speer (1984).

average analysis is given in Appendix II.) The smectite is commonly surrounded and crosscut by secondary laths of muscovite and green biotite. Although its origin is uncertain, the smectite grains are interpreted to be pseudomorphs after cordierite. Despite the widespread occurrence of both garnet and cordierite(?), they were not found together. Sillimanite occurs as acicular euhedral crystals that crosscut all essential minerals without regard to grain boundaries or crystallographic planes (Fig. 18f). They transect primary-looking and large secondary muscovite laths and are, in turn, crosscut by microfractures filled with very fine grained secondary muscovite. No compositional change in the host minerals adjacent to sillimanite grains was detected by microprobe analysis.

Pluton chemistry

Analytical methods and accuracy

Chemical analyses of 176 rocks from the 33 granitoid plutons and 25 miscellaneous plutonic rocks (given in Appendix IV) were used to calculate average compositions and CIPW norms for each pluton (given in Appendix III). The average pluton compositions should only be considered as first approximations, especially for those calculated from fewer than five samples.

Samples were 0.3-1.0 kg in size and had weathered surfaces removed. They were pulverized to -200 mesh using a chrome steel mill. This method may have introduced an uncorrected FeO error of +0.05-0.15%. Major elements were analyzed by XRF by X-Ray Assay Laboratories Limited of Don Mills, Ontario. Fe_2O_3 was done by titration. Based on ten replicate analyses of one sample, precision is ±0.5% (relative) at the 70% concentration level and ±5% at the 1% level. Comparison of three samples analyzed by different techniques at three different laboratories suggests that accuracy is about ±2% and ±10% at the 70% and 1% levels of concentration respectively.

Trace elements were determined by a combination of wet chemistry and instrumental methods by Bondar-Clegg and Company Limited of Ottawa, Ontario, and by X-Ray Assay Laboratories. Precision is ±10% at the 100 ppm level. Inter-laboratory results were inconsistent and more data are needed to assess accuracy limits. The absolute values of Ba and Rb should be used with caution.

Rare-earth elements were determined by instrumental neutron activation analysis by X-Ray Assay Laboratories. They estimate precision at about ±10% at levels well above the detection limits.

Effect of deformation on rock chemistry

Many of the chemical analyses used to calculate average pluton compositions were obtained from variably deformed and metamorphosed rocks. The effects of deformation and metamorphism on chemical composition were tested using samples from the Whitehead and Port Howe plutons, which were collected at varying distances from the Harbour Island shear zone. In general, rocks within 400 m of the centre of the shear zone are strongly deformed and recrystallized, with well developed S-C fabrics. In outcrops, they are very platy, somewhat friable, and rust-stained. Rocks more than 1 km from the centre of the shear zone are very weakly deformed to undeformed. The only sign of recrystallization is minor subgrain formation in quartz.

When selected major and trace elements are plotted against distance from the centre of the shear zone (Fig. 24), no systematic change in element abundance

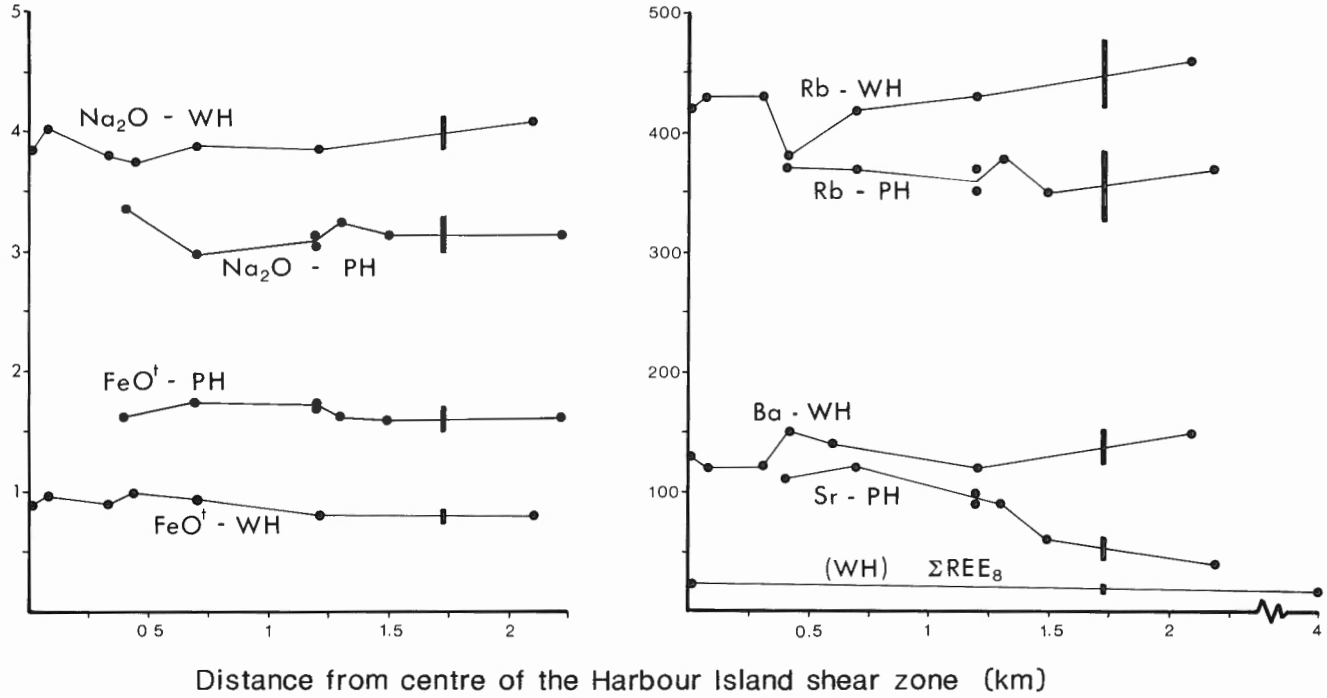

Figure 24. Variation of selected elements in samples of the Port Howe and Whitehead plutons with distance from the centre of the Harbour Island shear zone. In general, samples within 400 m of the centre are strongly mylonitic whereas those more than 1 km from the centre are essentially undeformed. Vertical bars indicate variation due to analytical error.

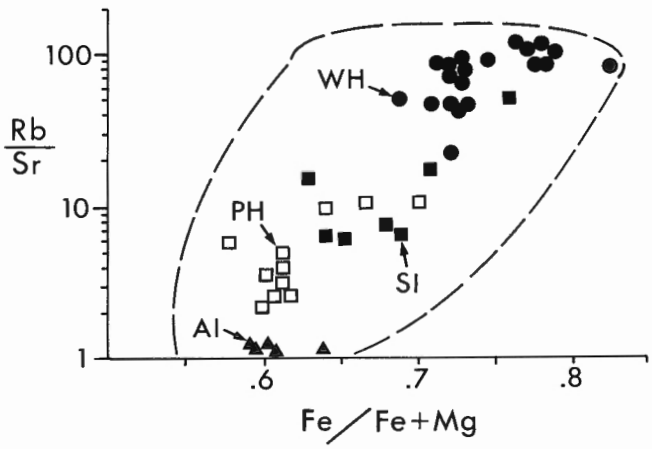

Figure 25. Compositional variation within the Andrew Island, Port Howe, Sheep Island, and Whitehead plutons compared to the total range for granitic rocks in the Canso area (dashed line).

with degree of deformation is evident. The data appear to reflect only minor variation in internal pluton composition and analytical error.

Major and trace element variation

Variation in composition within four intrusions is compared to the total range of granitic rocks in the Canso area (Fig. 25). The Andrew Island, Port Howe, and Whitehead plutons appear to be lithologically homogeneous in the field. The Sheep Island pluton is one of the few to show some heterogeneity, varying slightly in both grain size and biotite content from east to west. Figure 25 demonstrates significant inter-sample variation within single plutons, although some of this variation may be caused by inhomogeneity at hand specimen rather than outcrop scale. However, it is also clear that individual plutons are relatively homogeneous in composition compared to the total group of rocks, a group that is already compositionally restricted.

Major and selected trace elements for the 33 granitoid plutons are plotted against MgO in Figure 26. As expected, the three tonalite plutons (unit D_T) are high in Fe, Ti, Mg, Ca, and Sr and low in P, K, Sn, and Rb compared to the granitic plutons. Their large degree of variation in Si, Al, and differentiation indicators such as Ca and Mg reflect their different mineralogies. The Garry Lakes hornblende-biotite tonalite is the most primitive, being lowest in Si and highest in Mg and Ca. The Oliver Island muscovite-biotite tonalite is the least primitive, with Si content comparable to that in the most felsic granitic plutons. The Shag Cove biotite tonalite is intermediate in composition between the other two.

The 30 granitic plutons (unit D_G) define a rather narrow compositional spectrum, with 70.6-75.5% SiO_2 and 0.1-0.8% MgO. Obvious bivariate trends are evident between Mg and only Ti, Fe, Ba, Sr, and Zr (Fig. 26). The remaining elements (including those analyzed but not plotted) show weak to little correlation with MgO. Even greater variability is revealed if individual samples, including the miscellaneous plutonic rocks, are plotted instead

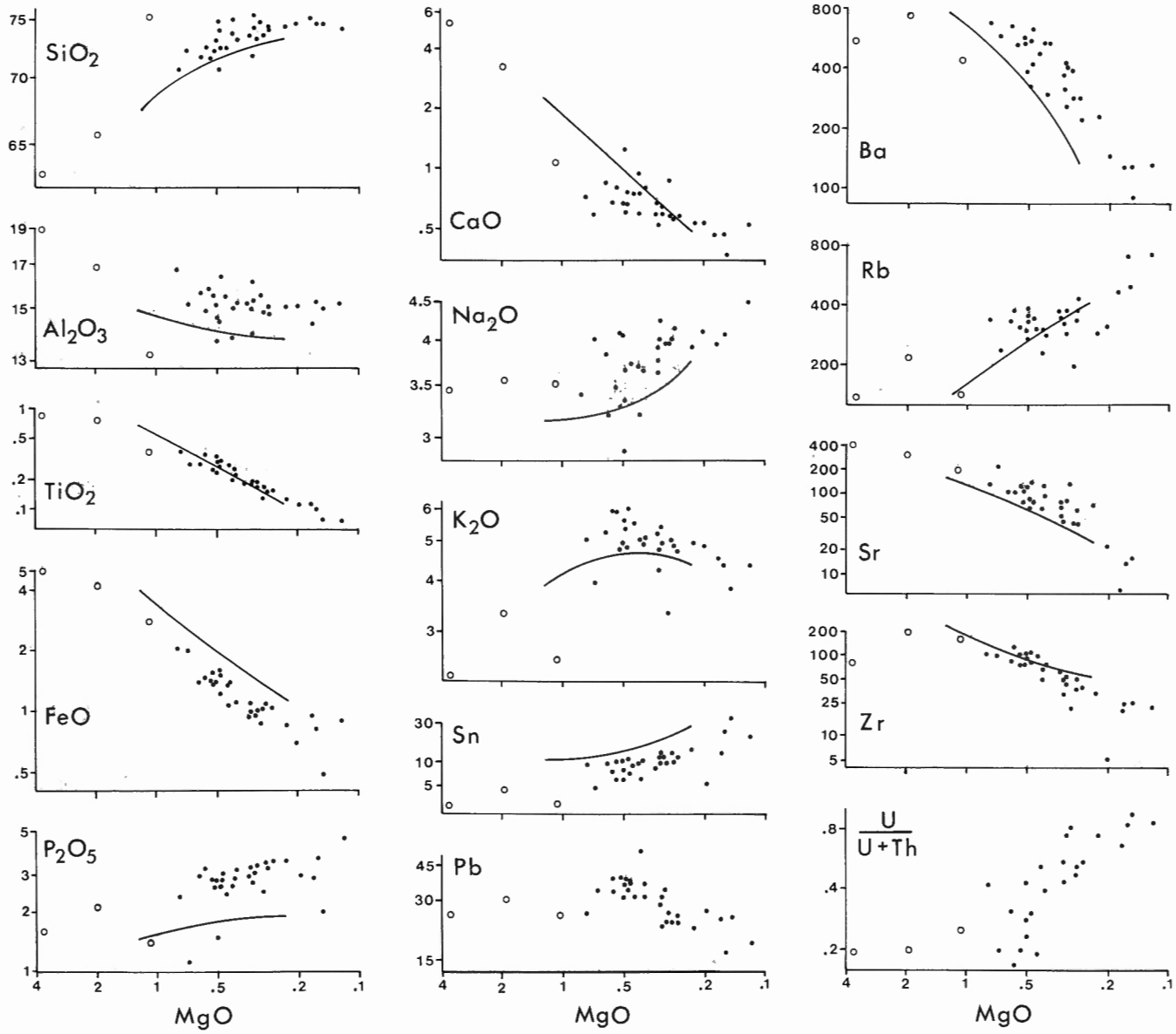

Figure 26. Log-log plots of major and selected trace elements against MgO. Closed and open circles are granitic (unit D_G) and tonalite (unit D_T) plutons respectively, taken from Appendix III. Curved lines define the average compositional trends of the South Mountain batholith (Smith, 1974; McKenzie and Clarke, 1975).

of average pluton compositions. Because of their relatively uniform mineralogy, the chemistry of the granitic plutons depends primarily on the proportions of biotite and muscovite. High-Mg plutons belong mainly to units D_{Gb} and D_{Ge} (i.e., with biotite > muscovite) whereas those with low Mg belong to units D_{Ga}, D_{Gdl} and D_{Gf} (i.e., with muscovite > biotite).

Using a modified ACF diagram (Fig. 27), the granitoid plutons define a relatively simple trend. The Garry Lakes hornblende-biotite tonalite plots within the plagioclase-biotite-hornblende triangle. The Andrew Island and Shag Cove plutons, which contain abundant biotite and almost no muscovite, fall close to the plagioclase-biotite tie-line. As the muscovite to biotite ratio increases in the granitic plutons, the points move increasingly toward muscovite. The interpretation that smectite grains are pseudomorphs after cordierite receives some support from Figure 27. The five plutons in which cordierite(?) is an important accessory plot within the plagioclase-cordierite-biotite triangle.

All the granitoid rocks are peraluminous. Normative corundum is 1.3-2.9% in the tonalite plutons and 1.5-4.8% in the granitic plutons. Unlike the South Mountain batholith, in which normative corundum increases as MgO decreases (McKenzie and Clarke, 1975), normative corundum in unit D_G plutons shows no correlation with MgO (Fig. 28a). The peraluminous nature of the plutons depends mainly on the amount of mica and the muscovite to biotite ratio. Al/Na + K + 2Ca varies from 1.4-1.7 in unit D_T biotites to 1.9-2.3 in unit D_{Gf}

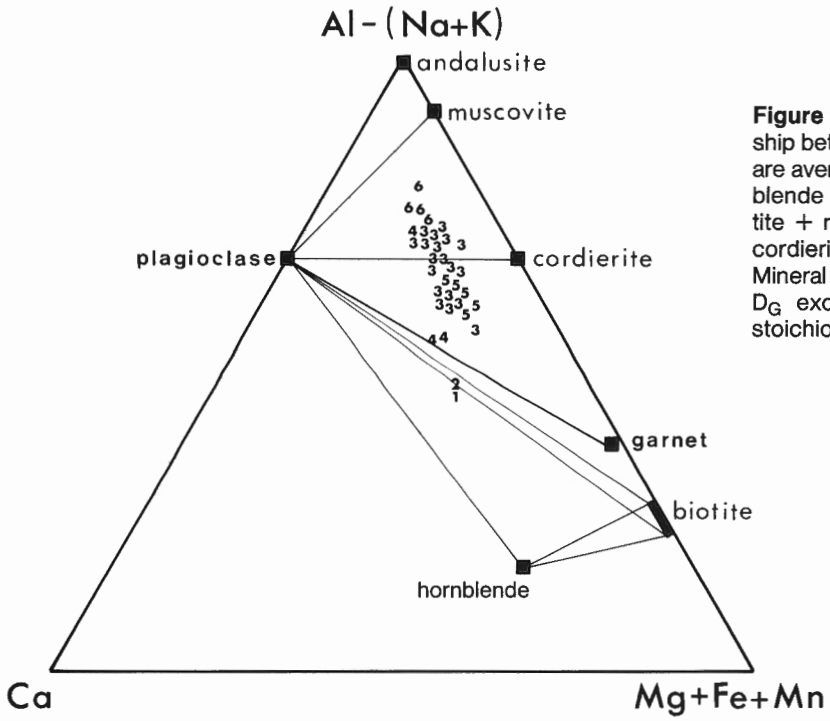

Figure 27. Modified ACF diagram showing the relationship between pluton mineralogy and chemistry. Numbers are average compositions for plutons with biotite + hornblende (1), biotite only (2), biotite + muscovite (3), biotite + muscovite + garnet (4), biotite + muscovite + cordierite(?) (5), and essentially muscovite only (6). Mineral compositions are those observed in units D_T and D_G except for cordierite and andalusite, which are stoichiometric.

siderophyllites to 2.7 in muscovite. Thus, within unit D_T, the Garry Lakes hornblende-biotite tonalite is the least peraluminous (1.3% co), the Oliver Island muscovite-biotite tonalite is the most peraluminous (2.9% co), and the Shag Cove biotite tonalite (2.0% co) is intermediate. Within unit D_G, biotite-rich plutons, such as the Andrew Island pluton, are generally the least peraluminous whereas muscovite-rich plutons such as Rocky Lake and Snyders Lake are the most peraluminous (Fig. 28a). The Lookout Hill pluton has an unusually high normative corundum content because of high total mica (22% mica). The Sloans Pond pluton has unusually low normative corundum because of its small mica content (6% mica).

The level of differentiation of each granitic unit is illustrated in Figure 28b,c using Na/Na+Ca and Rb/Rb+Sr plotted against MgO (N.B.–a single parental magma or source is not implied). Although other differentiation indices could have been used, the results would have been the same. In general, units D_{Gb} and D_{Ge} are the least evolved; units D_{Ga} and D_{Gc} lie at intermediate values and unit D_{Gf} is the most evolved. These values correspond to a general decrease in Mg/Fe and absolute abundance of biotite, increase in muscovite content, and decrease in anorthite content in plagioclase. The wide range of unit D_{Gd} reflects the lithological variety of the intrusions included in that unit, most of which have unknown age. The least evolved granitic pluton of all is the Andrew Island granodiorite (unit D_{Gb}), which contains 8% biotite and 1% muscovite. No simple correlation is observed when the MgO differentiation index is plotted against relative pluton age (Fig. 28d). The resulting pattern in Figure 28d could be even more complicated (but not less so) if the relative ages of all the plutons were known precisely.

Rare-earth elements

Rare-earth element analyses of 28 samples are given in Appendix IV. Representative samples from nine plutons are plotted in Figure 29, showing the complete range in REE contents. They are characterized by moderate LREE enrichment and variably sized negative europium anomalies. Total rare-earth contents (ΣREE_8), slopes (La_N/Yb_N), and europium anomalies (Eu/Eu*) are plotted against MgO in Figure 30. Tonalite plutons do not lie on trend lines for ΣREE_8 and La_N/Yb_N defined by the granitic plutons. They have large but variable total REE contents and highly variable La_N/Yb_N values. Granitic plutons show good positive correlation between MgO and both ΣREE_8 and La_N/Yb_N, which corresponds with a gradual decrease in biotite and increase in muscovite toward lower MgO values. It may also reflect generally lower contents of REE-rich accessory minerals in the more muscovite-rich rocks. REEs in the South Mountain batholith show similar trends (Muecke and Clarke, 1981). However, unlike the South Mountain batholith, the size of the europium anomaly in unit D_G rocks is unrelated to MgO content (Fig. 30).

Isotopic data and geochronology

U-Pb data

All U-Pb isotopic work was carried out by T.E. Krogh at the Royal Ontario Museum. General techniques of sample preparation and analysis are described by Krogh (1973); results are presented in Figure 31. The raw data are available from T. Krogh[1].

[1] T.E. Krogh, Department of Geology and Mineralogy, Royal Ontario Museum, 100 Queen's Park, Toronto, Ontario, M5S 2C6.

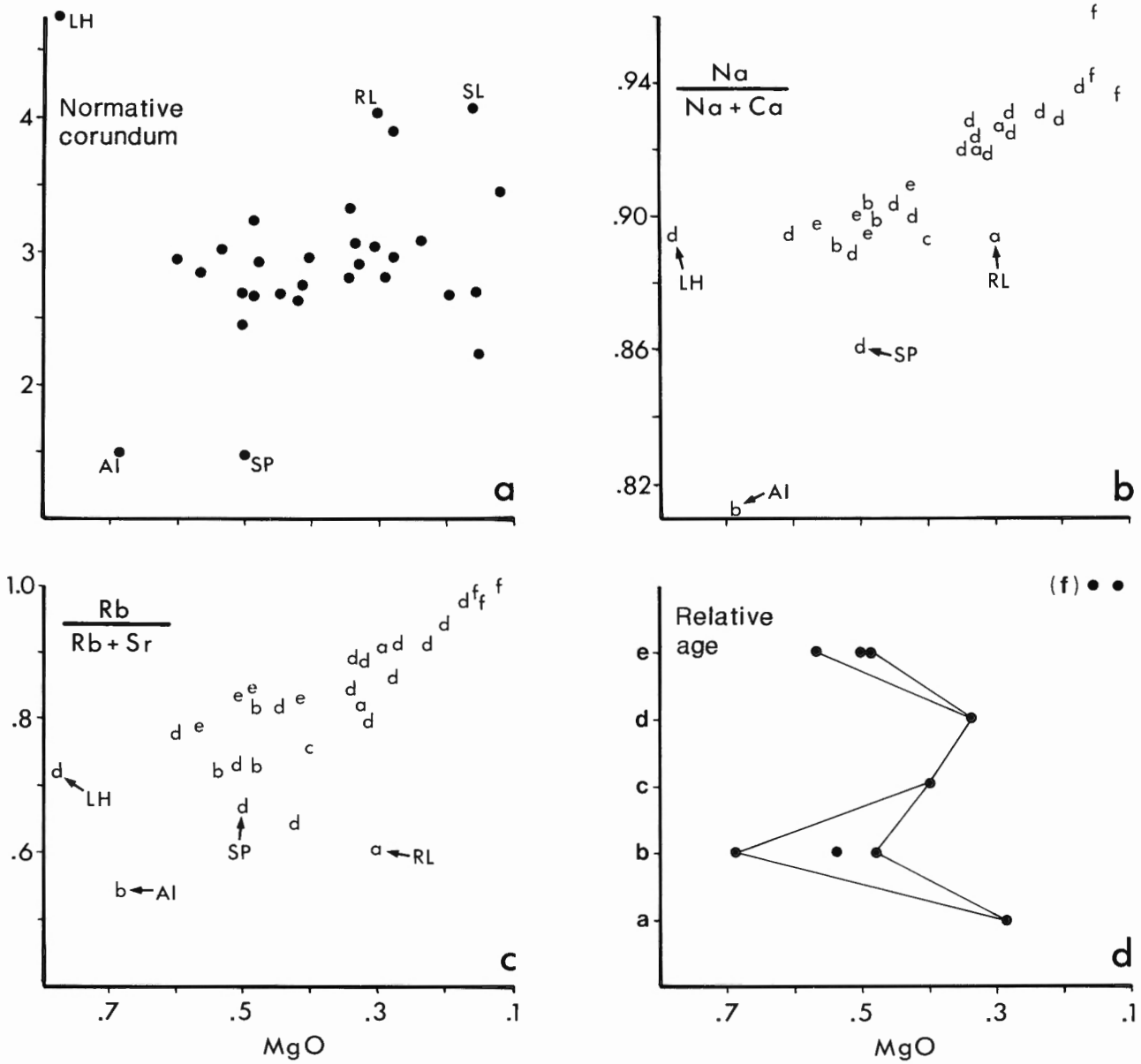

Figure 28. Selected parameters plotted against weight percent MgO for granitic plutons (n = 30). (a) CIPW normative corundum. The Lookout Hill, Andrew Island, Sloans Pond, Rocky Lake, and Snyders Lake plutons are indicated. (b and c) Na/Na+Ca and Rb/Rb+Sr. Small letters indicate the unit of each granitic pluton (e.g., a = unit D_{Ga} pluton). (d) relative age, using only the nine granitic plutons with well established relative ages. Plutons assigned to unit D_{Gf}, which have unknown relative age, are also plotted.

Clear, yellow, euhedral monazite was analyzed from the Sheep Island pluton (sample 606, unit D_{Ga}), Madeline Point pluton (sample 489A, unit D_{Gb}), and Ketch Harbour pluton (sample 492, unit D_{Gc}). Possible sources of contamination and alteration are described in Table 5. The data for 489A are 1.6% above concordia whereas 492 and 606 are concordant (Fig. 31). They define $^{207}Pb/^{235}U$ ages of 371 ± 2 Ma for the Madeline Point pluton, 372 ± 1 Ma for the Ketch Harbour pluton, and 370 ± 3 Ma for the Sheep Island pluton. The data for the three monazite samples overlap within analytical error and hence do not define an age sequence. According to Krogh (personal communication, 1987), the $^{207}Pb/^{235}U$ age is the best indicator of time of magmatic crystallization of these rocks, as monazite is Th-rich and may contain excess ^{206}U.

Clear, colourless zircons were separated from hornblende-biotite tonalite (sample 114B, unit D_{Th}) in the Garry Lakes pluton. The rock is weakly to moderately deformed, relatively unaltered, and contains scattered Goldenville xenoliths and pegmatite dykes. Three types of zircons were analyzed: crack-free euhedral grain tips, abraded crack-free cores, and unabraded cores from cracked grains. All fractions are concordant within analytical uncertainty, defining an age of 378.5 ± 2 Ma.

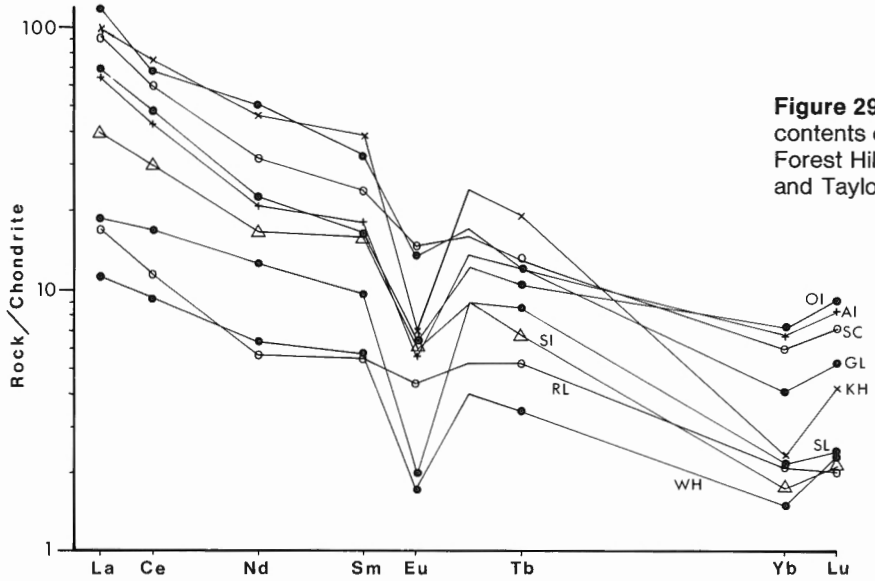

Figure 29. Chondrite-normalized rare-earth element contents of selected granitoid plutons in the Canso and Forest Hill areas. Chondrite values are from McLennan and Taylor (1980).

Zircons have also been analyzed from the Shag Cove pluton. Preliminary evaluation of the data suggest that the Shag Cove and Garry Lakes plutons were essentially coeval.

Rb-Sr data

Rb-Sr isotopic work was completed by R. Theriault at Geological Survey of Canada, and methods of sample preparation and analysis are described by Whalen et al. (1987). Two tonalite (unit D_T) and seven granitic samples (unit D_G) were analyzed. The analytical data are given in Table 6. Samples were selected to encompass a large range of Rb-Sr ratios. Although it was impossible to find pristine rock in perfectly homogeneous intrusions, the least altered and deformed were chosen from each pluton wherever possible and samples were selected to maximize the distances to dykes and xenoliths. Possible sources of contamination and chemical mobilization are listed in Table 5. Rocks with very weak deformation have essentially igneous textures with partial subgrain formation in quartz. Moderately deformed rocks have well developed tectonic foliations defined by recrystallized quartz and mica. Deuteric alteration includes sericitization of feldspar, especially plagioclase, minor chloritization of biotite, and the formation of grain coatings and tiny inclusions of iron oxide in feldspar.

The seven granitic samples (unit D_G) define an inexact line corresponding to an age of 373 ± 24 Ma with an initial $^{87}Sr/^{86}Sr$ ratio of 0.7070 ± 0.0023 (Fig. 32). This age agrees with the U-Pb monazite dates of ca. 372 Ma. The steeper slope of the line defined by the two tonalite samples implies an older age relative to the granitic plutons, assuming that the Shag Cove and Garry Lakes plutons are genetically related. Initial $^{87}Sr/^{86}Sr$ ratios recalculated using U-Pb crystallization ages of 372 Ma for granitic rock and 378 Ma for tonalite are given in Table 6.

STRUCTURE AND METAMORPHISM

General statement

The structure and metamorphism of the Canso and Forest Hill areas are summarized in Table 7. Although their dominant structures are somewhat different, the two areas appear to have been subjected to similar sequences of events, in which three main events are recognized. D_1 is correlated with regional folding and metamorphism in the Meguma Terrane, as defined by Dallmeyer and Keppie (1987). D_2 is attributed to dextral shearing adjacent to the Cobequid-Chedabucto fault system and is subdivided into five phases of deformation (D_{2a} to D_{2e}) as well as periods of static (M_S) and contact (M_K) metamorphism. D_3 includes all brittle deformation that is Carboniferous or younger.

D_1

Tenuous evidence for D_1 is preserved mainly in the southern parts of the two areas where the effects of D_2 are weak or absent. Six separate features point to one or more phases of deformation and metamorphism that predate D_{2a}. They are tentatively assigned to D_1 as all could be related to one tectonic event, although correlation between these features is virtually impossible.

a) Stratigraphic repetition in the Meguma Group implies the presence of east-trending macrofolds. The absence of broad closures suggests that they may be gently plunging. Examples include the syncline-anticline-syncline sequence in the western part of the Canso area (Fig. 4) and the Loon Lake synclinorium in the Forest Hill area (see lower frontispiece). A parasitic macrofold with sinistral vergence on the north side of the Loon Lake synclinorium near Tom Lake is tentatively grouped with D_1 as well.
b) Tight folds with wavelengths of 50-300 m are exposed in Halifax Formation hornfels (unit CO_{Hb}) between the Port Howe and Prices Island plutons in Whitehead Harbour. They are moderately inclined to the

southeast and plunge about 30° to the east-northeast (Fig. 33). Coticules define centimetre-scale parasitic folds on the limbs which plunge 15-45° to the northeast and southwest, suggesting that the larger folds are doubly plunging. A single cleavage, barely visible on weathered surfaces because of the overprinting effects of contact metamorphism, is axial planar to the folds. These structures could be related to either D_1 or D_{2a}, both of which predate granite intrusion and contact metamorphism. However, the lack of pronounced fold asymmetry, which is characteristic of D_2 folds, favours correlation with D_1.

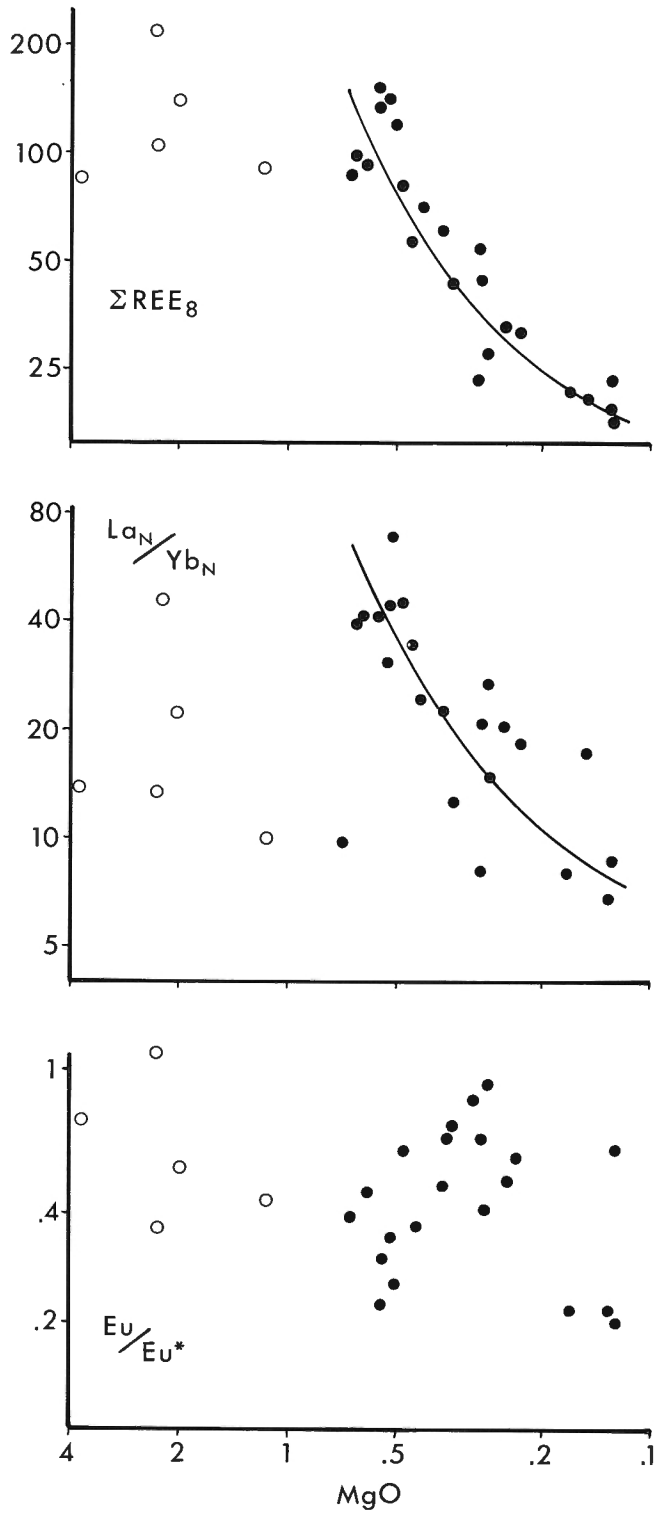

Figure 30. Variation in ΣREE, chondrite-normalized La/Yb, and Eu/Eu* with weight percent MgO. Closed and open circles are granitic rocks and tonalite respectively. Trend lines for the granitic rocks are visually fitted.

c) Goldenville metawacke (unit CO_G) adjacent to, and south of, the East Branch pluton in the southern part of the Forest Hill area is distinguished by a single, weakly developed mica schistosity that is oriented approximately parallel to bedding. Strain-free quartz grains up to 1.5 mm in diameter are common and quartzo-feldspathic laminae have polygonal-granoblastic texture (see Fig. 5a). The schistosity is truncated by small biotite porphyroblasts (correlated with the static metamorphic event). These rocks are texturally distinct from D_2 mylonites farther north, and for this reason the schistosity is correlated with D_1.

d) A transposition foliation, interpreted to be S_{2a}, is well developed in the Halifax Formation in the southwest corner of the Canso area. Near Spears Cove, S_{2a} is represented by a crenulation cleavage that locally preserves remnants of an older foliation (Fig. 34a, inset A). At Poule Point farther south, S_{2a} postdates an older fabric defined by parallel bands of garnet in coticule nodules (see Fig. 3, Hill and Raeside, 1988). These two pre-S_{2a} foliations are interpreted to be S_1.

e) Parasitic mesofolds of coticule beds are common on the limbs of F_{2a} macrofolds near Spears Head. Although most can be correlated with the F_{2a} macrofolds, a few mesofolds show the wrong asymmetry and could be F_1 in age.

f) Straight inclusion trails in the cores of small garnet grains are typically oriented at large angles to S_{2a} in the southwest part of the Canso area (Fig. 34a, inset B). The inclusion trails are parallel to crenulated remnants of S_1 in the single thin section where S_1 was observed. These features suggest that some of the garnet cores formed during or after D_1 but prior to D_{2a}, preserving traces of S_1 as inclusion trails.

The grade of regional metamorphism during D_1 is difficult to determine because of widespread recrystallization during D_2. The only evidence comes from the southern part of the Forest Hill area where S_1 appears to be the sole tectonic fabric. The following assemblage was observed:

quartz + muscovite + biotite ± Ca-plagioclase ± garnet

This assemblage corresponds to upper greenschist to lower amphibolite facies and is in agreement with the grade of metamorphism recognized farther south (Keppie, 1983) where D_2 structures are absent.

D_2–Dextral shearing event

General statement

To place the granitoid intrusions within the structural and metamorphic history of the area, D_2 is subdivided into

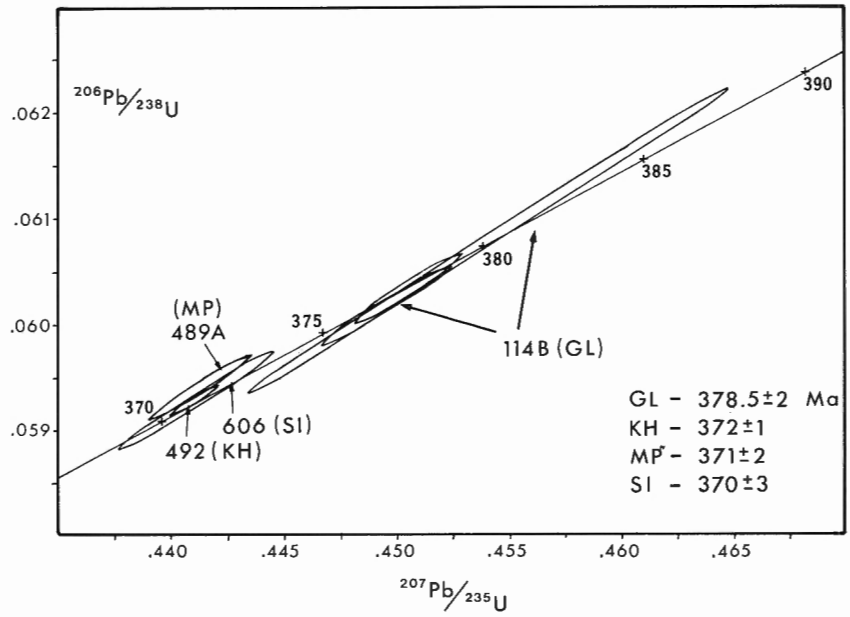

Figure 31. Concordia plot showing monazite fractions from the Sheep Island (unit D_{Ga}), Madeline Point (unit D_{Gb}), and Ketch Harbour (unit D_{Ge}) granitic plutons and three zircon fractions from the Garry Lakes tonalite pluton (unit D_{Th}).

Table 5. Outcrop features where U-Pb and Rb-Sr samples were collected

Sample	Degree of deformation	Deuteric alteration	Granitic dykes	Sedimentary xenoliths	Plutonic xenoliths
114B	Weak	3%	5%	10%	None
275	Weak	2%	1%	1%	10%
489A	Very weak	6%	20%	< < 1%	None
492	Weak	7%	1%	< < 1%	20%
512	Very weak	5%	None	None	None
582	Moderate	5%	1%	None	None
587A	Moderate	4%	5%	None	5%
606	Moderate	10%	< < 1%	None	None
724	Very weak	4%	None	None	None

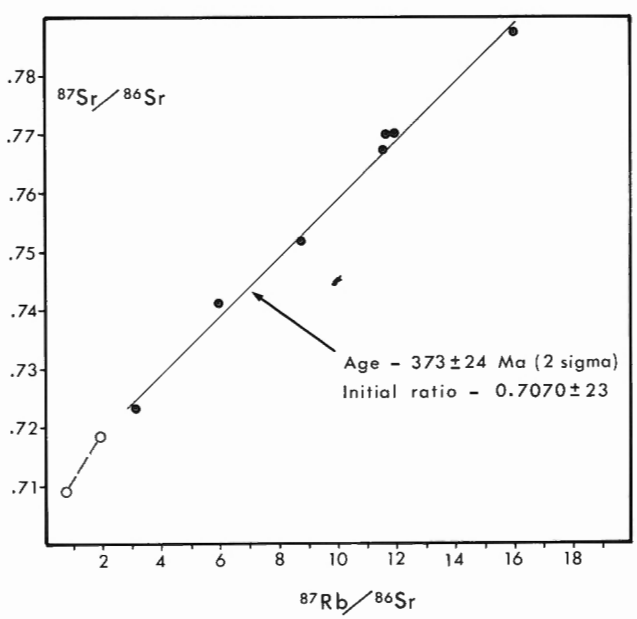

Figure 32. Rb-Sr diagram for seven granitic (closed circles) and two tonalite samples (open circles) from the Canso and Forest Hill areas. (Data are given in Table 6.)

five generations of structures (D_{2a} to D_{2e}) as well as periods of static (M_S) and contact (M_K) metamorphism. Metasedimentary rocks affected by D_2 are characterized by at least three generations of schistosity and intrafolial asymmetric folds with dextral vergence. Granitoid rocks are mylonitic with S-C fabric and subhorizontal lineations developed in areas of high strain. Ductile fabrics were overprinted locally by cataclastic textures as temperature decreased during the late stages of D_2. These features are part of a single event of progressive deformation that began with repeated transposition by isoclinal folding and ended with faulting. Correlation is a significant problem because structures associated with D_{2a}, D_{2b}, and D_{2c} have similar orientations and styles. In this regard, structures are correlated mainly relative to porphyroblast growth (M_S) and granite intrusion, two events that separate D_{2a} and D_{2b} and that appear to be approximately coeval.

D_{2a}

The first phase of D_2 is defined by well developed transposition foliation associated with asymmetric folds having

half-wavelengths ranging from 1 mm to about 100 m. They are mainly preserved in the southwest part of the Canso area. D_{2a} structures are largely obliterated by younger D_2 deformation farther north in the Canso area and throughout most of the Forest Hill area north of the East Branch pluton.

The only macrofolds recognized with certainty lie between Spears Cove and Loon Point (Fig. 34a). The occurrence of paired closures and the dominance of Z-shaped (looking down plunge) parasitic folds indicate dextral vergence. S-shaped mesofolds are confined to the short limbs of larger structures. The folds are defined by

Table 6. Rb-Sr whole-rock isotopic data. $^{87}Sr/^{86}Sr_i$ is the initial ratio calculated at 378 and 372 Ma for tonalite and granite respectively

Sample	Pluton	Unit	Rb(ppm)	Sr(ppm)	$^{87}Rb/^{86}Sr$	$^{87}Sr/^{86}Sr$	$^{87}Sr/^{86}Sr_i$
114B	GL	D_{Th}	83.15	352.6	0.6817	0.709256	0.7057
587A	SC	D_{Tb}	160.9	243.6	1.910	0.717173	0.7069
275	PH	D_{Ge}	294.4	73.78	11.614	0.770115	0.7088
489A	MP	D_{Gb}	248.8	123.1	5.844	0.740128	0.7093
492	KH	D_{Ge}	257.4	84.53	8.801	0.751847	0.7054
512	PH	D_{Ge}	284.0	69.77	11.849	0.771228	0.7087
582	AI	D_{Gb}	163.2	154.5	3.0594	0.722815	0.7067
606	SI	D_{Ga}	288.0	52.06	15.99	0.787461	0.7030
724	FH	D_{Gd}	259.5	65.31	11.48	0.767034	0.7064

Table 7. Summary of the structural, metamorphic, and intrusive history of the Canso and Forest Hill areas

Event	Age (Ma)	Description
D_3		Vertical movement on Guysborough County fault; sinistral transcurrent movement on northwest-trending Country Harbour and Kyak Brook faults; near-surface P-T conditions
	≈360	
D_2		D_{2e}: Riedel shear package of transcurrent faults and brittle-ductile shear zones; rare kink folds and kink bands; lower greendschist facies (and lower?)
		D_{2d}: regionally non-penetrative crenulation cleavages and small open folds; partly overlapped D_{2c} and possibly D_{2b}; lower greenschist facies
		D_{2c}: isoclinal asymmetric folds; east-trending crenulation cleavage and S-C fabric; upper greenschist to lower amphibolite facies
		D_{2b}: isoclinal asymmetric folds; east to NE-trending transposition foliation in metasedimentary rocks and mylonitic S-C fabric in granitic rocks; subhorizontal lineation; overlapped granitic plutonism and static metamorphism; upper greenschist to lower amphibolite facies
	372 ± 1	Granitic plutonism and contact metamorphism (M_K): numerous two-mica granite and minor granodiorite plutons; overlapped D_{2b}; hornblende hornfels facies developed locally
		Static metamorphism (M_S): widespread growth of fibrolite knots and porphyroblasts of biotite, andalusite, cordierite, and staurolite in schistose metapelites; overlapped D_{2a} and D_{2b}; upper greenschist to middle amphibolite facies
		D_{2a}: isoclinal asymmetric folds; east-trending transposition foliation; overlapped static metamorphism; upper greenschist to lower amphibolite facies
	378 ± 2	Tonalite plutonism: intrusion of several small bodies of tonalite; contact metamorphic effects unknown
D_1	≈400	Structures largely obliterated by D_2; kilometre-scale synclines and anticlines inferred from stratigraphic repetition; small folds and schistosity locally preserved where D_2 weak or absent; upper greenschist to lower amphibolite facies

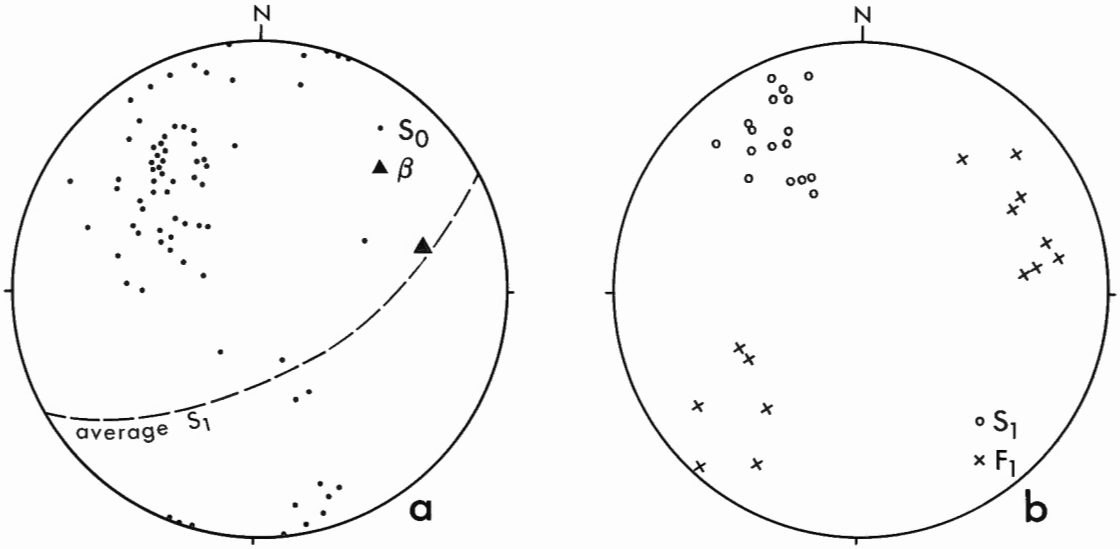

Figure 33. Lower hemisphere equal area projections of structural data from the area between Prices and Burnt islands in Whitehead Harbour. (a) Poles to bedding. (b) F_1 mesofold axes and poles to S_1. (Data taken in part from Eddy, 1987.)

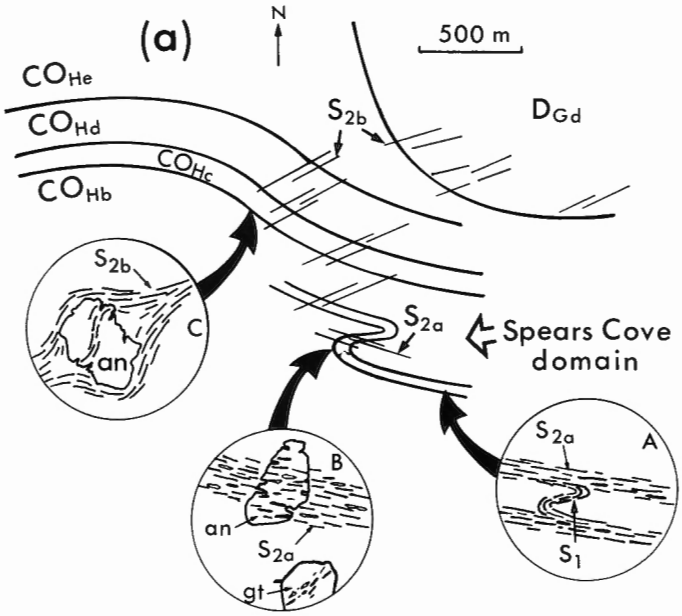

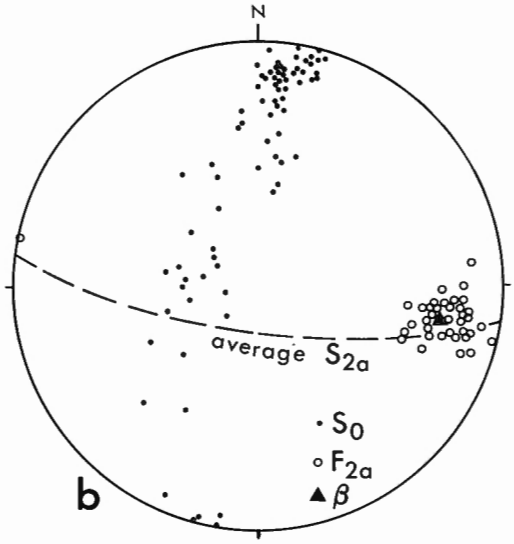

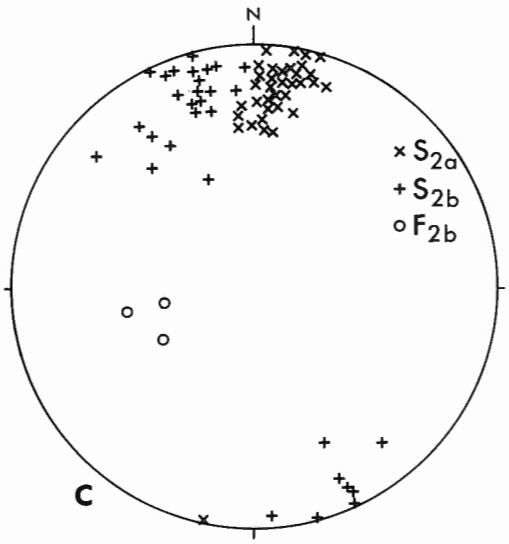

Figure 34. Structural relationships in the area around Spears Cove and Doughboy Point north of Whitehead. (a) Sketch map showing the relationships between F_{2a} (lower right) and F_{2b} folds (centre). S_{2a} transposition foliation locally preserves relicts of S_1 (inset A). Andalusite (an) porphyroblasts overprint S_{2a} whereas garnet (gt) contains inclusion trails oriented at large angles to S_{2a} (inset B). S_{2b} crenulation cleavage deforms porphyroblasts (inset C) and is concordant with a flattening foliation in adjacent granite (unit D_{Gd}). (b) Lower hemisphere, equal area projection of poles to bedding and F_{2a} mesofold axes in the Spears Cove domain. (c) Lower hemisphere, equal area projection of poles to S_{2a} and S_{2b}, and F_{2b} mesofold axes in the Spears Cove domain.

coticule beds and plunge 10-30° to the east (Fig. 34b). Farther south and west, possible F_{2a} mesofolds are indicated by mushroom-shaped interference patterns in coticule nodules (Eddy, 1987) and by the rare occurrence of S-shaped parasitic folds on the long limbs of Z-shaped F_{2b} macrofolds.

S_{2a} transposition foliation, which varies from slaty cleavage to fine grained schistosity (Fig. 35a,c), has been described in detail by Mawer and Williams (1986). It is typically oriented subparallel to bedding and is the oldest tectonic fabric recognized in most outcrops. The domainal nature of S_{2a} is clearly visible in many thin sections where D_{2b} strain is relatively weak. As stated by Mawer and Williams (1986), it is impossible to determine the number of cycles of transposition involved in the formation of S_{2a}. However, only one older fabric (S_1) has been recognized. Variably oriented xenoliths of tonalite (unit D_{Tb}) in granite (unit D_{Ge}) at Haulover Ledge contain a tectonic foliation that appears to be correlative with S_{2a} (see Fig. 12a). The tonalite (dated at ca. 378 Ma, in the previous section) must have been deformed after D_1 (dated at 384-415 Ma, e.g., Dallmeyer and Keppie, 1987) but prior to D_{2b} (which closely followed granite intrusion).

Recrystallization during D_{2b} has made recognition of D_{2a} mineral assemblages difficult. The following are believed to be preserved:

i) quartz + muscovite + chlorite ± albite(?) ± graphite
ii) quartz + muscovite + chlorite + biotite
iii) quartz + Ca-plagioclase + muscovite + biotite ± garnet
iv) quartz + Ca-plagioclase + microcline + muscovite + biotite
v) quartz + Ca-plagioclase + biotite ± microcline

Assemblages (i) to (iv) occur in pelitic rocks in the southwest part of the Canso area where D_{2a} fabrics are locally well preserved; of these, assemblage (iii) is the most widespread. Assemblage (iii) also occurs in a few outcrops north of the East Branch pluton in the Forest Hill area which contain a single domainal schistosity tentatively correlated with S_{2a}. The tectonic foliation in tonalite xenoliths at the south end of Andrew Passage in the Canso area (where D_{2b} is relatively weak) is defined by assemblage (v).

Static metamorphism (M_S)

The static metamorphic event (defined by Keppie, 1983) is recognized in schistose pelitic rocks in the Meguma Group by the occurrence of porphyroblasts of one or more of biotite, andalusite, cordierite, and staurolite as well as knots of fibrolitic sillimanite. Keppie (1983) has assigned garnet porphyroblasts to this event in the Isaacs Harbour area. However, garnet in the Canso and Forest Hill areas is manganiferous and forms small porphyroblasts and matrix-sized grains (Fig. 35b) that appear to have been stable from D_1 to D_{2c}. Although the term "static" is retained here, it is not entirely satisfactory because textural evidence suggests that this metamorphic event overlapped both D_{2a} and D_{2b}.

Biotite is the most widespread porphyroblast (Fig. 35a), forming inclusion-poor subhedral laths up to 0.7 mm long throughout both map areas. Staurolite, which occurs as subhedral poikiloblasts 0.1-0.5 cm in diameter, was found only in five outcrops in the Forest Hill area and in four outcrops in the Canso area. Cordierite and andalusite are common, usually occurring in close proximity. Cordierite forms ovoid anhedra ($\leq$2 cm long) that are filled with tiny inclusions and are commonly altered to green or yellow pinnite. Two types of andalusite are present. Equant subhedral andalusite (0.2-2.0 cm in diameter) is so loaded with small inclusions that it is dark grey in hand specimen and cloudy in thin section (Fig. 35e). It is stratigraphically confined to unit CO_{Hd}. Inclusion-poor, prismatic, subhedral to euhedral andalusite, which is light grey to pink in hand specimen and colourless to pleochroic pink in thin section (Fig. 35c,d), occurs in other members of the Halifax Formation. Prismatic andalusite grains are generally similar in size to the equant variety, although prismatic porphyroblasts up to 12 cm long occur in graphite schist (unit CO_{Ha}) south of Black Point in the Canso area. The pink colour may be caused by Fe_2O_3 contents up to 2.6% (Raeside et al., 1988). Sillimanite was found in one outcrop in the Canso area and in nine outcrops in the Forest Hill area (Fig. 35f).

Textural evidence suggests that porphyroblast and sillimanite growth occurred mainly between D_{2a} and D_{2b}. Where D_{2b} is relatively weak, porphyroblasts are decussate in the plane of S_{2a} and both truncate and overprint S_{2a} (Fig. 35a,c). Sillimanite fibres invariaby crosscut and replace porphyroblasts and S_{2a} mica. Both porphyroblasts and sillimanite are deformed by S_{2b} (Fig. 35d) where the presence of D_{2b} structures is obvious. However, textural relationships in three places where D_{2b} is weak or absent suggest that porphyroblast growth overlapped at least the end stages of D_{2a} as follows:

a) Andalusite porphyroblasts partly truncate, and are partly enveloped by, S_{2a} along the east side of the Northwest Branch of Whitehead Harbour.
b) South of Trout Lake, biotite porphyroblasts have weakly sigmoidal inclusion trails that are concordant at their terminations with S_{2a} in the matrix.
c) At Spears Head and Witch Cove Point, biotite porphyroblasts that truncate S_{2a} are locally kinked, with kinkband boundaries oriented parallel to S_{2a} (Fig. 35a). In the same manner, biotite porphyroblasts 5 km southeast of Stewart Lake (outside the Forest Hill area) overprint and are kinked by a locally developed subhorizontal crenulation cleavage. The crenulation cleavage postdates S_1 and predates S_{2a} (see Keppie, 1983).

Two other lines of textural evidence indicate that both porphyroblast and sillimanite growth overlapped at least the initial stages of D_{2b}:

a) Inclusion trails in cordierite and andalusite porphyroblasts between Whitehead and Doughboy Point are

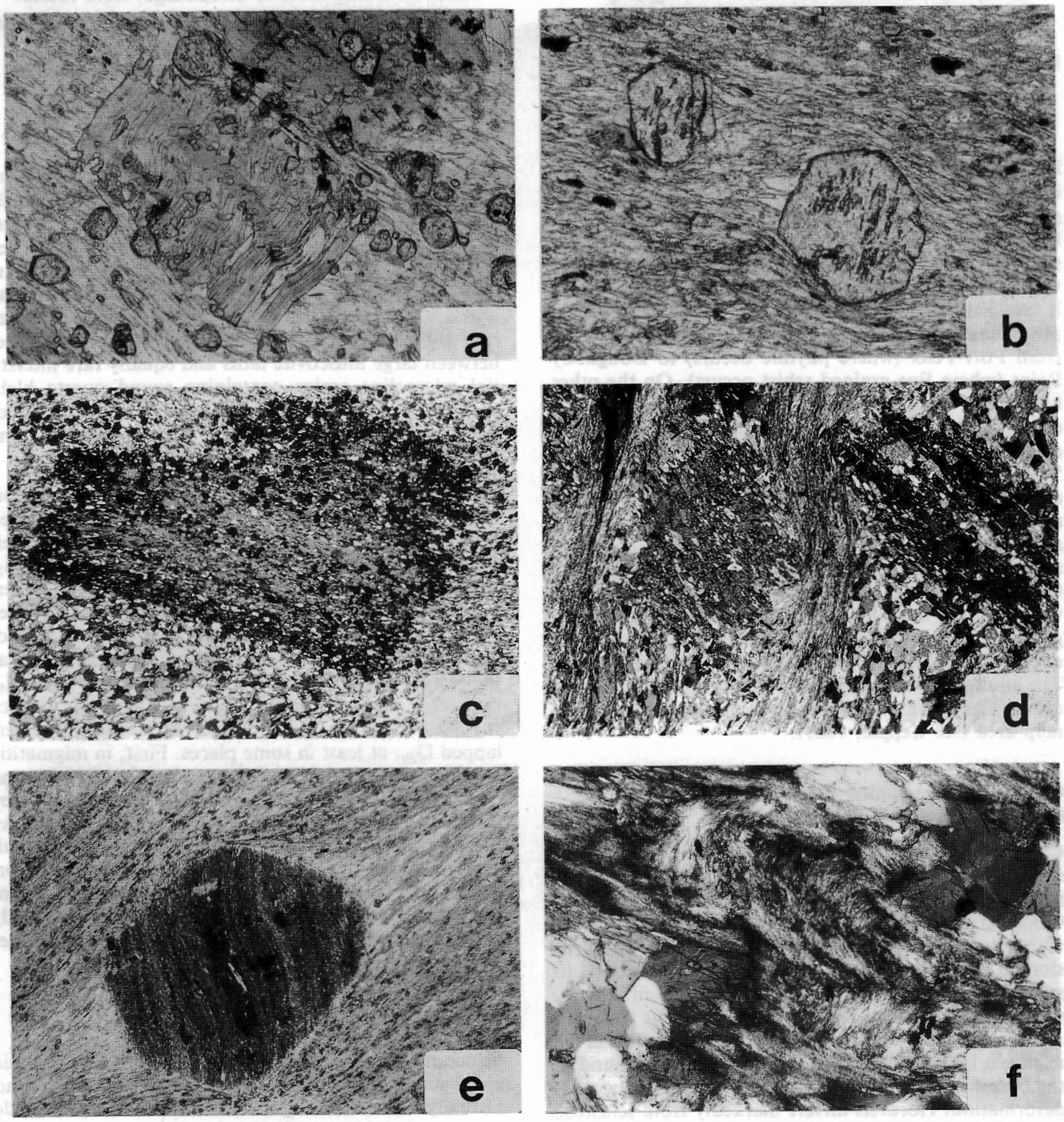

Figure 35. Deformation and metamorphic textures in the Meguma Group in the Canso area. Field widths (e.g., 3 mm) and light polarization (plane polarized or crossed nicols) given in brackets. (a) Biotite porphyroblast (M_S) truncates S_{2a} and has kink band boundaries oriented parallel to S_{2a} in unit CO_{Gb} at Sheep Island near Whitehead (4 mm; ppl). (b) Garnet porphyroblasts in unit CO_{Hb} north of Whitehead. Inclusion trails in the garnet cores are oriented at large angles to S_{2b} in the matrix (2 mm; ppl). (c) Andalusite poikiloblast overprints S_{2a} in unit CO_{Hb} north of Whitehead (3 mm; X-nicols). (d) Two andalusite porphyroblasts (dark grey) overprint an older foliation, inferred to be S_{2a}, and are deformed by S_{2b} crenulation cleavage in unit CO_{He} on the north side of the Northeast Branch. S_{2b} crosscuts the Flagstaff Hill granite 1 m to the north (3 mm; X-nicols). (e) Equant andalusite porphyroblast in unit CO_{Hd} north of Port Felix. Sigmoidal inclusion trails are partly concordant with S_{2b} in the matrix (5 mm; ppl). (f) Fibrolite (centre) in Goldenville schist at the north end of Dover Lake is crenulated by S_{2b} and has locally recrystallized along the crenulation axes (6 mm; X-nicols).

locally sigmoidal and concordant with S_{2b} (Fig. 35e). Other inclusion trails are weakly crenulated, with crenulation axes oriented parallel to S_{2b} in the matrix.

b) At the north end of Dover Lake, sillimanite is crenulated by S_{2b} and new fibres have locally grown parallel to S_{2b} along crenulation axes (Fig. 35f).

The limited areal extent of pelitic rocks and the irregular distribution of porphyroblasts and sillimanite make it difficult to delineate isograds. In general, metamorphic grade increases toward areas containing granitic plutons. For example, cordierite, staurolite, and prismatic andalusite only occur within 0.5-2 km of intrusions along the western side of the Canso area. This limited occurrence is coupled with a gradual increase in matrix and porphyroblast grain size toward the Flagstaff Hill pluton from Port Felix (where phyllite occurs) to Doughboy Point (where fine grained schist occurs). On the other hand, the stratigraphically controlled occurrence of equant andalusite in unit CO_{Hd} appears to be as much a function of composition as metamorphic grade (see "Geology of the country rocks"). Lines marking the first appearance of staurolite and/or cordierite run approximately north-south in the Canso area. This "isograd" also approximates the first appearance of prismatic andalusite (rather than equant andalusite), except near Gaulman Point where prismatic andalusite occurs farther west. In the Forest Hill area, the highest metamorphic grade is marked by the appearance of sillimanite, which occurs at distances of <10 to 300-600 m from plutons. The boundary between greenschist and amphibolite conditions lies south of Stewart Lake, possibly outside the map area (see Keppie, 1983).

Contact metamorphism (M_K) caused by granitic plutonism

Contact metamorphic hornfels are preserved only in the southern part of the Canso area where post-granite deformation is weak or absent. The main exposure lies in unit CO_{Hb} between the Port Howe and Prices Island plutons, with a maximum distance of 300 m to the nearest intrusion. Other hornfels occurrences are restricted to xenoliths (from <1 m long to 350 m by 200 m in size), which are scattered inside several plutons between Andrew Island and Whitehead Harbour. Xenoliths in the northern half of the Canso area and all those found in the Forest Hill area are schistose because of younger D_2 deformation. Hornfels differs markedly from schistose rocks in the same general area, being darker, harder, and denser. They ring and splinter when struck with a hammer. Matrix grain size varies from 0.05 to 1.0 mm, even within the same thin section. Poikiloblasts of andalusite and cordierite, where present, are clear, irregular in shape, and spongy with numerous inclusions of quartz, mica, opaques, and garnet (Fig. 36a). In contrast to andalusite and cordierite porphyroblasts in schistose rocks, which are related to static metamorphism (M_S), the inclusions are commonly coarser than 0.1 mm and include abundant biotite.

The following mineral assemblages were found:

i) quartz + Ca-plagioclase + cordierite + andalusite + biotite + muscovite + garnet
ii) quartz + Ca-plagioclase + biotite + muscovite ± microcline
iii) quartz + Ca-plagioclase + cordierite + biotite + muscovite ± microcline

In addition, half of the hornfels thin sections examined contain fibrolitic sillimanite. The sillimanite typically crosscuts and replaces all minerals listed in assemblages (i) to (iii). The highest grade of metamorphism recognized is indicated in one sample of metapelite collected 0.5 m from the contact with the Prices Island pluton on a small island 500 m northeast of Burnt Island. In this specimen, rare sillimanite fibres are restricted to the boundaries between large muscovite laths and equally rare interstitial microcline grains containing round quartz blebs (Fig. 36b). These relationships suggest formation of microcline and sillimanite at the expense of quartz and muscovite.

In general, granitic intrusion and contact metamorphism, like the static metamorphic event, occurred between D_{2a} and D_{2b}. No evidence was found to suggest that S_{2a} crosscuts any granitic plutons whereas S_{2b} clearly deforms all intrusions in both map areas wherever D_{2b} strain is even moderately strong (e.g., see Fig. 34a). Although the textural relationships are not clearly defined, hornfels textures (related to M_K) appear to overprint static metamorphic porphyroblasts (M_S) between Prices and Burnt islands. Two lines of evidence suggest that plutonism, like static metamorphism, overlapped D_{2b}, at least in some places. First, in migmatitic tonalite (unit D_{Tm}) east of Canso, nearly all aplite and pegmatite dykes (correlated with unit D_G) are sheared by S_{2b}. However, a few partly crosscut F_{2b} folds and have locally intruded parallel to S_{2b} in F_{2b} closures. Second, sillimanite fibres in two hornfels xenoliths in the Port Howe and Dover Head plutons locally define a faint schistosity. Although the surrounding granite is virtually undeformed, the foliation is concordant with S_{2b} farther north and south.

D_{2b}

Structures related to D_{2b} comprise the dominant tectonic elements in most of the metasedimentary rocks and virtually all of the granitoid rocks. They include asymmetric folds at scales ranging from 1 mm to several hundred metres, schistosity in pelitic rocks, S-C fabric in granitoid rocks, mineral lineation, and slickensides. The spatial distribution of D_{2b} structures is shown in Figure 10.

No F_{2b} folds were recognized with certainty in the Forest Hill area. However, Z-shaped macrofolds defined by aeromagnetic data in the core of the Loon Lake synclinorium (see lower frontispiece) may be F_{2b} in age. F_{2b} folds are common in the Canso area. Most are tight to isoclinal and plunge gently to moderately to the east and west. They have dextral vergence except for parasitic folds

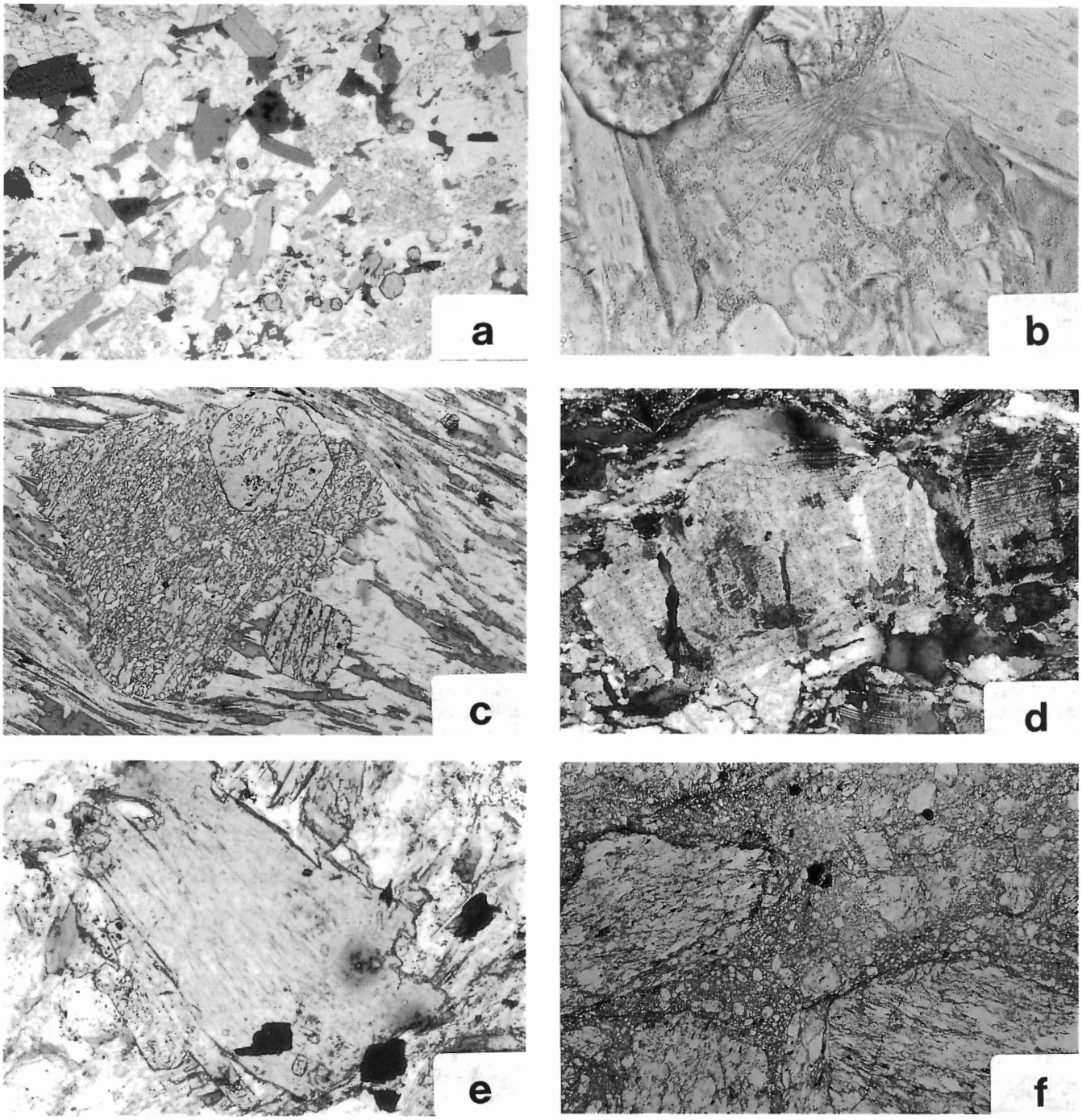

Figure 36. Deformation and metamorphic textures in the Meguma Group and granitoid plutons. Field widths (e.g., 3 mm) and light polarization (plane polarized or crossed nicols) are given in brackets. (a) Pelitic hornfels from unit CO_{Hb} on Raspberry Island, containing decussate biotite (dark), garnet (high relief), spongy andalusite (light grey, right), quartz and muscovite (2 mm; ppl). (b) Unit CO_{Hb} hornfels collected 0.5 m from the Prices Island pluton. Sillimanite fibres (top centre) occur along the boundary between microcline (centre) containing quartz blebs (lower centre) and muscovite (top right–0.3 mm; ppl). (c) Staurolite and garnet porphyroblasts are enveloped by S_{2b} in unit CO_{Ga} pelitic metawacke north of Trout Lake in the Canso area (3 mm; ppl). (d) Pull-apart cracks in a plagioclase porphyroclast in the Lumsdens Lake pluton near Canso. The cracks are oriented approximately perpendicular to S_{2b} and are filled with strained quartz and microcline (3 mm; X-nicols). (e) Chlorite porphyroblast (centre) truncates and is weakly deformed by S_{2b} in unit CO_{Hb} schist north of Whitehead (2 mm; ppl). (f) Meguma-derived cataclasite from the Guysborough County fault, 1 km northwest of Cutler Lake (6 mm; ppl).

on short limbs of larger structures. Most are defined by bedding in the Meguma Group, which is oriented subparallel to S_{2a} (Fig. 37a). Granite sheets are also folded in some places, particularly in migmatite (unit D_{Tm}) east of Canso (Fig. 37b). The two best examples of F_{2b} macrofolds are well exposed north of Whitehead. The larger one lies just north of Poule Point and has been studied in detail by Eddy (1987). It is inclined to the north, is isoclinal, and plunges about 50° to the east-southeast (Fig. 38). A well developed schistosity (S_{2b}) crenulates S_0 and S_{2a} at closures whereas S_0 and S_{2a} are transposed parallel to S_{2b} on limbs. In spots, S_0 laminae are dextrally offset up to 1 mm along single S_{2b} cleavage planes. Quartz veins and coticule beds are boudinaged on fold limbs. Parasitic mesofolds defined by coticules (Fig. 38c) generally plunge 30-60° to the east. They have highly variable axial surface orientations and are virtually identical to F_{2a} coticule folds (see Fig. 37c). The second macrofold is an open flexure defined by units CO_{Hc} and CO_{Hd} just west of Doughboy Point (see Fig. 34a). It plunges about 65° to the west-southwest. Both bedding and S_{2a} are crenulated by S_{2b} at the closure and on the limbs.

Although most F_{2b} folds are tight to isoclinal and gently plunging, open folds and steeply plunging folds are present. Mawer and Williams (1986) have attributed the change from open and steep to isoclinal and gently plunging to increasing D_{2b} strain. Although this relationship holds true in many places, it fails in some others. For example, the two macrofolds described above have similar plunges but vastly different interlimb angles. Elsewhere, mesofolds in unit CO_{Ha} just east of Fox Bay along the north shore of the Canso area vary from open to isoclinal yet maintain relatively constant plunges of about 25-35°.

The nature of S_{2b} varies considerably with respect to both host lithology and intensity of D_{2b} deformation. In pelitic rocks, it ranges from an open crenulation of S_{2a} without new mineral growth to a strong transposition schistosity, which has deformed porphyroblasts and obliterated most traces of older fabrics (e.g., Fig. 36c). L_{2b} lineation defined by the intesection of S_{2a} and S_{2b} is typically well developed, whereas mineral-aggregate lineation is confined to zones of high strain. Both lineations are oriented more or less parallel to F_{2b} fold axes. In more competent rocks such as Goldenville metawacke (unit CO_G), S_1 or composite S_1-S_{2a} pressure solution cleavage is commonly preserved, transposed parallel to S_{2b}. In granitoid rocks, S_{2b} varies from weakly aligned mica to a strong mylonitic foliation defined by ribbon quartz and very fine grained mica and feldspar (grain size = 0.01-0.1 mm), which wrap around large feldspar augen (Fig. 39). At moderate to high D_{2b} strain, the S_{2b} grain-flattening foliation (S-surface) is dextrally sheared along discrete C-planes (Fig. 39c). C-planes are slickenside surfaces of very small but finite thickness, containing ribbon quartz, very fine grained mica, and minor feldspar (see Fig. 11d). Subhorizontal mineral-aggregate lineation, defined by ribbon quartz and tailed feldspar augen, is well developed in the more deformed rocks and imparts a small-scale corrugation to C-planes. Both mineral-aggregate lineation and plate-shaped xenoliths are oriented parallel to S-surfaces. Feldspar augen are deformed cataclastically, with pull-apart cracks oriented approximately perpendicular to S-surfaces and filled with deformed quartz, microcline, and chlorite (see Fig. 36d). A second set of shear surfaces (C'-planes) crosscuts the initial S-C fabric in a few highly strained outcrops (e.g., Fig. 39c,d).

The effects of D_{2b} strain are most obvious in three narrow zones–the Tittle, Harbour Island, and Black Lakes shear zones (see Fig. 10). The Harbour Island shear zone is 500-1500 m wide, trends 093°, and is bounded on the north and south by virtually undeformed granite (Fig. 40). C-surfaces are oriented approximately parallel to the zone whereas S-surfaces describe a sigmoidal pattern, rotating toward the C-surfaces as the centre of the zone is approached. The angle between S and C-surfaces decreases from about 40° at the margin to an average of 20° in the centre. This change is accompanied by progressive decrease in average grain size as the rocks change from relatively undeformed granite through protomylonite to mylonite (terminology of Sibson, 1977). Ultramylonite was only observed in one outcrop south of Whitehead where the angle between S and C-surfaces is about 10° (see Fig. 39d). The other two shear zones are marked by the presence of strongly mylonitic rocks within larger areas of lower D_2 strain. The Black Lakes shear zone is distinguished by locally strong subhorizontal mineral-aggregate lineation. The Tittle shear zone is much broader although true mylonites are generally restricted to rocks within a few tens of metres of the Tittle. High strains are indicated by flattened metawacke xenoliths in granite, which have length to width ratios of up to 100:1. Although most appear to be plate-shaped, a few are elongate and parallel to F_{2b} fold axes. Similar xenoliths 6 km to the south where D_{2b} strain is much weaker are roughly equidimensional and angular.

D_{2b} mineral assemblages are well developed in both map areas. The following assemblages have been recognized:

<u>in pelitic rocks:</u>

i) quartz + muscovite + biotite + garnet ± Ca-plagioclase
ii) quartz + muscovite + biotite + chlorite
iii) quartz + muscovite + biotite + Ca-plagioclase ± microcline
iv) quartz + muscovite + chlorite ± garnet ± graphite ± epidote

<u>in calc-silicate rocks:</u>

v) quartz + Ca-plagioclase + biotite + clinozoisite + sphene

<u>in granitic rocks:</u>

vi) quartz + Ca-plagioclase + microcline + biotite + muscovite
vii) quartz + Ca-plagioclase + microcline + muscovite + chlorite

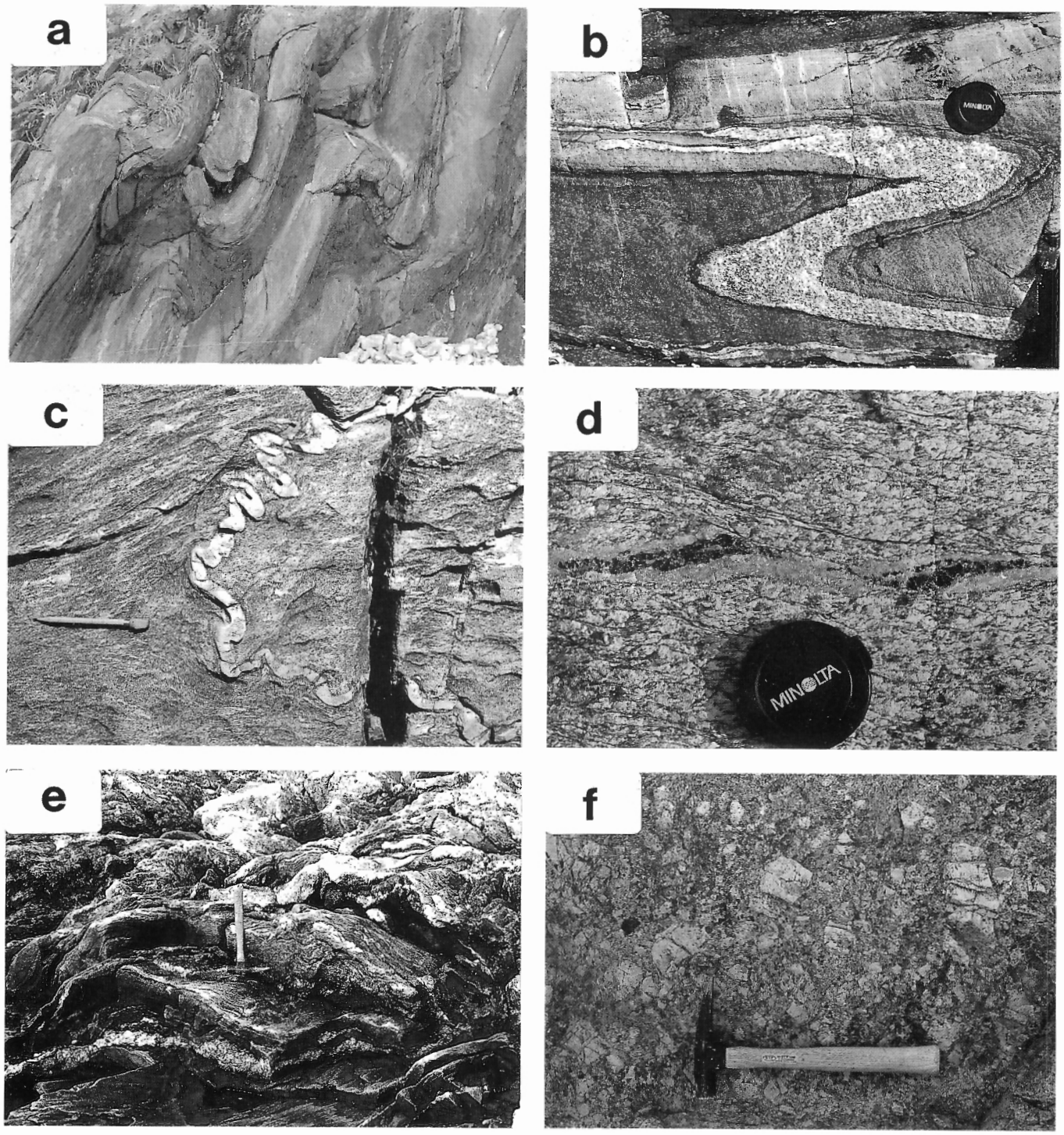

Figure 37. D_2 structures in the Canso area. (a) Subhorizontal Z-shaped F_{2b} fold in unit CO_{Ha} at Half Island Cove. Bedding and S_{2a}, which are parallel, are crenulated by S_{2b} at fold closures. GSC 204508-BB. (b) F_{2b} defined by boundinaged granite sheet in migmatitic metawacke on Durells Island. S_{2b} S-planes are oriented parallel to the axial surface of the fold. GSC 204508-S. (c) M-shaped parasitic folds of a coticule bed at the north anticlinal closure of the F_{2b} macrofold north of Poule Point. Pencil is parallel to S_{2b} crenulation cleavage whereas S_{2a} is parallel to bedding. GSC 204508-B. (d) D_{2b} S-C fabric in granite on Durells Island. Quartz-tourmaline vein is dextrally smeared along a single C-plane. GSC 204508-Q. (e) Subhorizontal F_{2c} fold with dextral vergence in migmatitic metawacke in unit D_{Tm} on Oliver Island. S_{2b} in granitic sheets is folded with bedding. GSC 204508-O. (f) Cohesive fault breccia in the Fogherty Lake granite pluton on the west side of Fox Bay. GSC 204508-X.

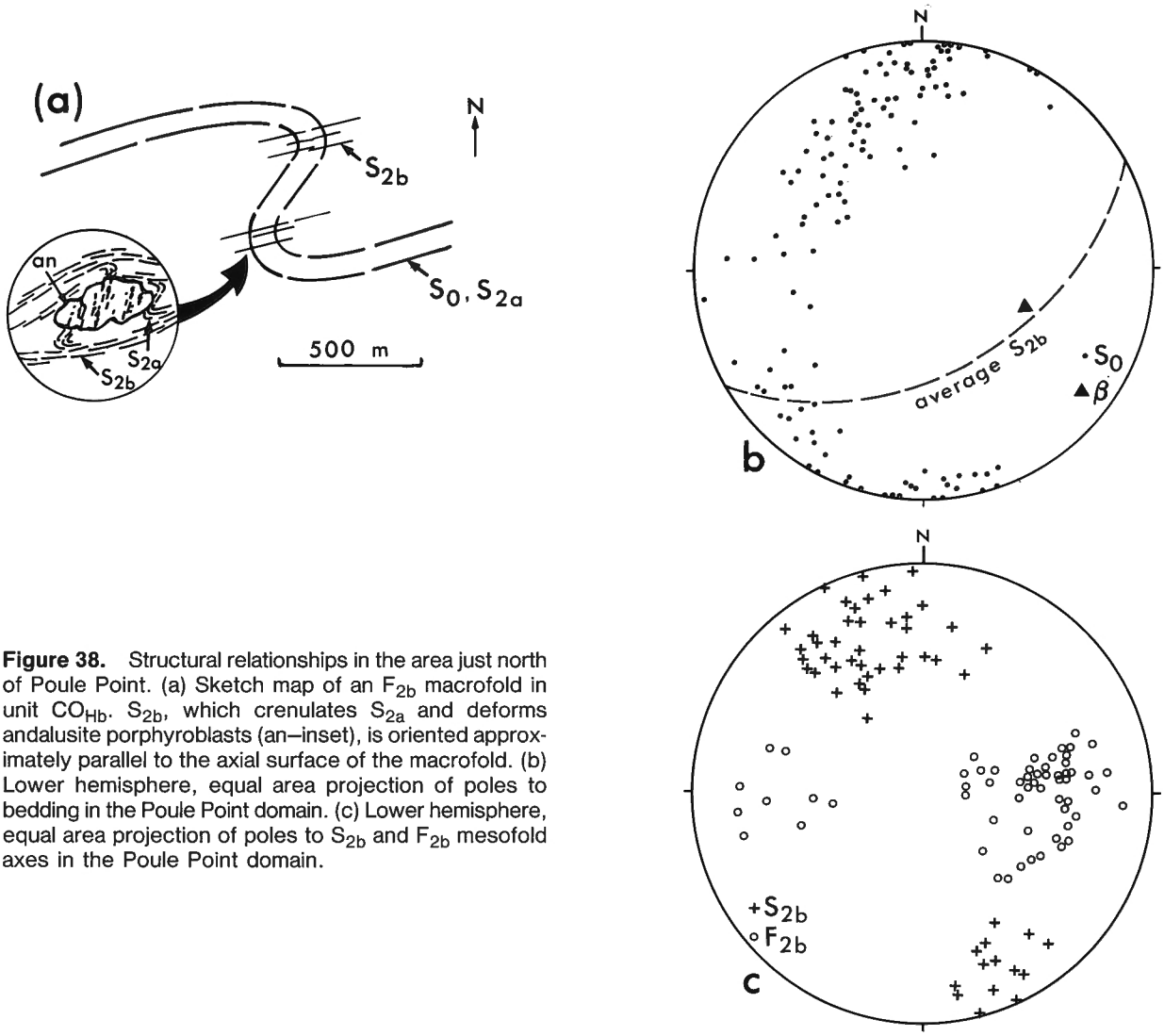

Figure 38. Structural relationships in the area just north of Poule Point. (a) Sketch map of an F_{2b} macrofold in unit CO_{Hb}. S_{2b}, which crenulates S_{2a} and deforms andalusite porphyroblasts (an–inset), is oriented approximately parallel to the axial surface of the macrofold. (b) Lower hemisphere, equal area projection of poles to bedding in the Poule Point domain. (c) Lower hemisphere, equal area projection of poles to S_{2b} and F_{2b} mesofold axes in the Poule Point domain.

Assemblages (i), (i), (iii), and (vi) are the most common. They imply upper greenschist to lower amphibolite facies metamorphism during most of D_{2b}. The significance of chlorite-bearing assemblages lacking biotite is uncertain. They may be related either to bulk rock composition or to post-D_{2c} retrograde alteration of biotite, which is locally pervasive, especially near fault zones. Albite-bearing assemblages were only recognized 1.5 km west of Port Felix, outside the Canso area (Raeside et al., 1988).

D_{2c}

This is the last phase of D_2 deformation which can be directly related to dextral ductile shearing along the south side of the Cobequid-Chedabucto fault system. It is defined by asymmetric folds, at scales from 1 cm to several tens of metres, and by locally developed crenulation cleavage, which overprint D_{2b} structures throughout the northern half of the Forest Hill area and in unit D_{Tm} in the northeast part of the Canso area.

The folds are similar in style and orientation to F_{2b} folds (see Fig. 37e). They are recognized by the fact that S_{2b} (which deforms porphyroblasts and granite) is folded along with older structures. East of Canso, bedding transposed parallel to S_{2b} and boudinaged granite sheets are deformed into a series of Z and M-shaped mesofolds, which mainly plunge gently to the west (Fig. 41a). A weak S_{2c} cleavage defined by muscovite and biotite locally crenulates S_{2b} at closures. Within some granite sheets, S and C-surfaces formed during D_{2b} are folded and a new set of S_{2c} dextral shear planes are developed, maintaining constant orientation across both limbs (Keppie, 1985). These new C-surfaces may be correlative with C'-surfaces that occur elsewhere in areas where D_{2b} strain is high (see preceding section). Where F_{2b} and F_{2c} folds occur together, most F_{2c} folds have slightly steeper plunges (cf. Fig. 41a and b).

S_{2c} involved only partial recrystallization of quartz, biotite, and muscovite parallel to crenulation axes. This assemblage implies continuation of upper greenschist to lower amphibolite conditions that existed during D_{2b}.

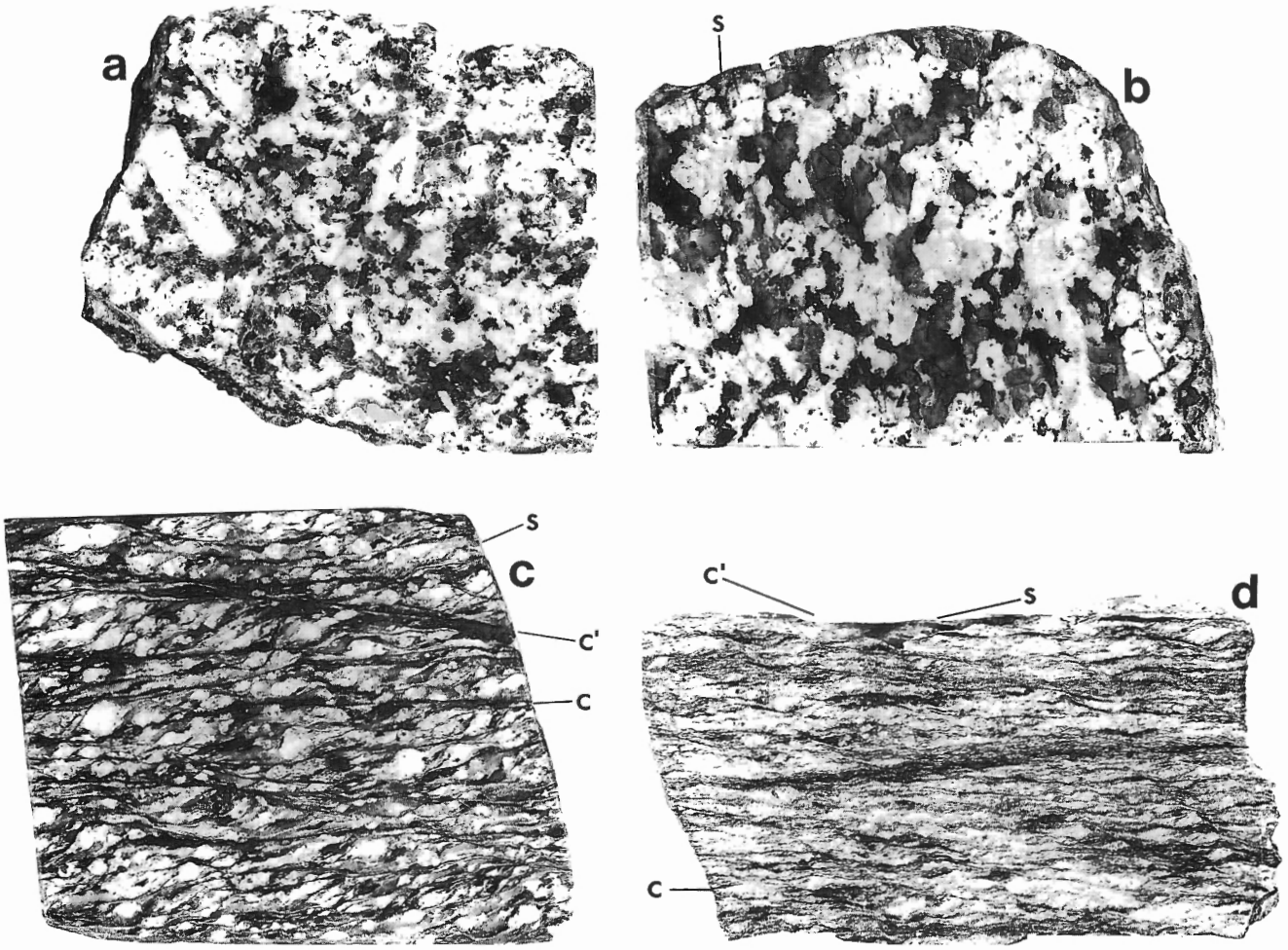

Figure 39. Differences in granitic rock texture due to variations in the intensity of post-granite D_2 strain. (a) Essentially undeformed Port Howe granite. (b) Protomylonite with a weakly developed S_{2b} mica foliation (S). (c) Mylonite from the centre of the Tittle shear zone. S, C, and C'-planes are visible, and the angle between S and C-planes is about 25°. (d) Ultramylonite from the centre of the Harbour Island shear zone south of Whitehead. S, C, and C'-planes are visible, and the angle between S and C-planes is about 10°.

Tectonic structures in the Minister Brook formation (unit DC_M) are correlated tentatively with D_{2c}. Bedding is deformed into centimetre- to decimetre-scale, tight to isoclinal folds with dextral vergence, which plunge gently east and west. A steeply dipping domainal slaty cleavage is axial planar to the folds. Discrete shear planes (C-surfaces) truncate and dextrally deform the slaty cleavage in a few outcrops. A mineral aggregate lineation is rarely developed on cleavage planes and plunges gently to the east. These structures are very similar to those developed in the Meguma Terrane during D_{2b} and D_{2c}. They are correlated with D_{2c} because the slaty cleavage is domainal and because only one generation of folding was recognized. The following metamorphic mineral assemblages were observed:

i) quartz + muscovite + chlorite + calcite + chloritoid
ii) quartz + muscovite + chlorite ± albite ± clinozoisite
iii) quartz + biotite + muscovite + albite + epidote

These assemblages imply greenschist facies conditions similar to, or slightly lower than, those developed during D_2 shearing in the Meguma Terrane.

D_{2d}

This phase of deformation includes a variety of variably oriented crenulation cleavages and associated small, open folds that appear to postdate D_{2b} and D_{2c}. They are restricted to pelitic rocks in the Meguma Group in both map areas and the Minister Brook formation in the Forest Hill area. They are regionally nonpenetrative, making it impossible to correlate the various structures from place to place.

Foliations are defined by open to tight crenulations of older D_2 fabrics. For example, a crenulation cleavage striking 200-220° and dipping 20-60° to the northwest is

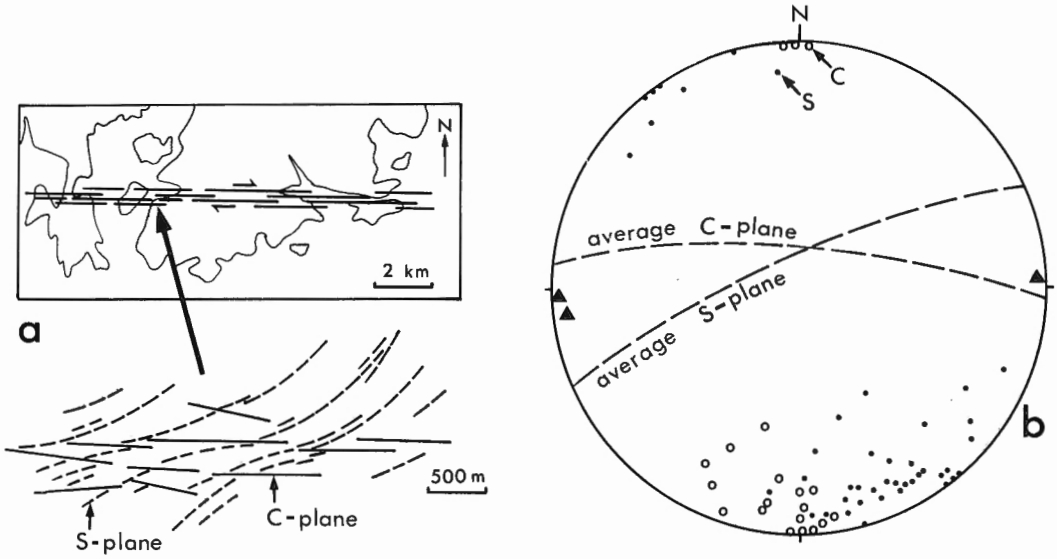

Figure 40. Structural relationships in the Harbour Island shear zone. (a) Sketch showing the orientations of S and C-planes in the area around Harbour Island. (b) Lower hemisphere, equal area projection of poles to S and C-planes and L_{2b} mineral aggregate lineation (triangles) in the area around and east of Harbour Island.

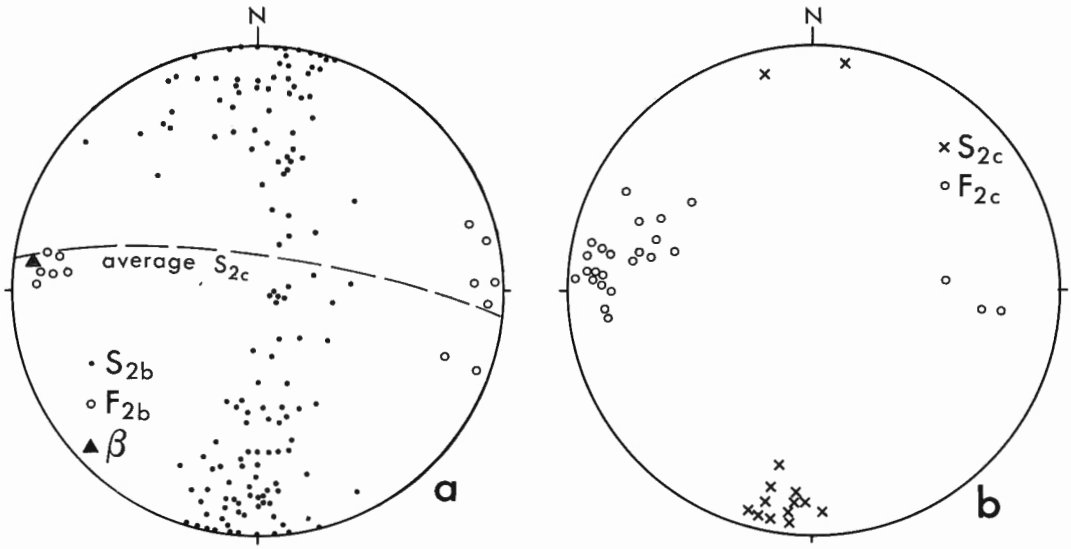

Figure 41. Lower hemisphere equal area projections of structural data from unit D_{Tm} on Oliver Island and George Island east of Canso. (a) Poles to S_{2b} in granitoid rocks and F_{2b} mesofold axes. (b) Poles to S_{2c} and F_{2c} mesofold axes.

developed between Poule and Doughboy points in the Canso area. It crenulates S_{2a} and is assumed to be younger than S_{2b} because it maintains a constant orientation across all limbs of the F_{2b} macrofold in that area. It is associated with centimetre- to decimetre-scale open warps of bedding and S_{2a}. A second post-D_{2b} crenulation cleavage, striking north-south and dipping moderately to the east is developed locally in the same area. The age relationship between the two crenulation cleavages is unknown. Crosscutting late foliations were also observed in one outcrop of unit CO_{Ha}, situated 1 km southeast of Gaulman Point on the north shore of the Canso area. There, a weak crenulation cleavage oriented 150°/47°SW is crosscut by a spaced cleavage oriented at 215°/69°NW. Neither foliation persists into adjacent outcrops.

Although the precise timing of D_{2d} textures and structures is unknown, they appear to have formed under lower greenschist facies conditions. Two lines of evidence are relevant. First, recrystallization of muscovite is minor and has only occurred in some places parallel to the axial planes of crenulations. Second, large decussate laths and radiating knots of chlorite and rare actinolite are a

distinctive feature of pelitic rocks in the southwest part of the Canso area and locally in the Forest Hill area. Individual grains are up to 2 mm long and crosscut both S_{2a} and S_{2b}. At the Forest Hill mine site and north of Whitehead, felty knots of chlorite truncate and are weakly kinked by S_{2c} at F_{2c} fold closures (see Fig. 36e). Chlorite is also weakly deformed by an S_{2d} crenulation cleavage that is developed in less competent layers. East of Doughboy Point in the Canso area, chlorite laths truncate S_{2b} and are slightly kinked with kinkband boundaries oriented parallel to S_{2b}. They are also deformed by a late crenulation cleavage. These relationships imply that growth of chlorite porphyroblasts overlapped D_{2c} and in some places D_{2b} as well. Widespread alteration of S_{2a} and S_{2b} biotite to chlorite may have occurred at that time.

D_{2e}

The last phase of D_2 represents the culmination of the dextral shearing event, when temperature had decreased to the point at which deformation became brittle. Structures include brittle-ductile shear zones, faults, and rare kink bands and conjugate kink folds.

Brittle-ductile shear zones can be traced for up to 10 m in outcrops of granite and the Meguma Group in the northern parts of both map areas. They occur only in areas in which ductile D_2 strain is relatively high. The planes of shear range from <1 mm to 5 m wide and show all gradations between the following six general types:

- open fractures
- comminuted country rock
- mylonitic country rock
- brecciated granite pervasively altered to a siliceous green material
- vein quartz locally brecciated
- altered pseudotachylite (observed in one outcrop in Harbour Island shear zone)

Bedding and ductile tectonic fabrics are either displaced or dragged into the shear planes, with offsets of up to 1.5 m observed across single shear zones. Two groups have been recognized–east-northeast to southeast-trending dextral shears and north-northwest to northeast-trending sinistral shears (Fig. 42). The dextral shears probably include rejuvenated D_{2b} S and C-surfaces in granitoid rocks that locally pass along strike into fractures filled with comminuted material. Conflicting age relationships were observed. Dextral shears truncate sinistral shears in four separate places whereas the reverse relationship was observed in one other outcrop.

Faults are common, especially along the northern margins of both map areas where they comprise segments of the Cobequid-Chedabucto fault system. Rocks adjacent to faults are highly fractured, altered, and locally crosscut by irregular veinlets of cataclasite (terminology of Sibson, 1977). Polished surfaces are commonly marked by subhorizontal striations. Actual fault zones are poorly defined by discontinuous exposures of breccia, protocataclasite, and cataclasite (see Fig. 36f and 37f) up to 15 m wide. In addition, protocataclasite and cataclasite locally overprint ductile fabrics in the centres of D_{2b} shear zones. The dominant matrix minerals are quartz, albite, microcline, muscovite, and chlorite. Veinlets of quartz and dolomite occur locally. Several X-ray diffraction patterns were determined for fault cataclasite in an attempt to identify zeolite and pumpellyite-grade minerals but the results were inconclusive. Where a fault crosses the Fogherty Lake pluton east of Fox Bay, the granite is brecciated and altered to a green material enriched in silica (cf. analyses 069A and 069C in Appendix IV). Two groups of strike-slip faults are recognized. They are identical in style and orientation to the brittle-ductile shear zones described above (Fig. 42). The most important of these is the Guysborough County fault, which separates the Meguma Terrane and Fundy Basin in the Forest Hill area. It is partly exposed in several places and is well exposed where an abandoned railway crosses Gunns Brook 1 km northwest of Cutler Lake.

Steeply dipping kink bands deform ductile D_{2a} and D_{2b} fabrics in a few places. They consist mainly of

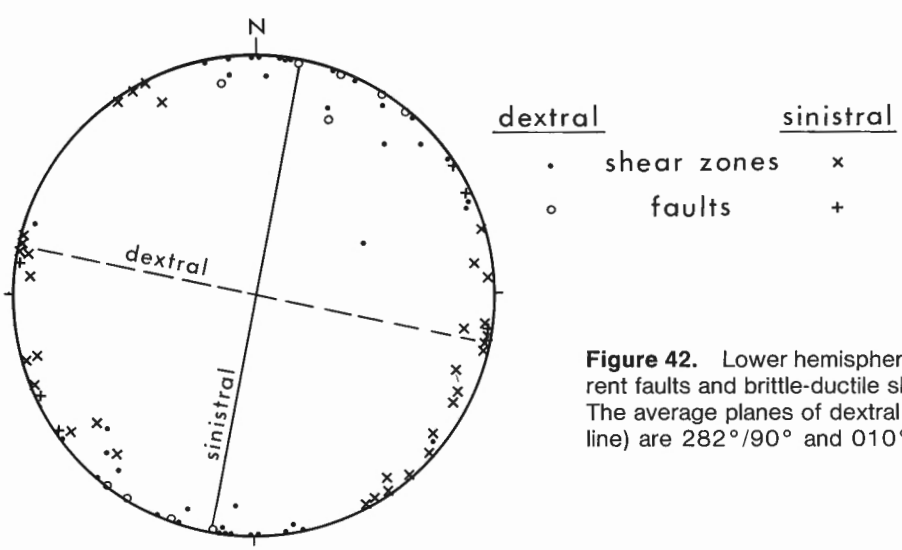

Figure 42. Lower hemisphere equal area projection of poles to transcurrent faults and brittle-ductile shear zones in the whole of the Canso area. The average planes of dextral (dashed line) and sinistral movement (solid line) are 282°/90° and 010°/90° respectively.

northwest-trending sinistral kink bands and northeast-trending dextral kink bands, which appear to comprise a conjugate pair. In unit CO_{Hb} between Whitehead and Burnt Island, coupled kink bands with opposing asymmetry form conjugate kink folds.

D_3–Late faulting

All fault movements that occurred during or after the early Carboniferous are assigned to D_3. However, temporal separation of D_{2e} and D_3 is tenuous and it would be equally profitable to consider D_3 as a prolonged extension of late D_2 brittle deformation.

Two types of fault movement are known to affect the early Carboniferous Gunns Brook formation in the Forest Hill area. The Horton Group (including the Gunns Brook formation) is partly confined to a graben structure between the Guysborough County and Chedabucto faults. The Gunns Brook formation contains abundant fanglomerate with Meguma-derived boulders up to 1 m long, which is spatially associated with the fault-controlled margin of the Meguma Terrane. Farther west, the Horton Group oversteps the Guysborough County fault and overlies unconformably the northern part of the Meguma Terrane (Belt, 1968; Bradley, 1982). These relationships suggest that ductile transcurrent movement (i.e., during D_{2a} to D_{2c}) on the Guysborough County fault had largely ended and vertical movement (i.e., D_3) had begun by early Carboniferous when the Gunns Brook formation was being deposited.

Two northwest-trending sinistral transcurrent faults have been recognized. The Country Harbour fault defines the southwest corner of the Forest Hill area. It offsets Meguma strata by 1-2 km south of the Forest Hill area (O'Brien, 1983). It is also believed to be responsible for the 110° counterclockwise rotation of the Guysborough County fault and ductile D_2 fabrics in the Meguma Terrane between Country Harbour Mines and Forest Hill (Keppie, 1983). Based on computer-enhanced radiometric images (see upper frontispiece), movement on the Country Harbour fault postdates at least part of the early Carboniferous Gunns Brook formation. The Kyak Brook fault in the Canso area is similar in style and orientation to the Country Harbour fault and the two faults are considered to be similar in age. The Kyak Brook fault is recognized on Landsat thematic mapper images by a 100-150 m sinistral offset of the D_{2b} Harbour Island shear zone.

SUMMARY AND DISCUSSION OF TECTONIC HISTORY AND GRANITOID PETROGENESIS

Tectonic history

Overview

Deformation and metamorphism in the Canso and Forest Hill areas are assigned to three events (D_1-D_3), which together represent continuous or almost continuous tectonism from early Devonian to early Carboniferous or later (Table 8). D_1 developed in response to initial continental collision between the Meguma and Avalon terranes (Keppie, 1977; Schenk, 1978). The boundary between the two terranes is defined by the Cobequid-Chedabucto fault system (see Fig. 1). D_1 was followed by a complex polyphase event (D_2) of ductile shearing and subsequent brittle deformation, which was associated with dextral transcurrent movements along the Cobequid-Chedabucto fault system. These movements appear to have been the result of post-accretionary adjustments and additional oblique collisions among the outboard blocks of that part of the Appalachian orogen (Keppie, 1985; Williams and Hatcher, 1982). The final phase of deformation (D_3) is defined by isolated brittle structures that affect rocks as young as early Carboniferous. They formed during development of the Fundy basin following continental collision (Keppie, 1977; Bradley, 1982; Dostal et al., 1983).

D_1–Regional deformation

Regionally, D_1 produced kilometre-scale, subhorizontal, open to tight synclines and anticlines associated with slaty to spaced cleavage defined by greenschist facies minerals. Its older age limit is given by the early Devonian Torbrook Formation (Emsian) in western Nova Scotia, which is folded by D_1 structures. Mica defining the slaty cleavage has been dated at 384-415 Ma (Reynolds and Muecke, 1978; Elias et al., 1987; Dallmeyer and Keppie, 1987). This age range is provisionally accepted for D_1 because D_2 has an older limit of about 378 Ma (discussed below).

D_1 structures are difficult to recognize in the Canso and Forest Hill areas because of overprinting effects of D_2. The clearest feature is folding inferred from kilometre-scale stratigraphic repetition in the Meguma Group. These folds are correlated with early Acadian structures farther southwest on the basis of similar style. Assignment of minor structures such as small folds and schistosity to D_1 is based on overprinting relationships by the earliest D_2 structures or because they occur in areas where D_2 is weak or absent.

D_2–Dextral transcurrent shearing

D_2 is comprised of a series of overlapping phases of deformation, metamorphism and granitoid intrusion. The first three phases of deformation (D_{2a}-D_{2c}) produced a 10-15 km wide ductile shear zone along the south side of the Cobequid-Chedabucto fault system, a feature that has been interpreted as part of a continental-scale shear zone that separated African and American-European plates during the late Paleozoic (Arthaud and Matte, 1977). Structures within the Cobequid-Chedabucto shear zone are remarkably similar to those developed in the South Amorican shear zone in France (Berthé et al., 1979) and northeast Gander Terrane in Newfoundland (Hanmer, 1981). D_2 structures have been described in some detail by Keppie (1985), Mawer and Williams (1986) and Mawer and White (1987). However, the occurrence of a distinct phase of deformation and metamorphism

Table 8. Summary of lithological, tectonic, and isotopic age relationships in the Canso and Forest Hill areas

Period	Lithology		Tectonic event
Early Carboniferous	Gunns Brook fm. (unit C_G)	FUNDY BASIN	D_3: faulting, with deposition of the Gunns Brook fm. partly controlled by vertical movements on the Guysborough County and Chedabucto faults.
Middle Devonian to Early Carboniferous	Minister Brook, Sunnyville, and Tower fms. (units $DC_{M,S,T}$)		
pre-Carboniferous	Inliers in DC_M		
Late Devonian	Peraluminous granitic plutons 372 ± 1 Ma[a] (unit D_G)	MEGUMA TERRANE	D_2: progressive, overlapping phases of deformation, granitic intrusion, and metamorphism caused by ductile shearing in the Cobequid-Chedabucto fault zone. Static metamorphism and dynamically recrystallized mica dated at 362-365 ± 7 and 365-373 ± 7 Ma[c] respectively. D_2 culminated with uplift and brittle deformation.
Middle Devonian	Tonalite plutons 378.5 ± 2 Ma[b] (unit D_T)		
Early to Middle Devonian			
Cambrian to Early Ordovician	Meguma Group		D_1: Regional folding. Metamorphism dated at 384-415 Ma[d].

a) U-Pb monazite, T. Krogh, this report.
b) U-Pb zircon, T. Krogh, this report.
c) $^{40}Ar/^{39}Ar$, Dallmeyer and Keppie (1984).
d) $^{40}Ar/^{39}Ar$, Reynolds and Muecke (1978), Dallmeyer and Keppie (1987), Elias et al. (1987).

prior to granite intrusion (D_{2a}) was not recognized. D_2 strain was heterogeneous, resulting in a high proportion of mylonitic rocks concentrated in narrow east-trending shear zones that are bounded to the north and south by less deformed rocks. At least three generations (D_{2a}-D_{2c}) of millimetre- to hundred-metre-scale tight to isoclinal folds with dextral vergence are intrafolial with respect to layer-parallel transposition foliation in metasedimentary rocks. Lineations defined by mineral aggregates, cleavage-bedding intersection and boudin plunge gently to moderately east and west and are parallel to fold axes. Sheath folds have been recognized locally (Keppie, 1985; Mawer and White, 1987). Similar structures of only one generation (correlated with D_{2c}) are developed in the Minister Brook formation on the north side of the Guysborough County fault in the Forest Hill area. They demonstrate that deformation related to ductile shearing was not completely asymmetrical with respect to the Cobequid-Chedabucto fault system (see also Mawer and White, 1987). Granitoid plutons were emplaced during D_2 and vary from relatively undeformed in the southern parts of both map areas to protomylonite and rare mylonite in D_{2b} shear zones farther north. S_{2b} transposition foliation in the Meguma Group passes into a penetrative S-fabric in granitoid rocks defined by polycrystalline quartz leaves, mica, and feldspar augen. Spaced shear planes (C-planes), composed mainly of very fine grained quartz and mica, and subhorizontal mineral-aggregate lineation developed with S-planes in areas of higher strain. As shear zone centres are approached, the proportion of C-planes increases to about 5-10 per cm and the angle between C and S-planes decreases to 10-20°.

The late stages of D_2 (D_{2d} and D_{2e}) were characterized by decreasing temperature and increasingly brittle conditions. D_{2d} includes a variety of small, open folds and crenulation cleavages that are regionally non-penetrative. D_{2e} is represented by minor kink folds, kink bands, brittle-ductile shear zones and transcurrent faults which overprint older D_2 ductile fabrics. The faults and brittle-ductile shear zones form a geometric package analogous to Riedel shears developed in a dextral transcurrent fault system (Fig. 43). A similar arrangement of brittle structures has been recognized at the west end of the Cobequid-Chedabucto fault system (Mawer and White, 1987).

D_2 appears to be tightly constrained within a 10-30 Ma period between about 380 and 350 Ma. D_2 structures overprint D_1 fabrics and therefore must be younger than about 384-415 Ma (see Table 8). Tonalite plutons in the Canso and Forest Hill areas provide a more precise older age limit. Shag Cove tonalite was deformed after crystallization (about 378 Ma) and prior to both intrusion of the Portage Cove granite pluton and D_{2b} deformation (about 372 Ma). The single tectonic fabric in the Shag Cove tonalite xenoliths shown in Figure 12a is correlated with S_{2a} as the tonalite was probably emplaced after D_1 and before D_{2b}. This interpretation places a maximum

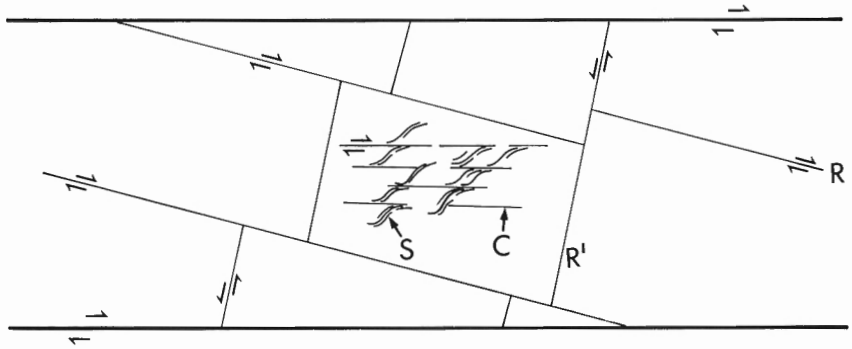

Figure 43. Simplified sketch of the relationships between S and C-planes, brittle-ductile shear zones and transcurrent faults along the north shore of the Canso area. C-planes dextrally shear and locally truncate S-planes in granitoid rocks. S-C fabric is crosscut by WNW-trending dextral (R) and NNE-trending sinistral (R') faults and brittle-ductile shear zones. These structures are analogous to a geometric package of Riedel shears (e.g., Wilson, 1970) developed within a dextral transcurrent shear zone (i.e., the Cobequid-Chedabucto fault system).

age of about 378 Ma on D_2. A minimum age of 350-360 Ma is defined by the presence of clasts of Meguma Terrane granite and metasedimentary rocks containing D_2 fabrics in the early Carboniferous Horton Group and by the fact that the Gunns Brook formation (Horton Group) lacks ductile D_2 structures.

The various phases of D_2 appear to overlap in time, forming a single event of progressive deformation and metamorphism. Textural evidence demonstrates that static metamorphism, which has been dated at 362-365 ± 7 Ma (Dallmeyer and Keppie, 1984), occurred between and overlapped both D_{2a} and D_{2b}. Granitic plutons, dated at 371-373 Ma, truncate S_{2a} and are deformed by S_{2b}, indicating that they were essentially coeval with static metamorphism. Textural and structural evidence described in the previous section indicate that granitic plutonism partly overlapped D_{2b}. Dynamically recrystallized S_{2b} mica has been dated at 365-373 ± 7 Ma (Dallmeyer and Keppie, 1984). Only limited evidence suggests that later phases of D_2 also overlapped in time. However, age constraints already described and the continuous decrease in metamorphic grade as D_2 waned (described below) point to close temporal relationships between D_{2c}, D_{2d}, and D_{2e}. Hanmer (1981) and Williams (1983) have suggested that overprinting relationships may not have any regional age significance in ductile shear zones. However, the consistent relative ages of D_2 structures and the fact that a period of static metamorphism and granite intrusion separate D_{2a} and D_{2b} imply that at least some of phases of D_2 recognized herein do have temporal significance. On the other hand, D_{2b} and D_{2c} could have been essentially contemporaneous.

The effects of D_2 are only developed within 10-15 km of the Cobequid-Chedabucto fault system in the eastern Meguma Terrane. As time progressed, structures became increasingly brittle and more localized closer to the fault zone. This spatial and time association is consistent with Keppie's (1985) interpretation that deformation was related to fault movements. Mineral-aggregate lineation indicates displacement was approximately subhorizontal. Kinematic indicators (e.g., Simpson and Schmid, 1983; Sugden, 1987) such as S-C fabric relationships, winged porphyroblasts, and asymmetric folds point to dextral sense of movement. No indication of sinistral motion was found (see also Mawer and White, 1987).

D_3—Carboniferous faulting

The brittle end stages of D_2 were closely followed by additional near-surface cataclastic deformation related to fault movements. These movements lasted at least until the early Carboniferous as they have affected the Gunns Brook formation in the Forest Hill area. The most significant effect was counterclockwise rotation of all D_2 structures (including the Guysborough County fault) in the western half of the Forest Hill area. This rotation is inferred to be the result of sinistral drag along the northwest-trending Country Harbour fault. Transcurrent D_2 movement on the Guysborough County fault must have given way to vertical D_3 movement by the early Carboniferous because the Gunns Brook formation lacks ductile D_2 fabrics and contains fanglomerates that are derived from, and localized against, the Meguma block.

Metamorphism and pressure-temperature conditions

The metamorphic history of the Canso and Forest Hill areas is depicted in Figure 44. Based on limited textural evidence in the southern parts of the two areas, regional metamorphism reached upper greenschist to lower amphibolite facies during D_1 and D_{2a}. The short time span between D_1 and D_{2a} ($\approx$5-20 Ma) suggests that P-T conditions may have been relatively constant during that period. Contact metamorphism related to intrusion of tonalite plutons at about 378 Ma has not been recognized

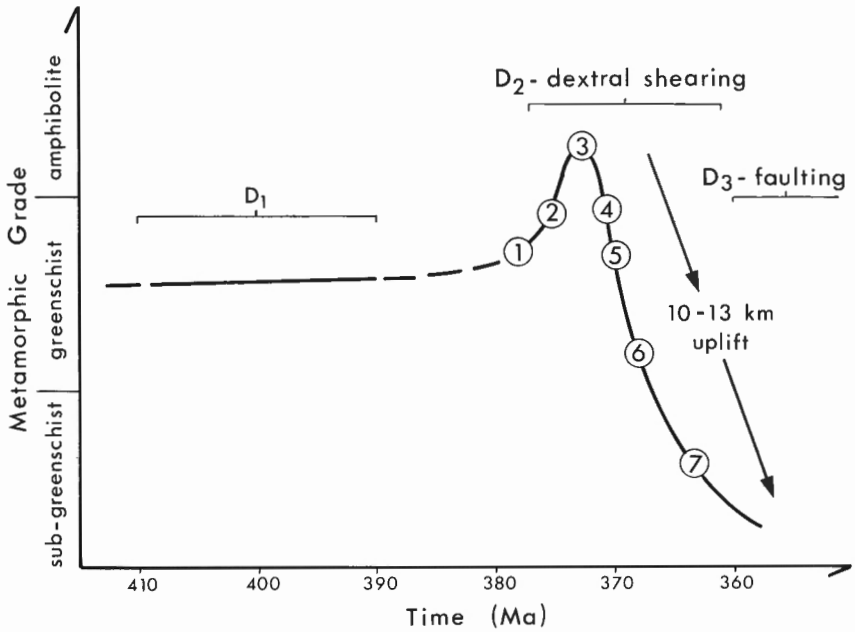

Figure 44. Inferred relationships between time, deformation, and metamorphic grade in the Canso and Forest Hill areas. D_2 is comprised of a series of overlapping phases, which began after tonalite intrusion (1) and included D_{2a} folding (2), static metamorphism and granitic intrusion (3), D_{2b} folding (4), D_{2c} folding (5), local minor D_{2d} ductile deformation (6), and D_{2e} brittle deformation (7). The change from peak metamorphic conditions during granitic intrusion to near-surface conditions during late D_2 and D_3 faulting corresponds to 10-13 km uplift of the eastern Meguma Terrane in about 10-20 Ma.

because of the overprinting effects of D_2. Temperature increased to lower to middle amphibolite conditions with the onset of static and contact metamorphism as D_{2a} ended. Static metamorphism produced sillimanite knots and porphyroblasts of biotite, andalusite, cordierite, and staurolite in schistose pelitic rocks throughout most of the two map areas. Identical mineral assemblages are developed in relatively rare hornfels. Hornfels is associated spatially with granitic plutons in the southern part of the Canso area where it is caused by local contact metamorphism. The origin of the static metamorphism is more enigmatic. Static metamorphic assemblages show generally increasing grade toward granitic plutons. On the other hand, the distribution of diagnostic minerals is somewhat irregular and cordierite and andalusite are found as much as 4 km away from small granitic plutons in the Forest Hill area. Although a direct causal relationship between plutonism and static metamorphism is probable, their precise relationship is made less important by the fact that both occurred at about the same time (ca. 372 Ma) under virtually identical P-T conditions. After metamorphism peaked at about 372 Ma, temperature progressively decreased to near-surface conditions as D_2 passed into D_3.

Biotite-garnet equilibration temperatures have been determined for nine pelitic schist and two hornfels samples collected from the Meguma Group in the Canso area and for one mylonitic inlier in the Minister Brook formation from the Forest Hill area. Sample locations are plotted on Figures 2 and 3, and the data are given in Table 9. Caution must be excercised in the use of these values because of the high Mn contents of most of the garnets. Except for sample 792B, which was collected 2.5 km west of Port Felix outside the map area and which gives an anomalously low temperature, calculated Meguma temperatures are consistent with the maximum grade of metamorphism recognized in each place, despite the fact that all samples are overprinted by younger deformation and show some retrograde effects. The data demonstrate the general increase in metamorphic grade toward granitic plutons. They also suggest that mineral compositions preserve peak conditions generated during static and contact metamosphism.

Seven lines of evidence constrain the maximum pressure developed at the current level of exposure during D_2:

a) The aluminosilicate sequence is andalusite-sillimanite; the lack of kyanite suggests that pressure was less than 380 MPa (Holdaway, 1971).
b) The presence of rare staurolite suggests a minimum pressure of about 150-300 MPa, based on the stability field of pure-Fe staurolite (Fig. 45), which is raised or lowered slightly by higher Mg and higher $f0_2$ respectively (Richardson, 1968).
c) Manganiferous garnet is common in both the Halifax Formation and some granitic plutons. Using the data of Green (1977), garnet in the Andrew Island pluton, which contains 26% spessartine, could have crystallized at pressures as low as 300 MPa.
d) The presence of subsolidus sillimanite crosscutting muscovite in granitic rocks in the southern part of the Canso area indicates a minimum pressure of about 220 MPa (i.e., above the intersection of the andalusite-sillimanite univariant line with the muscovite stability curve in Fig. 45). The same minimum pressure is implied by the static and contact metamorphic sequence of "sillimanite-in" before "muscovite-out". A minimum pressure of about 300 MPa is suggested if subsolidus recrystallization in the granitic plutons occurred at nearly magmatic temperatures, as inferred below.
e) Smectite aggregates in some of the granitic plutons are interpreted to be pseudomorphs after magmatic cordierite. If this is true, it suggests that crystallization occurred at a pressure of 500 MPa or less (Clemens and Wall, 1981).

Table 9. Biotite-garnet equilibration temperatures for Meguma pelitic rocks in the Canso area and a mylonitic inlier in the Minister Brook formation in the Forest Hill area, calculated from the data of Ferry and Spear (1978).

Sample	Mineral assemblage	% An	biotite Mg/Fe	biotite X_{Ti}	biotite $X_{Al^{vi}}$	garnet Mg/Fe	garnet X_{Ca}	garnet X_{Mn}	T °C
Meguma Group									
792B	ch + an	1	0.898	0.036	0.171	0.050	0.053	0.381	304
221B	ch + an	15	1.163	0.026	0.168	0.132	0.028	0.336	443
018	an	21	0.805	0.036	0.178	0.102	0.032	0.212	471
139	cd		0.986	0.030	0.168	0.127	0.022	0.332	476
050	st	24	0.752	0.031	0.161	0.107	0.050	0.082	502
794	an + cd + st	20	0.758	0.044	0.174	0.121	0.039	0.166	536
828	an + cd + si	17	0.598	0.069	0.137	0.097	0.023	0.360	541
835	an + cd + si	38	0.822	0.058	0.148	0.144	0.059	0.267	566
262B	an + cd + si	37	0.887	0.064	0.161	0.134	0.050	0.242	520
433C	an + cd + si	4	0.600	0.062	0.173	0.103	0.020	0.210	560
Inlier									
062	si + or	20	0.965	0.094	0.068	0.243	0.025	0.046	703

Rim compositions were used in all cases. Microprobe mineral analyses and calculations for Meguma samples were done by R. Raeside of Acadia University. Mineral assemblages are those found in the general area of the sample site, with quartz, biotite, plagioclase (given as % An), muscovite (not present in inlier) and garnet present in all samples. Note that the andalusite in sample 792B is the cloudy equant variety whereas all other andalusites are the prismatic type. All Meguma samples are schists except for 262B and 433C which are hornfels. Temperatures calculated using the calibration of Hodges and Spear (1982) are 10-30°C higher. Sample locations are given on Figures 2, 3. Mineral abbreviations indicate chlorite, andalusite, cordierite, staurolite, sillimanite, and orthoclase.

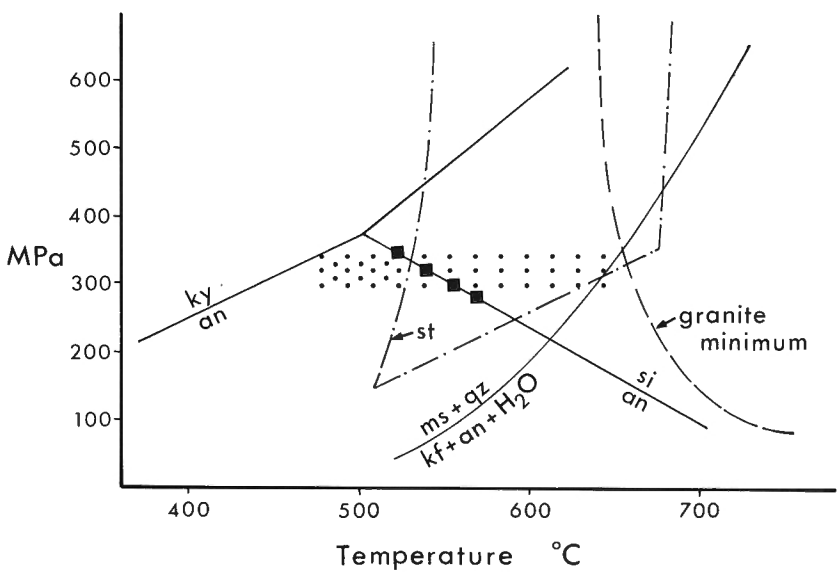

Figure 45. Probable pressure-temperature conditions during the peak of D_2 metamorphism in areas away from (heavily shaded) and close to (lightly shaded) granitic plutons. Solid squares are biotite-garnet equilibration temperatures for pelite samples containing both andalusite and sillimanite (data from Table 9). Al_2SiO_5 equilibria are from Holdaway (1971). Muscovite + quartz = alkali feldspar + Al_2SiO_5 + H_2O univariant curve is from Helgeson et al. (1978). The staurolite (st) stability field is from Richardson (1968). The minimum melting curve for granite is from Tuttle and Bowen (1958) and Luth et al. (1964).

f) Direct plotting on the aluminosilicate phase diagram of biotite-garnet equilibration temperatures determined in peltic rocks containing both andalusite and sillimanite gives pressures of 280-350 MPa (Fig. 45).
g) Approximate pressures derived using plagioclase-garnet geobarometry are in the range 324-542 MPa (Raeside et al., 1988).

These observations suggest that load pressure during the peak of D_2 metamorphism at about 372 Ma was most likely in the range 300-350 MPa (Fig. 45). This pressure corresponds to depths of 10-13 km, although inaccuracies in the established stability fields of the various minerals (e.g., Bohlen and Lindsley, 1987) could extend or decrease these depths by 1-2 km. The Meguma Terrane was uplifted and eroded to close to its present level of exposure by 350-360 Ma when the Gunns Brook formation was deposited, which implies an uplift rate of about 0.05-0.13 cm/a over the 10-20 Ma following static metamorphism and granitic plutonism.

Three main sources of heat might have caused granitic plutonism and regional and static metamorphism during D_2 as follows:

a) Crustal thickening by shortening or underplating during D_1 and the early part of D_2 (McKenzie and Clarke, 1975; Keppie, 1977);
b) Uprise of mafic magmas generated in the mantle or subducted oceanic crust (Keppie, 1977; Albuquerque, 1977); and
c) Large-scale frictional heating caused by shearing in the Cobequid-Chedabucto fault system (e.g., Hanmer, 1981).

The third model is incompatible with the fact that granitic plutons, and especially less evolved plutons (i.e., higher temperature), are not spatially associated with the Cobequid-Chedabucto fault system in the Meguma Terrane. The first model, crustal thickening, no doubt led to increased temperatures but appears to have been insufficient by itself to account for the inferred conditions. During D_2 but excluding the period of static and contact metamorphism, temperatures at the current level of exposure were likely about 500°C (i.e., upper greenschist to lower amphibolite facies—Turner, 1981). Accepting depths of 10-13 km as already inferred requires a geothermal gradient of 40-50°C/km. This gradient appears to be too high to be explained by crustal thickening alone. Thus, uprise of mafic magma seems to be required to impart additional heat to the crust. The presence of tonalite, which has liquidus temperatures of 1000-1100°C (Wyllie, 1977), suggests that mafic magma was involved in some way, either by supplying heat or ultimately giving rise to the tonalite plutons themselves. Under these conditions, significant partial melting could occur in the crust at depths greater than 25-35 km (Hyndman, 1981). In this scenario, uprise of granitic magma generated in the lower crust could account for elevated temperatures developed during the static metamorphic event. Thus, it is postulated that static and contact metamorphism were both caused by granitic plutonism within crust that was already preheated by mafic magma.

Porphyroclasts of plagioclase-quartz-biotite-garnet granofels in one sample from a mylonitic inlier in the Minister Brook formation in the Forest Hill area appear to have equilibrated at about 700°C (see Table 9). This high temperature suggests that the inliers are derived from much deeper crust than that currently exposed north of the Guysborough County fault.

Compositions of the granitoid plutons

The Meguma Group in the Canso and Forest Hill areas was intruded by two groups of granitoid plutons that are distinguished by age, composition, and areal extent. Small, widely separated bodies of tonalite (unit D_T) underlie <1% of both areas. All the tonalite plutons contain Meguma xenoliths and are intruded by pegmatite dykes believed to be related to granitic plutonism. In addition, the Shag Cove pluton is also intruded by at least four different granite and granodiorite plutons. Isotopic U-Pb zircon data indicate that at least some rocks in the Garry Lakes and Shag Cove plutons crystallized at about 378 Ma and this age is tentatively accepted for all the tonalite bodies. About 30 plutons and numerous miscellaneous small bodies and dykes of two-mica granite and minor granodiorite (unit D_G) comprise 37% of the two map areas. Concordant to nearly concordant U-Pb monazite dates of 371-373 Ma have been determined for three intrusions. Although isotopic age data do not cover the complete sequence of granitic intrusion, structural relationships (already described) suggest that all were emplaced at about the same time.

All the granitoid rocks are peraluminous, with Al/Na + k + 2Ca ranging from 1.05-1.25 in tonalite plutons to 1.08-1.34 in granitic plutons. Despite its small areal extent, the tonalite is quite variable in composition. Biotite, hornblende-biotite, and muscovite-biotite varieties are present and colour index of individual hand specimens varies from 10 to 40. The granitic plutons are much more uniform in composition. They contain subequal proportions of quartz, microcline, and plagioclase with <1-9% biotite and 1-13% muscovite. Comparison of deformed and undeformed rocks within single plutons shows that post-granite deformation and metamorphism did not significantly affect rock chemistry.

Although a large variety of granitic magmas can be generated in response to varying conditions of source composition, pressure, and temperature, recent work emphasizes four broad classes. In brief, these are peraluminous S-type granites, metaluminous I-type gabbro-granite suites, M-type quartz diorites, and A-type peralkaline granites (see summary by Pitcher, 1987). Granitic rocks in the Canso and Forest Hill areas have most of the characteristics of S-type granites such as high normative corundum, presence of Al-rich minerals, and restricted compositional range. However, compared to S-type granites in the Lachlan fold belt (Chappell and White, 1974), they have relatively high Na contents and unusually low initial $^{87}Sr/^{86}Sr$ ratios (Table 10).

In addition to metamorphic recrystallization in areas affected by D_2, mineral textures demonstrate that the undeformed granitic rocks suffered extensive subsolidus recrystallization. The only minerals that appear to preserve primary magmatic habits are plagioclase and accessories. Grain boundary relationships among the other essential minerals are consistent with a uniform subsolidus paragenetic sequence of microcline and quartz followed by biotite and muscovite. In addition, some plutons contain acicular sillimanite needles that crosscut all the essential minerals without regard to grain margins and that are in turn transected by muscovite-filled microfractures. Although biotite and muscovite display both primary-looking and secondary-looking habits, optical continuity and chemical homogeneity between different grain types within single thin sections indicate that all grains underwent virtually complete re-equilibration during subsolidus recystallization. The fact that each pluton has a characteristic range of rock and mineral compositions suggests that recrystallization was more or less isochemical at hand specimen scale. Compositional modifications appear to be restricted to the late formation of schlieren, fracture-fillings, and clots

Table 10. Characteristics of granitic plutons in the Canso and Forest Hill areas, compared with S-type criteria recommended by Chappell and White (1974), Ishihara (1977), Chappell (1978), and White et al. (1986)

Criteria	Canso-Forest Hill	S-type
Range of lithologies	Very restricted	Restricted
Na_2O	Generally 2.9-4.4%	Generally <3.2%
Al/Na + K + 2Ca	1.08-1.34	>1.1
Normative corundum	1.5-4.8%	>1.0
Inter-element plots	Very irregular	Irregular
Varietal minerals	Cordierite(?), garnet, subsoldus muscovite + biotite + sillimanite no hornblende	Cordierite, biotite, garnet, muscovite, Al_2SiO_5, no hornblende
Accessories	Ilmenite, monazite, zircon, tourmaline, large apatite grains, rare sphene	Ilmenite, monazite, zircon, large apatite grains, no sphene
Restite xenoliths	None recognized, locally derived Meguma xenoliths common	Metasedimentary
Initial $^{87}Sr/^{86}Sr$	0.703-0.709	>0.708
$Fe^3/Fe^2 + Fe^3$	0.02-0.33	<0.20

enriched in quartz and/or mica. The deformation of subsolidus grain textures by S_{2b} (which overlapped magmatism) in locally developed D_{2b} shear zones indicates that subsolidus recrystallization closely followed primary crystallization at nearly magmatic temperatures.

Comparison with other Meguma Terrane granitoid plutons

Granitoid rocks in the Meguma Terrane have relatively simple and uniform mineralogical compositions. Tonalite consists of quartz, plagioclase, and biolite locally with minor amounts of alkali feldspar and hornblende. Granite and granodiorite contain quartz, alkali feldspar, plagioclase, biotite, and muscovite with local cordierite. As a result, all the granitoid rocks in the Meguma Terrane are peraluminous and comparable lithologies have broadly similar major and trace element contents (Table 11) as well as rare-earth element patterns (Fig. 46). However, the eastern plutons, as represented by those in the Canso and Forest Hill areas, show four significant differences compared to the southern plutons and the South Mountain and Musquodoboit batholiths (see Fig. 1 for pluton locations) as follows:

a) Tonalite has only been found associated with the eastern and southern plutons. Based on limited data, tonalite in the eastern plutons is enriched in Al, K, Ba, and Rb compared to similar rocks in the southern plutons (see Table 11).
b) Granitic rocks in the eastern plutons and Musquodoboit batholith are generally restricted to true granite whereas granodiorite is abundant in the South Mountain batholith and southern plutons (references given in Table 11).
c) On average, muscovite is more abundant and biotite less abundant in granitic rocks in the Canso and Forest Hill areas compared to the southern plutons and the South Mountain and Musquodoboit batholiths (Fig. 47). Modal data from the River Lake (Thomas, 1982) and Bull Ridge (Chevalier, 1983) plutons suggest that this relationship may hold true for other eastern plutons as well.
d) Granitic rocks in the Canso and Forest Hill areas are enriched in Al, Na, K, and Rb and depleted in Fe, Mg and Ca compared to the southern plutons and the South Mountain and Musquodoboit batholiths (see Table 11). The South Mountain batholith and Canso-Forest Hill plutons can be effectively separated by plotting Al + Na + K against Fe + Mg (Fig. 48). The Musquodoboit batholith and southern plutons fall at intermediate values. Other eastern intrusions such as the Sherbrooke (Alizay, 1981), Mulgrave Lake (Dwyer, 1975), Bull Ridge (Chevalier, 1983), and River Lake (Thomas, 1982) plutons also fall in the Canso-Forest Hill field in Figure 48, which suggests that these chemical characteristics may apply to the whole of the eastern Meguma Terrane.

Granitoid plutons in the Meguma Terrane are remarkably similar considering their large areal extent. The eastern and southern plutons are broadly comparable because both groups form discrete bodies, contain tonalite, and occur in amphibolite facies rocks. However, the eastern

plutons are distinguished by restricted compositional range, high muscovite content, and high normative corundum.

Sequence and style of granitoid intrusion

Relative ages of the various tonalite bodies are unknown; 13 of the granitic plutons have partly or wholly known relative ages. They resolve into a minimum of five episodes of intrusion. To account for the remaining plutons, dykes, and miscellaneous bodies requires an intrusive sequence of at least six magmatic episodes (units D_{Ga} to D_{Gf}) and possibly more. All the granitic plutons were emplaced between D_{2a} and D_{2b} with crystallization of most of them between 371 and 373 Ma. This short time span raises the possibility, indeed the probability, that

Table 11. Average anhydrous analyses of granite in the Canso and Forest Hill areas (CFH), South Mountain batholith (SMB), Musquodoboit batholith (MB), and southern plutons (SP). Analyses exclude granodiorite as well as minor dykes and pegmatite. Average analyses of the Garry Lakes (GL) hornblende-biotite tonalite and Shag Cove (SC) biotite tonalite are compared to similar intrusions (Lyons Bay [LB] and Barrington Passage [BP]) associated with the southern plutons. Data are taken from Appendix III of this report and McKenzie and Clarke (1975), Smith (1974), MacDonald (1981), Albuquerque (1977), and Rogers (1986).

	Granite				Tonalite			
Analysis	CFH	SMB	MB	SP	GL	LB	SC	BP
SiO_2	73.3	74.0	73.1	73.6	60.2	59.3	65.6	66.0
TiO_2	0.2	0.3	0.3	0.2	0.8	1.0	0.8	0.7
Al_2O_3	15.1	14.0	14.8	14.8	18.8	17.6	16.8	16.1
FeO^t	1.2	1.9	1.7	1.6	5.1	5.4	4.3	4.1
MgO	0.4	0.5	0.5	0.5	3.7	3.6	2.0	1.9
CaO	0.7	0.9	0.9	0.9	5.4	5.6	3.2	3.1
Na_2O	3.8	3.3	3.7	3.6	3.4	3.6	3.6	3.7
K_2O	4.9	4.8	4.7	4.4	2.3	2.1	3.4	2.3
P_2O_5	0.3	0.2	0.3	0.2	0.2	0.4	0.2	0.2
Ba	377	307	253	559	543	362	725	513
Be	7			4			5	3
F	613			613	367		783	488
Li	102		182	90	89		87	58
Nb	13			12	9		18	11
Pb	30			41	26		31	16
Rb	355	267	294	172	138	73	220	89
Sn	11	16		5	3		5	3
Sr	75	63	97	98	400	373	288	324
Th	7	16	6	11	5		12	8
U	6		6	5	1		3	2
Y	10			17	13		20	18
Zn	57	60	54	50	95		98	65
Zr	62	85	94	112	76	132	210	173
CIPW co	3.0	2.2	2.7	3.0	1.3	0.3	2.0	2.3

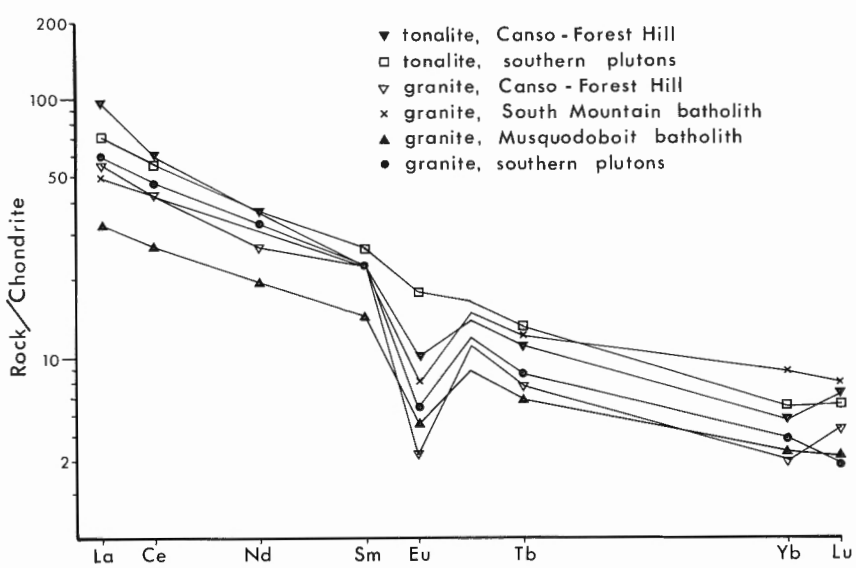

Figure 46. Chondrite-normalized plot of average rare-earth element contents in granitoid suites from the Meguma Terrane. Data for the southern plutons, South Mountain batholith, and Musquodoboit batholith are from Albuquerque (1977), Muecke and Clarke (1981), and MacDonald and Clarke (1985) respectively. Granite and granodiorite are averaged where they occur together. Chondrite values are from McLennan and Taylor (1980).

different granitic magmas coexisted. However, no age reversals or evidence of magma mixing were observed in the field, although the latter would be difficult to detect because of the similarity in composition of the magmas involved.

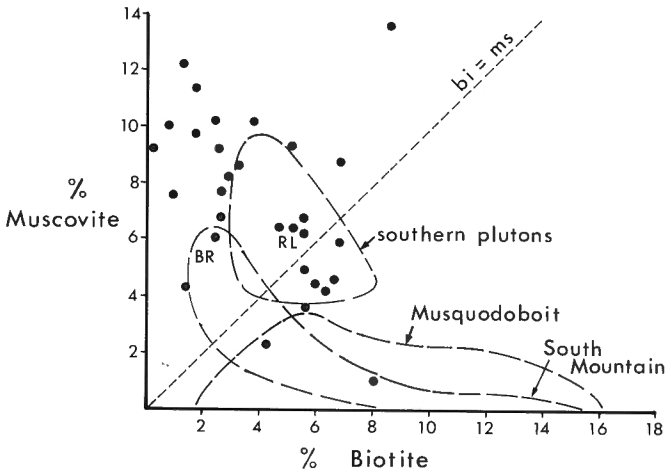

Figure 47. Variation in modal muscovite and biotite contents of plutons in the Canso and Forest Hill areas (solid circles). Fields for the Musquodoboit batholith (MacDonald, 1981), South Mountain batholith (McKenzie and Clarke, 1975; Ham and Horne, 1986), and southern plutons (Albuquerque, 1977; Rogers, 1986) are shown for comparison. Average compositions of the Bull Ridge (BR–Chevalier, 1983) and River Lake (RL–Thomas, 1982) plutons are also plotted.

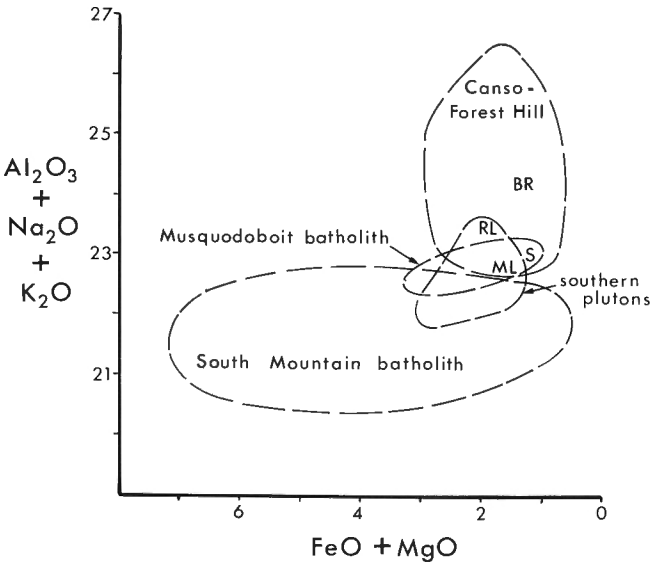

Figure 48. Bivariate plot illustrating the main chemical differences between granitic rocks in the Canso-Forest Hill area, South Mountain batholith (Smith, 1974; McKenzie and Clarke, 1975), Musquodoboit batholith (MacDonald, 1981), and southern plutons (Albuquerque, 1977; Rogers, 1986). The Sherbrooke (S–Alizay, 1981), Bull Ridge (BR–Chevalier, 1983), River Lake (RL–Thomas, 1982) and Mulgrave Lake (ML–Dwyer, 1975) plutons, which occur in the eastern Meguma Terrane, plot within the Canso-Forest Hill field.

Little is known about the shapes and mechanism of emplacement of the tonalite plutons because of their small sizes and the effects of later deformation and granite intrusion. Field relationships with the country rocks are similar to those observed for the granitic plutons. The granitic plutons occur as discrete intrusions except in the southern part of the Canso area where they comprise a large composite mass. Where post-granite deformation is weak, individual intrusions are roughly equidimensional in plan view. The few contacts observed suggest that plutons are steep-sided. A single gravity profile across the southern part of the Canso area has been calculated using all regional gravity data available up to April, 1986 (Fig. 49). The profile suggests that the granitic plutons in that area amalgamated to form a relatively thin, slab-like body extending to a maximum depth of about 3 km.

Meguma Group xenoliths up to 0.1 km² in size are dispersed within several plutons in the southern part of the Canso area. They have highly variable bedding orientations, which implies that they are not roof pendants. However, they could be roof fragments that have suffered significant sinking and rotation. Meguma xenoliths are also concentrated in widespread agmatite zones along the margins of many plutons. These features indicate that stoping played a major role during emplacement. A relatively high ductility contrast between granitic magma and country rocks is implied by the following observations in areas where post-granite deformation is weak or absent:

a) Xenoliths are blocky and have angular corners.
b) Pluton margins truncate bedding and S_1 at large angles.
c) Stringers of granite as narrow as a few millimetres thick locally penetrate highly fractured wall rocks (e.g., Fig. 13a).

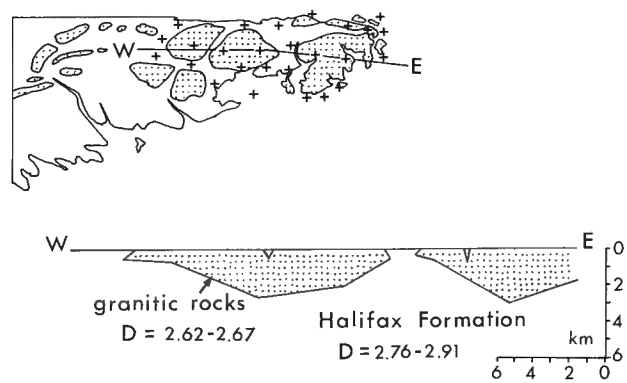

Figure 49. Profile of the upper crust in the easternmost Meguma Terrane, calculated from regional gravity data available up to April, 1986 (M. Thomas, personal communication, 1986). Densities were determined for five Halifax metapelites and seven granitic rocks. A density difference of 0.15 was used in the calculations. The sketch map shows the location of the profile and all gravity stations.

Although the exact proportions of liquid and crystals cannot be ascertained, the relationships described suggest that the granitic magmas were relatively fluid at the time of intrusion (i.e., less than about 70% crystals according to Hibbard and Watters, 1985). The formation of the composite granitic body in the southern part of the Canso area resulted in numerous interplutonic contacts that are well displayed in coastal exposures. The abrupt nature of the contacts and the occurrence of abundant plutonic xenoliths and dykes indicate that some intrusions were solid enough to fragment by the time the next intrusion was emplaced. The rounded shapes of many of the plutonic xenoliths suggest that a relatively small ductility contrast may have existed between successive phases of intrusion. In contrast, individual plutons must have been nearly solid when pegmatite and aplite dykes formed because dyke walls are locally marked by cataclasis and brittle offsets.

External pluton contacts are much more concordant with bedding and the dominant tectonic foliation in the country rocks in areas where post-granite deformation is relatively strong. This concordance probably reflects lower ductility contrast during D_{2b} and later because of progressive syntectonic crystallization of the magmas and strain softening in the country rocks.

Causes of lithological variation of the granitoid rocks

Five lines of evidence suggest that the tonalite and granitic plutons represent two different magmatic events:

a) There is a wide compositional gap between them.
b) There is a large difference in areal extent and presumably volume between the two groups.
c) Least squares mixing calculations using observed mineral compositions suggest that the tonalite and granitic plutons do not lie on any reasonable mixing trend lines. Therefore the tonalites are probably not cumulates or restite-rich members of the granite suite.
d) The Garry Lakes and Shag Cove tonalite plutons contain euhedral zircon crystals that lack visible cores and show no evidence of isotopic inheritance (T. Krogh, personal communication, 1987). This suggests that they had a different origin compared to the granitic plutons that contain zircons showing evidence of crustal inheritance.
e) They are separated in time by about 6 Ma without any indication of intervening igneous activity.

There are five possible causes of lithologic variation within each of the two groups of plutons:

- fractional crystallization of a homogeneous parental magma
- progressive fractional melting of a homogeneous source
- processes with variable effects (e.g., assimilation, volatile transfer)
- restite unmixing
- partial melting of heterogeneous source producing various magma types

Relationships among the tonalite plutons are poorly known and the following arguments apply mainly to the granitic plutons. The homogeneity of most plutons compared to the total range of granitic rock types and the lack of systematic correlation between composition and relative age indicate that differentiation must have operated below the current level of exposure. Thus, given the short time span inferred for intrusion and crystallization, individual plutons must have formed either independently or from magma (liquid plus crystals) that was tapped at different times from different parts of one or more zoned subchambers.

The small differences in composition between the various granitic plutons indicate that minor fractionation of the essential minerals in a single parental magma could have produced the rock types observed. However, this model is opposed by the large variation in initial $^{87}Sr/^{86}Sr$ ratios (0.703-0.709) and by irregular interelement plots (see Fig. 26). Furthermore, the large range in Rb/Sr (incoherent element pair) compared to K/Rb (coherent pair) suggests, but does not require, that fractional crystallization was relatively unimportant (Fig. 50). For these reasons, large-scale fractional crystallization of a single parental magma is discounted. Progressive fractional melting of a homogeneous source is also discounted for the same reasons. Local fractional crystallization appears to have resulted in the formation of some dykes and small bodies that are spatially associated with particular plutons. This aspect is discussed in more detail at the end of this section.

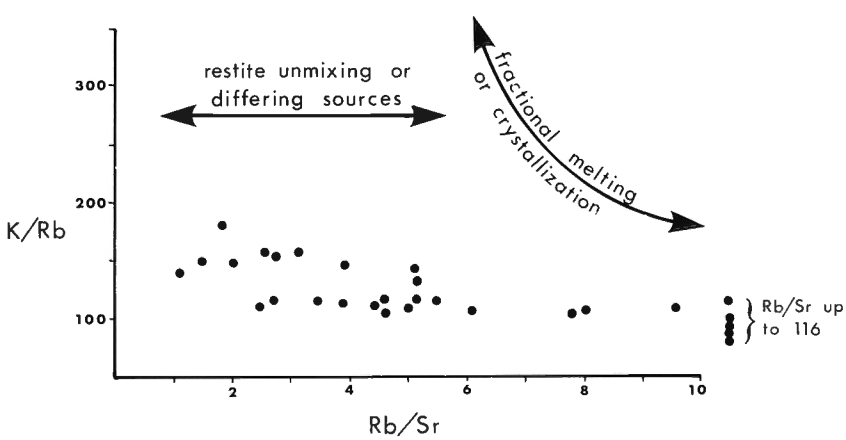

Figure 50. K/Rb versus Rb/Sr in granitic plutons in the Canso and Forest Hill areas. Arrows illustrate the most likely liquid trends generated by variations in source composition or restite unmixing and fractional melting or crystallization of a single parent.

Variable processes such as assimilation and volatile transfer are more difficult to evaluate simply because their results are harder to predict. The homogeneity of most plutons mitigates against these processes because their effects should vary from place to place within individual intrusions, unless efficient mixing occurred after differentiation. The only candidate for high-level assimilation is the Meguma Group. If this was significant, normative corundum would vary sympathetically with initial $^{87}Sr/^{86}Sr$, reflecting addition of variable amounts of Al-rich metasedimentary material with initial ratios of 0.711-0.718 (Clarke and Halliday, 1980). Instead, these two parameters show no correlation (Fig. 51). In addition, linear trends for the granitic plutons in the Canso area between Na_2O, FeO, and Zr do not intersect compositional fields defined by Meguma rocks (Fig. 52). Thus, large-scale contamination by Meguma-like material seems unlikely. Local contamination may be responsible for the unusual compositions of the Oliver Island tonalite and Lookout Hill granite plutons, both of which are abnormally peraluminous compared to other intrusions in their respective map units. This interpretation is compatible with the fact that the Lookout Hill pluton is displaced in more or less the appropriate direction from compositional trend lines defined by the other granitic plutons (Fig. 52). Volatile transfer appears unlikely as well because there is virtually no evidence for water-saturation, except perhaps at the very last stages of crystallization when pegmatite dykes and a few miarolitic cavities formed.

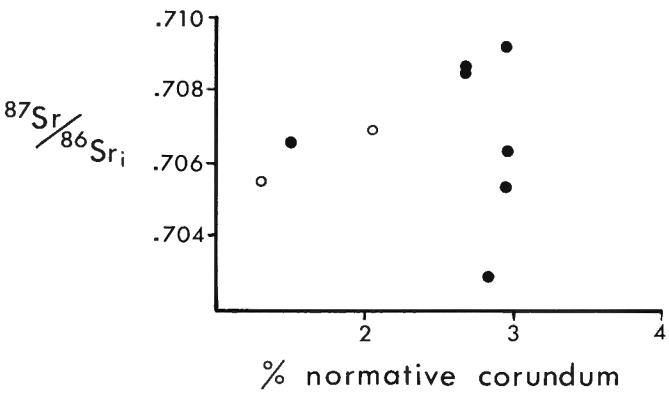

Figure 51. Variation in initial $^{87}Sr/^{86}Sr$ with CIPW normative corundum in tonalite (open circles) and granitic rocks (closed circles). (Isotopic data taken from Table 6.)

Restite-unmixing has been invoked to explain linear inter-element trends in a variety of I- and S-type granitic suites, especially in eastern Australia (e.g., Chappell, 1978). There is very little physical evidence for significant proportions of restite material in the Canso-Forest Hill plutons. Foliate or granoblastic aggregates of biotite (the only common mafic mineral) and unzoned, corroded, calcic cores in plagioclase grains are lacking. Xenoliths are restricted to locally derived metasedimentary and granitoid rocks. The highly felsic lithologies of the plutons (<10% biotite) and the fact that most of them have close to minimum melt compositions (Fig. 53) leave little room for a restite component, even in the most mafic intrusions. Linear trends are evident for several elements in Figure 26. These trends are revealed in more detail in Figure 54, which shows the variation of selected major and trace elements for granitic plutons in the Canso area alone. Good linear trends only occur for FeO, MgO, Na_2O, and Zr. Almost no correlation is shown between FeO and SiO_2, Al_2O_3, K_2O, and Rb. These data, coupled with the large range in initial $^{87}Sr/^{86}Sr$ ratios, suggest that restite unmixing was not important in controlling lithologic variation in unit D_G plutons.

The last process, partial melting of a heterogeneous source, appears to be the most acceptable. It would explain poor inter-element correlation in variation diagrams, the large range in initial $^{87}Sr/^{86}Sr$ ratios and unsystematic change in pluton composition with decreasing age of intrusion. It would also explain decoupled behaviour of some rare-earth, large ion lithophile, and high field strength elements (e.g., La, Rb, and Zr in Fig. 55) as each pluton or group of plutons would have its chemical characteristics determined by the composition of its respective source and P-T conditions during partial melting. It is impossible to ascertain the precise number of independent granitic magmas generated. The data

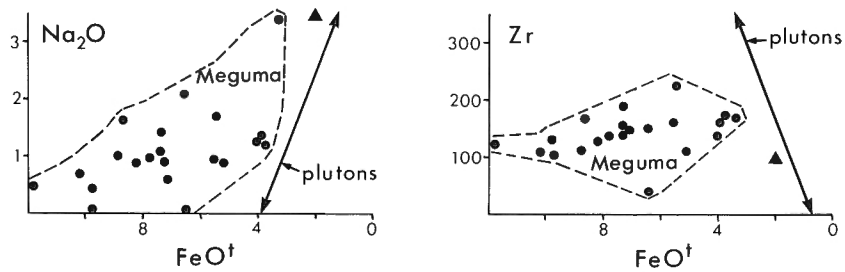

Figure 52. Linear Na_2O-FeO and Zr-FeO trends defined by granitic plutons fall outside the compositional range of Meguma metasedimentary rocks in the Canso area. This trend implies that large-scale lithological variation in unit D_G was not caused by contamination with Meguma-like material. Linear pluton trend lines are taken from Figure 54. (Meguma data are from Appendix IV.) The Lookout Hill pluton (shown by triangle), which has an unusually mica-rich composition, may have suffered high-level contamination.

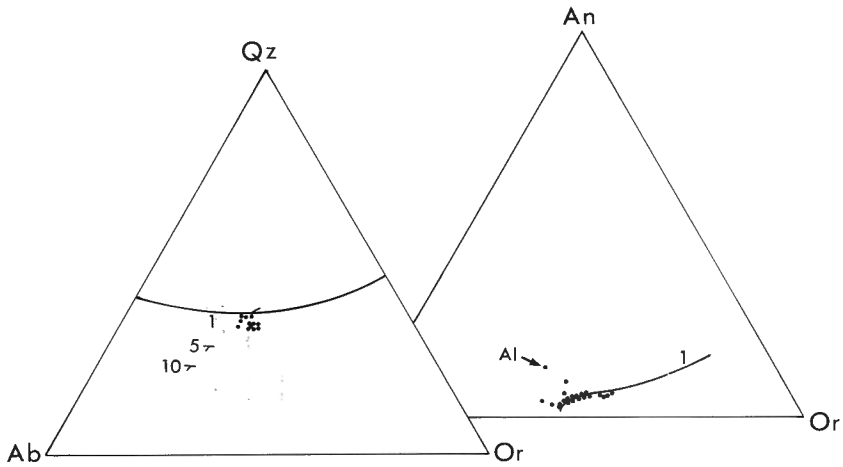

Figure 53. Proportions of normative quartz, albite, orthoclase, and anorthite in average granitic pluton compositions from the Canso and Forest Hill areas. Only pluton compositions calculated from three or more analyses are used and only those with <1% anorthite are plotted in the qz-ab-or-H_2O system. Al is the Andrew Island pluton. Numbers indicate boundary curves and minima for 1, 5, and 10 kb water vapour pressure (Luth et al., 1964; James and Hamilton, 1969).

do suggest, however, that they do not correspond exactly with unit designations. For example, the Andrew Island pluton (plots at 1.99% FeO in Fig. 54) appears to represent a different magma type from the three other plutons assigned to unit D_{Gb}.

The model of more or less simultaneous generation and uprise of several independent magmas from a heterogeneous source is only meant to explain the large-scale lithologic variation. Certainly, some variation within single plutons and groups of similar plutons may be the result of processes such as fractionation or restite-unmixing. Three lithologies in the granitic plutons appear to have formed by in situ differentiation:

a) Several dykes and small bodies of fine grained granite, grouped together as the False Cove pluton (unit D_{Gc}), intrude and are closely associated in space with three unit D_{Gb} plutons (Andrew Island, Madeline Point, and Dover Head plutons); the False Cove granite contains scattered small phenocrysts of quartz, microcline, plagioclase, muscovite, and biotite.
b) Small dykes and bodies of aplitic biotite-muscovite leucogranite intrude the medium- to coarse-grained Durells Island biotite-muscovite granite; the two rock types are similar in composition.
c) Small, poorly defined zones of quartz syenite occur within the Lumsdens Lake and Fogherty Lake granite plutons. Contacts between the granite and quartz syenite appear to be sharply gradational over about 1 cm; the two lithologies are very similar except for the difference in quartz content.

In situ differentiation has been tested by modelling the derivation of the aplitic and syenitic rocks from parental magmas defined by their associated host granitic plutons. Results are given in Table 12. Mineral compositions used were those observed in the parent plutons (data given in Appendices II and III). The data are consistent with the derivation of the False Cove granite from the Madeline Point and Dover Head plutons by minor gains and losses of the rock-forming minerals. Thus various dykes and small bodies of False Cove granite, which intrude the Madeline Point and Dover Head plutons, could have been produced by differential movements of crystals and residual liquid during the later stages of consolidation of the host intrusions. The calculations are less satisfactory for derivation of the False Cove granite from the Andrew Island pluton, which indicates either that some additional process such as assimilation was involved or that the False Cove and Andrew Island plutons are not related. The Durells Island aplite probably formed from the Durells Island granite pluton in the same manner as that described. The quartz syenite bodies in the Lumsdens Lake and Fogherty Lake plutons could have formed by the loss of a fluid containing about 99% Si with minor gains and losses of other elements. This interpretation favours formation of the quartz syenite by late stage loss of hydrothermal fluids rich in Si. The presence of numerous quartz veinlets in the host plutons supports this hypothesis.

Nature of source area

For reasons given in the preceding section, the tonalite and granitic plutons appear to have had different origins. The composition of the source from which the granitic magmas (unit D_G) were derived is considered first because more data are available for the granitic plutons. Following this, the tonalites are discussed.

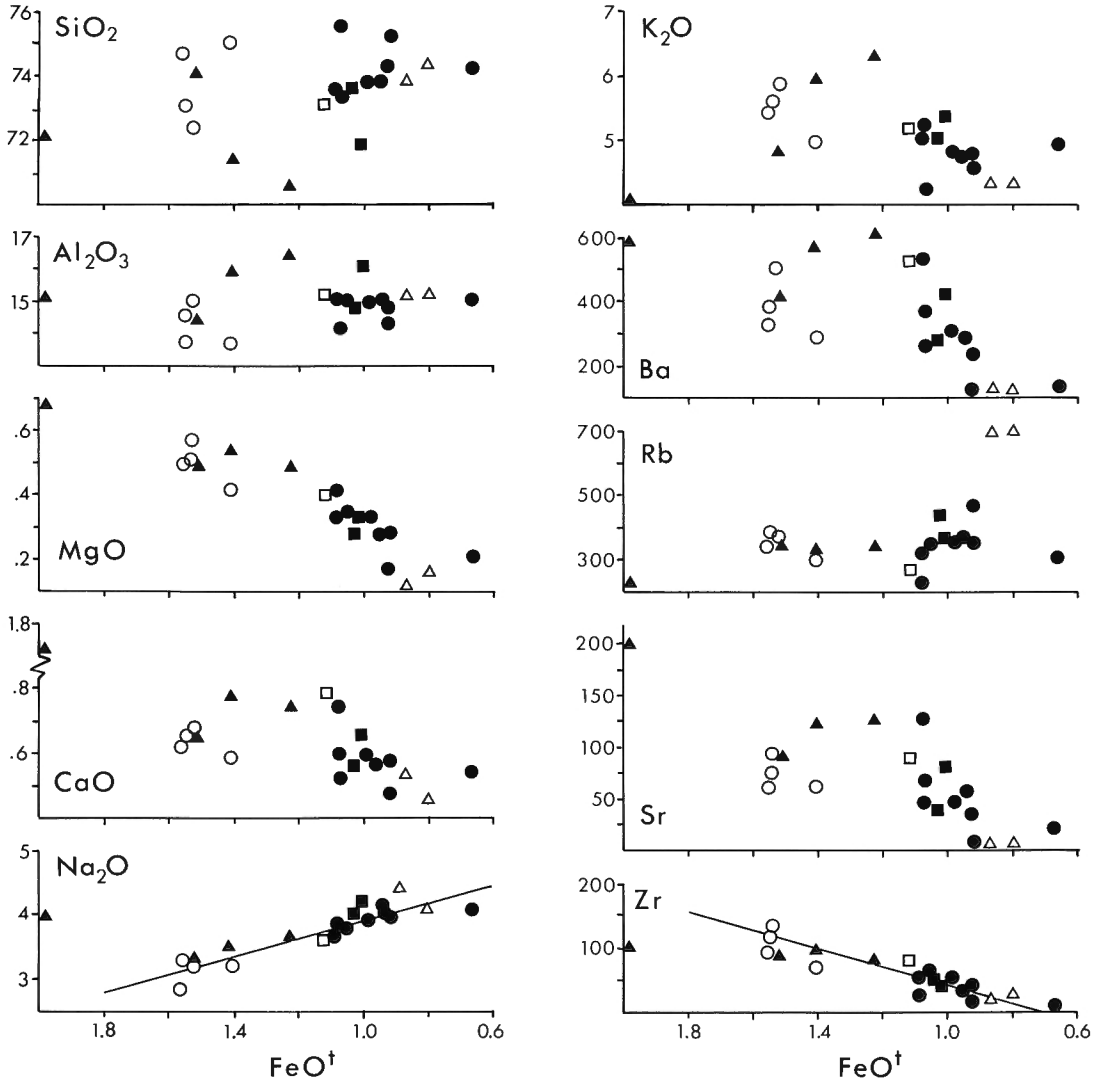

Figure 54. Variation of selected major and trace elements with FeO in granitic plutons from the Canso area. The Lookout Hill pluton is omitted because of its unusual and possibly contaminated composition. Lines have been visually fitted to the Na_2O-FeO and Zr-FeO plots for use in Figure 52. Symbols are solid square for unit D_{Ga}, solid triangle for unit D_{Gb}, open square for unit D_{Gc}, solid circle for unit D_{Gd}, open circle for unit D_{Ge}, and open triangle for unit D_{Gf} plutons.

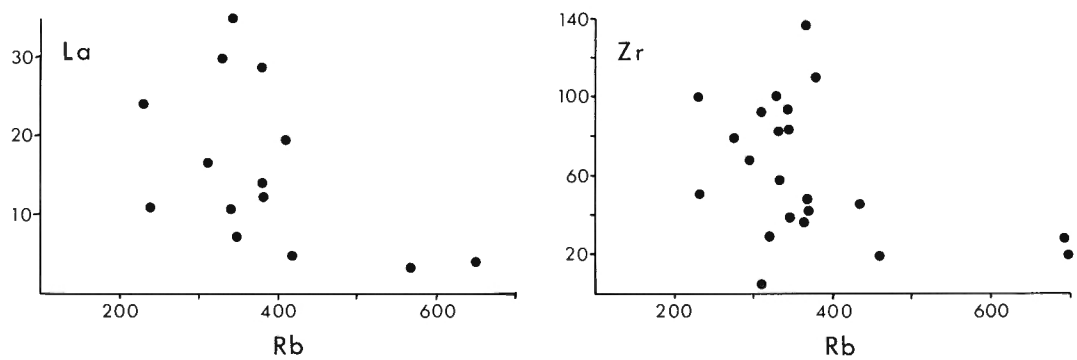

Figure 55. Variation in La (individual rock samples, Appendix IV) and Zr (pluton compositions, Appendix III) with Rb in unit D_G in the Canso area.

Table 12. Best-fit results of least squares mass balance calculations (Bryan et al., 1969) for derivation of the False Cove aplitic granite, Durells Island aplite, and Lumsdens Lake and Fogherty Lake quartz syenites from spatially associated plutons. Mixing components, expressed as weight fractions of the parent, are described in the text. ΣR2 is the sum of the squares of the residuals. (Parent and daughter compositions are given in Appendix III.)

			Mixing components				
Parent	Daughter	ΣR2	Pl	Kf	Qz	Bi	Ms
DH	FC	0.008		-.06	+.01	-.02	-.01
MP	FC	0.003	+.02	-.06	+.09		+.01
Al	FC	0.464	-.30	-.10	-.21	-.07	
Dl	Dla	0.029	-.02		-.02	-.01	
FL	FLs	0.011	+.03	+.10	-.32	+.01	-.03
LL	LLs	0.009	+.01	+.04	-.32		-.05

No direct evidence, such as lower crustal xenoliths, is available concerning the source area. A crustal source is inferred because of the large amount of uniformly felsic rocks produced having Rb/Sr ratios as high as 116. As most plutons have close to minimum melt compositions (see Fig. 53) and very low contents of cafemic components, an intermediate to felsic source containing quartz and two feldspars is favoured. Even small degrees of partial melting of mafic rocks produce liquids that are more like granodiorite than granite, with relatively high Fe, Mg, and Ca contents compared to granitic rocks in the Canso and Forest Hill areas (e.g., Holloway and Burnham, 1972; Helz, 1976). Initial $^{87}Sr/^{86}Sr$ ratios as low as 0.7030 raise the possibility that some plutons may contain a mantle component. However, the amount of possible mantle component is severely limited by the highly felsic compositions of the rocks (e.g., MgO generally less than 0.7%). Furthermore, there is no correlation between initial $^{87}Sr/^{86}Sr$ and MgO or FeO, as would be expected if contamination with mantle-derived material having low initial ratios had been significant.

The composition of the source area cannot be easily constrained because of the minimum melt compositions of the plutons and their lack of restite component (Chappell, 1984). The granitic intrusions are highly peraluminous (normative corundum = 1.4-4.8%), suggesting that their source contained a significant proportion of aluminous material such as pelite or peraluminous granite (Chappell and White, 1974; Clemens and Wall, 1981). Relatively high Na_2O contents imply that the Canso-Forest Hill source, if metasedimentary, was less mature than that involved in the generation of S-type plutons in the Lachlan fold belt in Australia (Chappell, 1978). The relatively low initial $^{87}Sr/^{86}Sr$ ratios, which overlap those for I-type granites, indicate that the source was either young or had low Rb/Sr; high Rb/Sr in many of the granitic rocks favours the former possibility. The initial ratios of the Canso plutons indicate that the Meguma Group was not the source if initial $^{87}Sr/^{86}Sr$ ratios of 0.711-0.718 at 372 Ma determined for the Meguma Group elsewhere (Clarke and Halliday, 1980) are applicable to the eastern Meguma Terrane.

In summary, granitoid plutons in the Canso and Forest Hill areas are believed to have formed from several independent magmas, generated at about the same time in a somewhat heterogeneous source composed of felsic to intermediate quartzofeldspathic rocks containing a significant peraluminous component. In this model, correlation between ΣREE, La/Yb, and Mg (see Fig. 30) corresponds to increasing degrees of partial melting in broadly similar source materials with increasing participation of such minerals as allanite and monazite in the melt and garnet in the residuum (Miller and Mettlefehldt, 1982). Moderate but variable negative Eu anomalies (see Fig. 30) reflect the retention of significant amounts of feldspar in the source with variable proportions taking part in the melting process. Given an average pluton thickness of 2 km (not counting material removed by erosion — see Fig. 49) and 20% partial melting requires a source volume represented by a cube about 11 km on a side. It is not surprising then that a crustal source of this dimension should yield partial melts of varying chemical characteristics.

The tonalite plutons have 1.3-2.9% normative corundum and initial $^{87}Sr/^{86}Sr$ ratios of 0.706-0.707, which suggests that continental crust was important in their formation as well. This interpretation is supported by their high K and Rb contents compared to tonalite generated within oceanic crust (e.g., Mason and McDonald, 1978). Two possibilities remain. The first is that basaltic magma generated in the upper mantle or subducted oceanic crust was contaminated by reaction with peraluminous crustal material during ascent. The second possibility is that tonalite magmas were derived by partial melting of mafic to intermediate rocks in the lower crust. The peraluminous nature of the magmas could have resulted by fractionation of amphibole (Cawthorn et al. 1976) or assimilation of peraluminous crust.

ECONOMIC GEOLOGY

General statement

Economic mineral showings occur in all three main lithologic divisions in the Canso and Forest Hill areas — the Cambro-Ordovician Meguma Group, Devonian granitoid plutons, and Devono-Carboniferous cover rocks. All established occurrences and a few new showings found during the 1985 and 1986 field seasons are described briefly in the following sections. The new showings are relatively small and most appear to have minimal economic significance.

Meguma Group

Gold

Gold in quartz veins in the Goldenville Formation is by far the most important type of mineralization in the eastern Meguma Terrane. It is known to occur northwest and southwest of Country Harbour Mines, southeast of Camerons Lake, and at Forest Hill in the Forest Hill area. It was first discovered in 1861 and mining has continued at various times and places since 1868 (Malcolm and Faribault, 1929). In addition, a new mine owned by Westminer Canada Limited is currently going into production at Forest Hill. Gold, arsenopyrite, pyrite, pyrrhotite, and minor chalcopyrite, sphalerite, and galena are generally confined to quartz veins carrying variable, small amounts of feldspar, mica, tourmaline, and chlorite. Individual veins range from <0.1 to 30 cm thick and are typically oriented parallel or subparallel to bedding on the flanks of large, anticlinal fold structures (Fig. 56). A few quartz veins are truncated by granite dykes at Forest Hill and Country Harbour Mines (Malcolm and Faribault, 1929). The fact that some veins are boudinaged (Fig. 56) and arsenopyrite crystals are deformed by S_{2b} suggests that vein formation (and presumably gold precipitation) occurred prior to D_{2b}. The bedding-parallel orientation of most of the veins may be the result of transposition during D_{2b} and D_{2c}, if variable orientation existed before D_{2b}.

Figure 56. Boudinaged quartz vein oriented parallel to bedding and S_{2b} in Goldenville metawacke and semi-schist at Forest Hill. GSC 204508-W.

Both syngenetic and epigenetic models have been used recently to explain the origin of auriferous quartz veins in the Goldenville Formation. McBride (1978) and Haynes (1986) favoured hydrothermal precipitation during clastic deposition on the sea floor. On the other hand, a syntectonic origin has been invoked by Mawer (1986), Crocket et al. (1986) and Smith and Kontak (1987), although the details of timing and origin of the hydrothermal fluids are unresolved. At this point it should be noted that Mawer (1986) has suggested that deposition was partly controlled by thermal conditions approximated by the chlorite-biotite isograd. This interpretation is untenable in the Forest Hill area where regional D_2 metamorphism reached lower to middle amphibolite facies, unless veins formed at lower grade prior to D_2 and were simply remobilized during subsequent D_2 deformation and metamorphism.

Recent work suggests several other places favourable for gold exploration in the Goldenville Formation in the Canso and Forest Hill areas. A regional lake sediment geochemistry survey (Rogers et al., 1985) found anomalous values of 15-21 ppm Au near Cooeycoff Lake and between Lawlor Lake and Country Harbour. The Cooeycoff Lake anomaly is only a few kilometres south of a gold showing indicated on Stevenson's (1964) map and the other anomalies are close to the old gold mines between Forest Hill and Country Harbour mines. (Gold analyses are given for 29 Meguma Group and quartz vein samples in Appendix IV). Most samples contain 1 ppb Au or less, in agreement with an average value of 1-2 ppb for unmineralized rocks in the Meguma Group (see Crocket et al., 1986). An anomalous value of 63 ppb Au was found for a coticule bed (sample 226) in unit CO_{Hb} on the coast about 1 km northeast of Whitehead. Slightly anomalous values of 5-13 ppb Au occur in several other samples (see Fig. 2, 3). In the area between Forest Hill and Country Harbour mines, known gold showings occur in a 200 m wide zone that lies 500-700 m structurally beneath the Halifax-Goldenville contact, on both flanks of the Loon Lake synclinorium. The implication is that the same zone farther east (e.g., between Costley Lake and Tom Lake) is also favourable for exploration. Its potential is enhanced by the presence of large folds (F_1?) recognized between Eight Mile and Tom lakes and the discovery by Esso Minerals of quartz veins containing accessory pyrite, arsenopyrite, and molybdenite near the gravel road south of Lawlor Lake (NSDME[1]). On the other hand, contrary to the suggestion of Haynes et al. (1986), most of the area between Camerons Lake and Country Harbour River is not a good exploration target for gold as it is mainly underlain by granitoid rocks.

[1] Reference denotes assessment files available at the Nova Scotia Department of Mines and Energy, Halifax, Nova Scotia.

Base metals

Tungsten mineralization has been found in two places along the north shore of the Canso area. The Lazy Head prospect, 2.5 km west of Durells Island, consists of scheelite and minor chalcopyrite, sphalerite, pyrite, and pyrrhotite in quartz veins stratabound within a 1-1.5 m thick orange-weathering coticule bed (Shaw, 1983). The coticule is fractured, locally brecciated, and consists of about 70% spessartine-rich garnet. Drilling and trenching undertaken since 1955 indicate that the horizon continues along strike for at least 80 m and down dip for more than 50 m. The coticule bed occurs within grey phyllite at the base of unit CO_{Ha}, about 30 m stratigraphically above the Halifax-Goldenville contact. Shaw (1983), using the base of the graphite schist horizon as the Halifax-Goldenville boundary, placed the mineralized coticule bed in the upper part of the Goldenville Formation. The best assay obtained to date is 2.19% WO_3 over a 30 cm section of drill core (NSDME). A grab sample of vein material (sample 059B, Appendix IV) was found to contain 3200 ppm W and 420 ppm Zn. A sample of the coticule bed (sample 059A) is only slightly anomalous in W and Sn. A similar showing of scheelite and pyrite is reported to occur a few metres north of Route 16 about 500 m west of Canso (NSDME). The showing lies within the Goldenville Formation and contains spessartine garnet. Although the composition of the host horizon is unknown, the presence of spessartine suggests that it could be similar to the one at Lazy Head.

Pyrite and pyrrhotite are abundant in unit CO_{Ha}, locally forming up to 50% of individual hand specimens. They occur as tiny veinlets with quartz, lensoid streaks up to 20 cm long and 5 cm wide, and disseminated grains. Chalcopyrite is associated with pyrite and pyrrhotite in four places in unit CO_{Ha} along the north shore of the Canso area. The best showing was found in andalusite-graphite schist at the bottom of the Tittle in 1953 when the channel was being deepened by blasting (NSDME). Grab samples returned copper values of 0.68-1.2%. However, later drilling showed that although pyrite and pyrrhotite persisted at depth, significant copper mineralization was confined to the surface. Samples of chalcopyrite-bearing graphite schist collected farther west (samples 086A, 086B, Appendix IV) were found to contain only 25-45 ppm Cu. Likewise, a mineralized quartz vein (sample 011) in graphite schist contained only 61 ppm Cu.

Aluminum

Schist with 20-30% andalusite porphyroblasts was bulk tested in the 1950s as a source for aluminum at two localities — Black and Doughboy points (NSDME). The Black Point occurrence is in graphite schist in unit CO_{Ha} whereas the Doughboy Point occurrence is in quartz-muscovite schist in unit CO_{Hd}. Grades were found to be too low for commercial exploitation.

Granitoid rocks

Granophile element deposits are associated with peraluminous granitic rocks throughout the world (e.g., Taylor, 1979; Strong, 1981). Within the Meguma Terrane, significant occurrences of Sn, Mo, U, W, Cu, F, Be, and Li are found in the Wedgeport pluton (Chatterjee and Keppie, 1981) and in several places in the South Mountain batholith (e.g., O'Reilly et al., 1982; Chatterjee et al., 1982). The most notable example is the East Kemptville tin mine, which has reserves of 38 million tonnes grading 0.2% Sn (Richardson et al., 1982). These deposits and showings point to the potential for granophile element mineralization associated with granitic plutons in the Canso and Forest Hill areas.

So far, only minor economic mineral showings have been found. Accessory beryl has been reported to occur in leucogranite pegmatite containing muscovite, garnet, and tourmaline in four places: on the north side of the highway about 2.2 km east of the intersection between Routes 16 and 316 in the Canso area (Shaw, 1983); on the east side of Route 316 about 700 m south of the same intersection (K.L. Ford, personal communication, 1987); at the southeast corner of the Buchanans Mountain pluton (G. O'Reilly, personal communication, 1987); and between Camerons and Grassy lakes in the Forest Hill area (Schiller, 1963). The pegmatite on Route 316 also contains traces of pyrite and molybdenite (Shaw, 1983). A 2 m thick dyke of pegmatite exposed in a series of old exploration pits south of Route 16 and 2.1 km east of the intersection contain minor pyrite and chalcopyrite. K. Adams (personal communication, 1986) found possible beryl and wolframite in pegmatite float north of the Forest Hill mine site. Traces of pyrite and chalcopyrite were also found in rare ovoid quartz-mica clots (2-4 cm long) in the Ketch Harbour and Madeline Point plutons at the east end of Little Dover Run in the Canso area. The most promising occurrence is at the southeast corner of the Buchanans Mountain pluton (unit D_{Gf}) in the Forest Hill area. The granite is leucocratic, fine to medium grained, muscovite rich, and protocataclastic. It contains disseminated pyrite and is everywhere orange-weathering because of iron oxide stain. The muscovite is typically lemon yellow in colour and may be enriched in F and Li based on whole rock analyses. The adjacent country rocks are quartz-mica schist belonging to the Goldenville Formation. Several horizons (<1-20 cm thick) contain up to 40% euhedral black tourmaline. Both the granite and the schist are crosscut by pegmatite dykes and quartz veins containing accessory muscovite, beryl, pyrite, and graphite. Dykes of fine- to medium-grained granite up to 3 m thick also intrude the metasedimentary rocks. Grab samples of the Buchanans Mountain pluton and a granite dyke in the country rocks (sample 088A) were found to contain 34 and 130 ppm Sn and 920 and 1400 ppm F respectively (Table 13). According to G. O'Reilly (personal commication, 1987), the tourmaline-bearing schist contains 180-620 ppm Sn, 661-2110 ppm Li, and 9-17 ppm Be. Thus, unit D_{Gf} granitic rocks show enrichment in the same elements, although to lower degrees, as the muscovite leucogranite that hosts the East Kemptville tin deposit (Kontak, 1987).

The general characteristics of mineralized granitic rocks which have been described by Tischendorf (1977), Taylor (1979), Darnley (1982), and Plimer (1987) include post-tectonic emplacement of anatectic granite in orogenic belts; associated granophile element mineralization at the marginal and apical parts of intrusions; accessories such as cassiterite, beryl, fluorite, topaz, and tourmaline; enrichment in volatiles and granophile trace elements; abundant hydrothermal alteration and fracturing; and an unusual order of mineral crystallization. Devonian granitic rocks (unit D_G) in the Canso and Forest Hill areas have some of these characteristics but lack others. For example, they are anatectic, slightly enriched in Sn, U, Li, and Rb compared to unmineralized granites (Table 13), and contain a few minor occurrences of beryl, chalcopyrite, and molybdenite. On the other hand, they are syntectonic with respect to D_2; pervasive alteration zones and greisen appear to be absent; and erosion has removed the highest parts of the plutons. The order of magmatic crystallization cannot be interpreted because of widespread deuteric recrystallization, a feature that in itself may indicate mineral potential. Tischendorf (1977) and Chatterjee et al. (1983) have suggested that low K/Rb is characteristic of mineralized granites. K_2O and Rb in granitic rocks from the Canso and Forest Hill areas are plotted in Figure 57 and are compared with fields delineating mineralized and unmineralized granitic rocks from the South Mountain batholith (after Chatterjee et al. 1983). The data suggest that the three unit D_{Gf} plutons (Gammon Islands, Snyders Lake, and Buchanans Mountain plutons) and three small dykes are the most likely candidates for mineralization. The Whitehead pluton, samples of which plot on both sides of the specialized-unspecialized granite boundary, may also have some potential. Chatterjee et al. (1983) separated uranium-specialized and tin-specialized granites in the South Mountain batholith using Li, P, U, and Th contents. Two of their triangular plots (Fig. 58) suggest that granitic plutons in the Canso and Forest Hill areas are more likely to host uranium mineralization than Sn. However, the single sample from the Buchanans Mountain pluton and an adjacent dyke (sample 088A) fall close to the tin field in Figure 58).

Thus, granitic plutons in the Canso and Forest Hill areas appear to be only moderately favourable as exploration targets for granophile element mineralization. This interpretation is supported by the lack of very strong U/Th airborne radiometric anomalies (see upper frontispiece), although mild anomalies that correlate with high muscovite content are associated with the Tom Lake, Whitehead, and Flagstaff plutons (Ford and Ballantyne, 1983). Trace element chemistry suggests that the best targets are the Gammon Islands, Snyders Lake, and Buchanans Mountain plutons in Unit D_{Gf}. These are rich in muscovite, contain plagioclase that is almost pure albite, and have siderophyllite instead of a more normal biotite (see "Petrography and chemistry..."). Of these three plutons, the Buchanans Mountain pluton and its envelope appear to offer the best chance of success because of high tin content and alteration and metasomatic effects.

Devono-Carboniferous rocks

Only very minor showings occur within the Devono-Carboniferous sedimentary and volcanic rocks north and west of the Guysborough County fault in the Forest Hill area. Gold has been reported from conglomerate in the

Table 13. Average trace element contents of Canso (CAN) and Forest Hill (FH) granitic rocks as well as selected plutons (GI, SL, BM) and samples (088A, 253). Average values for normal granites (NOR GNT - Tischendorf, 1977; Turekian and Wedepohl, 1961) and granites from the South Mountain batholith (McKenzie and Clarke, 1975; Smith, 1974, 1975; Chatterjee and Muecke, 1982; Chatterjee et al., 1983) are given for comparison. The South Mountain batholith analyses include granite (GNT), leucogranite (LGNT), tin-specialized (Sn), and uranium-specialized (U) granite averages.

	Canso-Forest Hill area								South Mountain bath.			
Element	CAN	FH	GI	SL	BM	088A	253	NOR GNT	GNT	LGNT	Sn	U
Ba	364	487	130	123	70	130	100	840	307	145	73	39
Be	7		21	4			81	5	14	8		
F	701	544	1433	1595	920	1400	890	850	1240	1600	3318	4532
Li	101	102	180	219	160	190	143	40	98	116	146	517
Rb	388	303	697	693	500	310	790	200	267	375	700	769
Sn	11	10	20	23	34	130	48	3	16	24	50	39
Th	10	6	2	3	1	1		17	16	7	25	5
U	6	4	10	15	12	10	21	3	6	8	23	14
Zn	57	58	78	77	20	22	29	39	60	51	43	86

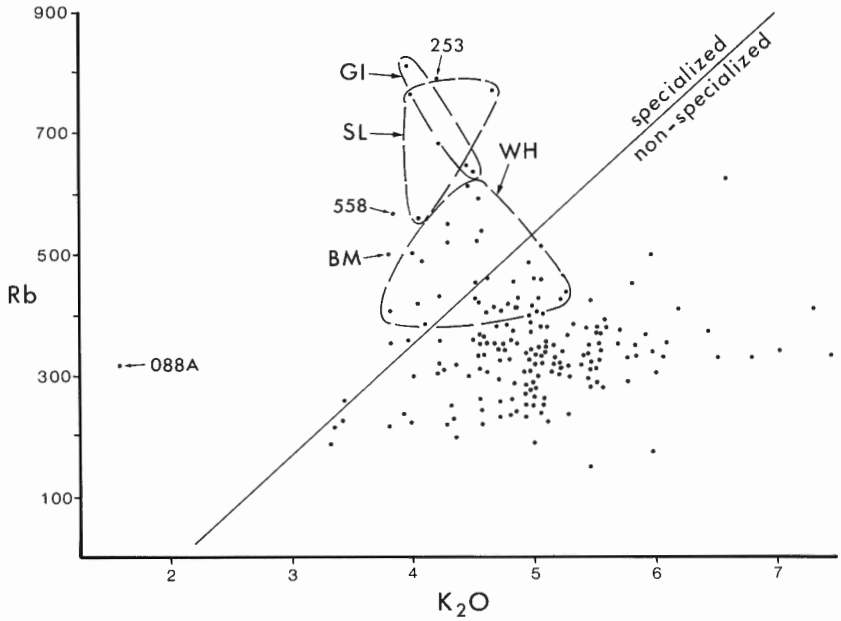

Figure 57. Rb-K_2O variation in granitic rocks from the Canso and Forest Hill areas. Boundary line separates specialized and non-specialized granitic rocks in the Meguma Terrane (Chatterjee et al., 1983). Anomalous rocks include all unit D_{Gf} plutons (Gammon Islands, Snyders Lake, Buchanans Mountain) and three miscellaneous samples (088A, 253, 558). The Whitehead pluton straddles the boundary. (All data are taken from Appendix IV.)

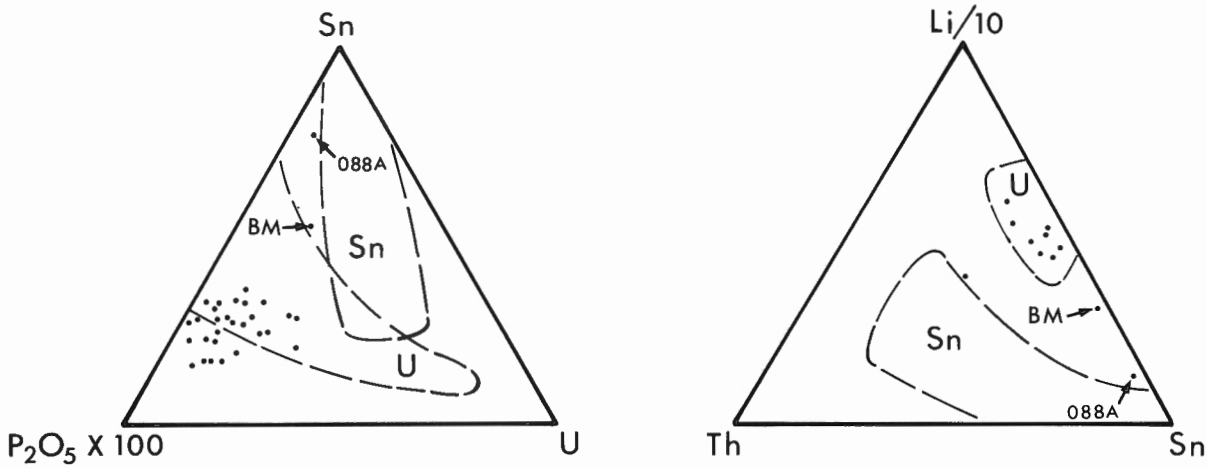

Figure 58. Ternary plots of all "specialized" granitic rocks from Figure 57. The Buchanans Mountain pluton and miscellaneous sample 088A are indicated. The fields for Sn-specialized and U-specialized granitic rocks in the South Mountain batholith are taken from Chatterjee et al. (1983).

Gunns Brook formation at two locations — in Gunns Brook 1 km northwest of Cutler Lake and along the river bank at the east end of Salmon River Lake (Keating, 1949). The best assays from bulk samples were 0.77-2.3 g/t. Pyrite and tiny amounts of chalcopyrite have been found in slightly graphitic phyllite in several places near Horton and McAllister brooks in the Minister Brook formation, both within and north of the map area. A grab sample from a new showing 1 km east of Horton Brook was found to contain only 68 ppm Cu. Pyrolusite was discovered along a fault zone near the mouth of Godfry Brook in the Minister Brook formation in the 1950s (NSDME). Specular hematite fills small fractures in various places in the Minister Brook, Tower, and Sunnyville formations.

REFERENCES

Albuquerque, C.A.R. de

1977: Geochemistry of the tonalitic and granitic rocks of the Nova Scotia southern plutons; Geochimica et Cosmochimica Acta, v.41, p. 1-13.

1979: Origin of the plutonic mafic rocks of southern Nova Scotia; Geological Society of America Bulletin, v.90, p. 719-731.

Alizay, K.M.

1981: Zur geologie und geochemie des Sherbrooke-plutons, Nova Scotia, Kanada; M.Sc. thesis, University of Hamburg, Hamburg, West Germany, 107 p.

Allan, B.D. and Clarke, D.B.

1981: Occurrence and origin of garnets in the South Mountain batholith, Nova Scotia; Canadian Mineralogist, v.19, p. 19-24.

Arthaud, F. and Matte, P.

1977: Late Paleozoic strike-slip faulting in southern Europe and northern Africa: result of a right-lateral shear zone between the Appalachians and the Urals; Geological Society of America Bulletin, v. 88, p. 1305-1320.

Belt, E.S.
1968: Post-Acadian rifts and related facies, eastern Canada; in Studies of Appalachian Geology, ed. E-An Zen, W.S. White, J.B. Hadley, and J.B. Thompson; Interscience, New York, p. 95-113.

Benson, D.G.
1967: Geology of Hopewell map-area, Nova Scotia; Geological Survey of Canada, Memoir 343, 58 p.
1974: Geology of the Antigonish Highlands, Nova Scotia; Geological Survey of Canada, Memoir 376, 92 p.

Berthé, D., Choukroune, P., and Jegouzo, P.
1979: Orthogneiss, mylonite and non-coaxial deformation of granites: the example of the South Amorican shear zone; Journal of Structural Geology, v. 1, p. 31-42.

Bohlen, S.R. and Lindsley, D.H.
1987: Thermometry and barometry of igneous and metamorphic rocks; Annual Review of Earth and Planetary Sciences, v. 15, p. 397-420.

Bradley, D.C.
1982: Subsidence in Late Paleozoic basins in the northern Appalachians; Tectonics, v. 1, p. 107-123.

Bryan, W.B., Finger, L.W., and Chayes, F.
1969: Estimating proportions in petrographic mixing equations by least-squares approximation; Science, v. 163, p. 926-927.

Cawthorn, R.G., Strong, D.F., and Brown, P.A.
1976: Origin of corundum-normative intrusive and extrusive magmas; Nature, v. 259; p. 102-104.

Chappell, B.W.
1978: Granitoids from the Moonbi District, New England Batholith, eastern Australia; Journal of the Geological Society of Australia, v. 25, p. 267-283.
1984: Source rocks of I- and S-type granites in the Lachlan Fold Belt, southeastern Australia; Philosophical Transactions of the Royal Society of London, v. A310, p. 693-707.

Chappell, B.W. and White, A.J.R.
1974: Two contrasting granite types; Pacific Geology, v. 8, p. 173-174.

Chatterjee, A.K. and Keppie, J.D.
1981: Polymetallic mineralization in the endo- and exocontact of the Wedgeport pluton, Yarmouth County; Nova Scotia Department of Mines and Energy, Report 81-1, p. 43-46.

Chatterjee, A.K. and Muecke, G.K.
1982: Geochemistry and the distribution of uranium and thorium in the granitoid rocks of the South Mountain batholith, Nova Scotia: some genetic and exploration implications; *in* Uranium in Granites, ed. Y. T. Maurice, Geological Survey of Canada, Paper 81-23, p. 11-17.

Chatterjee, A.K., Robertson, J., and Pollock, D.
1982: A summary on the petrometallogenesis of the uranium mineralization at Millet Brook, South Mountain batholith, Nova Scotia; Nova Scotia Department of Mines and Energy, Report 82-1, p. 57-66.

Chatterjee, A.K., Strong, D.F., and Muecke, G.K.
1983: A multivariate approach to geochemical distinction between tin-specialized and uranium-specialized granites of southern Nova Scotia; Canadian Journal of Earth Science, v. 20, p. 420-430.

Chevalier, B.A.M.
1983: Petrography and geochemistry of the Bull Ridge pluton, Guysborough County, Nova Scotia; B.Sc. thesis, Acadia University, Wolfville, Nova Scotia, 104 p.

Clarke, D.B.
1981: The mineralogy of peraluminous granites: a review; Canadian Mineralogist, v. 19, p. 3-18.

Clarke, D.B. and Halliday, A.N.
1980: Strontium isotope geology of the South Mountain batholith, Nova Scotia; Geochimica et Cosmochimica Acta, v. 44, p. 1045-1058.

Clarke, D.B., McKenzie, C.B., Muecke, G.K., and Richardson, S.W.
1976: Magmatic andalusite from the South Mountain batholith, Nova Scotia; Contributions to Mineralogy and Petrology, v. 56, p. 279-287.

Clarke, D.B., Muecke, G.K., and Chatterjee, A.K.
1985: The South Mountain batholith: geology, petrology, geochemistry; Nova Scotia Department of Mines and Energy, Paper 85-3, p. 1-14.

Clemens, J.D. and Wall, V.J.
1981: Origin and crystallization of some peraluminous (S-type) granitic magmas; Canadian Mineralogist, v. 81, p. 111-131.

Crocket, J.H., Fueten, F., Clifford, P.M., Kabir, A., and Henderson, J.R.
1986: Distribution of gold and arsenic in turbidites at Harrigan Cove, Nova Scotia: implications on gold mineralization; *in* Turbidite-hosted Gold Deposits, ed. J.D. Keppie, R.W. Boyle, and S.J. Haynes; Geological Association of Canada, Special Paper 32, p. 149-159.

Cumming, L.M.
1985: A Halifax slate graptolite locality, Nova Scotia; *in* Current Research, Geological Survey of Canada, Paper 85-1A, p. 215-221.

Dainty, A.M., Keen, C.E., Keen, M.J., and Blanchard, J.E.
1966: Review of geophysical evidence on crust and upper-mantle structure on the eastern seaboard of Canada; *in* The Earth Beneath the Continents, ed. J.S. Steinhart and T.J. Smith; American Geophysical Union, Monograph Number 10, p. 349-369.

Dallmeyer, R.D. and Keppie, J.D.
1984: Geochronological constraints on the accretion of the Meguma Terrane with North America; *in* Program with Abstracts, Geological Society of America, v.16, p. 11.
1987: Polyphase Late Paleozoic tectonothermal evolution of the southwestern Meguma Terrane, Nova Scotia: evidence from $^{40}Ar/^{39}Ar$ mineral ages; Canadian Journal of Earth Sciences, v. 24, p. 1242-1254.

Darnley, A.G.
1982: Hot granites: some general remarks; *in* Uranium in Granites, ed. Y.T. Maurice; Geological Survey of Canada, Paper 81-23, p. 1-10.

Dostal, J., Keppie, J.D., and Dupuy, C.
1983: Petrology and geochemistry of Devono-Carboniferous volcanic rocks in Nova Scotia; Maritime Sediments and Atlantic Geology, v. 19, p. 59-71.

Dwyer, G.J.
1975: Petrology of the Mulgrave Lake adamellite pluton; B.Sc. thesis, Dalhousie University, Halifax, Nova Scotia.

Eddy, B.G.
1987: Deformation and metamorphism of the Whitehead Harbour area, Guysborough County, Nova Scotia; B.Sc. thesis, Acadia University, 94 p.

Elias, P., Reynolds, P.H., and Muecke, G.K.
1987: Thermal history of an Appalachian exotic terrane: the Meguma Zone, Nova Scotia, Canada; Geological and Mineralogical Associations of Canada, Program with Abstracts, v. 12, p. 41.

Faribault, E.R.
1893a: Whitehaven sheet, Nova Scotia; Geological Survey of Canada, map sheet No. 26.
1893b: Guysborough Town sheet; Geological Survey of Canada, map sheet No. 25.
1893c: Country Harbour sheet; Geological Survey of Canada, map sheet No. 30.

Ferry, J.M. and Spear, F.S.
1978: Experimental calibration of the partitioning of Fe and Mg between biotite and garnet; Contributions to Mineralogy and Petrology, v. 66, p. 113-117.

Ford, K.L. and Ballantyne, S.B.
1983: Uranium and thorium distribution patterns and lithogeochemistry of Devonian granites in the Chedabucto Bay area, Nova Scotia; *in* Current Research, Geological Survey of Canada, Paper 83-1A, p. 109-119.

Foster, M.D.
1960: Interpretation of the composition of trioctahedral micas; United States Geological Survey, Professional Paper 354-B, 49 p.

Green, T.H.
1977: Garnet in silicic liquids and its possible use as a P-T indicator; Contributions to Mineralogy and Petrology, v. 65, p. 59-67.

Ham, L.J.
1988: The mineralogy, petrology and geochemistry of the Halfway Cove-Queensport plutons, Nova Scotia, Canada; unpublished MSc thesis, Dalhousie University, Halifax, N.S., 294 p.

Ham, L.J. and Horne, R.J.
1986: Geology of the South Mountain batholith on the eastern half of NTS Map Sheet 21A/16; Nova Scotia Department of Mines and Energy, Report 86-1, p. 149-159.

Hanmer, S.
1981: Tectonic significance of the northeastern Gander zone, Newfoundland: an Acadian ductile shear zone; Canadian Journal of Earth Science, v. 18, p. 120-135.

Harmeson, B.
1986: Integration of Landsat and aeromagnetic digital imagery: Meguma Terrane, Guysborough County, Nova Scotia; diploma report, Nova Scotia College of Geographic Sciences, Lawrencetown, Nova Scotia, 93 p.

Haynes, S.J.
1986: Geology and chemistry of turbidite-hosted gold deposits, greenschist facies, eastern Nova Scotia, Canada; *in* Turbidite-hosted Gold Deposits, ed. J.D. Keppie, R.W. Boyle, and S.J. Haynes; Geological Association of Canada, Special Paper 32, p. 161-177.

Haynes, S.J., Reilly, B.A., and Kiely, L.A.
1986: Structural setting of the Mile Lake gold prospect, Guysborough County, Nova Scotia; *in* Current Research, Geological Survey of Canada, Paper 86-1A, p. 141-150.

Helgeson, H.C., Delany, J.M., Nesbitt, H.W., and Bird, D.K.
1978: Summary and critique of the thermodynamic properties of rock-forming minerals; American Journal of Science, v. 278A, 229 p.

Helz, R.T.
1976: Phase relations of basalts in their melting ranges at P_{H_2O} = 5 kb. Part II. Melt compositions; Journal of Petrology, v. 17, p. 139-193.

Hibbard, M.J. and Watters, R.J.
1985: Fracturing and diking in incompletely crystallized granitic plutons; Lithos, v. 18, p. 1-12.

Hill, J.D.
1986: Granitoid plutons in the Canso area, Nova Scotia; *in* Current Research, Part A, Geological Survey of Canada, Paper 86-1A, p. 185-192.
1987a: Geology of the Guysborough-Country Harbour area, Nova Scotia; *in* Current Research, Geological Survey of Canada, Paper 87-1A, p. 415-422.
1987b: Time constraints on the emplacement and petrogenesis of Acadian peraluminous granitoid plutons in the eastern Meguma Terrane, Nova Scotia; *in* Program With Abstracts, 1987 Annual Meeting of the Geological and Mineralogical Associations of Canada, v. 12, p.56.

Hill, J.D. and Raeside, R.P.
1988: Discussion of "structural study of highly deformed Meguma phyllite and granite, vicinity of White Head Village, S.E. Nova Scotia" by C.K. Mawer and P.F. Williams; Maritime Sediments and Atlantic Geology.

Hodges, K.V. and Spear, F.S.
1982: Geothermometry, geobarometry and the Al_2SiO_5 triple point at Mt. Moosilauke, New Hampshire; American Mineralogist, v. 67, p. 1118-1134.

Holdaway, M.J.
1971: Stability of andalusite and the aluminum silicate phase diagram; American Journal of Science, v. 271, p. 97-131.

Holloway, J.R. and Burnham, C.W.
1972: Melting relations of basalt with equilibrium water pressure less than total pressure; Journal of Petrology, v. 13, p. 1-29.

Howie, R.D. and Barss, M.S.
1974: Upper Paleozoic rocks of the Atlantic Provinces, Gulf of St. Lawrence and adjacent continental shelf; Geological Survey of Canada, Paper 74-30, p. 35-50.

Hyndman, D.W.
1981: Controls on source and depth of emplacement of granitic magma; Geology, v. 9, p. 244-249.

Ishihara, S.
1977: The magnetite-series and ilmenite-series granitic rocks; Mining Geology, v. 27, p. 293-305.

James, R.S. and Hamilton, D.L.
1969: Phase relations in the system $NaAlSi_3O_8$-$KAlSi_3O_8$-$CaAl_2Si_2O_8$-SiO_2 at 1 kilobar water vapour pressure; Contributions to Mineralogy and Petrology, v. 21, p. 111-141.

Keating, B.J.
1949: The basal conglomerates of Nova Scotia; *in* Annual Report on Mines for 1948, Nova Scotia Department of Mines, p. 136-142.

Keppie, J.D.
1977: Tectonics of southern Nova Scotia; Nova Scotia Department of Mines and Energy, Paper 77-1, 34 p.
1983: Geological history of the Isaacs Harbour area, Parts of 11F/3 and 11F/4, Guysborough County, Nova Scotia; *in* Report of Activities, Nova Scotia Department of Mines and Energy, Paper 83-1, p. 109-143.
1985: Geology and tectonics of Nova Scotia; *in* Appalachians Geotraverse (Canadian Mainland), Geological and Mineralogical Associations of Canada Annual Meeting, guidebook to excursion 1, p. 23-108.

Keppie, J.D., Odom, L., and Cormier, R.F.
1983: Tectonothermal evolution of the Meguma Terrane: radiometric controls; *in* Abstract with Programs, Geological Society of America, Northeastern Section, v. 15, p. 136.

Kontak, D.J.
1987: The East Kemptville leucogranite: a possible mid-Carboniferous topaz granite; Nova Scotia Department of Mines and Energy, Report 87-1, p. 81-94.

Krogh, T.E.
1973: A low-contamination method for hydrothermal decomposition of zircon and extraction of U and Pb for isotopic age determinations; Geochimica et Cosmochimica Acta, v. 37, p. 485-494.

Leveson, D.J.
1966: Orbicular rocks: a review; Geological Society of America Bulletin, v. 77, p. 409-426.

Luth, W.C., Jahns, R.H., and Tuttle, O.F.
1964: The granite system at pressures of 4 to 10 kilobars; Journal of Geophysical Research, v. 69, p. 759-773.

MacDonald, M.A.
1981: The mineralogy, petrology and geochemistry of the Musquodoboit batholith; M.Sc. thesis, Dalhousie University, Halifax, Nova Scotia, 272 p.

MacDonald, M.A. and Clarke, D.B.
1985: The petrology, geochemistry and economic potential of the Musquodoboit batholith, Nova Scotia; Canadian Journal of Earth Sciences, v. 22, p. 1633-1642.

MacDonald, M.A. and Horne, R.J.
1986: The geology of the South Mountain batholith: NTS sheets 11D/05 and 11D/12; *in* Report of Activities, Nova Scotia Department of Mines and Energy, Report 86-1, p. 119-135.

Malcolm, W. and Faribault, E.R.
1929: Gold fields of Nova Scotia; Geological Survey of Canada, Memoir 156, 253 p.

Mason, D.R. and McDonald, J.A.
1978: Intrusive rocks and porphyry copper occurrences of the Papua New Guinea-Soloman Islands region: a reconnaissance study; Economic Geology, v. 73, p. 857-877.

Mawer, C.K.
1986: The bedding-concordant gold-quartz veins of the Meguma Group, Nova Scotia; *in* Turbidite-hosted Gold Deposits, ed. J.D. Keppie, R.W. Boyle, and S.J. Haynes; Geological Association of Canada, Special Paper 32, p. 135-148.

Mawer, C.K. and White, J.C.
1987: Sense of displacement on the Cobequid-Chedabucto fault system, Nova Scotia, Canada; Canadian Journal of Earth Science, v. 24, p. 217-223.

Mawer, C.K. and Williams, P.F.
1986: Structural study of highly deformed Meguma phyllite and granite, vicinity of White Head Village, S.E. Nova Scotia; Maritime Sediments and Atlantic Geology, v. 22, p. 51-64.

McBride, D.E.
1978: Geology of the Ecum Secum area, Halifax and Guysborough Counties, Nova Scotia; Nova Scotia Department of Mines and Energy, Paper 78-1, 12 p.

McKenzie, C.B. and Clarke, D.B.
1975: Petroloy of the South Mountain batholith, Nova Scotia; Canadian Journal of Earth Sciences, v. 12, p. 1209-1218.

McKenzie, C. and MacGillivary, J.
1974: Eastern Nova Scotia granites project; internal report, Department of Geology, Dalhousie University, Halifax, Nova Scotia.

McLennan, S.M. and Taylor, S.R.
1980: Geochemical standards for sedimentary rocks: trace element data for USGS standards SCO-1, MAG-1 and SGR-1; Chemical Geology, v. 29, p. 333-343.

Miller, C.F. and Mettlefehldt, D.W.
1982: Depletion of light rare-earth elements in felsic magmas; Geology, v. 10, p. 129-133.

Miller, C.F., Stoddard, E.F., Bradfish, L.J., and Dollase, W.A.
1981: Composition of plutonic muscovite: genetic implications; Canadian Mineralogist, v. 19, p. 25-34.

Mooney, S.J.
1987: Stratigraphy and tectonic evolution of two mid-Paleozoic basins: Implications for the timing of final emplacement of the Meguma Terrane; Geological and Mineralogical Associations of Canada Annual Meeting, Program With Abstracts, v. 12, p. 74.

Muecke, G.K. and Clarke, D.B.
1981: Geochemical evolution of the South Mountain batholith, Nova Scotia: Rare-earth element evidence; Canadian Mineralogist, v. 19, p. 133-146.

Neilson, M.J. and Haynes, S.J.
1973: Biotites in calc-alkaline intrusive rocks; Mineralogical Magazine, v. 39, p. 251-253.

Nichols, D.
1976: The metamorphic and structural evolution of the metasediments and granites in the Whitehaven area, Guysborough County, Nova Scotia; B.Sc. thesis, Dalhousie University, 50 p.

Nockolds, S.R. and Richey, J.E.
1939: Replacement veins in the Mourne Mountains granites, N. Ireland; American Journal of Science, v. 237, p. 27-47.

O'Brien, B.H.
1983: The structure of the Meguma Group between Gegogan Harbour and Country Harbour, Guysborough County; *in* Report of Activities, Nova Scotia Department of Mines and Energy, Report 83-1, p. 145-181.
1986: Preliminary report on the geology of the Mahone Bay area, Nova Scotia; *in* Current Research, Geological Survey of Canada, Paper 86-1A, p. 439-444.

O'Reilly, G.A.
1988: Geology and geochemistry of the Sangster Lake and Larry's River plutons, Guysborough County, Nova Scotia; unpub. MSc thesis, Dalhousie Univ., Halifax, N.S., 290 p.

O'Reilly, G.A., Farley, E.J., and Charest, M.H.
1982: Metasomatic-hydrothermal mineral deposits of the New Ross-Mahone Bay area, Nova Scotia; Nova Scotia Department of Mines and Energy, Paper 82-2, 96 p.

Pitcher, W.S.
1982: Granite type and tectonic environment; *in* Mountain Building Processes, ed. K.J. Hsu; Academic Press, New York, p. 19-40.
1987: Granites and yet more granites forty years on; Geologische Rundschau, v. 76, p. 51-79.

Plimer, I.R.
1987: Fundamental parameters for the formation of granite-related tin deposits; Geologische Rundschau, v. 76, p. 23-40.

Poole, J.
1984: An example of structural deformation of the Halifax Formation in the Whitehead area, Meguma Terrane, eastern Nova Scotia; B.Sc. thesis, St. Francis Xavier University, 89 p.

Poole, W.H.
1976: Plate tectonics evolution of the Canadian Appalachian region; *in* Current Research, Geological Survey of Canada, Paper 76-1B, p. 113-126.

Raeside, R.P., Hill, J.D., and Eddy, B.G.
1988: Metamorphism of Meguma Group metasedimentary rocks, Whitehead Harbour area, Guysborough County, Nova Scotia; Maritime Sediments and Atlantic Geology.

Reynolds, P.H. and Muecke, G.K.
1978: Age studies on slates: applicability of the $^{40}Ar/^{39}Ar$ stepwise outgassing method; Earth and Planetary Science Letters, v. 40, p. 111-118.

Reynolds, P.H., Zentilli, M., and Muecke, G.K.
1981: K-Ar and $^{40}Ar/^{39}Ar$ geochronology of granitoid rocks from southern Nova Scotia: its bearing on the geological evolution of the Meguma Zone of the Appalachians; Canadian Journal of Earth Sciences, v. 18, p. 386-394.

Richardson, J.M.G., Spooner, E.T.C., and McAuslan, D.A.
1982: The east Kemptville tin deposit, Nova Scotia: an example of a large tonnage, low grade, greisen-hosted deposit in the endocontact zone of a granite batholith; *in* Current Research, Geological Survey of Canada, Paper 82-1B, p. 27-32.

Richardson, S.W.
1968: Staurolite stability in part of the system Fe-Al-Si-O-OH; Journal of Petrology, v. 9, p. 467-488.

Rogers, H.D.
1986: Geology and igneous petrology of Shelburne and eastern Yarmouth Counties, Nova Scotia; Geological Survey of Canada, unpublished open file report, 127 p.

Rogers, P.J., MacDonald, M.A., and Rigby, D.W.
1985: Regional lake sediment survey of the Meguma zone, southern Nova Scotia: New analytical data; Nova Scotia Department of Mines and Energy, Open File Report 605, 65 p.

Schenk, P.E.
1970: Regional variation of the flysch-like Meguma Group (Lower Paleozoic) of Nova Scotia, compared to recent sedimentation off the Scotian shelf; Geological Association of Canada, Special Paper No. 7, p. 127-153.
1975: A regional synthesis; Maritime Sediments, v. 11, p. 17-24.
1978: Synthesis of the Canadian Appalachians; Geological Survey of Canada, Paper 78-13, p. 111-136.

Schiller, E.A.
1959: Petrography and petrology of the andalusite schists in the Port Felix area, Nova Scotia, Canada; M.Sc. thesis, Michigan State University, 50 p.
1961: Guysborough, Nova Scotia; Geological Survey of Canada, Map 27-1961.
1963: Mineralogy and geology of the Guysborough area, Nova Scotia, Canada; Ph.D. thesis, University of Utah, 162 p.

Schiller, E.A. and Taylor, F.C.
1965: Spessartite-quartz rocks (coticules) from Nova Scotia; American Mineralogist, v. 50, p. 1477-1481.

Shaw, W.G.
1983: A geological investigation of the Lazy Head tungsten prospect, Guysborough County and a comparison with the Moose River deposit, Halifax County, Nova Scotia; M.Sc. thesis, Dalhousie University, 217 p.

Sibson, R.H.
1977: Fault rocks and fault mechanisms; Journal of the Geological Society of London, v. 133, p. 191-213.

Simpson, C. and Schmid, S.M.
1983: An evaluation of criteria to deduce the sense of movement in sheared rocks; Geological Society of America Bulletin, v. 94, p. 1281-1288.

Smith, P.K.
1981: Geology of the Sherbrooke area, Guysborough County, Nova Scotia; **in** Report of Activities, Nova Scotia Department of Mines and Energy, Report 81-1, p. 77-94.

Smith, P.K. and Kontak, D.J.
1987: Nova Scotia gold deposits: the secrets unfold; Geological and Mineralogical Associations of Canada, Program with Abstracts, v. 12, p. 90.

Smith, T.E.
1974: The geochemistry of the granitic rocks of Halifax County, Nova Scotia; Canadian Journal of Earth Sciences, v. 11, p. 650-657.
1975: Layered granitic rocks at Chebucto Head, Halifax County, Nova Scotia; Canadian Journal of Earth Sciences, v. 12, p. 456-463.

Speer, J.A.
1981: Petrology of cordierite and almandine-bearing granitoid plutons of the southern Appalachian Piedmont, U.S.A.; Canadian Mineralogist, v. 19, p. 35-46.
1984: Micas in igneous rocks; *in* Micas, ed. S.W. Bailey, Reviews in Mineralogy, v. 13, p. 299-356.

Stevenson, I.M.
1964: Chedabucto Bay, Nova Scotia; Geological Survey of Canada, Map 1156A.

Streckeisen, A.
1976: To each plutonic rock its proper name; Earth-Science Reviews, v. 12, p. 1-33.

Strong, D.F.
1981: Ore deposit Models–5. A model for granophile mineral deposits; Geoscience Canada, v. 8, p. 155-166.

Sugden, T.
1987: Kinematic indicators: Structures that record the sense of movement in mountain chains; Geology Today, v. 3, p. 93-99.

Taylor, R.G.
1979: Geology of tin deposits; Developments in Economic Geology, v. 11, Elsevier Scientific Publishing Company, New York, 543 p.

Thomas, W.C.
1982: Petrology and geochemistry of the River Lake pluton, Halifax County, Nova Scotia; M.Sc. thesis, Acadia University, Wolfville, Nova Scotia, 133 p.

Tischendorf, G.
1977: Geochemical and petrographic characteristics of silicic magmatic rocks associated with rare-element mineralization; *in* Metallization Associated with Acid Magmatism, v. 2, ed. M. Stemprok; Geological Survey of Czechoslovakia, p. 41-96.

Turekian, K.K. and Wedepohl, K.H.
1961: Distribution of the elements in some major units of the Earth's crust; Geological Society of America Bulletin, v. 72, p. 1723-1728.

Turner, F.J.
1981: Metamorphic Petrology; McGraw-Hill Book Company, New York, 524 p.

Tuttle, O.F. and Bowen, N.L.
1958: Origin of granite in the light of experimental studies in the system $NaAlSi_3O_8$-$KAlSi_3O_8$-SiO_2-H_2O; Geological Society of America, Memoir 74, 153 p.

Vernon, R.H.
1983: Restite, xenoliths and microgranitoid enclaves in granites; Journal and Proceedings, Royal Society of New South Wales, v. 116, p. 77-103.

Waldron, J.W.F.
1987: Sedimentology of the Goldenville-Halifax transition in the Tancook Island area, South Shore, Nova Scotia; Geological Survey of Canada, Open File Report 1536, 26 p.

Webb, G.W.
1969: Paleozoic wrench faults in Canadian Appalachians; *in* North Atlantic - Geology and Continental Drift, ed. M. Kay; American Association of Petroleum Geologists, Memoir 12, p. 754-786.

Weeks, L.J.
1960: Cape Canso, Guysborough and Richmond Counties, Nova Scotia; Geological Survey of Canada, Map 1074A.

Whalen, J.B., Currie, K.L., and van Breeman, O.
1987: Episodic Ordovician-Silurian plutonism in the Topsails igneous terrane, western Newfoundland; Transactions of the Royal Society of Edinburgh, Earth Sciences, v. 78, p. 17-28.

White, A.J.R., Clemens, J.D., Holloway, J.R., Silver, L.T., Chappell, B.W., and Wall, V.J.
1986: S-type granites and their probable absence in southwestern North America; Geology, v. 14, p. 115-118.

Williams, H. and Hatcher, R.D.
1982: Suspect terranes and accretionary history of the Appalachian Orogen; Geology, v. 10, p. 530-536.

Williams, P.F.
1983: Large scale transposition by folding in northern Norway; Geologische Rundschau, v. 72, p. 589-604.

Wilson, G.
1970: Wrench movements in the Aristarchus region of the Moon; Proceedings of the Geological Association, v. 81, p. 595-608.

Wyllie, P.J.
1977: Crustal anatexis: an experimental review; Tectonophysics, v. 43, p. 41-71.

Zentilli, M., Graves, M.C., Mulja, T., and MacInnis, I.
1986: Geochemical characterization of the Goldenville-Halifax transition of the Meguma Group of Nova Scotia: preliminary report; *in* Current Research, Geological Survey of Canada, Paper 86-1A, p. 423-428.

APPENDIX I

Pluton Descriptions

A brief description of each pluton is given, in the sequence (A) composition and mineralogy, (B) notable features, and (C) observed age relationships with other intrusions. Two-letter codes (see Fig. 9 for pluton locations), unit designation, and map size are given in brackets for each pluton. Abbreviations for biotite, muscovite, and hornblende are bi, ms, and hb. Subscripts indicate modal percentages. Fine, medium, coarse, and very coarse grain sizes are <1, 1-5, 5-10, and >10 mm.

Canso area

Andrew Island (AI, unit D_{Gb}, 5.4 km^2)

A) Very coarse grained, porphyritic to seriate, ms_1-bi_8 granodiorite. Subhedral microcline phenocrysts, comprising about 10-30% of the rock, are 1-4 cm long with rare individuals 4-8 cm long. Phenocrysts >2 cm long are absent in the western part of AI around Mahons Lake. Rocks are typically foliate as a result of moderate deformation. Accessories include garnet (usually visible in outcrop, grains <3 mm in diameter), apatite, monazite, zircon, and ilmenite.

B) Commonly agmatitic with up to five rock types present in individual outcrops. These include xenoliths of SC and Meguma Group and dykes and larger masses of PC and GH. Pegmatite and minor aplite are locally abundant.

C) 1. Occurs as numerous xenoliths in GH at Whistler Point.
2. Intruded by dykes of PC in many places (e.g., north shore of Portage Cove).
3. A few xenoliths of probable AI occur in possible CL about 250 m southwest of the mouth of Gaspereaux Brook on the northeast side of the northwest-trending arm of Mahons Lake.
4. Xenoliths of SC occur in AI in several places along the southeast shore of Andrew Island.
5. Intruded by dykes of FC at Castle Rock and Gannet Point.

Big Branch (BB, unit D_{Ga}, 1.3 km$_2$)

A) Fine grained, bi_3-ms_9 granite. Equigranular except for scattered mica flakes up to 10 mm in diameter. Weakly deformed but foliate fabric is difficult to see in hand specimen because of the fine grain size. Accessories include apatite, zircon, monazite, allanite, and garnet (found in one specimen).

B) Fairly homogeneous in outcrop except for a few pegmatite dykes (<20 cm thick) and quartz veinlets.

C) 1. Occurs as a few small, rounded xenoliths in probable CL at sample site 830, about 750 m northwest of Dover Lake.

Canso Harbour (CH, unit D_{Gdl}, 0.1 km^2)

A) Medium- to coarse-grained, foliate, bi_2-ms_4 granite. Strongly deformed with feldspar augen 0.5-2 cm long, set in a finer grained mylonitic matrix. Accessories include apatite, zircon and monazite.

B) Pluton is poorly exposed. It appears to be agmatitically mixed with the Goldenville Formation in a few places.

Charles Lake (CL, unit D_{Ge}, 7.4 km^2)

A) Medium grained, ms_4-bi_6 granite, locally containing a few microcline phenocrysts up to 1 cm long. Most outcrops are equigranular. Rocks are foliate and some possess an S-C fabric as a result of deformation. Accessories include apatite, zircon, monazite, ilmenite, and garnet (found in one sample).

B) Rocks included in CL are somewhat variable in composition, with some approaching unit D_{Gd} in terms of mica porportions, which raises the possibility that CL may be composite in nature. It is correlated with D_{Ge} although it is finer grained than KH, PH, and most of PC. CL is agmatitically mixed with Goldenville Formation on the northwest and northeast sides and over a large area around Dover Basin. The Dover Basin agmatitic zone is intruded by numerous dykes and irregular lenses, typically <1 m thick, of pegmatite and minor aplite.

C) 1. Two xenoliths of SI occur in CL 300 m north of Meades Point on the north shore of Dover Harbour.
2. Small tabular bodies of CL in intrusive contact with probable GH about 700 m southwest of Hazel Hill Lake are inferred to be dykes.
3. See BB-C-1 and AI-C-3.

Dover Head (DH, unit D_{Gb}, 7.3 km$_2$)

A) Very coarse grained, seriate, ms_6-bi_7 granite. Typically contains 10-20% microcline phenocrysts, 1-6 cm long, that are subhedral in hand specimen. Groundmass grains lie in the 2-10 mm range. An impersistent magmatic foliation and rare lineation are developed locally, especially around Louse Harbour Island. The rocks are undeformed except along the Harbour Island shear zone. Accessories include zircon, monazite, apatite, ilmenite, allanite, sillimanite, and cordierite(?).

B) DH includes five to ten bodies that may once have been part of a single pluton, now segmented by the subsequent intrusion of PH. DH is similar in composition and texture to MP, and the two plutons may actually be part of the same body, the central portion of which is covered by Dover Bay. DH is agmatitic over large areas, caused by the intrusion of numerous dykes and small plutons of PH. Xenoliths of Halifax Formation hornfels up to 50 m across and pegmatite and aplite dykes <4 m in thickness are fairly common. Magmatic layering is developed locally, with good examples on Louse Harbour Island.

C) 1. Intruded by numerous dykes and bodies of PH over most of the pluton. Good contact relationships are exposed along the shoreline of Louse Harbour.
2. Intruded by several dykes of FC on Louse Harbour Island.
3. Probable DH occurs as rare, large xenoliths in WH on the east side of the entrance to Raspberry Cove West and on a small island 600 m to the southwest.

Durells Island (DI, unit D_{Gd}, 3.6 km^2)

A) Medium- to coarse-grained, bi_5-ms_7 granite. Strongly deformed with mylonitic S-C fabric developed throughout. Feldspar augen are up to 2 cm long except along the south side of Durells Island where the rocks are uniformly medium grained. Accessories include apatite, rutile, zircon, monazite, and ilmenite.

B) Tabular rafts of Goldenville Formation metawacke and minor schist form up to 30% of the outcrop in Derabies Islands and on the north side of Durells Island. The rafts are up to 40 m long and are oriented parallel to the tectonic foliation. Pegmatite dykes, up to 5 m thick and forming up to 15% of each outcrop, are oriented parallel and slightly oblique to the foliation. Mylonitic buff-coloured bi_1-ms_{3-6} leucogranite aplite intrudes DI as small masses and dykes up to several metres wide. The aplite is locally gradational with the pegmatite already described. The best exposures of aplite occur on Hog and Welsh islands.

C) 1. DI may be correlative with the abundant white-weathering leucogranite lenses and dykes that intrude OI.

False Cove (FC, unit D_{Gc}, 0.1 km^2)

A) Fine grained, porphyritic, ms_6-bi_6 granite. Typically contains 1-10% 1-2 mm phenocrysts of one or more of quartz, biotite, muscovite, microcline, and plagioclase. FC has a characteristic medium-grey colour on both weathered and fresh surfaces; it is undeformed. Apatite, zircon, monazite, and ilmenite are common accessory minerals.

B) FC is a collective term for widely separated small plutons and dykes that are spatially associated with, and intrusive into, unit D_{Gb}) (plutons DH, AI, and MP). The largest body has a map width of about 150 m.

C) 1. Two dykes of FC intrude MP at False Cove on Little Dover Island.
2. See AI-C-5 and DH-C-2.
3. Probable xenoliths of FC occur in PC on Pea Island in Andrew Passage.
4. Several xenoliths of FC occur in KH about 350 m southwest of Thrumcap Island on the southeast side of Little Dover Island.

Flagstaff Hill (FH, unit D_{Gdl}, 14.6 km^2)

A) Medium grained, equigranular, bi_3-ms_8 granite. It contains rare muscovite and microcline phenocrysts up to 1 cm long in a few outcrops. Accessory phases include apatite, zircon, monazite, ilmenite, allanite, sphene, and rare garnet, sillimanite, and cordierite(?). The rocks vary from undeformed to moderately deformed and locally possess a well-developed tectonic foliation defined by mica.

B) FH is quite massive and homogeneous in its interior, generally lacking xenoliths and dykes, although mica-rich schlieren, 0.1-10 cm thick, occur locally. In contrast, the margins of the pluton along Northwest and Northeast branches are agmatitic, with numerous xenoliths and whole outcrops of Meguma Group mixed with pegmatite and aplite dykes and the host granite. The eastern extension of FH toward Dover is poorly defined because of lack of exposure.

Fogherty Lake (FL, unit D_{Gdl}, 4.4 km^2)

A) Medium grained, foliate, bi_3-ms_7 granite. Accessories include apatite, ilmenite, zircon, monazite, and rare tourmaline. Biotite is commonly altered to chlorite. The pluton is moderately to strongly deformed.

B) FL is relatively homogeneous, containing only rare pegmatite dykes and sedimentary xenoliths. However, fault-related features such as breccia and numerous quartz veinlets are common in places along the coast. Irregular zones of quartz-bearing syenite, one to several metres in diameter, occur at the eastern end of the pluton about 2 km west of Indian Bay. They are sharply gradational over 1 cm with the host granite and are slightly finer grained and contain reddish feldspar. FL is virtually identical to LL and the plutons may actually be part of the same intrusion, separated by the Fox Bay fault.

Glasgow Harbour (GH, unit D_{Gd}, 8.2 km^2)

A) Medium grained, foliate, bi_4-ms_{10} granite. It contains rare muscovite and microcline phenocrysts (augen) up to 1 cm long. Biotite is commonly altered to chlorite. Apatite, zircon, monazite, and rare sillimanite are accessory phases. The rocks are moderately deformed and locally have an S-C fabric.

B) Outcrops in the vicinity of Chapel Gulley and Glasgow Head are agmatitic, containing numerous dykes and irregular masses of pegmatite and minor aplite as well as xenoliths and whole outcrops of Goldenville Formation. Magmatic layering was observed in one small outcrop on Sherewink Island. The western boundary between GH and CL is very poorly defined because of the lithological and textural similarities of the two plutons. A fault may be present along Chapel Gulley where quartz veins, hydrothermal alteration, and cataclasite are common.

C) 1. Numerous dykes of PC intrude GH at Whistler Point and along the shore to the west.
2. See AI-C-1 and CL-C-2.

Gammon Islands (GI, unit D_{Gf}, 0.5 km^2)

A) Medium grained, granular, bi_1-ms_{12} leucogranite. Both plagioclase and microcline contain abundant secondary muscovite. GI is undeformed and contains accessory apatite, ilmenite, zircon, monazite, and allanite.

B) GI is confined to several small islands just west of White Head Island. It is very homogeneous except for common schlieren enriched in mica and/or quartz. A few small miarolitic cavities occur on Shag Ledge.

Ketch Harbour (KH, unit D_{Ge}, 2.3 km^2)

A) Coarse grained, porphyritic to seriate, ms_5-bi_7 granite. Rocks contain <1-5% microcline phenocrysts that are subhedral in hand specimen and generally 1-3 cm long. Very rare phenocrysts are 4-8 cm long. The phenocrysts are generally blocky and decussate, except locally where they define a weak magmatic foliation or rare lineation. Accessories include apatite, zircon, monazite, ilmenite, sillimanite, cordierite(?), and rare fluorite. KH is undeformed except along Little Dover Run.

B) Agmatitically mixed with numerous xenoliths of Halifax Formation hornfels and MP (D_{Gb}) up to 200 m in diameter, which locally form up to 50% of the outcrop. Because of the agmatitic nature of all of the plutons in this area, the southern boundary with MP and PC is difficult to define at map scale. A few pegmatite and aplite dykes up to 2 m thick crosscut KH in a northwest direction. Biotite-enriched layers, 1-2 cm thick, were found in one outcrop. Biotite-rich schlieren crosscut KH outcrops in several places. KH is similar to PH and the two may be part of the same pluton.

C) 1. Dykes and plutons of KH intrude MP over a large area around Little Dover Island.
2. Dykes of KH intrude SC about 600 m north of Madeline Point.
3. See FC-C-4.

Lookout Hill (LH, unit D_{Gd}, 2.5 km^2)

A) Medium grained, foliate, bi_9-ms_{14} granite. Rocks are moderately deformed with 1-4 mm feldspar augen and muscovite laths set in a finer grained, recrystallized matrix. Accessories include apatite, ilmenite, zircon, and monazite.

B) Pluton is poorly defined and requires more detailed mapping. It has an unusually high content of mica compared to the other plutons grouped in unit D_{Gd}. The position of the boundary with FH is uncertain.

Lumsdens Lake (LL, unit D_{Gdl}, 5.5 km²)

A) Medium grained, foliate, bi_3-ms_{10} granite. Moderately to strongly deformed, especially along the Tittle where the rocks are platy as a result of the presence of well developed C-planes. Biotite is commonly altered to chlorite. Apatite, ilmenite, zircon, and monazite are common accessory phases.

B) Overall, LL is relatively homogeneous with pegmatite and xenoliths being rare. However, quartz veins are common, particularly along the coast where they locally permeate the granite in a cobweb fashion. A 50 m wide body of quartz-bearing syenite lies in abrupt contact with the host granite on the east side of Indian Bay. The two lithologies are similar in appearance and are only distinguished by close scrutiny. The relative age of the syenite was not determined. LL may be the eastern half of the FL pluton, separated along the Fox Bay fault.

Mahons Lake (ML, unit D_{Gdl}, 0.1 km²)

A) Medium grained, bi_1-ms_8 leucogranite. It is relatively inequigranular in outcrop, containing scattered microcline phenocrysts up to 1 cm long as well as patches of pegmatitic and aplitic granite that are gradational with the host. Garnet is an important accessory with individual grains measuring up to 5 mm in diameter. Other accessory phases include apatite, zircon, monazite, and sillimanite. ML is only weakly deformed.

C) 1. Small xenoliths of ML occur in PC along the north shore of Mahons Lake and 300 m northeast of Gun Cove Island.

Madeline Point (MP, D_{Gb}, 3.7 km²)

A) Very coarse grained, seriate, ms_5-bi_6 granite. Microcline phenocrysts form up to 30% of the rock and are 4-8 cm long, with rare individuals up to 15 cm long. The phenocrysts are generally decussate or form an impersistent magmatic foliation or rare lineation where the rocks are undeformed. Accessories are apatite, zircon, monazite, ilmenite, anatase, sillimanite, cordierite(?), and rare sphene and garnet. MP varies from undeformed to moderately deformed, with the greatest deformation occurring along Little Dover Run.

B) Most outcrops are agmatitic, characterized by the presence of numerous dykes and larger undefined masses of KH (north part) and PC (south part). This feature makes PC, KH, and MP difficult to separate at map scale. In addition to younger granite, xenoliths of SC and the Meguma Group are abundant on the west side of MP. A few pegmatite and aplite dykes, up to 3 m thick, intrude MP in a northwest trend. Five layers, 5-10 cm thick each and slightly enriched in mica compared to the host granite, are spaced at 0.5-1.5 m intervals in an outcrop on the east side of Seal Cove. Small clots and streaks enriched in biotite and ovoid knots of quartz (up to 5 cm long) are rare features. MP closely resembles DH and the two plutons may actually be parts of the same intrusion, the central portion of which is covered by Dover Bay.

C) 1. Numerous xenoliths of SC occur in MP between Gun Cove Island and Andrew Island.
2. See KH-C-1 and FC-C-1.
3. Four small xenoliths of SI occur in MP on the northwest side of Wreck Island.
4. Xenoliths of MP occur in PC just west of Pea Island.

Oliver Island (OI, unit D_{Tm}, 2.9 km²)

A) Fine- to medium-grained, schistose to gneissose, ms_8-bi_{13} tonalite (plots along tonalite-granodiorite join). The composition is highly variable at hand specimen scale because of the presence of numerous streaks and clots (0.1-3 cm thick) enriched in mica and scattered ovoid knots of pegmatite (5-20 cm long). Accessories include apatite, zircon, monazite, ilmenite, and sphene. The tonalite is highly deformed and contains plagioclase augen and muscovite flakes up to 1 cm long set in a mylonitic matrix.

B) The tonalite is the host lithology in a zone of migmatite composed of three additional rock types. These rocks are enclaves of Goldenville metawacke and minor schist, lenses and dykes of medium grained bi_{1-2}-ms_{2-6} leucogranite, and dykes and irregular masses of leucogranite pegmatite. All have been deformed into schlieric and layered migmatite marked by discontinuous bands, lenses and streaks from 1 mm to 40 m thick.

C) See DI-C-1.

Portage Cove (PC, unit D_{Ge}, 1.3 km²)

A) Coarse grained seriate ms_4-bi_6 granite with 1-15% microcline phenocrysts 0.5-3 cm long. One 8 cm long phenocryst was observed in a dyke at Sherewink Cove. PC lacks obvious phenocrysts in the western part of the pluton around Mahons Lake and in many of the numerous dykes intruding GH and AI north of the pluton. Where igneous textures are preserved, the phenocrysts are typically decussate, although they define a weak foliation in a few places. Ilmenite, zircon, monazite, apatite and minor garnet, sillimanite, and cordierite(?) are accessory phases. The rocks vary from weakly to moderately deformed.

B) Outcrops are commonly agmatitic, containing numerous xenoliths of SC, MP, AI and Halifax Formation. Dykes of pegmatite and minor aplite are locally abundant. The overall result is a very diffuse pluton that is difficult to separate at map scale from MP and AI. Dykes of PC have been recognized as far north as Glasgow Harbour, as far east as the east side of Andrew Island, as far west as Wreck Island, and as far south as Little Dover Run (where they are indistinguishable from KH). Magmatic layers 1-3 cm thick occur at Haulover Ledge.

C) 1. Contains numerous xenoliths of SC along the west side of Andrew Passage.
2. See AI-C-2, GH-C-1, MP-C-4, ML-C-1, and FC-C-3.
3. A large dyke of PC, containing xenoliths of SI, intrudes SI about 200 m north of Wreck Island.

Port Howe (PH, unit D_{Ge}, 25.2 km²)

A) Coarse grained seriate ms_4-bi_6 granite. Contains <1-20% microcline phenocrysts, 0.5-3 cm long, that range from blocky to thin subhedral tablets in hand specimen. Very rare individuals are up to 5 cm long. The phenocrysts define a decussate to weakly foliate or lineate fabric. Accessories include ilmenite, zircon, monazite, apatite, sillimanite, cordierite(?), and rare sphene and tourmaline. PH is virtually undeformed except along the Harbour Island shear zone.

B) PH is agmatitic with up to six lithologies present in single and small groups of outcrops, which include xenoliths of Halifax Formation hornfels, DH, and miscellaneous granitic rocks types. The Halifax Formation xenoliths vary from angular blocks <1 m across to large rafts up to 200 by 300 m that show diverse bedding orientations. Igneous layers, 1-10 cm thick and slightly enriched in biotite, are common with good examples occurring on Whale Island. Schlieren, enriched in biotite and/or quartz, occur in some outcrops. The contact with WH was not observed in outcrop, but was found to be abrupt within 20 m along the east side of Raspberry Cove West. However, coastal

exposures of PH between Raspberry Cove West and Crane Cove gradually become more like WH (in terms of mica proportions and grain size) toward the west. Thus the WH-PH contact may actually be gradational, although an intrusive contact is inferred until better data become available. PH is very similar in lithology to KH, raising the possibility that the two plutons may actually be parts of the same intrusion.

C) 1. See DH-C-1.

Prices Island (PI, unit D_{Gb}, 2.7 km²)

A) Coarse to very coarse grained seriate bi_5-ms_7 granite. Microcline phenocrysts, which comprise 10-20% of the rock, are generally 0.5-2 cm long, with scattered crystals up to 6 cm long. They are decussate, except in a few places where they define an impersistent igneous foliation or rare lineation. Accessories are apatite, ilmenite, zircon, and monazite. The rocks are undeformed to weakly deformed except along the Harbour Island shear zone where they are strongly deformed.

B) PI contains numerous blocks of Halifax Formation hornfels, ranging from <1 m in diameter to individual outcrops, around Prices Island. It is the only pluton in unit D_{Gb} that has more muscovite than biotite. Magmatic layers 1 cm to 1 m thick occur on Prices Island.

Shag Cove (SC, unit D_{Tb}, 0.5 km²)

A) Medium grained foliate bi_{22} tonalite containing 0-5% plagioclase phenocrysts up to 1 cm long. Zircon, monazite, ilmenite, apatite and rare epidote, garnet, and sphene are accessory minerals. The rocks are invariably moderately deformed and possess a well developed biotite foliation.

B) SC is a collection of pluton fragments ranging from obvious xenoliths <1 m long to larger mappable bodies up to 0.3 km² in area, all surrounded by younger granite. They lie in an east-trending band between Gun Cove Island and Andrew Island. The various tonalite fragments are somewhat variable in composition, containing from about 13-37% biotite. This composition suggests that more than one tonalite pluton may have been present prior to granite emplacement. The tonalite is characterized by the presence of 1-10% disc-shaped xenoliths (autoliths?, up to 1 m long) of fine grained tonalite similar in composition to their host. The xenoliths contain medium grained phenocrysts of quartz and plagioclase and are oriented parallel to the tectonic foliation.

C) 1. See AI-C-4, KH-C-2, MP-C-1, and PC-C-1.

Sheep Island (SI, unit D_{Ga}, 4.0 km²)

A) Fine- to medium-grained bi_3-ms_9 granite. The rocks are equigranular except for one outcrop containing 1% microcline phenocrysts 1-3 cm long and scattered muscovite crystals up to 1 cm long. Biotite is commonly partly altered to chlorite. Accessories include apatite, zircon, and monazite. SI is weakly to moderately deformed.

B) Si is fairly homogeneous in that dykes and xenoliths are rare. It is one of the few plutons that shows obvious variation at map scale. The eastern third is fine grained, having an average grain size of about 1 mm. The western part, which is similar in composition, has a grain size of 1-3 mm. The contact between the two textural phases is sharply gradational over 1-5 cm and is irregular in orientation at outcrop scale. It is exposed 600 m north-northeast of Meades Point on the north shore of Dover Harbour. Schlieren enriched in quartz and/or mica occur locally. The western boundary with PH, SL, and DH is poorly defined because of the lack of outcrop in that area.

C) 1. See CL-C-1, MP-C-3 and PC-C-3.

Snyders Lake (SL, unit D_{Gf}, 2.5 km²)

A) Medium grained bi_1-ms_{10} leucogranite. The rocks are equigranular except for scattered muscovite flakes up to 1 cm in diameter. Biotite is commonly partly altered to chlorite. Zircon, monazite, apatite, and allanite are accessory minerals. The pluton is undeformed.

B) Outcrops at Louse Head are notable for several unusual features. They contain rounded autoliths, up to several metres in diameter, of fine grained granodiorite of similar composition. Just east of the autoliths the host granodiorite is obicular, containing 0-30% spherical orbicules 2-4 cm across that differ from their host by having only about 1% fine grained muscovite. The same outcrops have scattered miarolitic cavities and are crosscut by a single 10 cm thick dyke of granodiorite that is virtually identical to the host. Discontinuous streaks enriched in quartz and/or muscovite, 1-10 cm thick, crosscut a few of the outcrops. The boundary with SI is poorly defined because of the lack of exposure in that area.

Whitehead (WH, unit D_{Gdl}, 16.6 km²)

A) Medium grained bi_2-ms_6 granite. The pluton is equigranular except for very rare microcline phenocrysts up to 2 cm long and muscovite flakes up to 5 mm in diameter. Biotite is typically partly altered to chlorite. Accessories include zircon, ilmenite, monazite, apatite and rare sillimanite, garnet, sphene, and spinel (one grain found). It is undeformed except along the Harbour Island shear zone.

B) WH is remarkably homogeneous except for small variations in muscovite content and the common occurrence of micaceous schlieren (0.1-3 cm thick) and mica-enriched layers (1-30 cm thick). These structures are particularly well displayed along the west side of White Head Island. Rounded autoliths, up to 0.5 m long and similar in composition to their host, occur at Flying Point. Miarolitic cavities lined with euhedral quartz, microcline, muscovite, and tourmaline occur at the north end of White Head Island. Pegmatite and minor aplite dykes, trending mainly northwest, and Meguma Group xenoliths are uncommon features. A 3-5 cm thick vein of pseudotachylite fills the centre of a small, north-trending sinistral shear plane on the mainland just east of Yankee Island.

C) 1. See DH-C-3.

Forest Hill area

Buchanans Mountain (BM, unit D_{Gf}, 0.5 km²)

A) Fine grained ms_9 leucogranite (plots on granite-granodiorite boundary). The rocks are orange-weathering from iron oxide stain. Accessory phases are apatite, zircon, pyrite, and monazite. The rocks are moderately deformed and possess a weak mica foliation.

B) BM is defined by only two outcrops. Although it lies just east and contigous with the elongate CR pluton, the two bodies are quite different in composition and texture and are mapped as separate intrusions. Quartz veins and pegmatite lenses, both with accessory muscovite and graphite, occur in the eastern end of BM.

Bantry Road (BR, unit D_{Gd}, 14.5 km²)

A) Medium grained bi_6-ms_7 granite, locally carrying a few muscovite laths up to 1 cm long and microcline phenocrysts 0.7-2 cm long. BR is somewhat heterogeneous in texture (varying from medium grained granular to medium to coarse grained seriate) and in composition (varying from bi > ms to ms > bi). The rocks are moderately to strongly deformed and have a well developed mica foliation. Accessories include monazite, apatite, and zircon.

B) Although the compositional and textural variability raises the possibility that BR is composite, no evidence of internal contacts was found in the field. Garnet-bearing bi_1-ms_3 granite aplite was found as an isolated outcrop east of Whites Lake. It is mapped as a dyke although contact relationships with the host pluton are unknown. Abundant irregular lenses and dykes of pegmatite and minor aplite, up to 5 m thick, intrude the margins and adjacent country rocks of BR.

Costley River (CR, unit D_{Gd}, 10.5 km^2)

A) Medium- to coarse-grained foliate bi_5-ms_9 granite. CR lies along the Black Lakes shear zone and is strongly deformed, possessing feldspar augen up to 2 cm long and a well developed S-C fabric and mineral lineation. Zircon, apatite, monazite, and minor garnet are accessories.

B) The eastern end of CR is poorly exposed and its contact relationship with adjacent BM is unknown.

Doctors Brook (DB, unit D_{Gd}, 16.4 km^2)

A) Medium grained foliate bi_7-ms_9 granite. DB is somewhat variable in grain size between outcrops and locally has feldpsar augen and muscovite flakes up to 1 cm long. It is moderately deformed. Accessory minerals include apatite, zircon, and monazite.

B) The northwest margin of DB is agmatitically mixed with lenses of Goldenville Formation in a 500-800 m wide zone. Pegmatite dykes and lenses up to 2 m thick are locally abundant within, and adjacent to, the pluton. Near the mouth of Doctors Brook, outcrops are locally highly fractured and altered. An isolated outcrop of fine- to medium-grained bi_2-ms_{10} granite south of Cutler Lake is mapped as a dyke, although contact relationship with the host was not determined.

East Branch (EB, unit D_{Gdl}, 11.9 km^2)

A) Medium grained granular bi_3-ms_8 granite, locally containing 1-5% reddish microcline phenocrysts up to 1 cm long. Accessories are apatite, zircon, and monazite. This pluton is the only in the Forest Hill area that is essentially undeformed.

B) EB is poorly exposed, and its shape is uncertain. The position of the eastern boundary of the pluton is particularly speculative.

Garry Lakes (GL, unit D_{Th} and D_{Tb}, 1.0 km^2)

A) On average, GL is fine- to medium-grained hb_4-bi_{23} tonalite, locally containing 1-5% weakly aligned to decussate plagioclase phenocrysts 2-6 mm long. Three of the small bodies that comprise GL carry both biotite and hornblende whereas the other two have only biotite. In addition, the body southeast of White Lake has minor augite. Other accessory minerals are zircon, ilmenite, and sphene. Individual samples vary from relatively fresh to highly altered. Most of the tonalite outcrops are moderately deformed, although the outcrop 300 m north of Garry Lakes is remarkably undeformed considering its proximity to the Guysborough County fault.

B) GL is a collective term for five small tonalite bodies in the northern part of the Forest Hill area. Because of the poor exposure and intrusion of younger granite, the relationships between the five plutons are unknown. The body just north of Garry Lakes is the only one defined by more than one outcrop. It contains biotite streaks and inclusions of Goldenville Formation metawacke oriented parallel to a very weak biotite foliation. The tonalite is intruded by a few stringers and lenses of granite pegmatite up to 1 m thick.

Rocky Lake (RL, unit D_{Ga}, 2.1 km^2)

A) Fine- to medium-grained foliate bi_2-ms_{12} granite. It is moderately deformed and contains feldspar augen up to 3 mm long set in a finer grained recrystallized matrix. Accessories include apatite, ilmenite, sphene, and tourmaline.

B) RL is charaterized by the presence of abundant irregular dykes and lenses of pegmatite (generally up to about 1 m thick) that form up to 75% of individual outcrops. The pegmatite, found both within and along the margins of the pluton, is typically oriented parallel to the tectonic foliation.

Sloans Pond (SP, unit D_{Gd}, 5.2 km^2)

A) Medium grained foliate ms_2-bi_4 granite. This pluton is the only one grouped in unit D_{Gd} that appears to have more biotite than muscovite. However, individual outcrops are quite variable in biotite and muscovite proportions, as well as texture. Apatite and garnet are accessory minerals. SP is moderately deformed and has feldspar augen up to 2 cm long and a locally developed S-C fabric.

B) The textural and compositional variability suggest SP may be composite. Lenses and dykes of pegmatite, up to 3 m thick, are locally abundant. The rocks are crushed and altered along the Guysborough County fault.

Tom Lake (TL, unit D_{Gdl}, 5.1 km^2)

A) Medium grained foliate bi_2-ms_{10} granite. This pluton is relatively equigranular although one microcline phenocryst 2 cm long was found. Biotite is commonly altered to chlorite. Accessories include apatite, ilmenite, zircon, and monazite. The rocks are moderately to strongly deformed.

B) TL is quite homogeneous with very few xenoliths and dykes. The eastern end of the pluton is intruded by a few pegmatite dykes up to 3 m thick.

APPENDIX II

Representative mineral analyses

Representative mineral compositions of feldspars, micas, and accessory minerals are given, selected from a total of more than 350 microprobe analyses. Each mineral composition is an average of one to six spot analyses. Grain types are core and rim for feldspars and primary-looking (P), secondary (S), metamorphic (M), and augen (A) for micas.

	Biotite												Muscovite						
pluton	GL	SC	AI	PH	PH	PH	PH	KH	KH	WH	GI	SL	AI	PC	WH	WH	WH	WH	GI
sample	114B	571	411A	686	686	641	641	477	477	338	502	562C	411A	445	328	338	340	340	502
grain	P	A	M	P	S	M	S	P	S	P	P	P	M	S	M	P	P	S	P
SiO_2	36.50	35.76	35.34	34.51	34.80	34.30	34.65	33.98	35.25	34.16	35.15	39.65	47.67	47.29	47.36	47.39	47.25	47.59	46.94
TiO_2	3.27	4.07	2.72	3.74	3.00	3.32	3.64	3.49	3.25	1.71	1.29	2.46	1.39	0.82	0.40	0.31	0.26	0.25	0.17
Al_2O_3	15.07	18.15	17.39	18.72	18.23	17.56	18.15	17.84	18.22	20.03	20.37	26.33	32.77	34.63	33.79	33.76	33.80	33.48	33.64
Cr_2O_3	0.08	0.00	0.03	0.08	0.08	0.08	0.00	0.15	0.00	0.13	0.00	0.00	0.02	0.00	0.00	0.00	0.01	0.06	0.00
FeO^t	17.69	19.58	22.38	21.10	21.51	23.00	22.50	21.81	20.90	27.22	25.90	18.07	1.51	1.02	1.60	1.89	1.74	1.84	2.01
MnO	0.26	0.52	0.44	0.26	0.35	0.34	0.43	0.35	0.26	0.59	0.43	0.17	0.04	0.00	0.00	0.00	0.00	0.00	0.00
MgO	12.91	8.99	7.30	6.63	6.76	6.53	6.49	7.01	7.70	3.41	0.81	0.53	0.79	0.56	0.49	0.56	0.65	0.79	0.36
CaO	0.23	0.05	0.00	0.14	0.19	0.09	0.09	0.05	0.05	0.00	0.00	0.05O	0.07	0.10	0.00	0.02	0.02	0.06	0.05
Na_2O	0.55	0.00	0.00	0.29	0.29	0.58	0.29	0.29	0.57	0.00	0.30	0.27	0.71	0.44	0.52	1.24	1.06	0.88	0.67
K_2O	9.01	9.98	9.59	9.59	9.33	9.57	9.24	9.58	9.90	8.75	9.31	9.87	10.48	10.91	10.54	10.14	9.95	10.18	10.40
	95.57	97.10	95.19	95.06	94.54	95.36	95.48	94.55	96.10	96.01	93.56	97.40	95.45	95.77	94.70	95.31	94.74	95.13	94.24
	(on basis of 22 oxygens)																		
Si	5.52	5.38	5.49	5.34	5.42	5.36	5.37	5.33	5.40	5.35	5.62	5.73	6.35	6.26	6.34	6.32	6.32	6.35	6.33
Al^{IV}	2.48	2.63	2.51	2.66	2.58	2.64	2.63	2.67	2.60	2.65	2.39	2.27	1.66	1.74	1.66	1.68	1.68	1.65	1.67
Al^{VI}	0.21	0.59	0.67	0.76	0.77	0.60	0.68	0.62	0.69	1.05	1.45	2.22	3.49	3.66	3.67	3.62	3.65	3.62	3.68
Ti	0.37	0.46	0.32	0.44	0.35	0.39	0.42	0.41	0.37	0.20	0.16	0.27	0.14	0.08	0.04	0.03	0.03	0.03	0.02
Cr	0.01	0.00	0.00	0.01	0.01	0.01	0.00	0.02	0.00	0.02	0.00	0.00	0.00	0.00	0.00	0.00	0.00	0.01	0.00
Fe	2.24	2.46	2.91	2.73	2.80	3.01	2.92	2.86	2.68	3.57	3.46	2.19	0.17	0.11	0.18	0.21	0.20	0.21	0.23
Mn	0.03	0.07	0.06	0.03	0.05	0.05	0.06	0.05	0.03	0.08	0.06	0.02	0.01	0.00	0.00	0.00	0.00	0.00	0.00
Mg	2.91	2.01	1.69	1.53	1.57	1.52	1.50	1.64	1.76	0.80	0.19	0.12	0.16	0.11	0.10	0.11	0.13	0.16	0.07
Ca	0.04	0.01	0.00	0.02	0.03	0.02	0.02	0.01	0.01	0.00	0.00	0.01	0.01	0.01	0.00	0.00	0.00	0.01	0.01
Na	0.16	0.00	0.00	0.09	0.09	0.18	0.09	0.09	0.17	0.00	0.09	0.08	0.18	0.11	0.14	0.32	0.28	0.23	0.18
K	1.74	1.91	1.90	1.89	1.86	1.91	1.83	1.92	1.93	1.75	1.90	1.82	1.78	1.84	1.80	1.72	1.70	1.73	1.79

	Plagioclase																Microcline		
pluton	GL	GL	SC	SC	AI	AI	DH	DH	KH	KH	PH	MP	WH	WH	WH	GI	AI	PH	WH
sample	114B	114B	571	571	411A	411A	680	680	477	477	686	472A	328	331	338	502	411A	269	338
grain	core	rim	core	rim	core	rim	core	rim	core	rim	core	core	core	core	core	core	core	core	core
SiO_2	54.54	57.28	58.97	61.60	63.32	63.98	63.22	64.55	62.97	67.23	62.52	64.42	66.95	63.55	64.27	67.91	64.53	64.90	64.99
Al_2O_3	28.71	26.83	26.34	24.11	23.47	22.67	23.36	22.66	23.58	21.25	23.45	22.76	19.29	22.47	21.58	19.63	19.04	19.18	19.28
FeO^t	0.14	0.28	0.14	0.14	0.10	0.12	0.00	0.00	0.14	0.14	0.14	0.00	0.04	0.02	0.00	0.14	0.00	0.00	0.03
CaO	10.76	8.57	7.71	5.04	4.55	3.60	3.70	2.82	4.16	1.47	3.99	3.05	0.29	2.96	2.11	0.06	0.22	0.17	0.17
Na_2O	5.55	6.99	7.42	8.83	8.96	9.43	9.48	10.37	9.26	10.80	9.29	9.92	11.77	9.77	10.34	11.74	0.53	2.13	1.41
K_2O	0.10	0.14	0.24	0.24	0.35	0.27	0.34	0.20	0.39	0.10	0.24	0.34	0.12	0.26	0.18	0.20	15.82	14.08	14.66
	99.80	100.09	100.82	99.96	100.75	100.07	100.10	100.60	100.50	100.99	99.63	100.49	98.46	99.03	98.48	99.68	100.14	100.46	100.54
(on basis of 32 oxygens)																			
Si	9.87	10.28	10.47	10.95	11.14	11.30	11.17	11.33	11.11	11.68	11.11	11.32	11.91	11.33	11.49	11.93	11.90	11.87	11.89
Al	6.12	5.68	5.51	5.05	4.86	4.72	4.86	4.69	4.90	4.35	4.91	4.71	4.04	4.72	4.54	4.06	4.13	4.13	4.16
Fe	0.02	0.04	0.02	0.02	0.01	0.02	0.00	0.00	0.02	0.02	0.02	0.00	0.01	0.00	0.00	0.02	0.00	0.00	0.01
Ca	2.09	1.65	1.47	0.96	0.86	0.68	0.70	0.53	0.79	0.27	0.76	0.58	0.05	0.58	0.41	0.01	0.04	0.03	0.03
Na	1.95	2.43	2.56	3.04	3.06	3.23	3.25	3.53	3.17	3.64	3.20	3.38	4.06	3.37	3.59	4.00	0.19	0.76	0.50
K	0.02	0.03	0.06	0.06	0.07	0.06	0.08	0.04	0.08	0.02	0.06	0.08	0.03	0.06	0.04	0.04	3.72	3.29	3.42
mole %																			
An	51.5	40.1	36.0	23.6	21.5	17.1	17.4	12.9	19.5	7.0	18.9	14.3	1.3	14.2	10.1	0.3	1.1	0.8	0.8
Ab	48.0	59.1	62.7	75.0	76.7	81.3	80.7	86.0	78.4	92.5	79.7	83.8	97.9	84.2	88.8	98.6	4.8	18.6	12.7
Or	0.5	0.8	1.4	1.4	1.9	1.6	1.9	1.1	2.2	0.6	1.4	1.9	0.8	1.6	1.1	1.1	94.1	80.6	86.5

	Ilmenite				Spinel	Garnet	Hornblende	Smectite
pluton	GL	PH	DH	MP	WH	Al	GL	PH,DH
sample	114B	686	680	472A	340	411A	114B	average
SiO_2						37.49	47.20	50.54
TiO_2	53.40	53.71	52.82	53.72	0.07	0.00	0.57	0.04
Al_2O_3					53.39	21.59	8.02	36.74
Cr_2O_3					0.04	0.00	0.00	0.01
FeO^t	43.32	43.72	42.02	35.88	17.75	25.98	15.24	4.74
ZnO					28.28			
MnO	3.69	2.57	4.21	8.56	0.50	12.02	0.72	0.19
MgO	0.18	0.18	0.00	0.00	0.93	2.05	12.26	1.95
CaO	0.14	0.05	0.19	1.14		0.82	11.44	0.41
Na_2O						0.00	0.98	0.09
K_2O						0.00	0.27	2.88
	100.73	100.23	99.24	99.30	100.96	99.95	96.70	97.59
	(on basis of 3, 4, 24 and 23 oxygens for ilmenite, spinel, garnet and hornblende)							
Si						6.04	7.03	
Ti	1.00	1.01	1.01	1.02	0.00	0.00	0.06	
Al					1.91	4.10	1.41	
Cr					0.00	0.00	0.00	
Fe	0.91	0.92	0.89	0.76	0.45	3.50	1.90	
Zn					0.63			
Mn	0.08	0.05	0.09	0.18	0.01	1.64	0.09	
Mg	0.01	0.01	0.00	0.00	0.04	0.49	2.72	
Ca	0.01	0.00	0.01	0.03		0.14	1.83	
Na						0.00	0.28	
K						0.00	0.05	

APPENDIX III

Average pluton compositions and norms

Average major and trace element analyses and CIPW norms are given for each pluton. Data are in weight percent oxides and parts per million. Blanks indicate no data. Individual analyses were recalculated to 100% anhydrous prior to averaging. For individual trace element values lower than the detection limit, one-half of the detection limit was used to calculate the average analysis. Plutons are separated into Canso area, miscellaneous bodies associated with plutons in the Canso area, and Forest Hill area. The miscellaneous bodies are aplite associated with the Durells Island pluton (DIa) and quartz-bearing syenite associated with the Fogherty Lake and Lumsdens Lake plutons (FLs and LLs).

Canso area

pluton	AI	BB	CH	CL	DH	DI	FC	FH	FL	GH	GI	KH	LH	LL	ML	MP	OI	PC	PH
unit	D_{Gb}	D_{Ga}	D_{Gd}	D_{Ge}	D_{Gb}	D_{Gd}	D_{Gc}	D_{Gd}	D_{Gd}	D_{Gd}	D_{Gf}	D_{Ge}	D_{Gd}	D_{Gd}	D_{Gd}	D_{Gb}	DT	D_{Ge}	D_{Ge}
n	5	3	1	8	5	5	3	7	6	8	3	5	2	10	1	5	4	6	11
SiO_2	72.05	71.81	75.49	75.06	71.40	73.55	73.08	73.79	73.93	73.49	73.89	72.37	70.66	74.24	74.23	70.57	75.20	74.68	73.06
TiO_2	0.28	0.17	0.17	0.26	0.29	0.18	0.21	0.15	0.17	0.19	0.08	0.36	0.38	0.15	0.11	0.25	0.38	0.32	0.33
Al_2O_3	15.15	16.13	14.13	13.73	15.84	14.98	15.21	14.99	14.95	14.98	15.25	14.99	16.62	14.76	14.95	16.44	13.09	13.67	14.65
Fe_2O_3	0.14	0.26	0.10	0.14	0.36	0.22	0.13	0.20	0.28	0.14	0.30	0.19	0.74	0.27	0.01	0.23	0.94	0.12	0.47
FeO	1.86	0.78	0.98	1.28	1.09	0.88	1.00	0.77	0.74	0.94	0.60	1.36	1.33	0.69	0.66	1.02	1.95	1.45	1.13
MnO	0.07	0.03	0.04	0.04	0.05	0.04	0.03	0.05	0.03	0.03	0.04	0.05	0.05	0.04	0.03	0.04	0.08	0.04	0.04
MgO	0.69	0.33	0.33	0.42	0.54	0.42	0.40	0.28	0.33	0.34	0.12	0.57	0.78	0.28	0.20	0.48	1.07	0.49	0.50
CaO	1.71	0.66	0.52	0.59	0.77	0.74	0.79	0.56	0.59	0.59	0.53	0.67	0.73	0.56	0.54	0.75	1.07	0.62	0.66
Na_2O	4.00	4.18	3.66	3.22	3.48	3.71	3.63	4.11	3.91	3.76	4.41	3.22	3.42	4.01	4.06	3.67	3.52	2.90	3.29
K_2O	3.92	5.37	4.25	4.97	5.91	5.02	5.19	4.77	4.77	5.21	4.33	5.89	5.04	4.66	4.92	6.28	2.56	5.40	5.57
P_2O_5	0.11	0.28	0.31	0.28	0.29	0.27	0.32	0.34	0.31	0.32	0.46	0.32	0.24	0.34	0.30	0.28	0.14	0.31	0.29
Ba	582	417	260	289	568	522	523	281	302	360	130	506	680	229	140	612	423	322	390
Be	4	7		5	8	5	9	7	5	7	21	8		4	5	8	3	6	6
F	524	510	450	509	396	334	403	516	583	447	1433	666	680	560	310	428	289	580	984
Li	113	190	51	87	77	51	90	119	66	100	180	85		52	63	73	46	97	85
Nb	14	10	30	16	12	16	13	12	17	16	17	16	13	11	10	10	20	16	12
Pb	33	31	23	51	38	36	31	25	22	28	18	38	26	23	27	38	25	34	35
Rb	228	370	320	293	312	228	277	363	368	336	697	368	330	346	310	342	140	340	379
Sn	5	10	11	9	6	6	9	10	13	11	20	8	10	12	5	6	3	7	8
Sr	198	83	40	58	122	128	87	59	47	65	6	96	130	36	20	126	200	62	75
Th	8	4		8	16	3		3		4	2	26	8	6		14	6		21
U	2	3	9	5	4	3	4	3	8	5	10	5	6	7	3	6	2	5	6
Y	28	12	10	7	14	8	10	9	9	11	23	12	8	7	5	8	25	12	11
Zn	49	45	34	57	54	38	58	42	35	43	78	75	44	33	36	50	59	69	77
Zr	98	43	30	70	94	50	80	37	48	58	20	136	100	40	5	84	173	93	110
Ap	0.24	0.62	0.68	0.62	0.64	0.59	0.70	0.75	0.68	0.70	1.01	0.70	0.53	0.75	0.66	0.62	0.31	0.68	0.64
Il	0.53	0.32	0.32	0.50	0.55	0.34	0.40	0.29	0.32	0.36	0.15	0.69	0.72	0.29	0.21	0.48	0.72	0.61	0.63
Mt	0.20	0.38	0.15	0.20	0.52	0.32	0.19	0.29	0.41	0.20	0.44	0.28	1.08	0.39	0.01	0.33	1.37	0.17	0.68
Hm																			
Or	23.15	31.73	25.11	29.36	34.92	29.66	30.66	28.18	28.18	30.78	25.59	34.80	29.77	27.53	29.07	37.11	15.12	31.90	32.91
Ab	33.84	35.37	30.97	27.25	29.45	31.39	30.72	34.78	33.09	31.82	37.32	27.25	28.94	33.93	34.36	31.06	29.78	24.54	27.84
An	7.76	1.44	0.55	1.10	1.93	1.91	1.83	0.56	0.90	0.84	-0.38	1.23	2.05	0.56	0.72	1.89	4.39	1.05	1.38
Hy	4.68	1.81	2.33	2.93	2.66	2.26	2.43	1.79	1.72	2.20	1.10	3.26	3.24	1.57	1.58	2.54	4.98	3.33	2.46
Ol																			
Co	1.48	2.92	3.31	2.65	3.02	2.75	2.95	2.87	3.03	2.85	3.45	2.87	4.79	2.92	2.69	2.92	2.92	2.67	2.71
Qz	28.07	25.41	36.56	35.39	26.34	30.79	30.10	30.51	31.68	30.23	31.33	28.91	28.87	32.06	30.72	23.07	40.41	35.04	30.75

Appendix III (cont.)

	Canso area (continued)								Forest Hill area								
pluton	Pl	SC	Sl	SL	WH	Dla	FLs	LLs	BM	BR	CR	DB	EB	GL	RL	SP	TL
unit	D_{Gb}	DT	D_{Ga}	D_{Gf}	D_{Gd}				D_{Gf}	D_{Gd}	D_{Gd}	D_{Gd}	D_{Gd}	DT	D_{Ga}	D_{Gd}	D_{Gd}
n	5	4	7	4	20	2	2	1	1	6	4	3	3	3	1	4	7
SiO_2	74.03	65.62	73.66	74.41	75.15	73.56	62.07	63.14	74.54	72.30	72.20	71.86	73.27	60.19	74.69	72.44	74.16
TiO_2	0.28	0.78	0.17	0.10	0.12	0.13	0.21	0.14	0.08	0.25	0.27	0.28	0.17	0.81	0.12	0.23	0.12
Al_2O_3	14.46	16.82	14.90	15.30	14.28	15.13	21.25	20.64	15.09	15.44	15.49	15.68	15.31	18.83	15.55	15.14	14.89
Fe_2O_3	0.36	0.41	0.17	0.14	0.26	0.23	0.43	0.27	0.31	0.34	0.39	0.32	0.43	0.64	0.62	0.44	0.32
FeO	1.20	3.93	0.88	0.67	0.69	0.73	1.15	1.06	0.20	1.00	0.96	1.05	0.57	4.48	0.30	1.01	0.55
MnO	0.06	0.16	0.04	0.04	0.03	0.04	0.03	0.05	0.04	0.03	0.03	0.03	0.03	0.12	0.03	0.04	0.03
MgO	0.49	1.97	0.29	0.16	0.17	0.29	0.43	0.45	0.15	0.51	0.45	0.60	0.32	3.66	0.30	0.50	0.23
CaO	0.66	3.20	0.56	0.46	0.47	0.79	0.34	0.84	0.37	0.93	0.72	0.83	0.64	5.39	0.85	1.19	0.53
Na_2O	3.36	3.56	3.95	4.02	3.94	3.63	5.50	5.99	5.21	4.08	3.72	3.84	4.02	3.44	3.95	4.03	3.93
K_2O	4.81	3.35	5.02	4.31	4.59	5.17	7.62	6.98	3.80	4.85	5.53	5.21	4.90	2.28	3.32	4.83	4.87
P_2O_5	0.29	0.21	0.36	0.38	0.30	0.30	0.47	0.44	0.20	0.27	0.24	0.30	0.34	0.16	0.25	0.15	0.37
Ba	408	725	280	123	123	385	430	500	70	542	458	643	397	543	390	540	220
Be	7	5	6	4	3	8	4	7									
F	552	783	770	1595	729	350	578	500	920	552	800	627	360	367	300	398	470
Li	107	87	124	219	111	52	46	38	160	94	120	117	105	89	28	90	91
Nb	12	18	16	20	13	8	14	10	8	10	7	9	13	9	12	9	14
Pb	33	31	23	16	24	36	14	25	24	31	31	32	32	26	26	36	21
Rb	336	220	433	693	457	255	370	480	500	292	380	320	280	138	190	268	297
Sn	9	5	13	23	11	9	10	17	34	9	9	9	13	3	10	11	14
Sr	74	288	41	13	6	100	100	130	14	107	84	92	71	400	130	134	58
Th		12	8	3	3		15		1	6	16	6	2	5	1	7	2
U	6	3	7	15	5	5	7	5	12	5	4	3	6	1	4	3	5
Y	13	20	7	13	9	15	1	10	1	8	5	6	9	13	10	9	8
Zn	71	98	57	77	56	33	16	194	20	64	64	82	45	95	16	44	23
Zr	84	210	47	28	20	40	80	70	27	85	99	81	54	76	21	75	33
Ap	0.64	0.46	0.79	0.84	0.66	0.66	1.03	0.97	0.44	0.59	0.53	0.66	0.75	0.35	0.55	0.33	0.81
Il	0.53	1.49	0.32	0.19	0.23	0.25	0.40	0.27	0.15	0.48	0.51	0.53	0.32	1.54	0.23	0.44	0.23
Mt	0.52	0.60	0.25	0.20	0.38	0.33	0.63	0.39	0.45	0.49	0.57	0.47	0.63	0.93	0.72	0.64	0.47
Hm															0.13		
Or	28.42	19.79	29.66	25.46	27.12	30.54	45.04	41.26	22.45	28.65	32.67	30.78	28.95	13.47	19.61	28.53	28.77
Ab	28.43	30.12	33.43	34.02	33.34	30.72	46.57	50.71	44.08	34.53	31.48	32.50	34.02	29.11	33.42	34.10	33.28
An	1.38	14.50	0.43	-0.20	0.37	1.96	-1.39	1.29	0.53	2.85	2.00	2.16	0.95	25.70	2.58	4.92	0.21
Hy	2.77	10.79	1.99	1.42	1.33	1.73	2.54	1.28	0.43	2.47	2.17	2.75	1.26	15.68	0.74	2.43	1.18
Ol								1.06									
Co	3.22	2.02	2.82	4.10	2.70	2.85	4.47	2.76	2.21	2.44	2.65	2.94	3.05	1.29	4.52	1.48	3.08
Qz	34.08	20.23	30.32	33.95	33.88	30.96	0.21		29.25	27.50	27.41	27.22	30.07	11.92	37.48	27.13	31.98

APPENDIX IV

Rock chemical analyses

Major and trace element analyses of all individual rock samples are tabulated in the order (1) Canso area plutons, (2) Forest Hill area plutons, (3) miscellaneous plutonic rocks (described below), (4) Meguma Group metasedimentary rocks (all from the Canso area), and (5) quartz veins (all from the Canso area). DIa is aplite associated with the Durells Island pluton and FLs and LLs are quartz-bearing syenite associated with the Fogherty Lake and Lumsdens Lake plutons. Data are in weight percent and parts per million, except for gold which is in parts per billion. Sample locations are plotted on Figures 2, 3 (in back pocket). Loss on ignition and total iron are given as H_2O^+ and FeO for incomplete analyses. Analytical techniques and precision are described in the section entitled "Petrography and chemistry of granitoid plutons". Data for sample numbers beginning with the letter "F" have been supplied by K. Ford of Geological Survey of Canada (see Ford and Ballantyne, 1983).

Miscellaneous plutonic rocks

041 - cataclastic leucogranite dyke, adjacent to BM
051 - biotite-muscovite granite dyke, adjacent to TL
069A - altered granite from fault zone, FL pluton
088A - muscovite leucogranite dyke, adjacent to BM
153 - muscovite leucogranite aplite dyke(?), adjacent to DB
154B - biotite-muscovite granite dyke(?), adjacent to DB
236, 253, 802 - felsite sills, Halifax Formation, Whitehead
248A - pegmatitic granite, margin of FH pluton
346A, 384A - leucogranite lens in OI migmatite
411C - biotite-muscovite leucogranite, in abrupt contact with AI and FC
414 - xenolith of medium grained biotite-muscovite granite in PC
441A - xenolith of medium grained muscovite-biotite granite in PC
458A - medium grained biotite-muscovite granite (correlative with GH?)
458B - dyke of muscovite-biotite granite, intrudes 458A, Black Island
463 - leucogranite aplite dyke, intrudes AI
472B, 485 - leucogranite aplite-pegmatite dykes, intrude MP
547 - altered PH granite, from Harbour Island shear zone
553 - biotite-muscovite leucogranite dyke, intrudes DH
558 - leucogranite aplite dyke, intrudes PH
587B - leucogranite aplite dyke, intrudes SC
F68A3 - altered granite, fault zone, LL pluton

Canso area plutons

pluton	AI					BB			CH	CL							
	410	411A	449	467A	582	654	830	831	480	147	149	152A	580	603	616B	676	814
SiO_2	70.90	71.50	70.00	71.10	72.20	72.30	72.10	69.20	74.80	72.00	75.70	74.10	72.90	74.60	75.40	74.00	73.90
TiO_2	0.26	0.28	0.32	0.26	0.28	0.19	0.16	0.16	0.17	0.21	0.26	0.19	0.35	0.18	0.25	0.25	0.31
Al_2O_3	14.90	15.20	15.30	15.20	14.20	15.10	15.70	17.20	14.00	15.00	12.50	13.70	14.00	13.90	12.80	13.50	13.00
Fe_2O_3	0.09	0.16	0.17	0.23	0.03	0.10	0.56		0.10	0.17	0.31	0.11	0.02	0.01	0.06	0.26	
FeO	1.74	1.86	1.99	1.58	2.00	0.97	0.40	1.04	0.97	1.17	1.23	0.96	1.45	1.08	1.33	1.22	1.84
MnO	0.07	0.08	0.07	0.08	0.07	0.04	0.02	0.04	0.04	0.05	0.05	0.03	0.04	0.03	0.05	0.04	0.04
MgO	0.65	0.75	0.75	0.66	0.62	0.34	0.35	0.28	0.33	0.42	0.43	0.29	0.48	0.35	0.46	0.39	0.49
CaO	1.62	1.91	1.69	1.63	1.60	0.70	0.54	0.72	0.52	0.76	0.51	0.56	0.59	0.66	0.49	0.57	0.48
Na_2O	3.94	4.03	4.03	4.04	3.72	3.81	4.12	4.50	3.63	3.65	3.11	3.37	2.95	3.34	3.01	3.17	2.83
K_2O	3.97	3.37	3.90	4.29	3.83	5.01	5.19	5.78	4.21	4.98	4.25	4.86	5.28	4.92	4.57	5.05	5.36
H_2O^+	0.93	0.70	0.70	0.54	0.62	0.93	1.08	0.93	0.93	1.00	0.85	0.77	0.93	0.93	1.16	0.93	0.54
H_2O^-																	
P_2O_5	0.11	0.12	0.12	0.11	0.09	0.28	0.18	0.38	0.31	0.30	0.23	0.27	0.27	0.29	0.28	0.30	0.30
Total	99.18	99.96	99.04	99.72	99.26	99.77	100.40	100.23	100.01	99.71	99.43	99.21	99.26	100.29	99.89	99.68	99.09
Ba	610	570	620	550	560	380	430	440	260	460	260	220	330	300	300	180	260
Be	5	4	5	5	3	7				5	5	6	4	5	9	4	
F	440	430	510	580	660	600	420		450	460	580	400	660	340	640	480	
Li	95	123	109	124	113	190			51	78	127	70	103	51	121	62	
Nb	10	10	20	10	20	< 10	20	< 10	30	10	20	20	10	20	10	20	20
Pb	37	33	32	35	28	27	34		23	185	26	26	28	30	27	32	
Rb	220	230	240	230	220	320	340	450	320	290	310	250	370	230	310	300	280
Sn	4	7	7	3	3	10	10		11	6	12	11	9	7	7	9	
Sr	200	200	210	190	190	90	70	90	40	100	50	30	60	100	40	30	50
Th				8			4				8						
U	3	1	2	2	2	4	< 2		9	1	6	7	7	5	7	5	
Y	20	30	30	20	40	20	10	< 10	10	< 10	< 10	10	< 10	< 10	< 10	10	10
Zn	47	47	53	52	46	49	40		34	60	65	59	76	33	60	43	
Zr	100	110	100	80	100	60	30	40	30	60	60	50	140	40	90	60	60
La				24.0							17.0						
Ce				41							32						
Nd				15							15						
Sm				4.12							4.23						
Eu				0.49							0.48						
Tb				0.7							0.6						
Yb				1.67							0.48						
Lu				0.31							0.08						

Appendix IV (cont.)

Canso area plutons (continued)

pluton	DH					DI					DIa		FC		
	167B	525A	556A	680	709	126	131	348A	352	373A	348B	350	167A	411B	488
SiO_2	71.70	71.60	68.70	68.00	72.00	74.10	72.40	71.40	73.10	72.40	72.40	72.50	72.20	72.10	71.90
TiO_2	0.34	0.26	0.25	0.29	0.27	0.18	0.14	0.19	0.23	0.14	0.13	0.13	0.23	0.19	0.20
Al_2O_3	14.70	14.50	16.40	17.40	15.10	14.10	15.00	15.30	14.20	15.40	14.90	14.90	15.10	15.10	14.80
Fe_2O_3	0.50	0.42	0.22	0.34	0.31	0.47	0.25	0.29	0.02	0.06	0.25	0.21	0.17	0.04	0.18
FeO	1.22	1.01	1.03	1.10	1.00	0.71	0.78	0.72	1.19	0.96	0.77	0.66	1.10	0.92	0.95
MnO	0.04	0.05	0.04	0.05	0.05	0.03	0.04	0.03	0.03	0.05	0.03	0.04	0.03	0.03	0.03
MgO	0.55	0.48	0.45	0.62	0.55	0.46	0.34	0.40	0.47	0.40	0.30	0.27	0.49	0.34	0.36
CaO	0.71	0.66	0.73	0.96	0.72	0.63	0.81	0.82	0.74	0.65	0.78	0.77	0.72	0.98	0.63
Na_2O	3.41	3.09	3.58	3.81	3.27	3.60	3.53	3.88	3.37	3.97	3.56	3.60	3.42	3.53	3.80
K_2O	5.62	5.41	6.53	6.03	5.53	4.65	4.84	5.31	4.98	5.02	5.14	5.04	5.08	5.11	5.15
H_2O^+	0.77	1.08	1.00	1.00	1.08	0.93	1.08	0.93	0.93	0.77	1.31	1.08	1.00	1.00	1.23
H_2O^-															
P_2O_5	0.31	0.25	0.26	0.33	0.26	0.25	0.31	0.30	0.25	0.21	0.30	0.30	0.35	0.23	0.37
Total	99.87	98.81	99.19	99.93	100.14	100.11	99.52	99.57	99.51	100.03	99.87	99.50	99.89	99.57	99.60
Ba	490	460	610	740	540	510	410	570	470	650	410	360	580	520	470
Be	7	9	8			5	7	6	4	3	7	9	9	9	8
F	410	380	420	470	300	310	400	340	400	220	330	370	380	400	430
Li	90	72	68			34	35	59	103	24	38	66	105	69	97
Nb	20	< 10	10			20	10	20	20	10	< 10	10	20	10	10
Pb	35	37	44	40	32	31	39	34	35	41	37	34	33	34	27
Rb	330	310	330	300	290	220	240	240	250	190	240	270	250	260	320
Sn	8	3	5	10	4	4	9	6	7	5	6	12	7	8	12
Sr	100	110	140	150	110	90	100	150	110	190	110	90	80	120	60
Th	25			12	10		3								
U	5	6	1	6	< 2	1	5	4	3	2	6	3	3	4	4
Y	20	10	10	20	10	10	10	10	< 10	< 10	20	10	10	10	10
Zn	72	51	40	56	50	28	39	55	48	18	30	35	63	45	67
Zr	110	90	80	100	90	50	40	60	70	30	40	40	90	90	60
La	30.3						11.3								
Ce	62						20								
Nd	32						8								
Sm	7.50						2.37								
Eu	0.66						0.63								
Tb	0.9						0.6								
Yb	0.68						0.62								
Lu	0.10						0.09								

pluton	FH							FL						FLs		GH	
	289	293	647	651	714	724	725	067A	069C	074	080	081A	742	F55A	F55B	358	392
SiO_2	73.90	72.60	71.50	73.60	72.50	72.40	73.60	71.10	72.00	74.40	73.20	73.40	72.60	60.80	61.90	73.20	71.60
TiO_2	0.13	0.15	0.17	0.14	0.17	0.11	0.15	0.19	0.20	0.10	0.17	0.16	0.19	0.20	0.22	0.19	0.29
Al_2O_3	14.70	14.80	15.10	14.50	14.60	15.00	14.90	14.70	14.90	14.70	14.90	14.70	14.60	21.30	20.70	14.60	14.80
Fe_2O_3	0.17	0.16	0.48	0.20	0.17	0.06	0.16	0.21	0.13	0.37	0.22	0.43	0.27			0.25	0.18
FeO	0.69	0.89	0.71	0.76	0.91	0.54	0.80	0.96	0.89	0.31	0.86	0.57	0.77	1.59	1.46	0.95	1.31
MnO	0.05	0.06	0.06	0.04	0.04	0.04	0.06	0.03	0.03	0.03	0.03	0.04	0.03	0.03	0.03	0.04	0.04
MgO	0.28	0.29	0.36	0.20	0.31	0.24	0.28	0.43	0.32	0.21	0.36	0.33	0.29	0.46	0.38	0.36	0.50
CaO	0.54	0.56	0.60	0.51	0.64	0.51	0.51	0.63	0.59	0.50	0.60	0.59	0.57	0.88	0.79	0.56	0.51
Na_2O	4.01	4.02	4.27	3.90	3.81	4.61	3.81	3.59	3.77	4.20	3.94	3.80	3.83	5.30	5.58	3.69	3.30
K_2O	4.48	4.72	4.82	4.59	4.71	5.05	4.57	4.93	5.12	3.89	4.54	4.62	5.11	7.48	7.59	4.64	5.50
H_2O^+	0.77	1.00	0.93	0.93	1.00	0.85	1.16	1.47	1.08	1.00	0.93	0.93	0.77	1.31	0.93	1.00	1.08
H_2O^-																	
P_2O_5	0.32	0.34	0.35	0.36	0.36	0.32	0.30	0.31	0.32	0.30	0.31	0.29	0.33	0.49	0.43	0.31	0.23
Total	100.04	99.59	99.35	99.73	99.22	99.73	100.30	99.55	99.35	100.01	100.06	99.86	99.36	99.84	100.01	99.79	99.34
Ba	310	290	360	100	290	390	230	410	330	110	300	340	320	440	420	270	540
Be	6	5	12	5	7	9	6	4	6	2	4	8	8	3	4	7	2
F	435	450	570	620	550	450	540	510	550	470	630	695	640	700	455	520	330
Li	92	163	109	136	106	73	154	42	36	18	97	93	111	52	40	105	32
Nb	10	10	10	20	20	< 10	10	30	10	20	10	20	10	16	12	20	10
Pb	29	30	20	18	26	27	22	23	23	11	24	24	28	15	12	25	28
Rb	360	350	360	420	350	350	350	360	360	360	370	360	400	380	360	350	320
Sn	12	10	11	12	6	10	10	14	17	13	11	13	11	5	14	10	5
Sr	60	80	50	10	80	90	40	50	60	20	30	60	60	110	90	50	100
Th							3							15	15		
U	2	4	3	4	3	5	3	7	3	14	8	7	10	7	6	5	7
Y	10	10	10	< 10	10	10	< 10	< 10	10	10	20	< 10	< 10	0	0	20	10
Zn	38	69	34	42	51	17	44	33	37	23	33	35	50	20	12	57	39
Zr	30	40	60	30	50	30	20	60	60	10	60	50	50	90	70	50	110
La							7.3										
Ce							13										
Nd							6										
Sm							1.77										
Eu							0.37										
Tb							0.1										
Yb							0.34										
Lu							0.05										

Canso area plutons (continued)

pluton	GH (continued)						GI			KH					LH	
	407	408	416B	424B	448	737	502	505	506	415B	433A	477	489B	492	751	818
SiO_2	72.80	73.50	71.90	72.40	72.90	72.30	72.50	73.20	73.30	70.50	72.00	71.50	71.30	70.50	69.50	69.50
TiO_2	0.16	0.15	0.19	0.16	0.17	0.19	0.07	0.08	0.08	0.32	0.36	0.39	0.37	0.35	0.36	0.38
Al_2O_3	14.80	14.50	15.00	14.70	15.10	14.80	15.40	14.90	14.90	15.20	14.10	14.60	14.70	15.10	16.60	16.10
Fe_2O_3	0.07	0.08	0.10	0.25	0.06	0.10	0.16	0.31	0.41	0.07	0.26	0.21	0.23	0.18	0.73	
FeO	0.93	0.77	0.95	0.67	0.89	0.99	0.59	0.60	0.60	1.21	1.35	1.50	1.35	1.28	1.30	1.97
MnO	0.03	0.02	0.03	0.03	0.04	0.04	0.04	0.04	0.03	0.05	0.04	0.05	0.05	0.05	0.05	0.05
MgO	0.35	0.26	0.31	0.29	0.29	0.35	0.10	0.13	0.13	0.49	0.57	0.62	0.57	0.55	0.78	0.76
CaO	0.58	0.65	0.64	0.56	0.57	0.58	0.72	0.41	0.45	0.63	0.69	0.69	0.62	0.65	0.71	0.72
Na_2O	3.93	3.82	4.05	3.59	3.57	3.79	4.41	4.22	4.43	3.31	3.08	3.07	3.05	3.34	3.49	3.24
K_2O	4.72	5.26	5.19	5.51	5.35	4.95	3.90	4.41	4.52	5.88	5.54	5.79	5.81	5.96	4.82	5.10
H_2O^+	1.23	0.77	0.77	0.85	0.85	1.00	1.31	0.50	0.50	0.93	0.77	0.77	1.08	0.93	1.31	1.47
H_2O^-								0.10	0.10							
P_2O_5	0.32	0.32	0.32	0.38	0.31	0.35	0.63	0.35	0.37	0.42	0.28	0.29	0.31	0.28	0.24	0.24
Total	99.92	100.10	99.45	99.39	100.10	99.44	99.83	99.25	99.82	99.01	99.04	99.48	99.44	99.17	99.89	99.53
Ba	360	390	350	320	340	310	110	140	140	500	400	490	520	620	690	670
Be	11	5	7	9	9	7	21			11	3	8	10	8		
F	400	320	440	395	470	700	1800	1300	1200	900	600	630	600	600	680	
Li	115	80	119	105	98	148	189	180	170	120	68	75	66	97		
Nb	20	10	20	20	10	20	20	20	10	20	20	10	20	10	< 10	20
Pb	24	28	33	28	26	30	12	20	22	32	39	40	41	36	26	
Rb	330	300	320	350	340	380	810	650	630	500	340	330	330	340	330	330
Sn	12	8	11	13	13	14	23	20	16	13	8	8	7	4	10	
Sr	60	70	70	50	60	60	8	< 10	< 10	100	80	80	110	110	130	130
Th					4			3	2					26	8	
U	7	6	3	2	6	5	10	9	14	5	5	3	9	5	6	
Y	< 10	< 10	20	10	10	10	30	20	20	10	< 10	20	20	< 10	10	< 10
Zn	38	36	50	35	41	44	69	64	100	72	80	79	77	67	44	
Zr	50	50	60	40	50	50	20	20	20	110	130	140	150	150	100	100
La					10.6			3.8						35.5		
Ce					20			8						72		
Nd					10			5						33		
Sm					2.92			1.32						8.86		
Eu					0.65			0.05						0.58		
Tb					0.6			0.3						1.1		
Yb					0.35			0.41						0.58		
Lu					0.07			0.06						0.16		

pluton	LL										LLs	ML	MP				
	046A	047B	118	157	668	670	F68A1	F68A2	F68B	F68C	015B	577	415A	432B	433B	472A	489A
SiO_2	73.10	73.00	73.90	72.20	72.80	73.50	73.20	74.90	74.10	73.60	62.10	73.50	69.50	70.40	68.50	71.60	68.00
TiO_2	0.11	0.16	0.18	0.18	0.19	0.17	0.13	0.07	0.12	0.17	0.14	0.11	0.25	0.31	0.20	0.28	0.19
Al_2O_3	14.90	14.90	14.20	14.70	14.80	14.30	15.00	14.30	14.50	14.40	20.30	14.80	16.50	15.50	16.80	14.90	17.40
Fe_2O_3	0.39	0.44	0.36	0.17	0.14	0.20					0.27	0.01	0.08	0.47	0.09	0.40	0.11
FeO	0.51	0.53	0.72	0.78	0.90	0.77	1.09	0.70	0.76	0.97	1.04	0.65	1.17	1.10	0.88	1.06	0.83
MnO	0.04	0.04	0.07	0.03	0.03	0.03	0.05	0.02	0.02	0.02	0.05	0.03	0.04	0.05	0.03	0.05	0.03
MgO	0.21	0.35	0.36	0.34	0.31	0.29	0.29	0.12	0.19	0.31	0.44	0.20	0.47	0.61	0.39	0.51	0.37
CaO	0.52	0.59	0.62	0.55	0.60	0.60	0.61	0.40	0.49	0.55	0.83	0.53	0.64	0.80	0.75	0.72	0.77
Na_2O	4.42	3.80	3.97	3.62	3.87	3.85	4.48	3.91	4.00	3.77	5.89	4.02	3.79	3.41	3.71	3.30	3.87
K_2O	4.16	4.64	4.48	5.30	5.04	4 75	4.18	4.35	4.47	4.73	6.86	4.87	6.18	5.48	6.82	5.40	7.07
H_2O^+	1.16	1.00	0.70	1.08	1.00	0.70	0.93	1.00	1.00	1.00	1.08	0.85	0.93	1.08	0.70	0.85	0.70
H_2O^-																	
P_2O_5	0.37	0.34	0.30	0.30	0.31	0.31	0.40	0.34	0.35	0.31	0.43	0.30	0.25	0.33	0.27	0.26	0.25
Total	99.89	99.79	99.86	99.25	99.99	99.47	100.36	100.11	100.00	99.83	99.43	99.87	99.80	99.54	99.14	99.33	99.59
Ba	120	280	310	360	320	290	170	70	170	200	500	140	600	580	710	450	720
Be	3	8	4	5	6	4	2	2	2	2	7	5	10		2	10	8
F	545	770	410	450	670	530	490	490	840	400	500	310	440	520	340	540	300
Li	34	110	35	34	99	66	36	31	40	37	38	63	120		50	75	46
Nb	10	10	10	10	10	< 10	19	13	11	14	10	10	10	< 10	10	20	< 10
Pb	19	23	25	25	24	31	14	25	22	19	25	27	38	34	42	33	42
Rb	430	450	330	320	400	380	300	320	300	230	480	310	410	320	330	310	340
Sn	17	16	11	11	14	7	15	8	12	7	17	5	9	6	5	7	3
Sr	< 10	50	70	50	40	40	30	10	20	40	130	20	120	120	140	100	150
Th						8	6	2	6	9			12	16			
U	7	4	5	4	10	8	6	7	5	11	5	3	8	6	3	7	4
Y	< 10	10	10	< 10	< 10	30	0	0	0	0	10	< 10	< 10	20	< 10	< 10	< 10
Zn	27	62	31	33	50	54	15	13	24	24	194	36	45	62	40	60	41
Zr	20	30	50	60	60	50	30	0	40	60	70	< 10	90	130	50	90	60
La						12.2							20.1				
Ce						24							39				
Nd						14							17				
Sm						3.40							4.60				
Eu						0.37							0.72				
Tb						0.3							0.4				
Yb						0.30							0.30				
Lu						0.06							0.06				

Canso area plutons (continued)

pluton	OI				PC						PH							
	346B	346C	346D	384B	416A	424A	441B	445	467B	625	175	269	275	278	512	514	525B	532
SiO_2	73.90	72.80	75.60	74.10	73.60	74.60	74.00	72.10	75.00	72.20	70.90	72.20	72.80	73.80	71.80	72.80	71.20	71.70
TiO_2	0.29	0.41	0.40	0.41	0.38	0.26	0.20	0.41	0.29	0.34	0.36	0.34	0.34	0.28	0.30	0.21	0.35	0.37
Al_2O_3	13.70	13.20	12.00	12.70	13.00	13.30	13.80	14.10	12.60	14.00	15.00	14.10	14.50	13.90	14.70	14.30	14.70	14.30
Fe_2O_3	1.10	0.95	1.14	0.51	0.27	0.17	0.04	0.09	0.09	0.03	0.12	1.13	0.84	0.73	0.42	0.01	0.48	0.60
FeO	1.09	2.66	1.53	2.40	1.74	1.23	1.25	1.66	1.35	1.34	1.53	0.52	0.87	0.96	1.03	1.17	1.19	1.16
MnO	0.07	0.10	0.06	0.08	0.05	0.04	0.03	0.05	0.03	0.04	0.05	0.05	0.04	0.04	0.04	0.03	0.05	0.04
MgO	0.85	1.12	1.09	1.14	0.53	0.40	0.34	0.66	0.44	0.51	0.57	0.51	0.51	0.45	0.46	0.28	0.55	0.55
CaO	1.10	1.09	0.78	1.23	0.48	0.52	0.72	0.71	0.63	0.62	0.70	0.70	0.74	0.63	0.62	0.57	0.69	0.70
Na_2O	4.36	2.75	3.37	3.40	2.77	3.26	2.65	2.93	2.55	2.98	3.12	3.14	3.26	3.15	3.33	3.59	3.37	3.15
K_2O	2.46	2.59	2.38	2.66	5.34	5.10	5.08	5.42	5.15	5.83	5.65	5.47	5.41	4.82	5.92	5.40	5.50	5.56
H_2O^+	1.08	1.39	1.39	0.50	0.77	0.70	0.77	0.77	0.62	0.70	0.77	0.62	0.54	0.77	0.70	0.47	0.93	0.93
H_2O^-				0.10														
P_2O_5	0.12	0.08	0.13	0.23	0.31	0.31	0.35	0.28	0.30	0.29	0.28	0.29	0.29	0.26	0.27	0.25	0.30	0.30
Total	100.12	99.14	99.87	99.46	99.24	99.89	99.23	99.18	99.05	98.88	99.05	99.07	100.14	99.79	99.59	99.08	99.31	99.36
Ba	430	280	400	580	170	230	260	480	290	500	520	350	470	260	400	170	480	450
Be	4	2	2		7	3	8	8	3	4	5	5	6	6	9	3	8	7
F	245	315	265	330	660	550	540	750	420	560	700	630	4100	600	650	660	650	710
Li	27	73	29	55	155	124	108	71	75	51	112	84	85	106	75	77	74	75
Nb	20	20	20	20	30	20	10	< 10	10	20	10	< 10	20	10	10	20	20	10
Pb	29	23	17	30	29	28	32	33	35	48	66	31	32	26	37	28	33	36
Rb	130	150	140	140	380	350	320	340	300	350	380	350	380	370	370	420	370	370
Sn	3	6	3	< 2	9	11	6	10	5	2	13	7	12	7	6	7	7	6
Sr	240	130	190	240	30	50	50	80	70	90	80	60	90	40	70	30	110	90
Th				6									21					
U	1	4	< 1	< 2	6	5	6	5	3	3	2	6	3	6	10	6	10	9
Y	10	40	20	30	10	< 10	10	< 10	20	20	10	10	10	20	20	< 10	20	10
Zn	56	79	45	56	85	55	55	93	80	47	72	66	80	84	74	100	72	73
Zr	90	170	250	180	110	40	50	150	70	140	140	120	110	80	100	50	130	130
La				25.3									28.9					
Ce				43									57					
Nd				16									24					
Sm				3.83									7.18					
Eu				0.56									0.60					
Tb				0.6									1.1					
Yb				1.76									0.44					
Lu				0.35									0.10					

pluton	PH (continued)			PI					SC				SI				
	555	556B	731	262A	297A	303A	315	326	442	469	571	587A	496	565	605	606	616A
SiO_2	71.00	70.60	73.10	73.40	72.60	71.80	74.50	72.10	64.70	59.60	67.10	65.00	72.90	73.30	72.20	72.20	72.90
TiO_2	0.39	0.38	0.21	0.25	0.30	0.31	0.27	0.25	0.75	0.96	0.60	0.72	0.13	0.12	0.19	0.20	0.14
Al_2O_3	14.50	14.50	14.30	14.50	14.10	14.40	13.60	14.60	16.30	17.70	15.80	15.90	14.70	14.70	14.70	14.80	14.80
Fe_2O_3	0.29	0.20	0.33	0.53	0.43	0.30	0.28	0.22	0.25	0.67	0.23	0.43	0.17	0.01	0.09	0.31	0.10
FeO	1.50	1.54	0.82	0.98	1.07	1.41	1.29	1.16	3.98	4.49	3.10	3.77	0.66	1.02	0.99	0.96	0.74
MnO	0.05	0.05	0.04	0.06	0.06	0.06	0.06	0.05	0.17	0.16	0.12	0.16	0.04	0.05	0.04	0.04	0.04
MgO	0.63	0.60	0.29	0.44	0.52	0.49	0.53	0.45	2.03	2.22	1.51	1.94	0.19	0.18	0.33	0.36	0.26
CaO	0.71	0.69	0.45	0.59	0.73	0.58	0.69	0.67	2.81	4.04	2.46	3.19	0.52	0.52	0.58	0.56	0.55
Na_2O	2.96	3.06	3.53	3.22	3.13	3.40	3.19	3.62	3.22	3.44	3.83	3.40	4.04	4.18	3.68	3.71	4.09
K_2O	5.71	5.68	5.26	4.75	4.92	4.96	4.00	5.02	3.34	3.26	3.23	3.25	5.08	4.62	5.06	5.09	4.95
H_2O^+	1.08	1.16	1.00	0.93	1.08	1.08	1.08	1.00	1.00	1.23	0.85	0.93	1.00	1.08	1.16	1.39	0.93
H_2O^-																	
P_2O_5	0.30	0.29	0.31	0.29	0.26	0.30	0.28	0.28	0.19	0.26	0.18	0.19	0.36	0.38	0.35	0.34	0.34
Total	99.12	98.75	99.64	99.94	99.20	99.09	99.77	99.42	98.74	98.03	99.01	98.88	99.79	100.16	99.37	99.96	99.84
Ba	530	470	190	360	490	290	370	530	680	990	520	710	270	150	320	330	320
Be	8	8	6	7	8	5	8	8	3	12	4	2	6	4	5	6	7
F	650	710	760	560	490	660	520	530	700	810	860	760	870	1050	710	710	480
Li	66	76	106	109	75	169	96	87	104	61	102	80	132	145	112	133	86
Nb	10	< 10	10	20	10	10	10	10	20	20	20	10	20	10	10	20	10
Pb	32	42	26	41	35	30	28	29	31	36	33	25	22	18	22	26	23
Rb	370	350	440	340	310	410	300	320	220	180	260	220	510	540	390	380	330
Sn	7	8	12	10	8	14	7	6	7	< 1	5	7	11	16	14	12	13
Sr	120	100	30	60	80	60	70	100	270	390	200	290	30	10	60	50	50
Th										12		12				7	
U	3	7	4	5	7	7	8	5	6	2	< 1	4	7	12	7	5	5
Y	10	< 10	< 10	20	20	< 10	10	10	40	20	10	10	< 10	< 10	10	< 10	10
Zn	83	77	63	65	86	87	61	55	119	109	92	72	66	54	63	60	36
Zr	160	140	50	70	90	70	90	100	190	270	170	210	50	10	50	60	40
La										28.0		39.4				14.6	
Ce										48		68				29	
Nd										21		24				12	
Sm										4.70		6.27				3.80	
Eu										1.53		0.99				0.50	
Tb										0.6		0.9				0.4	
Yb										1.40		1.51				0.43	
Lu										0.23		0.30				0.08	

Canso area plutons (continued)

pluton	SI (continued)		SL				WH											
	618	755	562A	562B	562C	757	029	181	196	197	198	204	263	266	317	329	330	331
SiO_2	72.50	73.10	72.30	73.10	72.30	74.70	74.10	73.90	74.30	74.60	74.60	74.30	75.30	73.90	73.40	74.60	74.60	74.00
TiO_2	0.18	0.18	0.09	0.12	0.08	0.12	0.15	0.10	0.11	0.09	0.14	0.09	0.16	0.09	0.13	0.12	0.13	0.14
Al_2O_3	14.60	14.70	15.20	14.60	15.60	14.70	14.20	15.00	14.50	14.40	13.90	14.50	13.20	14.10	14.00	13.90	14.20	14.00
Fe_2O_3	0.06	0.45	0.12	0.01	0.08	0.36	0.29	0.08	0.31	0.20	0.01	0.13	0.44	0.28	0.09	0.17	0.43	0.10
FeO	1.02	0.70	0.63	0.94	0.56	0.50	0.72	0.85	0.63	0.72	0.95	0.84	0.65	0.57	0.80	0.71	0.60	0.86
MnO	0.04	0.04	0.04	0.05	0.04	0.03	0.03	0.04	0.04	0.04	0.03	0.04	0.04	0.04	0.03	0.03	0.03	0.04
MgO	0.29	0.36	0.13	0.15	0.10	0.24	0.21	0.15	0.21	0.13	0.20	0.16	0.20	0.12	0.18	0.18	0.19	0.20
CaO	0.56	0.58	0.44	0.49	0.48	0.41	0.48	0.47	0.50	0.46	0.56	0.45	0.35	0.42	0.46	0.53	0.53	0.47
Na_2O	3.80	3.78	4.08	3.76	4.34	3.62	3.80	4.26	4.11	4.16	3.84	3.96	3.13	3.97	3.71	4.01	3.74	3.85
K_2O	4.96	4.93	4.21	4.68	4.00	4.05	4.98	4.26	4.07	4.28	4.65	4.44	4.81	4.53	5.02	4.51	4.71	4.77
H_2O^+	1.16	1.00	1.39	1.31	1.31	1.00	0.75	0.93	0.85	0.62	0.70	0.77	0.85	0.93	0.85	0.77	0.70	0.85
H_2O^-																	0.10	
P_2O_5	0.35	0.38	0.38	0.41	0.39	0.30	0.28	0.34	0.32	0.32	0.24	0.35	0.26	0.35	0.28	0.33	0.28	0.28
Total	99.52	100.20	99.01	99.62	99.28	100.03	99.99	100.38	99.95	100.02	99.82	100.03	99.39	99.30	98.95	99.86	100.24	99.56
Ba	320	250	110	180	100	100	170	120	130	110	110	140	130	110	120	120	150	140
Be	7		4	5	4		3	3	5	2	2	3	3	3	2	3		2
F	660	910	1800	1700	1780	1100	650	870	740	670	640	1070	600	1070	490	470	640	510
Li	134		232	237	188		85	161	146	159	98	176	81	143	72	40	85	92
Nb	20	20	30	20	10	20	10	10	20	20	10	20	10	20	10	30	10	10
Pb	24	24	17	20	9	16	30	14	24	15	108	15	23	14	24	19	24	23
Rb	400	480	680	770	760	560	460	550	490	520	400	610	450	600	430	430	380	420
Sn	10	16	24	23	25	20	9	14	14	14	11	16	10	18	12	8	6	6
Sr	60	30	5	30	10	<10	10	<10	10	<10	<10	<10	10	<10	10	<10	<10	20
Th		8	4			<2				3							2	
U	5	8	23	8	21	6	7	2	11	6	6	3	<1	3	6	7	4	4
Y	10	<10	20	10	10	10	10	10	20	20	<10	10	20	<10	10	10	10	10
Zn	52	66	87	100	58	64	40	72	54	68	59	80	43	54	62	26	64	76
Zr	60	60	40	30	30	10	30	20	20	10	20	30	30	10	30	20	20	20
La			7.0							3.1								
Ce			12							8								
Nd			9							4								
Sm			2.25							1.16								
Eu			0.17							0.19								
Tb			0.5							0.1								
Yb			0.54							0.31								
Lu			0.09							0.06								

pluton	WH (continued)								BM	BR						CR	
	333	338	340	519	826	F36	F38A	F38B	040	059	060	123	139	141	145	143A	159
SiO_2	74.60	74.20	74.50	74.50	73.70	74.20	74.50	75.80	74.10	71.00	70.60	70.60	71.70	72.40	71.70	70.50	71.00
TiO_2	0.11	0.10	0.11	0.10	0.13	0.16	0.08	0.07	0.08	0.20	0.26	0.32	0.23	0.22	0.24	0.28	0.30
Al_2O_3	13.90	14.10	14.40	14.10	14.20	14.00	14.20	13.90	15.00	15.60	15.40	14.90	14.90	15.20	15.40	15.50	15.20
Fe_2O_3	0.32	0.44	0.65	0.11					0.31	0.35	0.34	0.36	0.37	0.27	0.30	0.12	0.53
FeO	0.50	0.39	0.25	0.71	0.87	1.31	0.84	0.75	0.20	0.60	0.90	1.50	0.90	1.10	0.90	1.10	1.00
MnO	0.03	0.03	0.03	0.04	0.03	0.04	0.02	0.02	0.04	0.02	0.03	0.04	0.04	0.04	0.03	0.03	0.03
MgO	0.15	0.14	0.15	0.15	0.17	0.20	0.09	0.11	0.15	0.38	0.61	0.64	0.36	0.51	0.53	0.47	0.48
CaO	0.46	0.47	0.49	0.48	0.47	0.45	0.42	0.39	0.37	0.67	0.86	1.42	0.68	1.11	0.79	0.73	0.75
Na_2O	3.82	4.04	4.08	4.04	3.76	3.85	4.21	3.76	5.18	3.93	3.99	4.05	3.38	4.84	3.96	3.52	3.54
K_2O	5.24	4.60	4.03	4.56	4.81	4.71	3.82	4.14	3.78	5.65	4.91	4.37	5.13	3.43	5.19	6.08	5.52
H_2O^+	0.40	0.62	1.00	0.54	0.93	1.00	1.08	1.00	0.30	0.40	0.40	0.50	0.60	0.40	0.30	0.50	0.50
H_2O^-	0.05								0.10	<0.10	<0.10	0.10	0.10	<0.10	0.10	0.10	0.10
P_2O_5	0.28	0.28	0.27	0.31	0.29	0.34	0.33	0.30	0.20	0.28	0.29	0.17	0.37	0.22	0.26	0.23	0.23
Total	99.86	99.41	99.96	99.64	99.36	100.26	99.59	100.31	99.81	99.13	98.64	98.97	98.76	99.79	99.70	99.16	99.18
Ba	120	150	100	130	130	160	60	60	70	740	550	780	320	310	550	570	490
Be		2	2	3		2	2	1									
F	520	650	660	620		980	1025	980	920	400	740	310	640	510	710	690	840
Li	71	95	91	98		117	127	167	160	60	140	54	150	64	95	100	110
Nb	10	10	10	<10	<10	14	9	12	8	8	8	10	16	10	6	6	8
Pb	26	20	17	21		13	11	13	24	32	28	34	32	28	30	34	30
Rb	430	460	430	450	420	410	410	380	500	280	330	200	350	260	330	350	380
Sn	8	12	13	10		11	7	15	34	6	8	6	14	12	10	12	6
Sr	<10	<10	<10	<10	10	0	0	0	14	100	86	200	72	100	82	100	88
Th	<2					9	2	1	<2	6	6	10	6	4	6	14	16
U	<2	5	7	4		5	4	3	12	4	2	4	6	6	6	6	6
Y	<10	<10	<10	<10	10	0	0	0	<2	6	4	12	12	8	6	6	6
Zn	56	60	55	87		40	22	46	20	40	96	42	66	64	74	28	120
Zr	20	10	30	20	20	40	0	0	27	72	90	120	90	57	78	110	110
La					5.1				5.6		23.3						
Ce					10				10		44						
Nd					5				4		19						
Sm					1.50				1.07		5.73						
Eu					0.11				0.18		0.62						
Tb					0.3				0.1		0.4						
Yb					0.42				0.22		0.39						
Lu					0.11				<0.01		0.06						

Forest Hill area plutons (continued)

pluton	CR (continued)		DB				EB			GL			RL	SP	
	211	236	191	195	215	218	240	250	253	014	114B	133	026	015	108
SiO_2	71.10	72.20	70.70	71.30	70.60	72.50	73.10	72.40	72.30	62.50	58.80	54.90	73.50	70.10	71.40
TiO_2	0.31	0.19	0.32	0.22	0.29	0.10	0.14	0.17	0.19	0.71	0.86	0.81	0.12	0.34	0.21
Al_2O_3	15.30	15.10	15.50	15.50	15.40	15.70	15.00	15.40	15.10	17.30	18.10	19.70	15.30	15.00	14.80
Fe_2O_3	0.50	0.38	0.29	0.22	0.43	0.31	0.35	0.50	0.43	0.50	0.77	0.59	0.61	0.43	0.46
FeO	1.00	0.70	1.20	0.90	1.00	0.30	0.60	0.50	0.60	3.50	4.60	5.00	0.30	1.70	0.90
MnO	0.03	0.03	0.03	0.03	0.03	0.03	0.03	0.03	0.02	0.10	0.12	0.13	0.03	0.05	0.04
MgO	0.53	0.31	0.74	0.39	0.65	0.17	0.25	0.34	0.37	2.24	3.62	4.84	0.30	0.76	0.44
CaO	0.73	0.62	0.92	0.65	0.89	0.70	0.58	0.63	0.70	3.38	5.38	7.01	0.84	1.51	1.10
Na_2O	3.54	4.06	3.66	3.80	3.90	4.16	4.15	3.92	3.88	3.75	3.09	3.23	3.89	3.94	4.25
K_2O	5.53	4.68	5.21	5.19	5.00	5.47	4.68	4.94	4.93	3.51	2.16	1.02	3.27	4.53	4.59
H_2O^+	0.50	0.40	0.40	0.50	0.40	0.40	0.50	0.60	0.70	0.70	0.90	1.00	0.60	0.50	0.50
H_2O^-	0.10	0.10	0.10	0.10	0.10	0.10	0.10	0.20	0.20	0.10	0.10	0.20	0.10	0.20	0.10
P_2O_5	0.23	0.24	0.27	0.32	0.30	0.30	0.33	0.33	0.35	0.19	0.15	0.14	0.25	0.18	0.16
Total	99.40	99.01	99.34	99.12	98.99	100.24	99.81	99.96	99.77	98.48	98.65	98.57	99.11	99.24	98.95
Ba	470	300	770	550	610	300	330	420	440	780	500	350	390	710	450
Be															
F	720	950	640	500	740	280	480	220	380	300	440	360	300	520	500
Li	110	160	110	100	140	60	140	79	96	160	55	52	28	160	100
Nb	6	8	6	12	8	10	12	12	14	10	8	8	12	10	10
Pb	30	28	28	32	36	34	32	32	32	38	24	16	26	32	34
Rb	380	410	320	300	340	300	290	280	270	220	150	44	190	260	310
Sn	4	14	6	12	10	4	18	8	12	4	4	<2	10	8	12
Sr	88	58	110	78	88	72	60	74	78	300	380	520	130	170	110
Th	20	12	8	4	6	<2	2	4	<2	10	4	2	<2	12	6
U	<2	<2	2	2	4	6	8	4	6	<2	<2	2	4	<2	2
Y	4	4	6	6	6	6	6	10	10	12	16	10	10	12	10
Zn	48	60	86	60	100	24	44	44	48	140	74	70	16	64	44
Zr	110	66	90	63	90	42	39	57	66	110	66	51	21	130	72
La	35.0				23.4		8.5			63.6	22.0		6.3		
Ce	68				45		15			93	36		11		
Nd	32				23		6			50	22		4		
Sm	7.75				5.96		2.21			10.10	5.05		1.26		
Eu	0.72				0.56		0.36			1.17	1.15		0.38		
Tb	0.7				0.4		0.4			0.7	0.7		0.3		
Yb	0.34				0.40		0.28			0.95	1.08		0.53		
Lu	0.05				0.10		0.04			0.20	0.20		0.08		

Miscellaneous plutonic rocks

pluton	SP (continued)		TL																
	113	119	046	047	053	F56	F63A	F63B	F65	041	051	069A	088A	153	154B	236	248A	253
SiO_2	72.10	72.60	73.00	72.50	72.70	74.40	72.60	73.70	72.90	79.00	72.90	85.90	75.00	71.90	71.00	74.20	70.90	70.00
TiO_2	0.20	0.14	0.14	0.12	0.13	0.10	0.13	0.11	0.11	0.03	0.10	0.09	0.07	0.11	0.21	0.04	0.24	0.04
Al_2O_3	14.90	15.10	14.60	14.90	15.00	13.40	15.00	14.80	15.10	11.40	15.00	7.12	14.50	15.10	15.30	14.40	16.00	16.80
Fe_2O_3	0.40	0.45	0.37	0.21	0.39					0.28	0.55	0.00	0.21	0.27	0.26	0.11	0.65	0.17
FeO	0.80	0.60	0.80	0.50	0.60	0.68	0.87	0.76	0.69	0.10	0.30	0.50	0.30	0.60	0.80	1.17	0.99	0.20
MnO	0.03	0.05	0.04	0.03	0.04	0.01	0.02	0.02	0.02	0.02	0.03	0.02	0.04	0.03	0.02	0.09	0.11	0.07
MgO	0.46	0.31	0.27	0.23	0.23	0.20	0.24	0.20	0.19	0.11	0.16	0.17	0.09	0.23	0.40	0.12	0.43	0.11
CaO	1.31	0.78	0.58	0.62	0.58	0.47	0.46	0.48	0.47	0.22	0.74	0.28	0.39	0.71	0.68	0.61	0.52	0.83
Na_2O	3.54	4.18	3.78	4.16	4.04	3.64	3.62	3.89	3.99	4.28	3.94	2.69	6.07	4.24	3.79	4.11	4.72	5.40
K_2O	5.17	4.81	4.72	5.05	4.89	4.32	4.77	4.96	4.91	3.35	4.86	1.90	1.65	4.72	5.75	4.28	3.78	4.22
H_2O^+	0.40	0.40	0.60	0.50	0.50	1.08	1.39	1.16	1.16	0.20	0.50	0.54	0.30	0.40	0.50	0.54	1.00	1.00
H_2O^-	0.10	0.10	<0.10	<0.10	0.10					0.10	0.10		<0.10	0.10	0.10			
P_2O_5	0.07	0.17	0.40	0.42	0.41	0.31	0.34	0.35	0.35	0.09	0.28	0.13	0.30	0.30	0.30	0.07	0.32	0.76
Total	99.48	99.69	99.35	99.29	99.61	98.61	99.44	100.43	99.89	99.18	99.46	99.34	98.92	98.71	99.11	99.74	99.66	99.60
Ba	650	350	200	280	260	170	230	240	160	190	300	180	130	460	740	480	120	100
Be						5	4	4	7			2				3	6	81
F	200	370	580	540	440	420	420	470	420	150	280	190	1400	310	290	215	820	890
Li	50	51	110	79	100	45	101	98	101	7	23	11	190	110	70	38	111	143
Nb	6	10	16	12	16	10	16	12	14	6	12	20	16	12	8	10	20	20
Pb	36	40	28	32	30	10	15	15	18	14	34	8	34	38	40	32	42	37
Rb	220	280	350	340	360	220	260	280	270	220	240	120	310	260	280	250	360	790
Sn	6	16	24	18	18	14	10	5	12	6	4	5	130	12	6	7	16	48
Sr	170	86	50	64	60	70	70	40	50	90	76	40	150	92	110	80	<10	80
Th	4	4	<2	<2	<2	2	3	3	2	<2	<2		<2	2	6			
U	<2	6	6	2	10	4	3	4	5	<2	4	<1	10	<2	4	6	3	21
Y	4	8	8	8	8					2	10	10	4	12	6	<10	<10	<10
Zn	26	40	34	36	38	14	13	13	14	40	20	42	22	30	48	46	68	29
Zr	54	42	42	38	39	20	30	30	30	3	35	10	18	36	81	30	60	10
La	15.5				8.1													
Ce	26				14													
Nd	12				7													
Sm	2.64				1.93													
Eu	0.87				0.34													
Tb	0.2				0.3													
Yb	0.30				0.30													
Lu	0.09				0.05													

Miscellaneous plutonic rocks (continued)

pluton	346A	384A	411C	414	441A	458A	458B	463	472B	485	547	553	558	587B	802	F88A3
SiO_2	74.30	69.70	72.50	73.50	73.80	74.60	70.40	70.10	73.40	73.60	69.50	69.00	73.30	74.20	61.80	84.70
TiO_2	0.08	0.13	0.07	0.18	0.12	0.14	0.39	0.38	0.04	0.05	0.38	0.16	0.05	0.08	0.81	0.04
Al_2O_3	14.10	16.40	14.80	14.70	14.30	13.90	14.80	15.40	13.90	14.90	15.00	16.60	14.90	14.50	17.30	8.13
Fe_2O_3	0.20	0.32	0.00	0.07	0.02	0.29	0.33	0.45	0.00	0.05	0.48	0.11	0.11	0.06		
FeO	0.49	0.70	0.45	0.96	0.86	0.64	2.07	1.47	0.86	0.52	1.44	0.54	0.48	0.52	4.81	0.37
MnO	0.04	0.03	0.02	0.04	0.05	0.07	0.07	0.05	0.31	0.15	0.07	0.04	0.03	0.07	0.20	0.01
MgO	0.22	0.40	0.17	0.30	0.26	0.19	0.62	0.78	0.09	0.08	0.60	0.24	0.13	0.17	3.02	0.08
CaO	0.60	0.63	0.30	0.60	1.05	0.46	0.60	0.96	0.22	0.27	0.77	0.48	0.44	0.52	4.11	0.18
Na_2O	3.52	4.26	2.99	3.63	3.95	3.76	4.09	3.00	2.36	4.89	2.47	4.15	4.93	4.52	3.78	2.92
K_2O	5.40	5.97	7.52	4.56	4.64	4.81	4.52	6.14	6.46	4.04	6.65	7.34	3.86	4.23	1.72	2.43
H_2O^+	0.70	0.30	0.62	1.00	0.54	0.70	1.00	1.00	0.70	0.70	1.23	0.93	1.00	0.77	1.16	0.54
H_2O^-		0.10														
P_2O_5	0.09	0.17	0.17	0.34	0.10	0.28	0.28	0.25	0.50	0.39	0.37	0.31	0.52	0.33	0.21	0.13
Total	99.74	99.11	99.71	99.88	99.69	99.84	99.17	99.98	98.84	99.64	98.96	99.90	99.75	99.97	98.92	99.53
Ba	1010	1470	560	290	480	100	350	880	160	90	520	690	120	170	470	80
Be	4		6	5	4	6	24	1	2	10	5	5	6	11		1
F	155	90	180	440	299	450	1200	790	220	500	620	315	590	600		<20
Li	13	24	20	81	72	88	200	167	21	58	44	37	40	20		12
Nb	<10	20	20	10	20	10	30	10	10	20	10	<10	10	20	10	0
Pb	72	54	41	24	36	26	29	48	27	17	26	43	11	15		8
Rb	150	170	340	340	240	420	540	330	380	500	630	410	570	360	200	130
Sn	4	<2	6	11	7	10	12	5	8	16	6	3	20	16		0
Sr	260	350	100	50	140	30	60	200	20	20	140	120	<10	30	380	10
Th		<2														1
U	2	2	<1	5	<1	4	15	5	6	11	12	5	29	3		4
Y	<10	<10	<10	20	20	<10	10	<10	10	<10	20	<10	10	10	30	0
Zn	12	16	10	52	29	50	91	55	20	20	86	26	35	14		9
Zr	30	30	<10	50	50	10	200	150	<10	20	150	30	20	10	140	0
La																
Ce																
Nd																
Sm																
Eu																
Tb																
Yb																
Lu																

	Halifax Formation																Goldenville Formation		
Unit	CO_{He} 024	CO_{Ha} 053	CO_{Ha} 059A	CO_{Ha} 071	CO_{Ha} 086A	CO_{Ha} 086B	CO_{Ha} 185	CO_{Hb} 224A	CO_{Hb} 226	CO_{Hd} 241	CO_{He} 245	CO_{Hb} 262B	CO_{Hd} 792A	CO_{Hc} 792B	CO_{Hb} 805A	CO_{Hd} 806	CO_{Ga} 020	CO_{Gb} 050	CO_{Gb} 081B
SiO_2	62.30	51.00	38.90	49.80	49.40	52.90	60.50	57.60	62.80	53.00	62.10	52.90	52.90	55.10	58.80	54.10	60.50	55.50	47.90
TiO_2	0.86	1.47	0.84	1.38	1.33	1.15	1.17	2.81	0.41	1.10	1.02	0.86	0.96	1.09	0.92	1.00	0.77	0.82	1.22
Al_2O_3	18.60	28.40	18.20	26.10	28.10	26.20	20.50	20.30	11.00	21.70	19.50	20.30	24.30	22.30	19.80	24.10	19.70	20.60	17.20
Fe_2O_3																			
FeO	7.25	3.79	9.81	7.28	3.92	4.02	5.50	8.19	6.52	10.17	5.38	9.72	8.77	7.21	7.32	7.79	5.19	8.62	11.88
MnO	0.10	0.04	18.60	0.06	0.12	0.10	0.13	1.04	14.20	3.77	0.08	1.82	1.55	0.38	1.65	1.31	0.08	0.14	8.23
MgO	2.02	1.89	2.80	3.38	1.55	1.75	1.43	2.13	0.49	1.24	1.73	2.98	1.60	1.90	1.65	1.73	2.66	3.08	4.36
CaO	0.38	0.01	6.14	0.08	0.07	0.22	0.09	0.37	1.54	0.42	0.75	0.80	0.33	0.21	0.42	0.35	0.43	0.82	4.02
Na_2O	0.89	1.32	0.01	1.07	1.36	1.25	0.94	0.90	0.01	0.73	1.67	0.46	0.98	0.62	1.41	0.99	0.87	1.64	0.40
K_2O	3.40	4.99	0.65	4.51	5.53	4.97	4.34	3.15	0.06	2.71	3.85	4.31	3.49	5.81	3.20	3.62	6.27	4.89	3.14
P_2O_5	0.17	0.05	0.21	0.12	0.07	0.12	0.05	0.21	0.18	0.20	0.19	0.22	0.15	0.12	0.19	0.14	0.19	0.15	0.27
C		1.29	0.07	0.99	1.24	1.09	0.33	0.10	0.06	0.08		0.10	0.05	0.10	0.06	0.06			0.16
S		0.02	0.00	0.87	1.26	0.39	<0.01	0.01	0.02	<0.01		0.59	0.00	0.00	0.00	0.00			0.30
H_2O^+	3.39	6.35	1.08	7.00	7.77	6.39	4.05	2.90	<0.05	2.30	3.00	2.10	3.31	3.93	3.00	2.85	2.62	2.08	0.75
H_2O^-																			
Total	99.36	100.10	97.31	102.20	101.09	100.36	99.03	99.71	97.28	97.42	99.27	96.87	98.39	98.77	98.42	98.04	99.28	98.34	99.68
As		3	140	2	57	12	13	4	58	2		17	9	42	9	12			87
Au		2	1	<1	5	<1	5	<1	63	<1		<1	<1	1	1	9			<1
Ba	840		250		1710	1380					960		950	1140	920	930	1210	980	
Co			14		18	12							42	26	40	42			
Cu		23	<1	57	45	25	2	2	2	5		53	14	33	15	10			29
Mo		14	<2	12	20	2	2	2	4	2		2	<2	<2	<2	<2			6
Nb	20		40		20	20					30		40	20	20	30	30	10	
Ni			24		48	24							74	56	80	92			
Pb		29	28	33	42	36	34	32	32	64		75	52	38	48	54			55
Rb	260		40		320	270					230		230	270	210	260	420	280	
Sb			9		9	<3							18	9	6	<3			
Sn		5	72	4	8	8	6	<1	4	<1		1	<2	6	6	<2			<1
Sr	140		30		210	340					210		240	60	280	260	80	130	
Th			<2		14	12							16	10	10	10			
Tl			8		18	16							14	10	8	16			
U		11	<2	11	10	6	5	8	2	7		4	2	<2	2	6			6
W		2	66	2	9	3	2	<2	4	<2		<2	<3	3	<3	6			4
Y	30		20		80	20					40		20	40	10	20	30	50	
Zn		62	22	240	64	120	59	94	41	66		263	130	110	110	130			133
Zr	190	174	130	151	170	140	165	133	38	114	230	99	110	150	140	140	110	170	124

Meguma Group metasedimentary rocks (continued)

	Goldenville Formation (continued)			Quartz Veins							
	CO_{Ga} 346E	CO_{Ga} 794		011	059B	219B	219C	224B	224C	224D	224E
SiO_2	75.60	62.10									
TiO_2	0.51	0.78									
Al_2O_3	10.80	17.90									
Fe_2O_3											
FeO	3.29	6.47									
MnO	0.08	0.10									
MgO	1.32	2.56									
CaO	2.11	1.04									
Na_2O	3.38	2.05									
K_2O	1.60	4.05									
P_2O_5	0.07	0.17									
C	0.04										
S	0.20										
H_2O^+	0.40	2.31									
H_2O^-											
Total	99.30	99.53									
As	<2		Ag			<0.5	<0.5	<0.5	<0.5	<0.5	<0.5
Au	<1		As	<3	380	<2	<2	9	6	23	14
Ba		950	Au	<1	1	13	1	<1	10	<1	8
Co			Ba	80	210						
Cu	1		Co	2	28						
Mo	2		Cu	61	100	6	8	3	9	5	40
Nb		20	Mo	10	<2	2	1	1	4	1	1
Ni			Nb	4	8						
Pb	26		Ni	26	56						
Rb		200	Pb	12	34	28	34	25	42	16	22
Sb			Rb	14	26						
Sn	4		Sb	6	3						
Sr		200	Sn	<2	32	13	5	7	2	11	4
Th			Sr	6	52						
Tl			Th	<2	<2						
U	3		U	<2	<2	6	9	1	6	<1	4
W	<2		W	9	3200	<2	<2	<2	2	2	2
Y		20	Y	4	6						
Zn	96		Zn	12	420	27	25	29	45	21	30
Zr	168	150	Zr	<3	27	33	80	39	30	41	56